Wnt Signaling Regulation of the Human Gastric Corpus Epithelium

by

Kevin Patrick McGowan

A dissertation submitted in partial fulfillment
of the requirements for the degree of
Doctor of Philosophy
(Molecular and Integrative Physiology)
in the University of Michigan
2023

Doctoral Committee:

Professor Linda C. Samuelson, Chair
Professor Howard Crawford
Professor Yatrik Shah
Professor Jason R. Spence

Kevin Patrick McGowan
kpmcg@umich.edu
ORCID iD: 0000-0001-8383-8789

DEDICATION

To my family and friends for the laughs, love,

and support that made this possible.

ACKNOWLEDGEMENTS

First, I would like to thank my mentor, Linda Samuelson, for everything she has done for me over the past nearly six years. For my entire time in the lab, Linda and I met every Thursday to discuss my ongoing experiments, data, plans, and, at times, just life. I truly appreciate how willing she was to always be there for me as a mentor in every way. Even when things were dark and experiments were failing, she was able to pick me back up and motivate me to keep moving forward to find that eventual success. Linda consistently pushed me to be the best scientist, as well as the best person, that I could possibly be, and I am truly grateful to have spent my years working towards my PhD in her lab.

Next, I would like to thank all my lab mates who were a part of my journey. From the moment I joined the lab during my first-year rotations, I felt like a welcomed and valued member. Specifically, I would like to thank Theresa Keeley for being a steadfast and warm presence as our lab manager during my years in the lab. Theresa made sure the lab always felt as if it ran itself (which it absolutely did not) and was always there to help in any way possible.

I would also like to thank my committee members – Drs. Yatrik Shah, Jason Spence, and Howard Crawford, for all their support and guidance throughout the years. I always felt that they wanted the best for me at every step and helped me to grow as a researcher during my committee meetings.

Finally, I would like to thank Scott Magness at the University of North Carolina for taking a chance on a random undergrad, welcoming me into his lab, and, unknowingly at the time, making all of this possible.

Moving on from people who influenced me scientifically, I would like to thank all the members of the two organizations, miLEAD Consulting and the Zell Lurie Commercialization Fund (ZLCF), that helped round out my graduate studies. Joining miLEAD my first year was one of the best decisions I made throughout my time in graduate school. It became an escape for me when experiments and lab were difficult and provided an outlet for me to explore facets of science and technology that I would never have been exposed to otherwise. This was only expanded upon with ZLCF, which truly helped inform my passion for innovation and career goals moving forward. I am grateful to have been elected as a leader within both groups, and I am excited to continue seeing them grow through the years.

I would also like to thank every single person who came out to one of Mike's and my football tailgates. Waking up at 5am on a freezing November Saturday to stand on a golf course for eight hours is not for everyone, but it was always worth it.

Next, I would like to thank my friends who helped keep me going for all these years. Starting with the old, I have always felt extraordinarily lucky to have a group of "boat friends" that I have been able to stay close with for all these years since undergrad. From annual New Years' trips and alumni regattas to now weddings, I never had to go more than a few months without spending some much-needed time with them. They have always been there for me, and I know moving forward that they always will be. For my newer "Michigan friends", I have no idea how I could have made it to

where I am today without them. From First Friday breakfast at Northside to coffee runs to happy hours to game nights to tailgates to Whisky Wednesday at Last Word to intramural sand volleyball to annual St. Patrick's Day and Halloween parties to Among Us over Zoom and so much more, they were there from start to finish to both help keep me focused and to distract me in the best way possible. For me they were more than just a support system but a new family that I got to grow with for six years.

I am also extraordinarily grateful to my actual family for the endless love and support they have been able to give me. Despite living multiple states away and at times not being able to be as present as I wish I could have been, they were always there to encourage me and cheer me on every step of the way.

Finally, I would like to thank Phoebe for being an incredible cheerleader, supporter, friend, and overall partner for my entire time in graduate school. She always pushed me to become the best version of myself and grounded me by reminding me about how much there is to life beyond a lab bench. Without her by my side, these past years would have been infinitely more challenging, so I am forever thankful to her, as well as Dem, Elle, and Birdy, simply for being there for me all these years.

TABLE OF CONTENTS

LIST OF FIGURES

CHAPTER I

CHAPTER II

CHAPTER III

CHAPTER IV

LIST OF TABLES

ABSTRACT

The gastrointestinal epithelium is one of the most proliferative tissues within the body and consistently undergoes complete cellular turnover. This renewal is fueled by resident populations of adult stem cells which asymmetrically divide to establish differentiated cells that carry out functions required for digestion, absorption, and barrier integrity. Wnt signaling is an essential pathway regulating stem cell identity throughout the gastrointestinal tract, and its dysregulation rapidly leads to disease. Interestingly, there appear to be regional differences in Wnt function along the gastrointestinal tract, including between the proximal corpus and distal antral regions of the human stomach. Despite similar gradients of Wnt signaling throughout each region, the corpus and antrum have strikingly different glandular architectures and proliferative zones. Furthermore, while Wnt target genes label active antral progenitors as demonstrated in the intestines, these markers localize to differentiated cells within the corpus. Currently, little is known about the role of Wnt signaling in regulating corpus epithelial cell homeostasis.

Gastric Wnt regionality is further suggested by the pathogenesis of Wnt activation diseases such as familial adenomatous polyposis (FAP). FAP is caused by germline loss-of-function mutation to *APC*, a negative regulator of the Wnt pathway. These patients develop abundant yet benign fundic gland polyps (FGPs) within the corpus but experience little polyp burden in the antrum. It remains poorly understood

how activation of Wnt signaling underscores FGP formation, why they are regionally restricted, and what mechanisms underly their benign nature. In this thesis, I sought to investigate the mechanisms through which activation of Wnt signaling regulates the human corpus epithelium to understand the role of Wnt during homeostasis and disease. Throughout my studies, I utilized cultures of three-dimensional, self-renewing organoids derived from primary human tissue.

Through comparative experiments, I demonstrated that peak growth of corpus organoids was induced by a lower concentration of GSK3β inhibitor and Wnt pathway activator CHIR99021 than in patient-matched antral organoids. In-depth analysis revealed region-specific, Wnt-dependent regulation of proliferation and that supramaximal CHIR99021 dose-dependently suppressed corpus organoid growth. Further, Wnt signaling regulated a bimodal axis of differentiation within corpus organoids, with activation promoting deep glandular cell differentiation. Paradoxically, deep glandular-enriched, slow-growing organoids established new organoids at enhanced rates. My findings suggest that high Wnt induces differentiated, quiescent cells that are poised to function as proliferative progenitors upon Wnt reduction.

To investigate the role of Wnt signaling activation in gastric disease, our lab established a biobank of patient-matched FGP and surrounding non-polyp sample pairs from FAP patients. I determined that FGP biopsies and organoids were associated with increased levels of Wnt signaling yet exhibited reduced tolerance for additional pathway upregulation. This aligns with a theory established to explain the association of specific *APC* mutations with the development of colon cancer, termed the ‘just-right’ hypothesis. Genomic sequencing demonstrated that in contrast to colon polyposis, second-hit

somatic *APC* mutations were infrequent in FGPs, indicating that most polyps arose without the need for loss-of-heterozygosity. Ultimately, these findings were translated into *Apc*-deficient mouse models where heterozygous deletion of *Apc* increased corpus proliferation, while homozygous deletion was required for antral hyperproliferation.

In conclusion, this work elucidates a role for Wnt signaling to drive growth and differentiation within the human gastric corpus. These studies provide translatable findings to the clinical manifestations of disease and offer insight for the continued study of human tissue in *ex vivo* systems.

CHAPTER I

Introduction

The gastrointestinal epithelium from the proximal stomach to the distal rectum is comprised of a continuous monolayer of columnar cells. Throughout the gastrointestinal tract, the epithelium is compartmentalized into submucosal invaginations known either as glands within the stomach or as crypts within the intestine. This architecture enables the distinct compartmentalization of various specialized cell types involved in critical processes of gastrointestinal function during homeostasis such as digestion, absorption, barrier integrity, microbial protection, and tissue renewal.

Renewal within the gastrointestinal epithelium occurs at an incredible rate, making it one of the most proliferative organs in the human body. Luminal facing foveolar (surface) cells in the stomach or enterocytes in the intestine are turned over every few days to maintain essential tissue functions and barrier integrity (1). This property makes the gastrointestinal tract an important target for studying the various pathways and mechanisms that drive progenitor cell function within adult tissues. Furthermore, stem or progenitor cells are also known to be the cells-of-origin for many human diseases, including cancer, as dysregulation of these pathways confers aberrant proliferation and cell identity which breaks down the typical mucosal cellular structure (2, 3).

Central to the regulation of gastrointestinal stemness is the highly conserved Wnt signaling pathway. Stem cells of the distal stomach, small intestine, and colon have all been shown to rely on Wnt signaling, with activation of the pathway conferring stemness and maintenance of homeostatic proliferation. In the proximal stomach, however, the role of Wnt signaling remains unclear. Despite the long-held belief that Wnt signaling was dispensable or even absent from corpus, recent studies have begun to demonstrate a role for Wnt in regulating epithelial cell proliferation and differentiation in unique ways compared to more distal regions. Activation of Wnt signaling through pathway gene mutations predisposes the corpus to abundant yet benign polyposis syndromes, therefore suggesting a role for Wnt underlying gastric hyperproliferative diseases. These mechanisms regulating homeostasis and disease however appear to be unique to the corpus, which contains differentiated cell types and mucosal architecture that is distinct from the antrum. Furthermore, most studies to date have focused on studying gastric homeostasis within mouse models, and therefore little is known regarding the role of Wnt or other pathways within human gastric tissue.

In this chapter, I discuss the current understanding of gastric corpus epithelial homeostasis and disease in mice and humans, including recent insights observed in the role of Wnt signaling in regulating these functions. First, I begin by providing an overview the anatomy of the human stomach, including highlighting the distinct features that comprise the corpus and antrum. Next, I review gastric corpus stem cells including their known markers and the pathways that regulate their identity and differentiation. This then leads to a discussion of organoid models as an experimental model to study human progenitor function *in vitro*. Following, I discuss the Wnt signaling pathway as a

master regulator of gastrointestinal stem cell function and examine emerging studies demonstrating its potential to regulate corpus epithelial homeostasis. Finally, I highlight the Wnt activation disease familial adenomatous polyposis (FAP), the pathogenesis of regional gastric polyps clinically observed within these patients, and a principle of Wnt signaling which may underly regional disease manifestation known as the 'just-right' hypothesis.

1.1 Overview of the Human Gastric Epithelium

Anatomy of the Human Stomach

The human stomach is divided into two major anatomical units: the proximal body, also known as the corpus, and the distal pylorus, or antrum (Figure 1.1). Rodent stomachs are slightly more complex than human stomachs as they contain an additional enlarged, peri-esophageal proximal compartment comprised of squamous tissue resembling the esophageal epithelium (4). The corpus and antrum are both lined with a monolayer epithelium connected by a transition zone containing characteristic features of both regions. Relative to antral glands, glands in the gastric corpus are elongated and contain populations of oxyntic parietal cells which are responsible for secreting acid to maintain acidity within the lumen. Gastric corpus versus antral specification occurs during development, with the transcription factor *PDX1* implicated as a key regulator of antral identity (5). As such, deletion of *Pdx1* in mice leads to a failure in antral development (6).

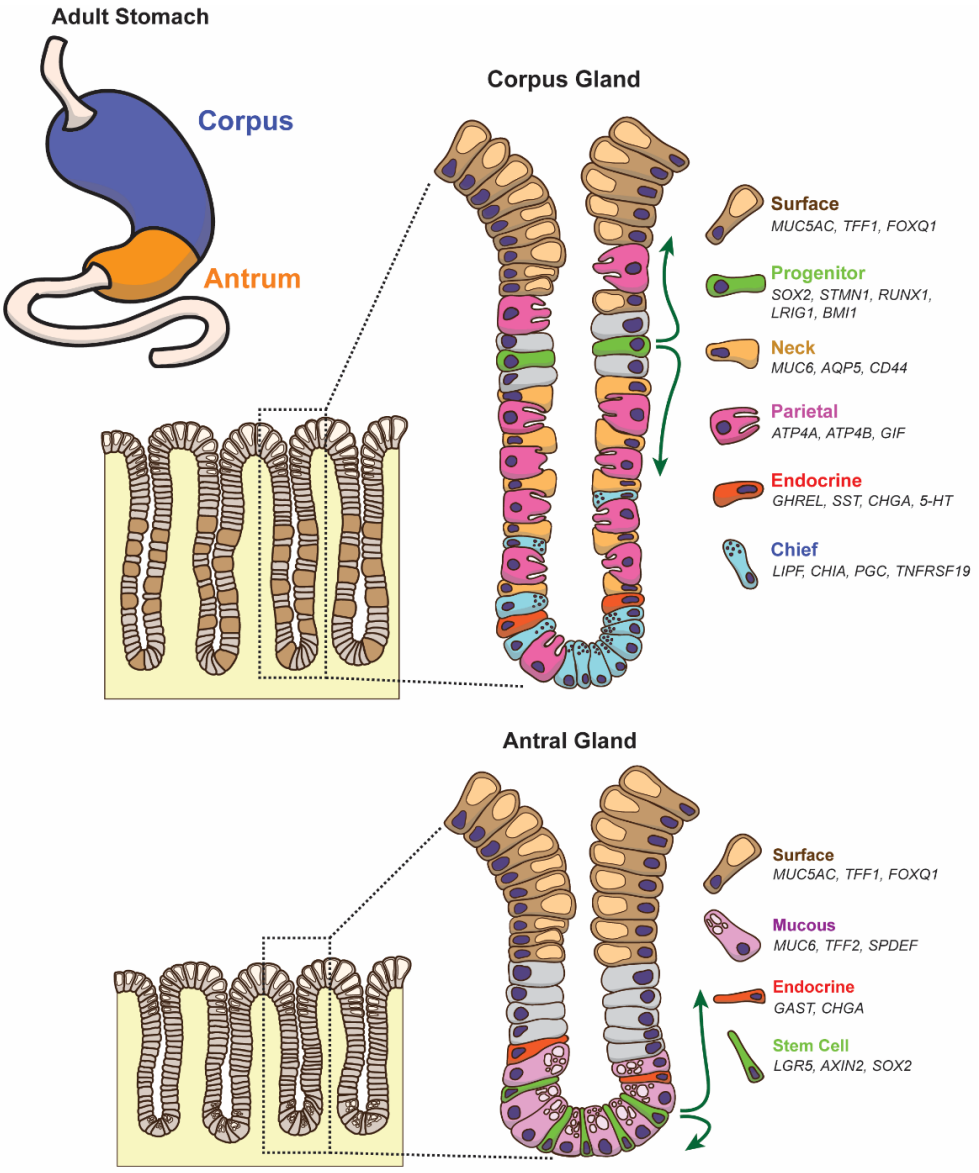

Figure 1.1: Corpus and antral epithelium

The human stomach is divided into two major anatomical compartments: the corpus and antrum. The corpus comprises most of the stomach and contains elongated glands containing acid secreting parietal cells and zymogenic chief cells secreting digestive enzymes. Undifferentiated progenitor cells of the corpus reside in the mid-gland region known as the isthmus and bidirectionally differentiate towards mucous-producing surface cells or towards deep glandular cell lineages. Corpus glands also possess a population of necks cells which intercalate between parietal cells, as well as endocrine cells secreting peptide hormones and biogenic amines (serotonin, somatostatin, histamine). Antral glands are shorter and more closely resemble crypts of the intestine. A resident population of active stem cells marked by *LGR5* exists at the base of glands and primarily gives rise to differentiated cells through a population of transit amplifying cells located in the isthmus. Mucous cells are located at the surface and in the base along with scattered endocrine cell populations expressing gastrin.

Corpus Glandular Architecture

Epithelial glands of the corpus are elongated invaginations containing compartmentalized pools of specialized cells that play integral roles in digestion and barrier protection within the stomach (Figure 1.1). The architecture of corpus glands can be further broken down into the surface, isthmus, neck, and base regions in order from most luminal to the deepest part of the mucosa. The luminal surface of the corpus gland contains mucus-secreting foveolar (also known as pit or surface) cells, which are the primary cells in contact with the caustic gastric lumen (7). They produce hallmark secretory proteins, the glycoprotein Mucin 5AC (MUC5AC) and lectin Trefoil factor 1 (TFF1). These cells are considered to be terminally differentiated and are constantly replenished through rapid cellular turnover from undifferentiated progenitor pools to maintain homeostasis and barrier integrity.

The isthmus of the corpus is in the upper middle region of the gland and is the primary proliferative compartment during homeostasis. Early high resolution microscopy of the corpus epithelium localized granule-free undifferentiated progenitor cells to this region (1). These cells give rise to differentiated cells that migrate towards the surface or towards the neck region. While a definitive, specific marker for isthmus progenitors remains elusive, lineage tracing studies in mice have shown that *Sox2*, *Lrig1*, *Stmn1*, *Bmi1*, and *Runx1* all label progenitor cells with the capacity to give rise to clonal expansions of differentiated cells and self-renew *in vivo* (8-12).

Below the isthmus is the neck region of the gland. This is the primary location for acid-secreting parietal cells, although these cells can be found throughout the gland aside from the most luminal surface. Their primary role is to maintain the acidic environment of the stomach through the secretion of hydrochloric acid into the lumen,

which is accomplished by H/K ATPase activity composed of two subunits, ATP4A and ATP4B. Parietal cells in humans are also the source of gastric intrinsic factor (GIF), which is essential for Vitamin B12 absorption (13). Intercalating between parietal cells are mucous-secreting neck cells labeled by their hallmark secretory product Mucin 6 (MUC6).

Finally, at the base of glands reside zymogenic chief cells whose primary function is to secrete digestive enzymes such as the protease precursor pepsinogen. These cells are thereby commonly marked by pepsinogen C (PGC), although single cell RNA-sequencing studies have shown that *PGC* localizes to a wider range of cells, including chief cell precursors and neck cells (14). Other prominent markers for chief cells include the digestive enzymes lipase F (LIPF) and chitinase acidic (CHIA), the cytokine receptor TROY (encoded by *TNFRSF19)*, and transcription factor class A basic helix-loop-helix protein 15 (BHLHA15), also known as MIST1. Interestingly, while GIF is localized to parietal cells in humans, GIF is localized to chief cells in mice (13).

The final major differentiated cell type of the gastric corpus is enteroendocrine cells which represent a broad class of scattered cells releasing various hormones and biogenic amines. The most prominent corpus-specific enteroendocrine cell, the X/A cell, releases the hormone Ghrelin (GHREL), which stimulates the hunger response (15). In the human corpus, endocrine cells have also been demonstrated to produce somatostatin (D cells), serotonin/5-HT (EC cells), and histidine decarboxylase (ECL cells) (4). Cells expressing these hormones appear to be distinct from one another, contrary to the intestine where there is significant colocalization of multiple hormones within a single cell (15). Interestingly, while intestinal enteroendocrine development

relies on the transcription factor NEUROG3, EC, ECL, and X/A cells of the corpus appear to be NEUROG3 independent (16). Another transcription factor, NEUROD, has also been implicated in enteroendocrine development, however only a portion of endocrine cells arise from *NeuroD*-expressing progenitors in mice (17).

Antral Glandular Architecture

Relative to those in the corpus, antral glands have a more classic architecture that closely resembles what is observed throughout the remainder of the intestinal tract. These glands are shorter, lack parietal cells, and contain populations of endocrine cells secreting the hormone gastrin (GAST) (4, 6). There is overlap in the differentiated cell types found within the corpus and antrum with the presence of MUC5AC-secreting surface cells. While in mice there is a definitive lack of chief cells within the antrum, in humans there are rare glands that contain scattered chief cells throughout this gastric region (4). Instead, the base of antral glands is comprised of large, mucous-secreting cells labeled by MUC6 and trefoil factor 2 (TFF2).

Cells of the isthmus, neck, and base region of the antral gland are clustered together in the deepest region of the gland, resulting in a smaller base compartment relative to the corpus (Figure 1.1). A definitive stem cell population resides within the base of antral glands that is marked by the Wnt target genes *LGR5* and *AXIN2* (3, 18). These cells give rise to transit amplifying cells of the gastric isthmus which ultimately differentiate to the various specialized lineages comprising the antral gland (19). This pattern of proliferation of stem/progenitor cells is consolidated to the base which contrasts to the mid-gland localization of progenitor cells in the corpus.

1.2 Gastric Stem Cells and Differentiation

Adult stem cells along the length of the gastrointestinal tract are responsible for giving rise to differentiated cell lineages (1, 20, 21). Normal turnover of stem cells is essential to maintaining proper tissue function, and dysregulation of niche signaling pathways regulating turnover can lead to gastrointestinal dysfunction and disease. Furthermore, their undifferentiated status and proliferative potential make them typical cells-of-origin for gastrointestinal cancer (2). Therefore, the study of adult stem cell populations is essential to understanding the molecular pathways underpinning both homeostasis and tumorigenesis.

Gastric Corpus Stem Cells

The first identification of gastric corpus stem cells was in 1948 when Leblond et al. used ^{32}P radiolabeling to observe DNA synthesis in the nuclei of cells within the isthmus region of gastric glands in mice (22). Continued work demonstrated pools of granule-free undifferentiated progenitor cells existing within the isthmus region that bidirectionally gave rise to differentiated cells at the surface or deep glandular regions (1, 23, 24).

Today, it is well described that the isthmus is home to the actively proliferating progenitor population within the adult corpus gland. However, a definitive specific molecular identity for the corpus isthmus stem cell remains elusive. The most widely used way to identify stem cell pools *in vivo* is through use of genetic mouse models to lineage trace progeny to observe clonal expansion from a specific labeled cell (25). This

analysis is commonly done using the Cre-Lox system driven by the promoter of a cell type-specific marker gene. A reporter gene, such as LacZ or fluorescent GFP, is inserted into the locus of a ubiquitously expressed gene (typically *Rosa26*) along with a transcriptional stop codon flanked by two loxP sites. As a result, Cre-recombinase activity within the candidate cell will excise the stop codon, leading to irreversible expression of the reporter. This genomic change will be carried through any subsequent progeny of the cell, thus specifically marking clonality and cell fate originating from the cell-of-origin.

In the corpus, one of the major confounding issues remains that a specific marker for isthmus progenitor cells has not been identified, which contrasts with stem cells in the intestine and antrum. In 2007, Barker et al. demonstrated that *Lgr5* labels intestinal stem cells which clonally expand to all differentiated cell types (21). This marker was also shown to mark stem cells in the antrum; however, *Lgr5* cells were surprisingly absent from the corpus epithelium (3). Additional intestinal stem cell markers such as *Olfm4* and *Axin2* have also fallen short in labeling corpus stem cells (18, 26).

Genetic Markers of Gastric Stem Cells

Overtime, numerous studies have identified cellular markers in mice that label lineage tracing stem/progenitor cells, although no consensus has been reached on identification of a marker. Thus far, *Sox2*, *Lrig1*, *Runx1*, *Bmi1*, *Stmn1*, and *Troy* have been demonstrated to label populations of cells with the capacity to clonally give rise to

all differentiated corpus cell types over time. However, in addition to labeling self-renewing progenitors, these drivers also mark differentiated cell types.

Sry-related high-mobility-box 2, or SOX2, is a transcription factor typically implicated in development and early cell fate determination of pluripotent embryonic stem cells (27). It is also considered critical for the development of anterior foregut endoderm, which eventually gives rise to the stomach (28). Arnold et al. demonstrated *Sox2* expression throughout the adult glandular stomach that labeled isolated isthmus and base cells of both the antrum and corpus epithelium (8). Lineage tracing studies from these cells demonstrate the generation of long-lasting clones encompassing full epithelial glands over time, thus marking them as stem cells. Importantly, *Sox2* expression is absent from the intestine, making the tamoxifen-responsive *Sox2-CreER^{T2}* driver a unique tool to study gastric epithelium while sparing the intestines from genetic manipulation.

Leucine-rich repeats and immunoglobulin-like domains protein 1 (LRIG1) was initially identified as a marker of intestinal stem cells using lineage tracing techniques (29). LRIG1 is a pan-ErbB negative regulator that functions as a tumor suppressor (30). Initial studies showed that *Lrig1*+ cells lineage traced as progenitors within the corpus and antrum, although the function of these gastric progenitor cells was not expanded upon (29). Eventually, Choi et al. confirmed the identity of *Lrig1*+ cells as progenitor cells within the corpus by demonstrating that *Lrig1*-YFP-marked cells induced by a *Lrig1-CreER^{T2};Rosa-LSL-YFP* transgenic mouse model gave rise to all gastric epithelial lineages (9).

Runx1, and its enhancer element eR1, was first discovered as a regulator of hematopoietic stem cells (31). Later, its expression was found in epithelial cells across a variety of other self-renewing tissue types, prompting its study within gastric tissue (11, 32). Matsuo et al. demonstrated that *Runx1+* cells were predominately located in the isthmus, as well as more sparsely in the base, and lineage-traced to all gastric lineages (33). Furthermore, single eR1^{high} cells generated organoids containing markers for the various differentiated gastric lineages. RUNX transcription factors may have a functional role as well within gastric stem cells as a R122C point mutation in RUNX3 leads to a precancerous phenotype including hyperplasia and lack of differentiation in isthmus progenitors in mice (34).

The polycomb group protein BMI1 has traditionally been used to label facultative stem cells in the intestine which activate to replace stem cells following injury (35). Recently, Yoshioka et al. observed that *Bmi1* also labels progenitor cells within both the gastric antrum and corpus (12). As has been observed with most of the other markers, *Bmi1*-expressing cells can also restore the epithelial following injury by high-dose tamoxifen, irradiation, or acetic acid.

The most recent progenitor cell marker to be identified is Stathmin1 (*Stmn1*). *Stmn1* was identified by Han et al. through bulk RNA-seq analysis of fluorescent-sorted proliferating cells to find candidate markers (10). Subsequent lineage tracing from *Stmn1-p2A-eGFP-IRES-CreERT2* mice demonstrated that *Stmn1+* cells can lineage trace throughout the surface-isthmus-neck compartment in the corpus. Unlike the other described markers, they show that *Stmn1* appears to specifically label isthmus progenitors without overlapping with the base chief cell compartment.

While lineage tracing studies can be used to study stem cells in animal models, identification of stem cell pools in humans is challenging. Single-cell RNA sequencing (scRNAseq) has emerged as a powerful tool to identify potential marker genes of progenitor populations within the human epithelium; however, follow-up confirmation of any expected markers would need to be conducted either *in vitro*, *ex vivo*, or within animals. A recent study by Busslinger et al. conducted scRNAseq on human and mouse gastric epithelium to identify expression patterns of specific cell types as well as differences in expression between the two species (14). Using the previously discussed bank of candidate marker genes, *STMN1* expression appears to label proliferating (MKI67+) human corpus isthmus progenitor cells most appropriately within their data set. The rest of the putative stem cell markers appear to label both progenitor and differentiated populations in humans and mice, although there is some cell-type specificity. *SOX2* localizes predominately to chief cells and zygomatic precursors, although it is expressed widespread throughout the gland. *LRIG1* on the other hand is most abundant within neck cells, especially in mice. *RUNX1* and *BMI1* are diffusely distributed amongst all cell types. The broad expression pattern of these various identified progenitor cell markers makes them poor markers for precisely following progenitor cell function within the gastric corpus. Therefore, there is a key need within the field for the development of novel, specific markers in both mice and humans to continue building on the current understanding of gastric corpus progenitor cell physiology.

The tissue necrosis factor (TNF) receptor superfamily member, TROY (encoded by *Tnfrsf19*), has also been demonstrated to label cell populations capable of driving

renewal within the corpus. *Troy* was initially identified to follow the expression pattern of *Lgr5*+ stem cells in intestinal crypts and *Troy*+ cells clonally expanded throughout the crypt-villus axis (36). In searching for new corpus stem cell markers, Stange et al. demonstrated that *Troy*+ at the gland base had reserve stem cell capacity and, over long periods of time (3 mo – 1.5+ yrs), can generate clones encompassing all lineages (37). However, rather than labeling isthmus progenitors, *Troy*-expression marked differentiated chief cells. They also demonstrated that *Troy*+ chief cells have the capacity to establish organoids in culture, a hallmark of stem cell function. Despite low rates of basal turnover, they did note increased tracing following injury, therefore labeling *Troy*+ cells as reserve stem cells akin to facultative stem cells of the intestine. Thus, while normal turnover is orchestrated by isthmus progenitors, differentiated cells types such as chief cells retain plasticity to act as a pool of reserve stem cells capable of dedifferentiating restoring glands following injury.

The Stem Cell Niche

Stem cells reside in a specialized microenvironment of signaling factors that support stem cell function known as the stem cell niche. Understanding the molecular underpinnings of stem cell maintenance and the niche will help elucidate the mechanisms underscoring epithelial cell homeostasis and identify potential drivers of tumorigenesis and disease. The glands and crypts of the gastrointestinal tract represent prototypical stem cell niches as their architecture enables distinct gradients of signals to be established along the mucosal axis (Figure 1.2) (38). This leads to a concentration of stem cell-supporting niche factors typically localized to the base, with pathways inducing

differentiation more concentrated towards the luminal surface. Several pathways have been identified to play key roles in maintaining gastric stem cell function, including Notch, bone morphogenetic protein (BMP), EGFR signaling, and, notably, Wnt (Figure 1.2).

The Wnt signaling pathway is considered a hallmark pathway governing stemness within the intestinal tract (39). However, its role is poorly understood within the gastric corpus, and has previously been assumed to be dispensable for normal homeostasis (40). More recent studies have demonstrated an important role for Wnt signaling in directing corpus cellular proliferation and differentiation in a unique manner from the rest of the distal columnar gastrointestinal epithelium. The primary goal of this thesis is to expand upon these recent findings and establish Wnt as a key pathway regulating corpus epithelial homeostasis in the human stomach. Before going into detail on Wnt, I will first discuss the other pathways that are important regulators of corpus stemness, function, and differentiation. Subsequently, the remainder of this thesis will be dedicated to an in-depth discussion on the mechanisms of Wnt signaling, the current understanding of Wnt-regulated gastric homeostasis, and its role in gastrointestinal disease.

Notch Signaling Regulation of Gastric Stem Cells

The Notch signaling pathway is a highly conserved cellular process that has been demonstrated to regulate proliferation and differentiation in many tissues, including the gastrointestinal tract (41). Briefly, Notch signaling occurs through juxtacrine signaling, with Notch ligands (Delta-like 1, 3, 4, and Jagged 1, 2) interacting

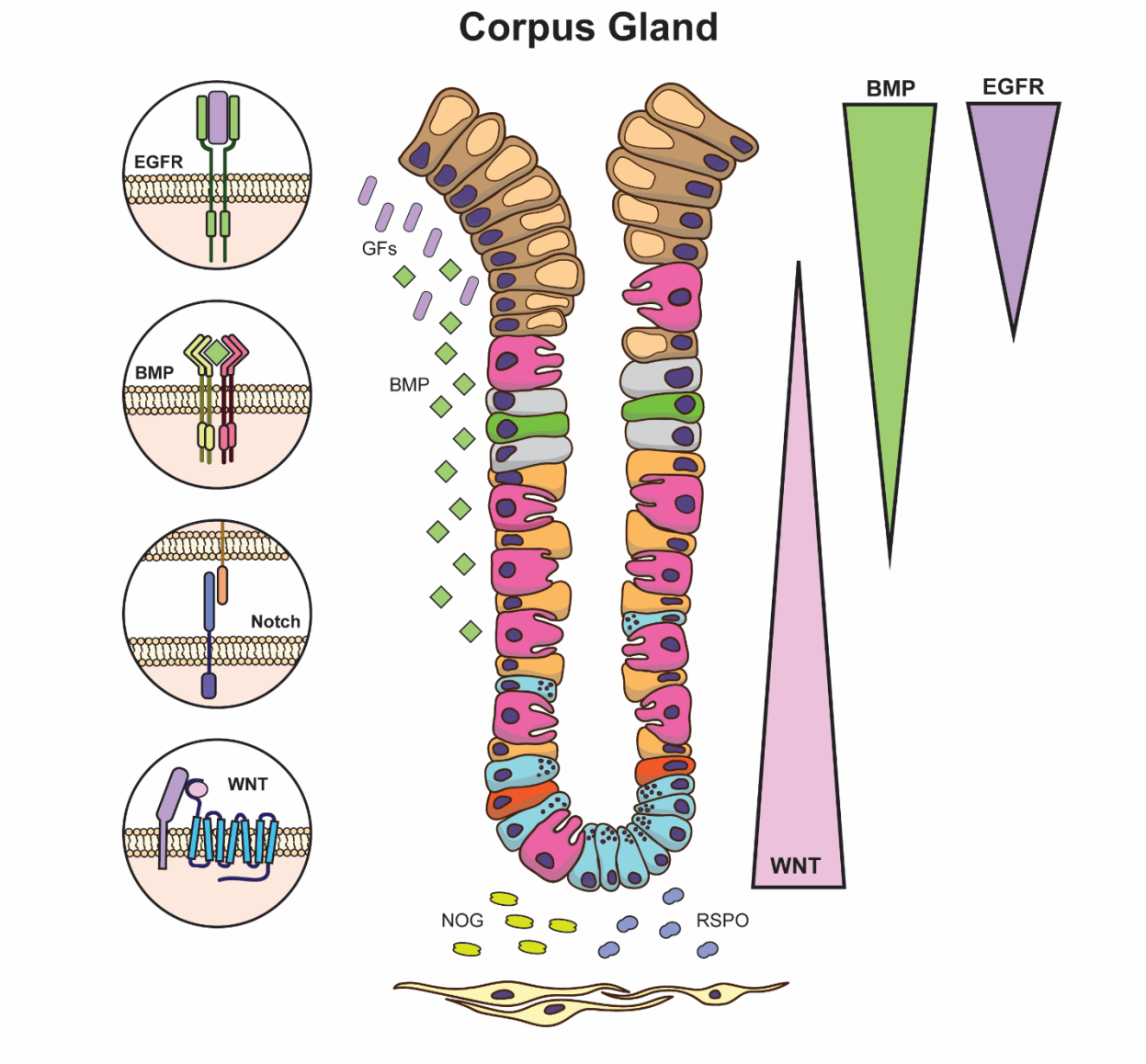

Figure 1.2: Pathways regulating gastric corpus stem cell function and differentiation.

Corpus gland homeostasis is regulated by paracrine, autocrine, and juxtacrine signaling pathways, including EGFR, BMP, Notch, and Wnt. Defined signaling gradients pattern epithelial glands to compartmentalize signaling and define the active stem cell niche. A Wnt signaling gradient is constructed through secretion of RSPO ligands (primarily RSPO3) by sub-epithelial stromal cells at the gland base, leading to high Wnt tone at the base and low Wnt tone at the surface. An inverse gradient of BMP signaling is established by expression of BMP2 and BMP4 within epithelial and stromal cells, respectively, as well as secretion of BMP inhibitors NOG and GREM1 by stromal cells at the gland base. EGFR signaling is also predominately localized towards the lumen as activation leads to surface cell development, although ligands for EGFR can be found throughout the gland. Notch ligands have been localized in mice to cells of the isthmus, indicating a role for Notch within the stem cell niche to regulate proliferation.

with Notch receptors (Notch1-4) on adjacent cells (42). This stimulates receptor cleavage and internalization of the Notch receptor intracellular domain (NICD) within receptor-expressing cells and subsequent activation of target genes. Notch target gene *Olfm4* is a specific marker for active stem cells in the intestinal tract where Notch signaling has been demonstrated to play an integral role in modulating proliferation and differentiation (26, 43). While *Olfm4*+ cells are not present in the gastric epithelium, Notch has still been demonstrated to be a key regulator of proliferation in both the antrum and corpus (44-46). Demitrack et al. demonstrated in adult mice that expression of NOTCH1 and NOTCH2, the dominant Notch receptors in the corpus, colocalized with EdU+ proliferating cells within the corpus isthmus, suggesting that progenitors are Notch-signaling cells (45). Inhibition of NOTCH1 and NOTCH2 resulted in reduced proliferation *in vivo* using mouse genetic and pharmacologic models, and *in vitro* using corpus-derived organoids from both mouse and human (45). On the contrary, activation of Notch through NICD overexpression led to hyperplasia and expansion of the undifferentiated progenitor zone. Thus, Notch signaling plays a key role in regulating gastric stem cell function through juxtacrine signaling and helps define the actively proliferating compartment of the stem cell niche.

BMP Signaling Regulation of Gastric Stem Cells

The BMP signaling pathway involves secretion of BMP ligands, which are members of the transforming growth factor beta superfamily, into the surrounding microenvironment and is considered to have anti-proliferative, pro-differentiation effects in the gastrointestinal tract (47-50). Initially it was proposed through studies of intestinal

stem cells in mice that BMP signaling suppressed stem cell identity through direct suppression of Wnt/β-catenin signaling, and additional studies suggest crosstalk between the BMP and Wnt pathway throughout the gastrointestinal tract (51, 52). More recently, BMP signaling has been demonstrated to restrict function of intestinal stem cells in a Wnt-independent manner with no impact upon expression of Wnt target genes or β-catenin nuclear localization (53). However, the authors noted that Smad proteins, the primary targets of BMP signaling, can bind to the promoter region of *Lgr5* and therefore they cannot exclude the possibility that BMP signaling can indirectly downregulate Wnt signaling through this mechanism.

BMP ligands are expressed by both stromal and epithelial cells throughout the gastric gland, with in situ hybridization localizing expression predominantly within the surface and isthmus regions (52, 54, 55). Over 20 BMPs have been identified, however the most prominent BMPs within the gastrointestinal tract are BMP4 (expressed by stromal cells), BMP2 (expressed by surface cells), and BMP7 (52, 55-58). BMP signaling is further structured by the expression of BMP antagonists, including NOG and GREM1, which primarily localize to stromal cells at the base of glands and contribute to the stem cell niche by inhibiting BMP signaling within stem cells (56, 59). Interestingly, NOG is expressed in the human stomach but is absent from gastric tissue in mice (52, 55). The localization of these ligands thus defines the stem cell niche by creating high BMP signaling within the surface and isthmus regions, associated with cellular differentiation, and low BMP signaling at the gland base to support stem/progenitor cell function.

BMP signaling has been demonstrated in mice to regulate proliferation within the stomach. Kapalcznska et al. recently demonstrated that loss of BMP receptor 1α (*Bmpr1a*) in *Axin2*+ antral stem cells using a transgenic mouse model led to hyperproliferation within glands (55). In the corpus, Shinohara et al. demonstrated that inducing *Nog* expression in parietal cells of transgenic mice to suppress BMP led to corpus hyperplasia and an induction of metaplastic cells that co-expressed markers of mucous neck and chief cells (60). Interestingly, two independent studies have also demonstrated that BMP regulates gastric epithelial homeostasis through a stromal axis. Transgenic mouse models constitutively deleting *Bmpr1a* in mesenchymal cells led to corpus hyperplasia, the formation of spontaneous polyps, and the emergence of metaplastic lineages (61, 62). Thus, active BMP signaling is necessary within both epithelial and stromal compartments to pattern zones of epithelial cell proliferation within the corpus.

1.3 Gastric Epithelial Cell Differentiation during Homeostasis and Injury

Outside of the stem cell niche, progenitor cells are rapidly exposed to various signaling factors that direct and influence cellular identity towards a differentiated state. The earliest studies observing cellular differentiation within the gastric corpus identified a bimodal axis of differentiation projecting outward from undifferentiated isthmus progenitor cells (1). This proliferative zone within the corpus exists closer to the lumen than in glands or crypts of the distal gastrointestinal tract thus leading to an expanded deep glandular region and a shorter surface zone exposed to the luminal interior. As a

result of this patterning, there is asymmetry in cellular turnover between the two compartments. Corpus surface cells turnover every few days, while parietal cell and chief cell lifespan is several months (7, 63).

Surface Cell Differentiation

Due to their rapid turnover, surface cells are the dominant cell fate resulting from isthmus progenitors. An analysis of proliferating isthmus cells in the murine gastric corpus identified 76% of those cells as MUC5AC-positive, confirming that cell renewal during homeostasis is heavily skewed towards a surface cell lineage (33). The expression of transcription factor *Foxq1* within progenitor cells has been implicated to drive differentiation of MUC5AC-positive surface cells (64). Numerous pathways have been implicated in directing surface cell differentiation within the stomach, and dysregulation of these pathways can lead to disease such as atrophic gastritis and cancer.

In the antrum, inhibition of Notch signaling through gamma secretase inhibitor dibenzazepine (DBZ) or αN1+αN2 inhibitory antibody treatment leads to a significant increase in surface cell differentiation (44, 46). However, in the corpus similar treatments resulted in no observed significant difference in surface cell differentiation (45). Of importance, these experiments may have been limited by the short duration of inhibition. Thus, while Notch signaling does play a key role in regulating the rate of proliferation within the isthmus progenitor zone, it remains unclear whether Notch plays a role in surface cell differentiation as well.

Numerous studies have demonstrated that the predominant pathway which regulates surface cell differentiation is likely EGF/EGFR signaling. EGFR is a receptor tyrosine kinase involved in the signal transduction of numerous pathways which play key roles in growth and cell function such as RAS-RAF-MEK-ERK, PI3K-AKT-mTOR, and JAK-STAT signaling (65). Aside from epidermal growth factor (EGF), EGFR signaling can be induced through binding with various other growth factors such as transforming growth factor alpha (TGFα), amphiregulin (AR), and epiregulin (EPR), among others (66). Within the human stomach, EGF ligands have been localized predominately to cells at the luminal surface; however, expression does also appear to be present within cells at the gland base as well (52).

Activation of EGFR and its downstream pathways has been demonstrated to be a dominant force in directing surface cell differentiation. Studies using transgenic *MT-TGFA* mice to overexpress TGFα within the gastric epithelium showed altered differentiation towards predominately surface mucous cells within the corpus (67). This aligns with findings of Ménétrier's disease, which is caused by pathologic overexpression of TGFα leading to overactivation of EGFR signaling (68). These patients exhibit significant surface cell hyperplasia, glandular atrophy, and overproduction of mucus (68). Treatment with EGFR inhibitors has been demonstrated to reduce surface cell hyperplasia and re-establish lost populations of parietal and chief cells within the corpus (69-71).

The observations that increased EGFR signaling directs preferential surface cell differentiation have also been confirmed through mechanistic studies. *In* vivo, Choi et al. demonstrated using transgenic mice that activation of KRAS, which is downstream of

EGFR, in *Lrig1*+ progenitor cells (*Lrig1CreER*^{T2}*;Kras*^{G12D}) leads to hyperplastic glands with an expanded surface cell compartment (72). *In vitro* studies of human gastric corpus cells have further demonstrated the essential role of EGFR signaling in directing surface cell differentiation. Using two-dimensional monolayers termed mucosoids, Wölffling et al. recently demonstrated that either withdrawal of EGF from culture media or treatment with MEK inhibitor PD0325901 prevented surface cell differentiation (52). While they demonstrated that activation of BMP signaling through withdrawal of NOG also led to surface cell differentiation, loss of EGFR signaling superseded this, thus demonstrating EGFR activation as a necessary signal directing surface cell differentiation.

The authors also note a role for EGF/EGFR in underscoring atrophic gastritis, a chronic precancerous inflammatory condition induced by *H pylori* infection. Glands in patients with atrophic gastritis have markedly reduced chief and parietal cells but maintain a large surface cell compartment, therefore suggesting altered differentiation. They observed remarkable EGF overexpression within these glands, which aligns with other reports of EGFR ligand overexpression in atrophic gastritis and cancer (52, 73). *H pylori* has also been demonstrated to activate EGFR signaling within gastric epithelial cells, which may stimulate a wound healing response (74-76). EGFR activation further plays a critical role in gastric ulcer healing which requires mucus and bicarbonate produced by surface cells to protect ulcers from the acidic luminal environment (66). Thus, in numerous different disease contexts EGFR signaling underscores preferential differentiation towards surface cells and appears to be essential for surface cell development.

Suppression of Wnt signaling has also been implicated in directing surface cell differentiation from an undifferentiated progenitor. These studies will be discussed at length in a dedicated section later within this chapter and are further expanded upon by my studies discussed in Chapter 2.

Parietal Cell Differentiation

The aforementioned mucosoid study by Wölffling et al. also demonstrated that BMP signaling directs parietal cell differentiation (52). They observed that BMP signaling, activated through the withholding of the inhibitor Noggin or supplementation of BMP4 in media, led to the development of parietal cells in the absence of EGF signaling. This finding is remarkable as parietal cells are typically missing from normal organoid cultures, although standard culture conditions require both the presence of EGF and inhibition of BMP to drive organoid formation and growth (77). Two independent studies that co-cultured mesenchymal cells with organoids formed either from adult tissue or from pluripotent stem cells (PSCs) were able to demonstrate improved parietal cell differentiation and function, potentially further implicating stromal factors in driving their fate (78, 79). Whether BMP was a key stromal factor remains to be determined. Early *in vitro* studies using isolated canine parietal cells also demonstrated that BMP4 promoted maintenance of a differentiated parietal cell phenotype (80).

BMP signaling has also been implicated *in vivo* in driving parietal cell differentiation from isthmus progenitors. Studies by Takabayashi and Shinohara et al. used a H^+/K^+-ATPase subunit beta promotor to drive expression of Noggin in parietal

cells of transgenic mice to inhibit BMP signaling (56, 60). These studies observed that inhibition of BMP signaling throughout the gland axis suppressed parietal cell differentiation and led to parietal cell atrophy throughout the corpus. Interestingly, infection with *H pylori* has recently been demonstrated to disrupt BMP signaling in the gastric antrum through manipulation of IFN-γ, although a connection to *H pylori*-induced oxyntic atrophy in the corpus has not been established (55). Therefore, numerous studies have demonstrated that activation of BMP signaling is necessary to direct parietal cell fate determination within isthmus progenitor cells.

Neck Cell Differentiation

Little is known about the regulation of neck cell differentiation aside from the fact that they originate from isthmus progenitors. Speer et al. demonstrated that while Fgf10 is dispensable for normal gastric proliferation, overexpression of this ligand led to an expansion of mucous neck cells in favor of other deep glandular lineages (81). While typically this phenotype is seen as a hallmark of a metaplastic injury response, they did not observe evidence of metaplasia, thus indicating altered differentiation originating from an isthmus progenitor.

A few studies have also demonstrated that BMP signaling may suppress neck cell differentiation in favor of a parietal cell fate. Maloum et al. demonstrated that deletion of *Bmpr1a* in the foregut endoderm using a *Foxa3Cre* mouse model led to an adult phenotype with increased mucous neck cells and decreased surface and parietal cells (54). In the study by Shinohara et al. that used a transgenic mouse model to drive Noggin expression in parietal cells, they noted a significant expansion of neck cells (60).

Furthermore, MUC6+ cells are maintained in culture using traditional media inhibiting BMP signaling, however differentiation to surface or parietal cells can be induced through activating the BMP pathway (52). Thus, low levels of BMP signaling likely influence neck cell fate determination within isthmus progenitors.

Chief Cell Differentiation

It has long been believed that chief cells arise over time from lineage committed neck cells arising themselves from undifferentiated isthmus progenitors (Figure 1.3) (63, 82, 83). This therefore connects cells at the base of glands to cellular renewal occurring within the isthmus region of the corpus epithelium. Initial studies have pinned transcription factor MIST1 as the key factor regulating epithelial transition from a neck to a chief cell (84). However, two recent studies have injected controversy into this assumption by suggesting that chief cells at the base of corpus glands self-renew with minimal input from renewal occurring within the isthmus region (Figure 1.3). Using a *Rosa26-LSL-Confetti* reporter and a ubiquitously expressed *CreER*^{T2} allele, Han et al. demonstrated that overtime (up to 1.5 years) clonal expansion within glands either arose rapidly from the isthmus or more slowly from the base (10). Interestingly, there was minimal intermixing between clonal expansions from these two regions, therefore defining the surface-isthmus-neck and base regions as two distinct self-renewing compartments during homeostasis. This was expanded upon by a later study by Burclaff et al, who used continuous BrdU labeling to follow the dynamics of chief and neck cell differentiation during homeostasis and injury (85). They demonstrated that there was not the expected association of BrdU incorporation in neck and chief cells that would label

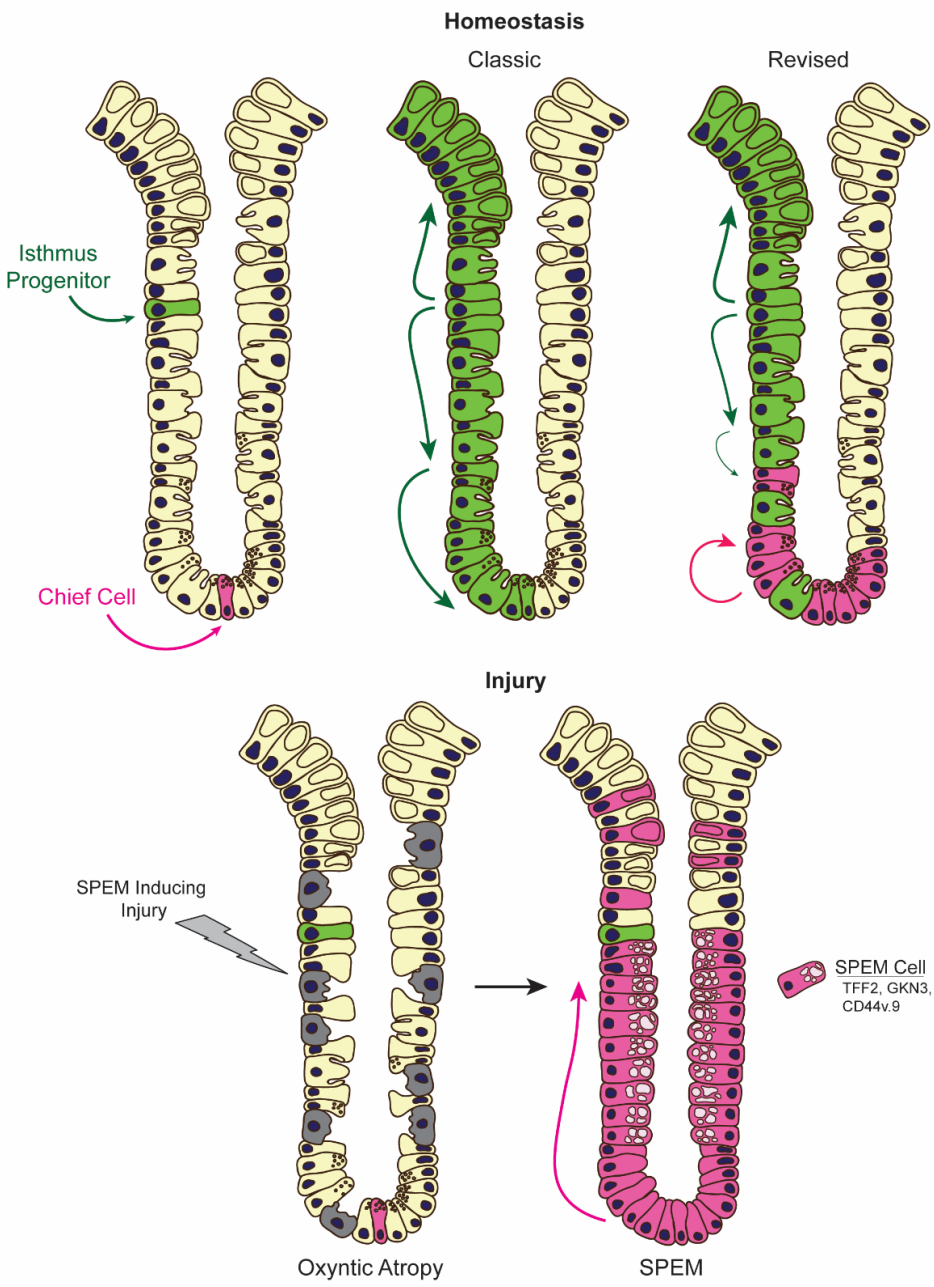

Figure 1.3: Epithelial renewal during homeostasis and injury

Isthmus progenitor cells give rise to differentiated cells bidirectionally during homeostasis. The classic model of glandular renewal proposes that isthmus progenitors give rise to all cell types, including neck cells that further differentiate to chief cells as they transition to the gland base. Recent studies however have suggested that the chief cell compartment is predominately self-maintained through low levels of chief cell turnover with only minor input by neck cells. Injury to the gland which induces SPEM, such as *H pylori* infection, high dose tamoxifen, or protonophore treatment, leads to oxyntic atrophy. Chief cells then transdifferentiate to a proliferative metaplastic SPEM cell expressing features of antral mucous cells (*TFF2*, *GKN3*) to repair the epithelium.

neck cells as zymogenic precursors, and therefore concluded that chief cell maintenance must be a consequence of low levels of turnover at the base independent from the isthmus. Although this paradigm of chief cell self-renewal remains controversial, it represents a significant shift in the understanding of gastric corpus physiology and may tie into the reported reserve stem cell function exhibited by chief cells.

The pathways regulating chief cell differentiation and maintenance remain unclear. Recent studies have shown that Wnt signaling may play a prominent role in defining the chief cell base, however it is poorly understood how this relates to their differentiation. These studies will be discussed further within the dedicated section on Wnt signaling later in within this chapter, and later expanded upon by my studies discussed in Chapter 2.

Role of Chief Cells in the Injury Response

While chief cells undergo low levels of turnover during homeostasis, a consensus has been reached in the field that chief cells possess facultative progenitor cell potential that can be activated in response to glandular injury (Figure 1.3). The most prominent form of injury response in the corpus is known as spasmolytic polypeptide-expressing metaplasia, or SPEM. SPEM is defined by a rapid induction of metaplastic antral-like cells resembling deep mucous cells expressing TFF2, with chronic SPEM proposed to act as a precursor to gastric dysplasia and eventually cancer (86). SPEM was first identified in mice infected with *H felis*, and then subsequently associated with equivalent human infection by *H pylori* (87). Since then, numerous models of injury have been

demonstrated to induce SPEM in mice such as treatment with high-dose tamoxifen, protonophore DMP-777, and structurally related protonophore L-635, with the common pathogenic hallmark of these treatments being oxyntic (parietal cell) atrophy (88-90).

Despite the well described emergence of SPEM, it long remained unclear which cells were responsible for giving rise to this metaplastic lineage. In 2010, Nam et al. demonstrated for the first-time using lineage mapping from a *Mist1Cre*$^{ER/+}$ mouse model that SPEM arises predominately from transdifferentiation of chief cells (88). Since then, many studies have come to the same conclusion that mature chief cells are the primary cell of origin for this metaplasia and further demonstrated that remodeled chief cells can function as regenerative cells to give rise to cells of all lineages to repair glandular injury (85, 91-95). Thus, chief cells are thought to be facultative stem cells within the corpus epithelium despite their highly differentiated and quiescent state. Stange et al. demonstrated that *Troy*+ chief cells share many markers with stem cells of the antrum and intestine and could on rare occasions be observed to clonally expand throughout the entire gland under homeostasis (37). They also demonstrated that FACS-isolated *Troy-GFP*+ cells could establish organoids *in vitro*, which is typically a hallmark of progenitor cell function.

The factors that regulate chief cell quiescence during homeostasis and progenitor function after tissue injury remain unclear. Notably, the columnar epithelium of the more distal regions of the gastrointestinal tract (antrum, intestine, colon) has a distinct cellular structure with proliferating stem/progenitor cells at the glands/crypt base. Therefore, the localization of differentiated, quiescence cells residing at the base of the corpus represents an anomaly in cellular identity. A recent mouse study by Lee et al.

identified the G1-S cell cycle regulator p57(Kip2) (CDKN1C) as a key protein involved in retaining chief cell quiescence during homeostasis (96). They demonstrated in mouse models that p57 expression was localized to chief cells during homeostasis but lost upon metaplastic transformation to SPEM. Overexpression of p57 using a stomach specific *Anxa10-CreER^{T2};R26loxpTA-p57$^{k/k}$* transgenic mouse model prevented chief cell activation in response to injury, therefore pinning it as a key regulator of chief cell quiescence. Single-cell studies of the human gastric epithelium have also localized *CDKN1C* predominately to chief cells, and its expression is negatively correlated with gastric cancer prognosis (14, 97). Interestingly, p57 also appears to be a regulator of cellular quiescence in other tissue systems, namely within hematopoietic stem cells (98-100). Therefore, chief cell quiescence may be maintained within the pro-proliferative environment at the base of glands through a unique mechanism of cell cycle regulation which preserves progenitor potential in case of injury.

1.4 Gastric Organoids

Most mechanistic studies within the gastrointestinal tract have focused predominately on mouse genetic models; however, these lack the same translatable impact of directly studying human tissue. Over the past decade, organoids have emerged as an *in vitro* model to directly study organized human gastric tissue. The high rate of cellular turnover and general plasticity of the gastrointestinal tract enable establishment of organoids from either pluripotent stem cells or adult tissues. Organoids are three-dimensional cysts of cells that self-organize into a monolayer and

polarize to develop a defined, apical lumen when grown in an extracellular matrix such as Matrigel (Figure 1.4). To grow, epithelial organoids require niche signaling factors typically supplied by the surrounding stroma to be included within growth media. Once established, organoids can grow almost indefinitely with regular media renewal and subculture.

A seminal study by Sato et al. described for the first time the establishment of organoids from adult mouse tissue by demonstrating that single *Lgr5*+ intestinal stem cells can form long lived “mini gut” cultures *in vitro* (101). This was later translated into the antrum, where Barker et al. demonstrated that *Lgr5*+ antral stem cells could likewise establish long-lived antral organoid cultures (3). In developing optimal conditions for organoid establishment and growth, they determined that Wnt regulated cellular differentiation, showing that an absence of Wnt leads to surface cell differentiation. However, the development of corpus organoids from these mice was hampered by the absence of *Lgr5*+ corpus cells observed within these initial mouse studies. Later, Stange et al. demonstrated that isolated *Troy*+ chief cells could establish long-lived corpus organoids in culture (37). Since, continued study has enabled establishment of long-lived cultures of corpus organoids from adult tissue for targeted *in vitro* analysis.

Development of Human Gastric Organoids

Organoids derived from human biopsies can be used to study epithelial cell growth, proliferation, differentiation, and stem cell function following targeted pathway manipulation. The use of adult human tissue-derived organoids provides translatable results and actionable insights into how these pathways regulate epithelial homeostasis

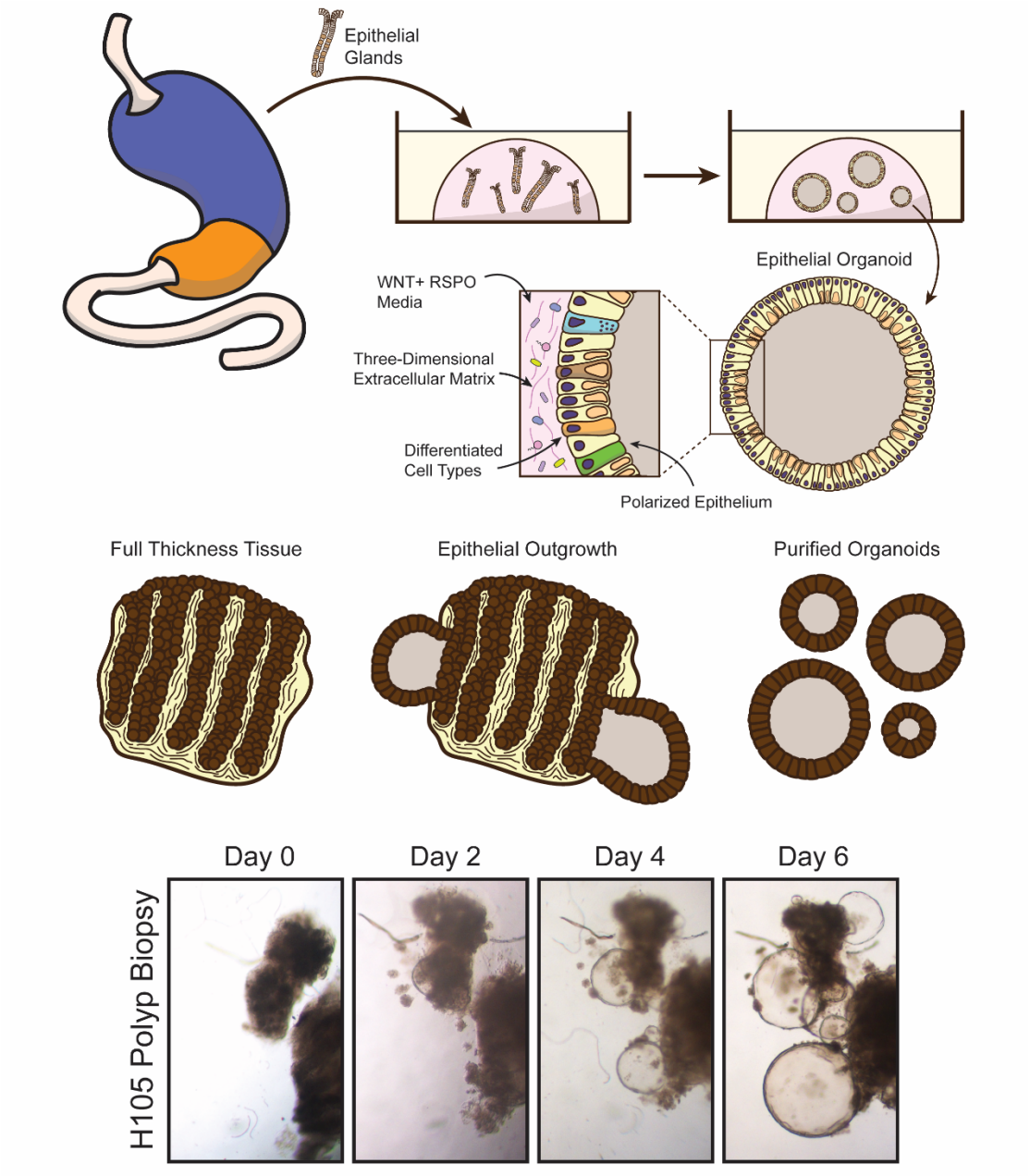

Figure 1.4: Gastric organoids

Gastric organoid establishment involves dissociation and purification of epithelial glands from tissue samples. Glands are suspended within a three-dimensional extracellular matrix, such as Matrigel, for culture. Over time epithelial growth transforms into spheroids of polarized cells known as organoids. Organoids require media rich in pro-proliferative, anti-differentiation factors such as WNT, RSPO, and NOG (WRN) for long-term maintenance. Differentiated surface, neck, and chief cells have been identified in culture, but not parietal cells. As an alternative approach to establishment, minced full thickness tissue can be embedded within Matrigel. Epithelial outgrowth rapidly occurs within culture, but not from stromal cells. Serial passages select for epithelial cells, thus resulting in pure cultures of epithelial organoids.

in the human stomach. However, while organoid models are currently the gold standard for human gastrointestinal work, they are still relatively new, and lack hierarchical structure that would enable studying cellular compartmentalization in response to signaling microenvironments. My studies have helped to define the cellular consequences of Wnt signaling on human gastric organoid growth, proliferation, and differentiation.

The original development of human gastric organoids focused on generating gastric tissue from pluripotent stem cells (PSCs). McCracken et al. first reported the de novo generation of gastric organoids *in vitro* from PSCs; however, these tissue structures were predominately antral-like (102). Continued work by the same group eventually established a protocol for the development of corpus-specific human organoids from PSCs (103). They determined that additional exposure to FGF10 and stimulation of Wnt signaling using CHIR99021 guided development towards a corpus fate rather than an antral fate. Interestingly, the addition of BMP4 and the MEK inhibitor PD0325901 for 48 hours induced parietal cell differentiation *in vitro* within their system, which aligns with more recent studies that have further explored the mechanisms underpinning parietal cell differentiation (52).

Continued advances in human gastric organoids have enabled establishment directly from patient tissue. These patient-derived organoids can then be used in the context of personalized medicine to screen drugs and devise targeted therapies for specific disease states, or to study fundamental mechanisms of proliferation and differentiation. Applications of human organoids include studying factors involved during

normal homeostasis, in the context of infection (such as *H pylori*), and in modeling diseases including with the use of CRISPR (104-106).

Bartfeld et al. demonstrated that corpus organoids could be derived from isolated glands of primary human tissue samples and defined media components necessary to support long-term growth (77). Ultimately, they determined that WNT, RSPO, NOG, and EGF were essential factors in the establishment and maintenance of human corpus organoids. Removal of any of these factors rapidly led to deterioration of the cultures. Interestingly, they also noted that TGFβ inhibitors were required for human corpus organoid establishment, but dispensable for human antral organoids. Gastrin and FGF10 also increased organoid lifespan within culture, but to a lesser extent than the previously mentioned factors.

Human epithelial organoids can also be grown from full-thickness tissue rather than from isolated glands or stem cells to speed up growth and ease the technical burden of tissue processing. Tsai et al. demonstrated this technique from both gastric and colonic tissue, and further showed that full thickness tissue can be frozen using conventional LN_2 cryopreservation techniques for later organoid retrieval with minimal impact upon cellular identity (107). Subsequent passaging enables the removal of stroma to eventually obtain purified epithelial cultures (Figure 1.4).

Novel Culture Models

As the use of organoids in studying human gastric physiology continues to grow, novel techniques are being developed to more accurately recapitulate the *in vivo* physiological environment. While *in vitro* epithelial organoids are typically suspended in

a homogenous medium of pro-proliferative factors, the *in vivo* mucosa exists within a complex environment of signaling gradients and contributions from non-epithelial niche cells to direct function. Mouse studies have demonstrated the potentially unappreciated importance of stromal cell contribution by describing parietal cell emergence with the inclusion of mesenchymal cells in organoid cultures (78, 79). Bioengineered systems which can recreate the *in vivo* mucosal architecture of glands could therefore unlock a new wave of insights into human physiology.

One such example of this has been developed specifically for the colonic epithelium. Hinman et al. demonstrated that scaffolds resembling the crypt architecture can be seeded with single colonic stem cells, expanded, and then polarized with exposure to signaling gradients to develop distinct compartmentalization of cellular subtypes (108). While this research has predominantly been focused on intestinal tissue, the same principles could be transferred to the gastric epithelium to create *ex vivo* patient-derived glands for study of human gastric homeostasis and diseases such as metaplasia.

Polarized monolayers of epithelium have also emerged as an important approach to study human gastric physiology. While traditional two-dimensional monolayers lack organization, Boccellato et al. demonstrated that subjecting antral epithelial monolayers to a transient air-liquid interface, as would be observed within the gastric lumen, resulted in the establishment of polarized mucous-secreting cells, which they termed mucosoid (109). More recently, the same group demonstrated that similar mucosoids could be developed using human corpus tissue where it proved to be a powerful tool to identify factors regulating corpus differentiation (52).

Overall, the emergence of organoids has opened a new door into the study of human gastric physiology. Advancements in organoid technology, through the use of new scaffolds, mixed cultures, bioengineered extracellular matrices, and novel techniques, could better our understanding of stem cell physiology, homeostasis, and the manifestation of disease to help drive the next generation of therapeutic interventions.

1.5 The Wnt Signaling Pathway

Thus far, I have discussed the current understanding of the gastric corpus epithelium, the tools used to study cellular physiology, and the various pathways shown to regulate epithelial homeostasis that are independent of Wnt signaling. The rest of the work presented within this thesis will focus on describing the important functions for Wnt within the corpus, with a goal to elucidate the complex mechanisms of this signaling pathway in regulating corpus homeostasis and disease.

The Wnt signaling pathway is a highly conserved signaling pathway that regulates cellular identity, proliferation, and stemness in various tissue types. In the gastrointestinal tract, Wnt signaling has emerged as an essential component of the stem cell niche. From the earliest studies, loss of Wnt was shown to disrupt stem cell function, while hyperactivation of the pathway rapidly leads to tumorigenesis. However, while Wnt has clear and profound effects upon the intestine and antrum, the role of Wnt signaling within the gastric corpus is poorly understood.

Overview of Wnt Signaling

Wnt signaling was initially discovered from studies in *Drosophila* and murine breast cancer. Baker first identified the gene *wingless* as a regulator of segment polarity in *Drosophila* and demonstrated its requirement for the generation of adult wings (110). The gene was subsequently determined to be a homolog of the murine mammary oncogene int-1, which led to the naming of Wnt when a similar homolog was found in humans (111).

The Wnt signaling pathway (Figure 1.5) is regulated by secreted ligands (WNT proteins) which signal to receptor-expressing cells to elicit an autocrine or paracrine response. In humans, there are 19 different WNT ligands, with specific ligands of interest in the gastrointestinal tract being WNT2B, WNT3A, and WNT5A (112). Secretion of ligands from cells requires a specialized lipid modification within the Golgi known as palmitoylation (112). Modification and secretion of WNT ligands is regulated by the proteins porcupine (PORCN) and wntless (WLS), making them popular targets for genetic or pharmacologic manipulation in Wnt inhibition studies (113-115).

Secreted WNT ligands then bind to a Wnt receptor complex composed of Frizzled (FZD), a seven-transmembrane receptor protein, and lipoprotein receptor-related proteins 5 and 6 (LRP5/6) (116, 117). Wnt signaling activates a canonical or non-canonical response, with many WNT ligands having functional roles in both pathways. The non-canonical Wnt pathway can influence functions such as cell polarity or calcium signaling (117). The canonical pathway, also known as Wnt/β-catenin signaling, is responsible for inducing stemness, proliferation, and identity within various

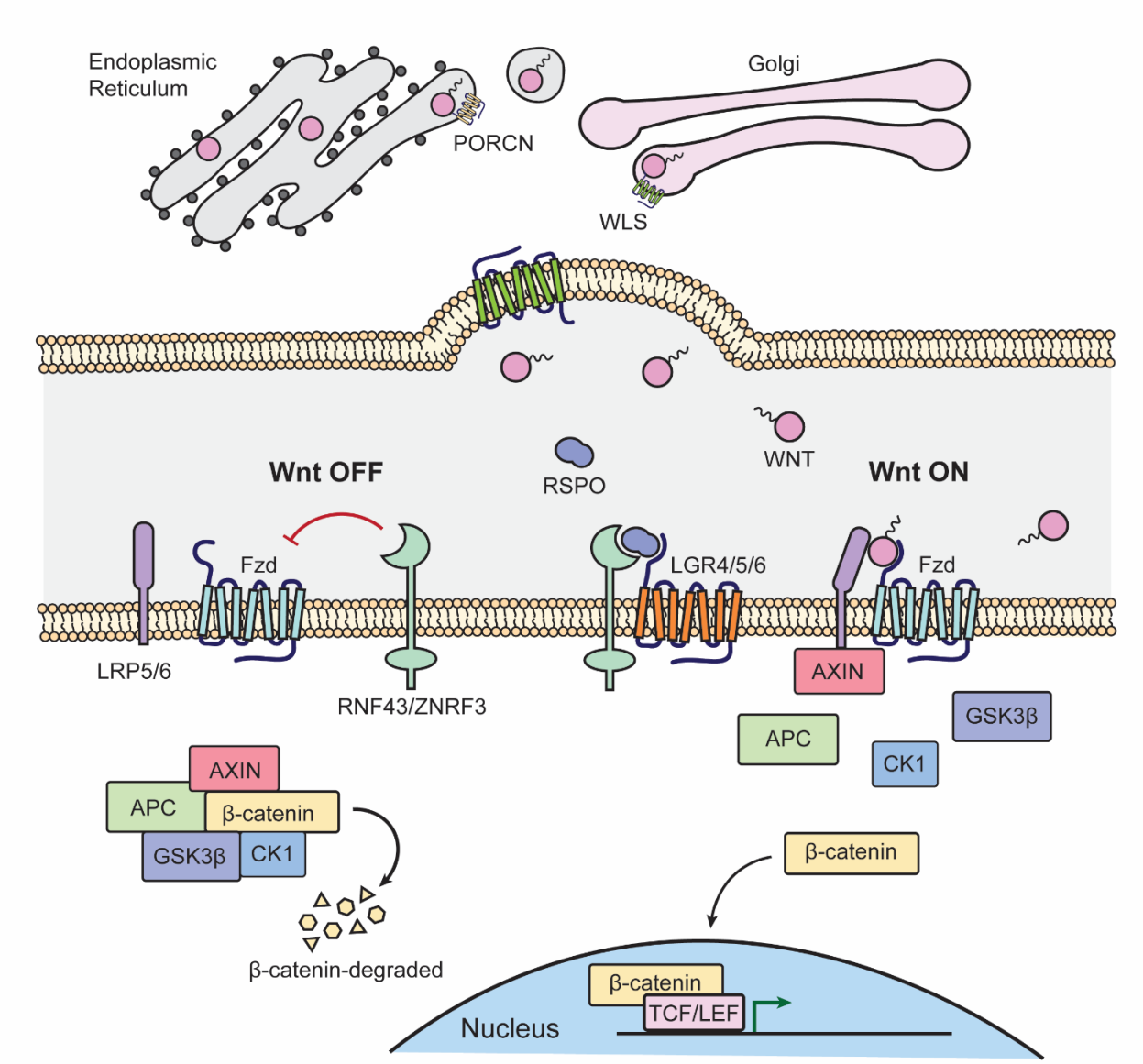

Figure 1.5: The canonical Wnt signaling pathway

The canonical Wnt signaling pathway is activated through autocrine or paracrine secretion of WNT ligands. Secretion of WNT ligands requires palmitoylation by PORCN in the endoplasmic reticulum and transport by WLS from the Golgi. In the absence of WNT ligands, the transmembrane E3 ubiquitin ligases ring finger 43 (RNF43) and zinc and ring finger 3 (ZNRF3) ubiquitinate the frizzled (FZD) and lipoprotein receptor related protein (LRP) receptor complex. A β-catenin destruction complex composed of axis inhibition protein (AXIN), adenomatous polyposis coli (APC), glycogen synthase kinase 3 (GSK3), and casein kinase 1 (CK1) cytosolically degrades β-catenin through GSK3-mediated phosphorylation. Binding of secreted WNT to the FZD/LRP complex recruits AXIN to the membrane and leads to dissociation of the β-catenin destruction complex. Simultaneous binding of RSPO ligands to leucine-rich G-protein coupled receptors (LGR4/5/6) potentiates WNT signaling by preventing RNF43/ZNRF3 mediated destruction of FZD/LRP. Destruction complex dissociation enables translocation of β-catenin to the nucleus where it interacts with TCF/LEF to drive transcription of Wnt target genes.

tissue systems, including the gastrointestinal tract, and is therefore the focus for studying the role of Wnt in homeostasis and disease (118).

The goal of canonical Wnt signaling is to induce β-catenin translocation to the nucleus where it can act as a transcription factor to upregulate genes involved in proliferation and stemness. In the absence of Wnt, a β-catenin destruction complex comprising of axis inhibition protein (AXIN), adenomatous polyposis coli (APC), glycogen synthase kinase 3 (GSK3), and casein kinase 1 (CK1) phosphorylates cytosolic β-catenin, therefore leading to its degradation and preventing its nuclear activity (117, 119). Upon activation of FZD and LRP5/6 receptors by WNT ligands, the destruction complex is recruited to the cell membrane where AXIN binds to LRP and the destruction complex dissociates. This frees β-catenin to actively shuttle to the nucleus where it interacts with TCF/LEF to drive transcription of target genes (120, 121). These target genes are involved in pathways regulating self-renewal, metabolism, survival, and proliferation, hence the pathway's function in regulating the stem cell niche (122, 123).

R-spondin and additional regulators of Wnt signaling

R-spondins (RSPOs) are another group of ligands that play an essential role in the Wnt/β-catenin signaling pathway. Signaling by RSPO through its receptors, leucine-rich repeat-containing G-protein coupled receptor 4, 5, or 6 (LGR4-6), acts as a potent activator of Wnt signaling and plays a key role in defining the Wnt signaling niche within the gastrointestinal tract, including the stomach (18, 124, 125). There are four different R-spondins (RSPO1-4) which can all bind each of the three LGRs; however RSPO3,

and to a lesser extent RSPO1, appear to be the dominant R-spondins within the gastrointestinal tract (124). In the absence of R-spondin signaling, the transmembrane E3 ubiquitin ligase proteins ring finger 43 (RNF43) and zinc and ring finger 3 (ZNRF3) ubiquitinate the FZD/LRP receptor complex to negatively regulate Wnt signaling (124, 126, 127). Both *RNF43* and *ZNRF3* are Wnt/β-catenin target genes, therefore constructing a negative feedback loop to regulate signaling. R-spondins bind to RNF43 and ZNRF3 in addition to LGRs to inhibit ubiquitinase activity, therefore stabilizing the Wnt receptor complex and potentiating Wnt signaling. Studies of *Rnf43* and *Znf3* knockout mice have demonstrated potentiation of Wnt signaling in their absence, however WNT ligand itself is still necessary for activating the pathway (126, 127). The critical role of R-spondins in activating Wnt/β-catenin signaling within gastrointestinal stem cells is demonstrated by the expression of *LGR5*, also a Wnt target gene, to faithfully label active stem cells in the antrum, small intestine, and colon (3, 21). In further demonstration of the role of R-spondin signaling in promoting proliferation, chromosomal rearrangements that result in *RSPO* fusion proteins have been shown to drive colorectal cancer, with *RSPO2*/*RSPO3* fusions being identified in 10% of colon tumors of one study (128). A recent study has also implicated LGR4 as a key RSPO receptor within *Axin2*+/*Lgr5*- progenitor cells of the mouse antrum, however a role for LGR4 has not yet been demonstrated within the corpus (129).

There are also many secreted negative regulators of Wnt/β-catenin signaling that confine the stem cell niche. Secreted frizzled-related proteins (sFRPs) were one of the first classes of Wnt antagonists to be discovered, and they function by binding WNT ligands using a FZD-like cysteine-rich binding domain to prevent activity (130, 131). The

secreted protein Dickkopf1 (DKK1) competitively binds with LRPs to inhibit Wnt signaling, and two independent studies have demonstrated that ectopic expression within the intestine suppresses Wnt-dependent proliferation (132-134). Additional antagonists of the pathway include sclerostin domain containing 1 (SOST), Wnt inhibitory factor 1 (WIF1), and insulin growth factor binding protein 4 (IGFBP-4) (135-137). Although DKK homolog expression has been demonstrated within the gastric antrum, no studies have analyzed the role of any of these secreted Wnt inhibitors in regulating gastric epithelial homeostasis (18).

Localization of WNT and RSPO Ligands

The key Wnt and R-spondin signaling cells of the gastrointestinal tract have long been debated, although recent studies have highlighted subepithelial stromal cells as the major source of WNT ligands to comprise the Wnt stem cell niche. A seminal paper by Farin et al. first demonstrated in mice that non-epithelial cells support stem cell function in the small intestine in the absence of epithelial WNT provided by Paneth cells expressing WNT3 at the base of crypts (138). Paneth cells, however, are unique to the small intestine, and therefore it follows that additional cells more consistently distributed across the gastrointestinal tract would provide essential sources of WNT.

Building on initial studies that showed epithelial Wnt was dispensable for stem cell function in the intestine, Kabiri et al. observed that stromal cells could support intestinal organoids in culture without supplementation of WNT or RSPO (113). While Paneth cells can support the stem cell niche *in vitro* through expression of WNT3, R-

spondins, considered essential for organoid growth, are solely expressed in stromal populations (139).

Additional studies continued to provide support for subepithelial stromal cell populations as key sources of WNT and RSPOs for the stem cell niche and began to define markers to label these cells. While it is clearly established that stromal cells are essential niche cells supporting Wnt signaling, there has been significant controversy identifying this cell population. In mice, canonical WNT and RSPO ligands have been localized to stromal cells expressing *Foxl1*, *Gli1*, *Pdgfra*, *Acta2*, *Myh11*, *Cd34*, *Grem1*, and *Cd81* (140-145). *Foxl1*+ pericryptal mesenchymal cells were one of the first labeled populations identified as the key sources of Wnt for epithelial cells, and these cells were determined to be distinct from myofibroblasts (143). These cells were later named telocytes for their elongated appearance, and they appeared to form a close network surrounding intestinal crypts and villi (146). Later studies built off this idea but identified telocytes as a distinct subset of stromal cells that contributed to epithelial function within the intestine. In a study by McCarty et al., canonical WNT, such as WNT2B, and RSPOs were instead localized to *Pdgfra*^{low}, *Cd34*+ subepithelial cells distinctly located at the gland base to a cell population which they labeled as trophocytes (144). They noted that telocytes, which expressed *Foxl1* and were *Pdgfra*^{high}, expressed WNT4/5A/5B but also higher amounts of BMPs, and were incapable of supporting epithelial cultures without *in vitro* supplementation with recombinant RSPO1 and NOG.

Significantly less work has been conducted to identify the key WNT/RSPO-expressing cells of the stomach, although, as in the intestine, it is believed that stromal cells comprise the key Wnt niche cells. Importantly, gastric epithelial cultures require

WNT supplementation *in vitro*, indicating that there is likely no Paneth-like epithelial cell which supplies WNT to the stem cell niche (77). Sigal et al. first demonstrated in the antrum that *Rspo3* localizes to subepithelial stromal myofibroblasts (*Myh11*+, *Acta2*+) at the gland base (18). In co-culture experiments, these cells could support antral organoids, therefore demonstrating their function as niche cells. These findings have recently been translated into the corpus, where *RSPO3*, the dominant gastric R-spondin, is localized to *MYH11*+ cells at the gland base in both mouse and humans (147). A broader study by Kim et al. conducted single cell analyses on stroma from both gastric and intestinal mouse tissue and found conserved populations of cells in each region (148). Thus, cell populations that have been demonstrated to support the stem cell niche in the intestines likely also exist in the stomach. Using the previously defined genetic mouse models targeting intestinal stromal populations could therefore translate to the stomach and help improve understanding of various niche pathways and stromal regulation of gastric epithelial stem cell function.

The localization of RSPO3 ligands to cells at the gland base constructs a Wnt signaling gradient along the base-lumen axis of gastric glands, with signaling concentrated at the base of glands and diminishing upwards towards the luminal surface. This leads Wnt signaling and target gene expression to be induced in epithelial cells at the gland or crypt base. Typically, these cells are considered to be active stem/progenitors cells which constantly divide to drive epithelial turnover. However, the cellular architecture is different in the corpus relative to the antrum and intestines, with stem/progenitor cell population residing in the mid-gland isthmus while chief cells are in the gland base.

Barker et al. identified the Wnt target gene *Lgr5* as the first definitive marker for active epithelial stem cells within the small intestine and colon, while also labeling cells at the base in the antrum (21). Continued work led to *Lgr5*+ cells, and eventually also *Axin2*+ cells, of the antrum being identified as stem cells as well (3, 18). Interestingly, in these studies *Lgr5*+ cells were notably absent from the corpus aside from rare instances along the lesser curvature. This long casted doubt regarding the role of Wnt within the gastric corpus as there was no clear Wnt signaling stem cell pool despite the presence of WNT and RSPO ligands within the mucosal environment. However, one of the original markers for chief cells, *Troy*, is also a Wnt target gene. Early studies observing *Troy*+ chief cell function identified that these cells also possessed Wnt target gene characteristics (*Lgr5*+, *Axin2*+) that were reminiscent of stem cells in the antrum and intestine (37). It wasn't until more recently though that Leushacke et al. used a new mouse model to demonstrate that the Wnt target gene and stem cell marker *Lgr5* labeled *Gif*+ chief cells at the gland base (91). This study also mapped *LGR5* mRNA to chief cells of the human stomach. However, in contrast to the antrum and intestine where *LGR5* marks active stem cells, these *LGR5*+ cells in the corpus are quiescent, differentiated cells.

The Role of Wnt Signaling within the Corpus

The role of Wnt signaling within the corpus epithelium is poorly understood. The expression of Wnt target genes in mature chief cells rather than stem/progenitor cells is in stark contrast to the rest of the gastrointestinal tract where active progenitor cells are high Wnt signaling. The presence of Wnt in mature, quiescent cells combined with the

absence of Wnt in active isthmus progenitors therefore suggests a different role for Wnt signaling in maintaining epithelial homeostasis within the corpus, with normal adult corpus stem/progenitor proliferation potentially being Wnt independent (40).

The first evidence for regionality in how Wnt may differentially regulate human corpus epithelial homeostasis emerges from developmental studies. Disruption of Wnt/β-catenin signaling in mouse embryos promoted an antral phenotype and absence of corpus epithelium (103). Furthermore, to generate differentiated gastric corpus organoids from human PSCs, McCracken et al. demonstrated that activation of Wnt signaling through addition of the GSK3β inhibitor CHIR99021 led to corpus specification, while disruption of Wnt signaling resulted in antral organoids (103, 149). Thus, high levels of Wnt signaling may underscore region-specific gastric determination and indicates that the corpus mucosa may be a high Wnt signaling environment relative to the antrum.

In mature corpus tissue the role of Wnt remains unclear, although recent studies have begun to demonstrate a role for Wnt in regulating cell fate. In defining the optimal media conditions for human-derived corpus organoids, Bartfeld et al. determined that WNT and RSPO were necessary for organoid formation and also regulated cellular differentiation (77). High WNT/RSPO media resulted in the presence of all differentiated subtypes (aside from parietal cells), while complete WNT/RSPO withdrawal rapidly led to surface cells becoming dominant. This was the first indication that Wnt regulates corpus epithelial differentiation and that it logically follows the Wnt gradient observed *in vivo*. In a more recent study, Fischer et al. investigated how overexpression or knockout of *Rspo3* in transgenic mouse models would alter homeostasis *in vivo* (147). They

observed that overexpression of *Rspo3* in *Myh11+* mesenchymal cells at the base of glands increased corpus proliferation, gland size, and led to a massive expansion of the *Gif+* chief cell compartment. On the contrary, *Rspo3* knockout in *Myh11+* cells shrunk the *Gif+* compartment, but interestingly did not have any impact upon proliferation or gland height. Thus, Wnt signaling appears to be essential for promoting chief cell differentiation and/or maintenance. However, in light of recent studies suggesting compartmentalization of renewal within the corpus epithelium, it is unknown whether chief cell expansion after *Rspo3* overexpression occurs via increased chief cell self-renewal, or through directing fate determination from an isthmus progenitor.

Beyond differentiation, there is a potential role for Wnt signaling in regulating the injury response, although the specific mechanism remains unclear. In the same Fischer et al. study, it was demonstrated that high-dose tamoxifen and chief cell ablation both led to increased *Rspo3* expression in mice and that *Rspo3* expression promoted glandular regeneration (147). Infection with *H pylori*, which induces SPEM, has also been demonstrated to activate Wnt signaling through increased R-spondin expression in both the corpus and antrum (18, 147, 150).

There is also increased expression of the Wnt target gene and cell-surface adhesion molecule CD44 during SPEM, with expression colocalizing with *TFF2+* metaplastic cells (151). In the antrum and intestines, CD44 is abundantly expressed and labels both active and facultative stem cells within the high Wnt base (152, 153). A functional role for CD44 has been established during SPEM as two independent knockout studies have demonstrated that ablation perturbs SPEM development following injury (153, 154). Interestingly, during homeostasis there is low expression of

Cd44+ cells within the isthmus region, although single cell studies have localized transcripts primarily to neck cells (14, 153). *Sox9*, another Wnt target gene, has also recently been implicated in neck cell development in mice as well as during SPEM, therefore further highlighting a potential role for Wnt signaling in regulating the gastric injury response (155).

Thus far, Wnt signaling has predominately been demonstrated to regulate basal chief cells within the corpus. Injury studies suggest that Wnt signaling may underscore chief cell progenitor function and the overall injury response, however this has not been definitively proven. Furthermore, it remains unclear how activation of Wnt signaling regulates progenitor cells within the isthmus. The work within my thesis focuses on exploring these concepts and establishing a role for Wnt in regulating human corpus epithelial proliferation, differentiation, and stem cell function.

1.6 Wnt in Gastrointestinal Disease

Dysregulated Wnt signaling has been implicated in driving disease across most tissue systems (123). Hyperactivation of the pathway, which can be caused by loss-of-function mutations in regulator genes or gain-of-function mutations to *CTNNB1* (encoding β-catenin), has been connected to the emergence of cancer throughout the body including breast cancer, hepatocellular carcinoma, lung cancer, pancreatic cancer, prostate cancer, colorectal cancer, and gastric cancer (156-160).

Adenomatous Polyposis Coli (APC) Function

The critical role of Wnt signaling in driving epithelial proliferation and stemness within the gastrointestinal tract makes it a common driver of tumorigenesis in the presence of oncogenic mutation. This is most notable within the colon, where 93% of colorectal cancers have been shown to carry a Wnt activating mutation (161). Somatic and germline mutations in many of the pathway's complex regulatory elements have been identified as key drivers for such diseases through predisposing tissue to acquiring further oncogenic mutation. Most prevalent among these mutations with respect to the gastrointestinal tract is loss-of-function mutations to *APC*.

APC, located on chromosome 5q21, encodes a large (310 kDa), multifunctional tumor suppressor protein that contains numerous binding regions that interact with various pathways to regulate cellular function. These include pathways involving cytoskeletal organization, adhesion, and migration (162). Most notably among its functions is to act as a scaffolding protein within the β-catenin destruction complex to enable efficient cytosolic degradation to negatively regulate Wnt/β-catenin signaling in the absence of WNT ligand. This is primarily accomplished by three 15 amino acid repeats (AARs) between codons 1021-1170 and seven 20 AARs between codons 1265-2035 that specifically bind β-catenin (163). Loss-of-function *APC* mutations prevents proper assembly of the β-catenin destruction complex, thereby suppressing efficient cytosolic degradation and enabling β-catenin translocation into the nucleus even in the absence of WNT ligand (Figure 1.6) (164). *APC* truncating mutations within colorectal tumors are most frequently described within the 20 AAR region between codons 1282-1581 as these mutations prevent its proper function within the Wnt signaling pathway

(163). While *APC* mutations have long been connected to tumorigenesis within the gastrointestinal tract, Barker et al. first demonstrated in mice that homozygous loss of *Apc* in intestinal stem cells was sufficient to drive colonic intestinal neoplasia and adenomatous transformation (2).

Familial Adenomatous Polyposis (FAP)

People who inherit a single copy of mutated *APC* are naturally predisposed to developing significant disease burden throughout their gastrointestinal tract. This condition is known as familial adenomatous polyposis (FAP), and is an autosomal dominant disorder characterized by the emergence of numerous adenomatous lesions within the colon (Figure 1.6) (165). The incidence of FAP is approximately 1 in 7,000 to 1 in 30,000 with equal distribution amongst men and women (165, 166). Interestingly, while most cases of FAP arise with familial history, approximately 20%-30% of new diagnoses are made without family history, thus indicating de novo germline acquisition of mutated *APC* (167). As a result of this mutation, patients have an effective 100% chance to develop colorectal adenomas and ultimately colorectal cancer, with cancer generally emerging between 35-45 years old (165, 168, 169).

In the stomach, mutations to *APC* have been reported in 7-34% of sporadic gastric cancers (170-172). Beyond somatic loss-of-function mutations, Ksiaa et al. demonstrated that *APC* is also commonly hypermethylated in gastric cancer as these epigenetic changes were observed in 52.9% of gastric cancer samples versus in 37.7% of healthy tissue (173). Interestingly, the rate of gastric cancer in FAP patients is

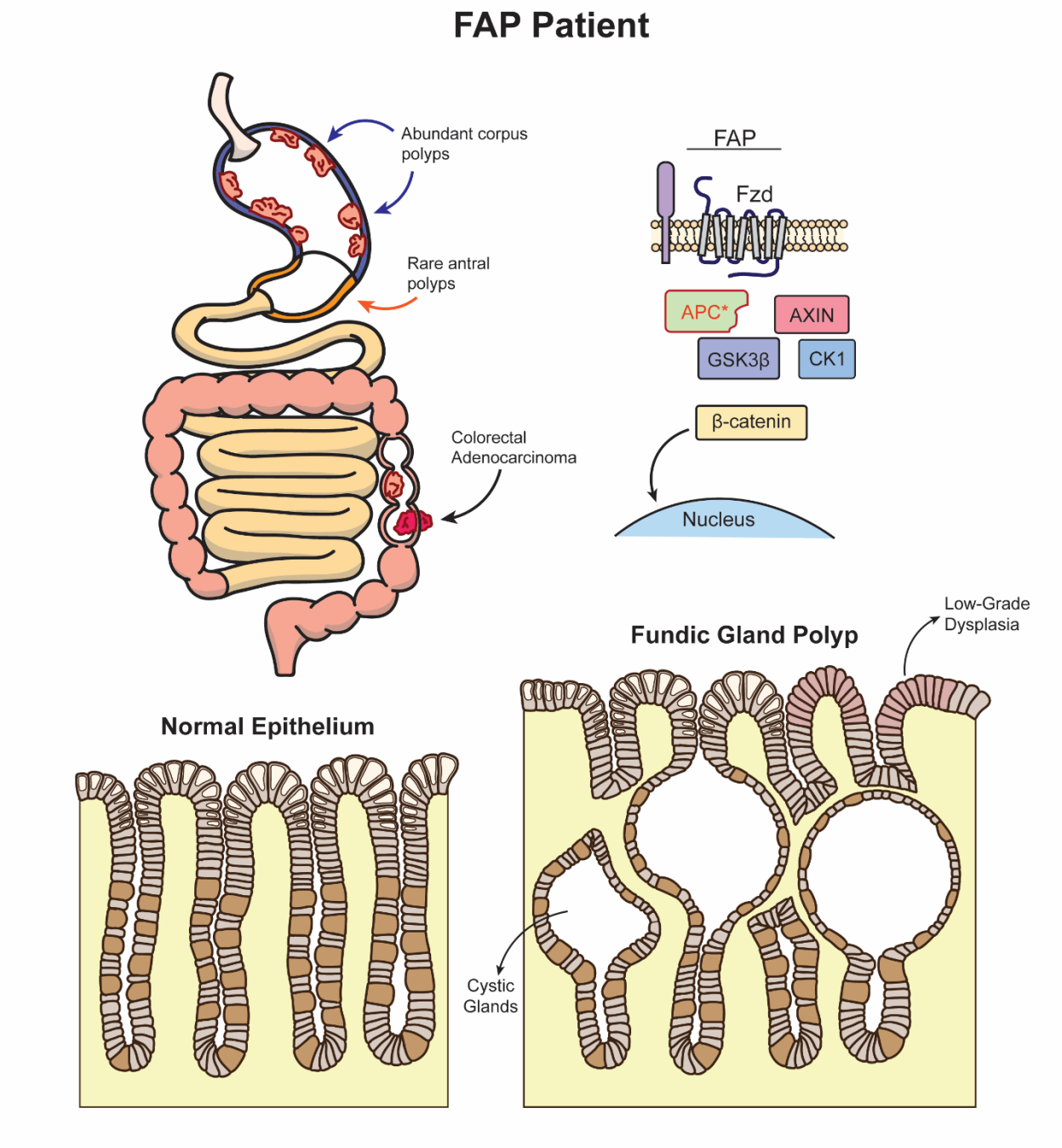

Figure 1.6: Familial adenomatous polyposis and fundic gland polyps

Patients with familial adenomatous polyposis develop gastrointestinal disease. The most severe phenotype occurs in the colon where patients develop colorectal adenocarcinoma. In the stomach, patients develop abundant yet benign polyposis within the corpus in the form of fundic gland polyps (FGPs). FGPs are defined by cystically dilated glands, increased proliferation, and a common presence of low-grade dysplasia. However, high-grade dysplasia and precancerous adenomatous change rarely arise. Polyps in the antrum are rare, but typically exhibit increased risk for cancer.

shockingly low relative to colorectal cancer, with a lifetime risk for FAP patients to develop gastric cancer only reported to be 0.5-1.3% (174, 175). However, FAP patients are at a heightened risk of developing gastric polyps in the form of benign neoplasms known as fundic gland polyps (FGPs).

FGPs are sessile, benign polyps characterized by cystically dilated glands (Figure 1.6). These dilations are typically lined with differentiated cells, including predominately chief, mucous neck, and attenuated parietal cells (176, 177). Fundic gland polyps have been described to occur in anywhere from 30-88% of FAP patients, with equal incidence in men and women (178-180). The frequency of emergence is also variable with patients manifesting 100’s to even 1000’s of FGPs, sometimes leading to complete carpeting of the gastric corpus mucosa (181).

Despite their name, FGPs are not solely localized to the fundus but are found throughout the corpus of the stomach (175). Interestingly, FGPs are notably absent from the antrum. However, although less common, FAP-associated antral polyps which do emerge have a significantly higher incidence of exhibiting adenomatous change (175). In the corpus, FGPs rarely exhibit adenomatous change or high-grade dysplasia, although low-grade dysplasia has been identified in approximately 50% of FAP-associated FGPs (181).

Therefore, there are stark regional differences in manifestation of polyps within the stomach. These regional differences highlight differences in sensitivity to activation of Wnt signaling between the corpus and antrum to underscore regional patterns of disease. Furthermore, the low risk of cancer progression directly contradicts observations in the colon, thus suggesting either a novel role for Wnt signaling in the

gastric corpus versus colon, or a different threshold for tumorigenesis. Throughout my dissertation, I explore how Wnt may differentially regulate proliferation and identity in the corpus versus antrum to provide insight on the clinical manifestations of FGPs resulting from Wnt activation disease.

Etiology of Fundic Gland Polyps

The etiology of FGPs, especially with respect to Wnt signaling, remains unclear. There is some evidence that suggests their emergence may be linked with parietal cell malfunction. In large part this is due to their association with long-term proton-pump inhibitor use to reduce the acidity of the gastric lumen (182-184). These sporadic FGPs regress when treatment is ended, therefore demonstrating the transient nature of this pathology (183, 185). Early studies surmised that polyp development in these patients could be due to increased gastrin production stimulated by the reduction in luminal acidity (186). Accordingly, Franic et al. demonstrated that while mice lacking H^+/K^+-ATPase Subunit β (encoded by *Atp4b*) experienced mucosal hypertrophy within the corpus, loss of gastrin negated these phenotypic effects (186). Additional studies have also demonstrated that H^+/K^+-ATPase malfunction due to *Atp4a* deletion in mice leads to an FGP-like phenotype within the corpus (187, 188). In humans however, while acid suppression therapy does appear to increase gastrin production, there has not been an established association between hypergastrinemia and the emergence of FGPs (189, 190).

It is unknown how, or if, sporadic FGPs in patients with acid suppressing therapy follow a similar etiological manifestation to Wnt-related FGPs in patients with FAP as it

is mostly unknown how Wnt regulates parietal cell differentiation. A recent mouse study by Fischer et al. using *Rspo3*-knockout or *Rspo3*-knock-in in *Myh11+* stromal cells demonstrated that while loss of *Rspo3* had no impact on parietal cell numbers, *Rspo3* overexpression did lead to an absolute increase in parietal cells. However, parietal cells remained equally distributed throughout the expanded glands, indicating that this may have been a function of an overall increase in epithelial cell numbers rather than a direct effect on parietal cell differentiation (147).

Other Wnt activation mouse models have produced variable effects within the proximal stomach, therefore leading to further uncertainty regarding the Wnt-dependent etiology of FGPs. Using an *AhCre* mouse model to broadly target gastric epithelial cells, Radulescu et al. induced Wnt activation through conditional deletion of either *Apc* or *Gsk3 (alpha* and *beta*), or through oncogenic activation of beta-catenin (*Ctnnb1*) (191). They observed that all Wnt activation models rapidly induced adenomatous changes within the antrum. In the corpus, they observed FGP development typically after 1 week, with all mice developing both FGPs and adenomatous change by Day 12. Using immunohistochemistry, they showed that parietal cells were rapidly lost, therefore demonstrating that activation of Wnt signaling reduced parietal cell differentiation. However, this study used tamoxifen to induce Cre recombination, which is known to cause oxyntic atrophy and lead to a metaplasia injury response. Thus, additional studies with other models would be required to conclude the causal relationship they observe between Wnt activation and parietal cell loss.

While the study by Radulescu et al. showed a distinct link between Wnt activation and the emergence of an FGP phenotype, similar studies from other groups have failed

to support this mechanism. Two independent studies using chief cell specific Cre drivers, *Pgc-CreER^{T2}* and *Mist1-CreER^{T2}*, observed that homozygous deletion of *Apc* failed to promote corpus hyperplasia or any form of phenotypic change (192, 193). However, successive oncogenic activation through combination with a *Kras^{G12D}* mutation was successful in driving tumorigenesis, therefore confirming the oncogenic potential of those cells. A study by Powell et al. took a different approach where they induced heterozygous loss of *Apc* in progenitors throughout the GI tract using a *Lrig1-CreER^{T2}; Apcfl$^{/+}$* mouse model, and monitored tumor formation over an extended period of time (100+ days) (194). They noted surface cell hyperplasia and a dramatic increase in proliferation in the corpus of mice at day 100 post-injection, although the glands did not exhibit the typical cystic dilation associated with fundic gland polyps. Altogether, these studies suggest that while homozygous loss of *Apc* does induce phenotypic change within the corpus, heterozygous loss of *Apc* may be sufficient to drive hyperplasia. In this dissertation, I continue to explore the consequences of *Apc* deletion within the gastric epithelium of mice and present rationale highlighting key regional differences within the stomach that shed light on the patterns of disease and Wnt-regulated cellular differentiation.

Wnt signaling is a clear driver for FGP emergence in humans. While syndromic FGPs are associated with familial conditions such as FAP with germline *APC* mutation, sporadic FGPs are also linked with activating mutations in *CTNNB1*, which encodes β-catenin (195, 196). Interestingly, sporadic FGPs are negatively correlated with *H pylori* infection, which may result in increased FGP prevalence in Western countries as *H pylori* infection rates are lowered (197, 198). There are typically no major phenotypic

differences between familial and sporadic FGPs, however *APC*-linked FGPs have been reported to have higher rates of dysplasia, perhaps because Wnt signaling is constitutively increased throughout life (181, 199-201).

Despite the prevalence of FGPs in FAP patients, the mutational landscape underscoring their emergence has been scarcely studied. One potential reason for this is that FGPs have a low rate of tumor progression. Compared to the distal GI tract where FAP patients have a near 100% incidence of developing colorectal cancer, gastric cancer risk is only modestly increased with a prevalence of 0.5-1.3% (174, 175). Although FGPs are benign neoplasms, FAP patients regularly undergo gastric endoscopy to monitor polyp progression in the adverse event of tumorigenesis.

The "Two-Hit" Hypothesis

Typically, polyp formation within the gastrointestinal tract of FAP patients is thought to depend on a second-hit mutation to *APC* to induce loss-of-heterozygosity. Knudson's "two-hit" hypothesis was, in part, based these observations within the colon where loss of the functional allele was necessary to initiate adenomatous change and the mutational cascade ultimately leading to colorectal cancer (202). In mice, homozygous *Apc* deletion drives immediate adenoma formation within the intestines while conditional loss of a single *Apc* allele only drives phenotypic change when mice are followed for multiple months and after loss of the remaining allele (203). Therefore, it would be expected that FAP patients would require a similar second hit to form an FGP. In one of the few studies analyzing the mutational state of FGPs from FAP patients, Abraham et al. observed somatic *APC* alterations in 21 out of 41 polyps (51%)

(204). They identified 15 of these cases to be due to somatic loss-of-function mutations and the remaining six to be due to allelic loss leading to loss-of-heterozygosity. Therefore, they were unable to demonstrate *APC* loss-of-heterozygosity within the remaining 20 polyps, thus demonstrating variability in the mutational landscape underscoring polyp formation. Interestingly, they did not observe a connection between loss-of-heterozygosity and grade of dysplasia within their sample set. In Chapter 3 of this dissertation, I further explore the mutational etiology of fundic gland polyp formation within the proximal stomachs of FAP patients through the use of genomic sequencing in patient-matched polyp and non-polyp sample pairs.

The "Just-Right" Hypothesis of Wnt Signaling

Traditionally, the Wnt signaling pathway could be thought of as a simple ON/OFF switch that promotes proliferation and stemness in the presence of ligand and induces differentiation in the absence of ligand. According to this and Knudson's 'two-hit' hypothesis, any two random mutations that lead to *APC* loss-of-function should result in upregulation of signaling and ultimately tumorigenesis (202). Most studies investigating this paradigm have focused on the intestine where *APC* loss-of-heterozygosity is thought to initiate polyp formation and eventual development of adenocarcinoma (164, 168, 169, 202). Early studies investigating the mutational landscape of *APC* within colorectal tumors demonstrated that *APC* mutations were not random (205). Analysis of colorectal tumor biopsies from FAP patients showed that somatic second-hit mutations within *APC* were highly dependent upon the nature of the germline mutation of the patient. Albuquerque et al. expanded upon these original findings and demonstrated

that within colorectal adenomas there was a coordination of loss-of-function mutations in the 20-amino-acid repeat regions responsible for downregulating β-catenin (206). In short, they determined that the two independent mutations (germline and somatic) combined to retain a few of these 20-amino-acid repeats, but complete loss of all repeats was never observed. Therefore, they concluded that selection of mutations in adenomas was titrated for an optimal level of Wnt signaling that retained some β-catenin regulating activity in a manner they termed the 'just-right' hypothesis.

This signaling paradigm describes a Goldilocks zone of Wnt signaling that leads to proliferation and stemness (Figure 1.7). Too little Wnt signaling improperly regulates stemness and ultimately leads to the initiation of differentiation. Too much Wnt signaling on the other hand is not tolerated, and those cells either no longer contribute to normal epithelial turnover or are lost through induction of apoptosis. Proper stem cell function and proliferation therefore occurs when Wnt signaling is 'just-right.'

Additional studies have added credence to this idea by demonstrating that high Wnt, but not excessive Wnt, is essential for gastrointestinal tumorigenesis. Using two distinct *Apc* knockout mouse models, Lewis et al. demonstrated that mutational severity and phenotypic severity did not correlate within the intestine (207). They found that while an Apc^{R850X} (Apc^{Min}) knockout model led to enhanced nuclear localization of β-catenin, a more distal Apc^{1322T} knockout model led to a more severe tumorigenic phenotype that favored stemness and stem cell function. Therefore, they concluded that an excess in Wnt signaling can actually suppress tumor growth in accordance with the 'just-right' hypothesis. In a more recent study, Lähde et al. demonstrated that induction

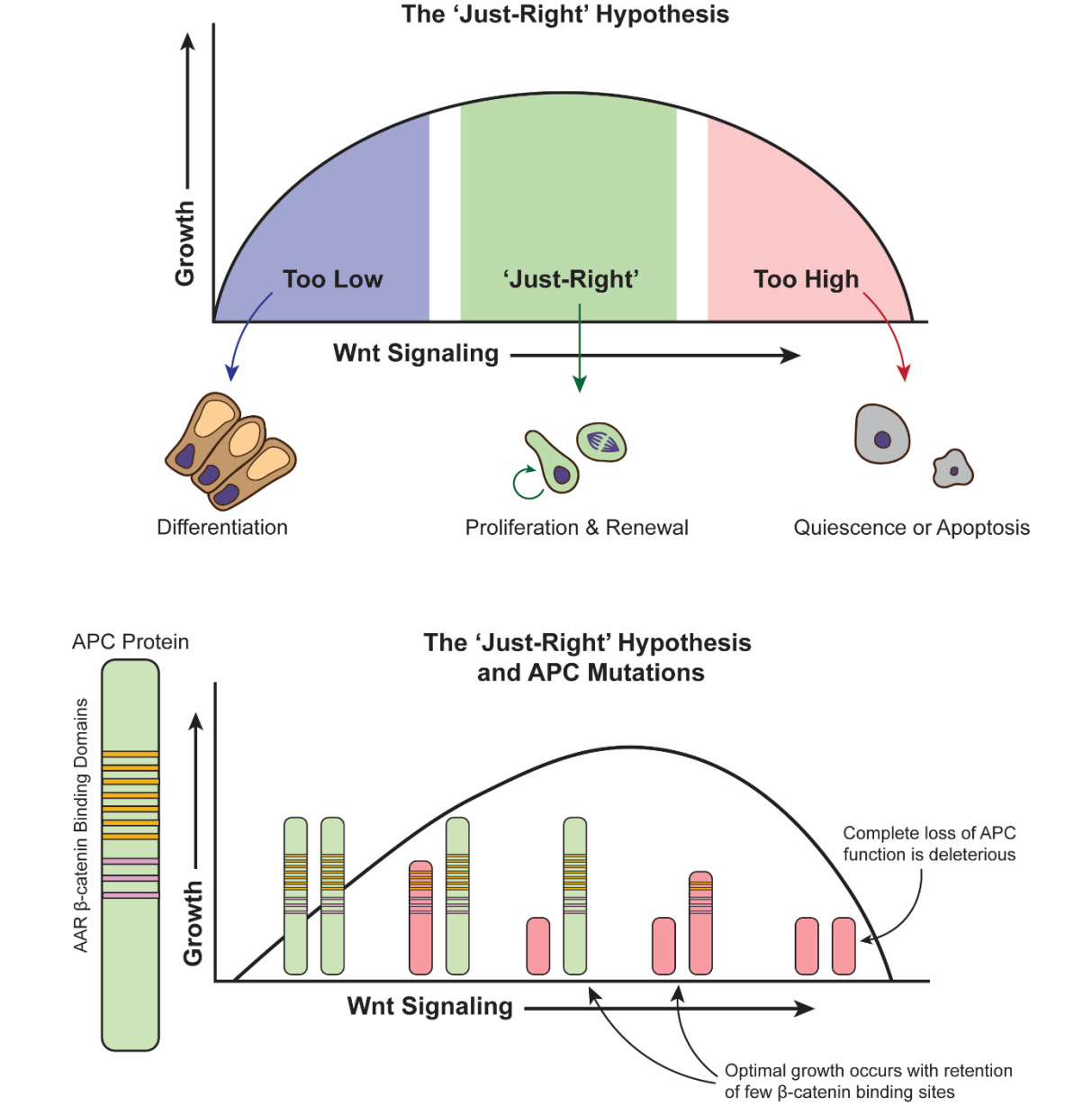

Figure 1.7: The 'Just-Right' Hypothesis

The 'just-right' hypothesis describes an optimal range of Wnt signaling which induces growth, proliferation, and renewal within a cell. Too low Wnt signaling leads to loss of stem cell character and induction of differentiation, such as towards terminally differentiated surface cells. Too high Wnt signaling suppresses proliferation of cells and potentially induces apoptosis. 'Just-Right' levels of signaling optimally maintain stemness and induce proliferation and self-renewal. Wnt activating mutations leading to cancer require pathway activation that drives signaling within this range to ectopically drive stemness and hyperproliferation. In the case of APC mutations, proliferation is optimally driven when only a few β-catenin binding sites are retained. Hyperactivation of the pathway beyond this level, such as a complete loss of all β-catenin binding activity in both *APC* alleles, poorly drives tumorigenesis within the colon.

of Wnt through overexpression of RSPO1 in mice can suppress intestinal adenoma formation driven by the *Apc*^{Min} allele (208). Upon injection with RSPO1, intestinal adenomas formed within *Apc*$^{Min/+}$ mice via second-hit mutations experienced increased apoptosis and reduced proliferation, ultimately resulting in fewer tumors and prolonged survival. A similar effect has been observed by Langlands et al. within *Apc*$^{Min/+}$ intestinal organoids in which excess Wnt in media, through addition of Wnt activator CHIR99021, suppressed *Apc*$^{Min/Min}$ organoid growth and instead favored organoids which retained a functional wild-type allele (*Apc*$^{Min/+}$) (209).

The concept that excess Wnt can be deleterious to proliferation has also been described in homeostasis. In mouse experiments, Yan et al. observed that adenoviral overexpression of *RSPO1* or *RSPO2* led to an expansion of *Lgr5*+ stem cells within the small intestine (210). However, these *Lgr5*+ cells were “trapped” at the base of crypts and no longer lineage traced to other regions of the crypt-villus axis, thus demonstrating that excess Wnt confined these cells to a stem cell identity while simultaneously suppressing their proliferation. A study by Sigal et al. within the gastric antrum showed a strikingly similar phenotype in which overexpression of *Rspo1* or *Rspo3* in *Myh11*+ cells led to a suppression of lineage tracing from *Lgr5*+ stem cells and demonstrated that they instead remined confined to the base of crypts (18). In both studies, the major proliferative pool following *Rspo* overexpression were *Lgr5*- cells; transit amplifying cells within the intestine and *Axin2*+/*Lgr5*- cells within the antrum. Overall, these studies demonstrate that Wnt signaling dose-dependently regulates proliferation and stemness of Wnt-responsive (*Lgr5*+) progenitors, with excessive Wnt being prohibitive towards normal proliferation and instead locking cells within a stem-like state.

The ‘just-right’ hypothesis has also been expanded through continued independent studies to describe the patterns of tumorigenesis throughout the gastrointestinal tract. Interestingly, mice are predisposed to develop small intestinal lesions in response to loss of *Apc*, while in humans, tumors predominately arise in the colon while the small intestine is mostly spared (211). Continued work by Albuquerque et al. demonstrated that there were distinct types of *APC* mutations underscoring tumorigenesis within the proximal versus the distal intestinal tract (212). Later, Leedham et al. investigated Wnt signaling levels of the intestinal tracts of both mice and humans and surmised that these patterns of polyp emergence were due to regional differences in basal Wnt sensitivity and signaling (211). Therefore, the appropriate Goldilocks zone of Wnt signaling which initiates adenoma formation is regionally dependent and relies on a combination of the cell-extrinsic environment as well as cell-intrinsic signaling tone.

The consequences of activation of Wnt signaling within the corpus stomach and how it relates to the ‘just-right’ hypothesis remains unclear. Using normal and FGP-derived human organoid lines, I explore within this thesis how Wnt signaling regulates cellular function within the corpus and provide novel insight into the Wnt-dependent manifestation of FGPs.

1.7 Dissertation Summary

The Wnt signaling pathway plays an essential role in regulating many of the facets necessary for adult gastrointestinal epithelial stem cell function including proliferative potential, cellular identity, and fate determination. Furthermore, it plays a

central role in disease manifestation, especially in the distal gastrointestinal tract where hyperactivation of the pathway through mutation confers adenomatous change and a significant risk for carcinogenesis. Interestingly, the epithelium of the gastric corpus appears to have a distinct response to Wnt signaling relative to the rest of the columnar epithelium in the antrum and intestines. Active progenitors of the corpus are not labeled by the typical Wnt target genes present in the antrum or intestines. Rather, Wnt targets localize to basal chief cells which are differentiated cells that play a critical role in digestion. However, chief cells also potentially undergo low levels of self-maintaining baseline turnover restricted to the gland base and demonstrate facultative progenitor potential in response to glandular injury.

Although it is clinically well documented that activation of Wnt signaling through mutations in *APC* and *CTNNB1* can lead to FGPs, the mechanism underlying this has remained elusive as a distinct role for Wnt signaling in regulating homeostasis is not clear. Further understanding the role of pathways such as Wnt signaling in regulating adult stem cell function within the corpus will enable the development of novel platforms to study tissue function *ex vivo* and help unlock the next generation of therapeutics targeting gastric disease.

The goal of my thesis research has been to elucidate how Wnt signaling regulates the human gastric corpus epithelium. This work broke down into two overlapping projects to investigate how activation of Wnt signaling regulates human corpus epithelial function during homeostasis (Chapter 2) and how activation of the pathway leads to disease in the form of fundic gland polyps (Chapter 3). Throughout my

studies, I directly studied human tissue using epithelial organoids derived from primary biopsies to provide translatable insights into human gastric physiology.

In Chapter 2, I use human epithelial organoids derived from genetically normal gastric tissue to characterize how Wnt signaling differentially regulates growth, proliferation, and differentiation in the corpus versus antrum. Using the pharmacologic Wnt activator and GSK3β antagonist CHIR99021 (CHIR), I subjected patient-matched corpus- and antral-derived organoids to varying levels of Wnt signaling and demonstrated that progenitor cells from each region have differential thresholds for Wnt signaling to induce optimal growth. Across three independent patient sample sets, I show that corpus organoids have a reduced threshold for Wnt signaling and reach optimal growth rates at lower concentrations of CHIR relative to their patient-matched antral organoids. Furthermore, I demonstrate that these findings are a function of proliferation with supramaximal CHIR rapidly conferring reduced corpus organoid size and EdU incorporation but not an increase in apoptosis. These findings lead to a more in-depth investigation of how Wnt signaling influences corpus progenitor cell function and identity. I show that Wnt signaling distinctly regulates a bimodal axis of differentiation within the corpus, with high levels of signaling leading to deep glandular chief and neck cells, while low levels allow differentiation towards surface cells. Despite high CHIR inducing low rates of proliferation, I demonstrate that these cells establish organoids at more efficient rates, as cells are paused in a quiescent yet primed G_1 cell cycle state. Ultimately, I show that the impact of high Wnt signaling on differentiation and growth are transient, and upon return to normal Wnt conditions, organoids regain typical growth rates, morphology, and patterns of differentiation.

In Chapter 3, I characterized gastric organoids derived from patients with familial adenomatous polyposis (FAP) to investigate how *APC* mutations and activation of Wnt signaling lead to the emergence of disease in the form of FGPs within the corpus. I utilize an extensive biobank of patient matched tissue derived from FGPs and surrounding non-polyp regions of these patients to conduct comparative experiments assaying Wnt tone and sensitivity to varying levels of Wnt signaling. I demonstrate that Wnt target genes are upregulated in FGP biopsies as well as within a subset of polyp-derived organoids, confirming that upregulation of Wnt signaling is an underlying driver of FGP manifestation. I next carry out several experiments to investigate Wnt tone and sensitivity within FGP-derived organoids and ultimately demonstrate that the principles of the 'just-right' hypothesis faithfully model organoid responses to induction of Wnt signaling. Using targeted genomic sequencing, I show that despite upregulated signaling, additional somatic *APC* mutation is rare in FGPs, indicating that most polyps emerge without *APC* loss-of-heterozygosity. This represents a stark contrast from the traditional understanding of adenomatous antral and colorectal lesions and suggests that *APC* loss-of-heterozygosity may not be tolerated within the corpus. Finally, I transition to a gastric specific *Apc*-knockout mouse model to determine the consequences of heterozygous and homozygous *Apc* loss of gastric homeostasis. I demonstrate that while heterozygous *Apc* deletion drives increased corpus proliferation, cells with homozygous *Apc* loss are not retained long-term. On the contrary, we observed no phenotypic change upon heterozygous *Apc* deletion in the antrum, but homozygous loss confers hyperplasia. These findings suggest that regional differences

in Wnt sensitivity underscore the emergence of different polyp types within the corpus and antrum.

Finally, in Chapter 4 I summarize my findings in the context of the current understanding of human corpus homeostasis and disease progression. I pose potential questions which arise from my work and present future directions for continued study of Wnt-dependent mechanisms of human corpus epithelial function.

1.8 References

1. Karam SM, and Leblond CP. Dynamics of epithelial cells in the corpus of the mouse stomach. I. Identification of proliferative cell types and pinpointing of the stem cell. *Anat Rec* 236: 259-279, 1993.

2. Barker N, Ridgway RA, van Es JH, van de Wetering M, Begthel H, van den Born M, Danenberg E, Clarke AR, Sansom OJ, and Clevers H. Crypt stem cells as the cells-of-origin of intestinal cancer. *Nature* 457: 608-611, 2009.

3. Barker N, Huch M, Kujala P, van de Wetering M, Snippert HJ, van Es JH, Sato T, Stange DE, Begthel H, van den Born M, Danenberg E, van den Brink S, Korving J, Abo A, Peters PJ, Wright N, Poulsom R, and Clevers H. Lgr5(+ve) stem cells drive self-renewal in the stomach and build long-lived gastric units in vitro. *Cell Stem Cell* 6: 25-36, 2010.

4. Choi E, Roland JT, Barlow BJ, O'Neal R, Rich AE, Nam KT, Shi C, and Goldenring JR. Cell lineage distribution atlas of the human stomach reveals heterogeneous gland populations in the gastric antrum. *Gut* 63: 1711-1720, 2014.

5. Stoffers DA, Heller RS, Miller CP, and Habener JF. Developmental expression of the homeodomain protein IDX-1 in mice transgenic for an IDX-1 promoter/lacZ transcriptional reporter. *Endocrinology* 140: 5374-5381, 1999.

6. Larsson LI, Madsen OD, Serup P, Jonsson J, and Edlund H. Pancreatic-duodenal homeobox 1 -role in gastric endocrine patterning. *Mech Dev* 60: 175-184, 1996.

7. Karam SM, and Leblond CP. Dynamics of epithelial cells in the corpus of the mouse stomach. II. Outward migration of pit cells. *Anat Rec* 236: 280-296, 1993.

8. Arnold K, Sarkar A, Yram MA, Polo JM, Bronson R, Sengupta S, Seandel M, Geijsen N, and Hochedlinger K. Sox2(+) adult stem and progenitor cells are important for tissue regeneration and survival of mice. *Cell Stem Cell* 9: 317-329, 2011.

9. Choi E, Lantz TL, Vlacich G, Keeley TM, Samuelson LC, Coffey RJ, Goldenring JR, and Powell AE. Lrig1+ gastric isthmal progenitor cells restore normal gastric lineage cells during damage recovery in adult mouse stomach. *Gut* 67: 1595-1605, 2018.

10. Han S, Fink J, Jorg DJ, Lee E, Yum MK, Chatzeli L, Merker SR, Josserand M, Trendafilova T, Andersson-Rolf A, Dabrowska C, Kim H, Naumann R, Lee JH, Sasaki N, Mort RL, Basak O, Clevers H, Stange DE, Philpott A, Kim JK, Simons BD, and Koo BK. Defining the Identity and Dynamics of Adult Gastric Isthmus Stem Cells. *Cell Stem Cell* 25: 342-356.e347, 2019.

11. Scheitz CJ, Lee TS, McDermitt DJ, and Tumbar T. Defining a tissue stem cell-driven Runx1/Stat3 signalling axis in epithelial cancer. *EMBO J* 31: 4124-4139, 2012.

12. Yoshioka T, Fukuda A, Araki O, Ogawa S, Hanyu Y, Matsumoto Y, Yamaga Y, Nakanishi Y, Kawada K, Sakai Y, Chiba T, and Seno H. Bmi1 marks gastric stem cells located in the isthmus in mice. *J Pathol* 248: 179-190, 2019.

13. Levine JS, Nakane PK, and Allen RH. Immunocytochemical localization of human intrinsic factor: the nonstimulated stomach. *Gastroenterology* 79: 493-502, 1980.

14. Busslinger GA, Weusten BLA, Bogte A, Begthel H, Brosens LAA, and Clevers H. Human gastrointestinal epithelia of the esophagus, stomach, and duodenum resolved at single-cell resolution. *Cell Rep* 34: 108819, 2021.

15. Fakhry J, Stebbing MJ, Hunne B, Bayguinov Y, Ward SM, Sasse KC, Callaghan B, McQuade RM, and Furness JB. Relationships of endocrine cells to each other and to other cell types in the human gastric fundus and corpus. *Cell Tissue Res* 376: 37-49, 2019.

16. Jenny M, Uhl C, Roche C, Duluc I, Guillermin V, Guillemot F, Jensen J, Kedinger M, and Gradwohl G. Neurogenin3 is differentially required for endocrine cell fate specification in the intestinal and gastric epithelium. *EMBO J* 21: 6338-6347, 2002.

17. Li HJ, Johnston B, Aiello D, Caffrey DR, Giel-Moloney M, Rindi G, and Leiter AB. Distinct cellular origins for serotonin-expressing and enterochromaffin-like cells in the gastric corpus. *Gastroenterology* 146: 754-764 e753, 2014.

18. Sigal M, Logan CY, Kapalczynska M, Mollenkopf HJ, Berger H, Wiedenmann B, Nusse R, Amieva MR, and Meyer TF. Stromal R-spondin orchestrates gastric epithelial stem cells and gland homeostasis. *Nature* 548: 451-455, 2017.

19. Leushacke M, Ng A, Galle J, Loeffler M, and Barker N. Lgr5(+) gastric stem cells divide symmetrically to effect epithelial homeostasis in the pylorus. *Cell Rep* 5: 349-356, 2013.

20. Bjerknes M, and Cheng H. Multipotential stem cells in adult mouse gastric epithelium. *Am J Physiol Gastrointest Liver Physiol* 283: G767-777, 2002.

21. Barker N, van Es JH, Kuipers J, Kujala P, van den Born M, Cozijnsen M, Haegebarth A, Korving J, Begthel H, Peters PJ, and Clevers H. Identification of stem cells in small intestine and colon by marker gene Lgr5. *Nature* 449: 1003-1007, 2007.

22. Leblond CP, Stevens CE, and Bogoroch R. Histological Localization of Newly-formed Desoxyribonucleic Acid. *Science* 108: 531-533, 1948.

23. Corpron RE. The ultrastructure of the gastric mucosa in normal and hypophysectomized rats. *Am J Anat* 118: 53-90, 1966.

24. Yang DH, Tsuyama S, Ge YB, Wakamatsu D, Ohmori J, and Murata F. Proliferation and migration kinetics of stem cells in the rat fundic gland. *Histol Histopathol* 12: 719-727, 1997.

25. Kretzschmar K, and Watt FM. Lineage tracing. *Cell* 148: 33-45, 2012.

26. Schuijers J, van der Flier LG, van Es J, and Clevers H. Robust cre-mediated recombination in small intestinal stem cells utilizing the olfm4 locus. *Stem Cell Reports* 3: 234-241, 2014.

27. Lefebvre V, Dumitriu B, Penzo-Mendez A, Han Y, and Pallavi B. Control of cell fate and differentiation by Sry-related high-mobility-group box (Sox) transcription factors. *Int J Biochem Cell Biol* 39: 2195-2214, 2007.

28. Que J, Okubo T, Goldenring JR, Nam KT, Kurotani R, Morrisey EE, Taranova O, Pevny LH, and Hogan BL. Multiple dose-dependent roles for Sox2 in the patterning and differentiation of anterior foregut endoderm. *Development* 134: 2521-2531, 2007.

29. Powell AE, Wang Y, Li Y, Poulin EJ, Means AL, Washington MK, Higginbotham JN, Juchheim A, Prasad N, Levy SE, Guo Y, Shyr Y, Aronow BJ, Haigis KM, Franklin JL, and Coffey RJ. The pan-ErbB negative regulator Lrig1 is an intestinal stem cell marker that functions as a tumor suppressor. *Cell* 149: 146-158, 2012.

30. Wang Y, Poulin EJ, and Coffey RJ. LRIG1 is a triple threat: ERBB negative regulator, intestinal stem cell marker and tumour suppressor. *Br J Cancer* 108: 1765-1770, 2013.

31. Jacob B, Osato M, Yamashita N, Wang CQ, Taniuchi I, Littman DR, Asou N, and Ito Y. Stem cell exhaustion due to Runx1 deficiency is prevented by Evi5 activation in leukemogenesis. *Blood* 115: 1610-1620, 2010.

32. Banerji S, Cibulskis K, Rangel-Escareno C, Brown KK, Carter SL, Frederick AM, Lawrence MS, Sivachenko AY, Sougnez C, Zou L, Cortes ML, Fernandez-Lopez JC, Peng S, Ardlie KG, Auclair D, Bautista-Pina V, Duke F, Francis J, Jung J, Maffuz-Aziz A, Onofrio RC, Parkin M, Pho NH, Quintanar-Jurado V, Ramos AH, Rebollar-Vega R, Rodriguez-Cuevas S, Romero-Cordoba SL, Schumacher SE, Stransky N, Thompson KM, Uribe-Figueroa L, Baselga J, Beroukhim R, Polyak K, Sgroi DC, Richardson AL, Jimenez-Sanchez G, Lander ES, Gabriel SB, Garraway LA, Golub TR, Melendez-Zajgla J, Toker A, Getz G, Hidalgo-Miranda A, and Meyerson M. Sequence analysis of mutations and translocations across breast cancer subtypes. *Nature* 486: 405-409, 2012.

33. Matsuo J, Kimura S, Yamamura A, Koh CP, Hossain MZ, Heng DL, Kohu K, Voon DC, Hiai H, Unno M, So JB, Zhu F, Srivastava S, Teh M, Yeoh KG, Osato M, and Ito Y. Identification of Stem Cells in the Epithelium of the Stomach Corpus and Antrum of Mice. *Gastroenterology* 152: 218-231 e214, 2017.

34. Douchi D, Yamamura A, Matsuo J, Lee JW, Nuttonmanit N, Melissa Lim YH, Suda K, Shimura M, Chen S, Pang S, Kohu K, Kaneko M, Kiyonari H, Kaneda A, Yoshida H, Taniuchi I, Osato M, Yang H, Unno M, Bok-Yan So J, Yeoh KG, Huey Chuang LS, Bae SC, and Ito Y. A Point Mutation R122C in RUNX3 Promotes the Expansion of Isthmus Stem Cells and Inhibits Their Differentiation in the Stomach. *Cell Mol Gastroenterol Hepatol* 13: 1317-1345, 2022.

35. Yan KS, Chia LA, Li X, Ootani A, Su J, Lee JY, Su N, Luo Y, Heilshorn SC, Amieva MR, Sangiorgi E, Capecchi MR, and Kuo CJ. The intestinal stem cell markers Bmi1 and Lgr5 identify two functionally distinct populations. *Proc Natl Acad Sci U S A* 109: 466-471, 2012.

36. Fafilek B, Krausova M, Vojtechova M, Pospichalova V, Tumova L, Sloncova E, Huranova M, Stancikova J, Hlavata A, Svec J, Sedlacek R, Luksan O, Oliverius M, Voska L, Jirsa M, Paces J, Kolar M, Krivjanska M, Klimesova K, Tlaskalova-Hogenova H, and Korinek V. Troy, a tumor necrosis factor receptor family member, interacts with lgr5 to inhibit wnt signaling in intestinal stem cells. *Gastroenterology* 144: 381-391, 2013.

37. Stange DE, Koo BK, Huch M, Sibbel G, Basak O, Lyubimova A, Kujala P, Bartfeld S, Koster J, Geahlen JH, Peters PJ, van Es JH, van de Wetering M, Mills JC, and Clevers H. Differentiated Troy+ chief cells act as reserve stem cells to generate all lineages of the stomach epithelium. *Cell* 155: 357-368, 2013.

38. Clevers H. The intestinal crypt, a prototype stem cell compartment. *Cell* 154: 274-284, 2013.

39. Clevers H, Loh KM, and Nusse R. Stem cell signaling. An integral program for tissue renewal and regeneration: Wnt signaling and stem cell control. *Science* 346: 1248012, 2014.

40. Mills JC, and Shivdasani RA. Gastric epithelial stem cells. *Gastroenterology* 140: 412-424, 2011.

41. Demitrack ES, and Samuelson LC. Notch regulation of gastrointestinal stem cells. *J Physiol* 594: 4791-4803, 2016.

42. Kopan R, and Ilagan MX. The canonical Notch signaling pathway: unfolding the activation mechanism. *Cell* 137: 216-233, 2009.

43. VanDussen KL, Carulli AJ, Keeley TM, Patel SR, Puthoff BJ, Magness ST, Tran IT, Maillard I, Siebel C, Kolterud A, Grosse AS, Gumucio DL, Ernst SA, Tsai YH, Dempsey PJ, and Samuelson LC. Notch signaling modulates proliferation and differentiation of intestinal crypt base columnar stem cells. *Development* 139: 488-497, 2012.

44. Demitrack ES, Gifford GB, Keeley TM, Carulli AJ, VanDussen KL, Thomas D, Giordano TJ, Liu Z, Kopan R, and Samuelson LC. Notch signaling regulates gastric antral LGR5 stem cell function. *EMBO J* 34: 2522-2536, 2015.

45. Demitrack ES, Gifford GB, Keeley TM, Horita N, Todisco A, Turgeon DK, Siebel CW, and Samuelson LC. NOTCH1 and NOTCH2 regulate epithelial cell proliferation in mouse and human gastric corpus. *Am J Physiol Gastrointest Liver Physiol* 312: G133-G144, 2017.

46. Gifford GB, Demitrack ES, Keeley TM, Tam A, La Cunza N, Dedhia PH, Spence JR, Simeone DM, Saotome I, Louvi A, Siebel CW, and Samuelson LC. Notch1 and Notch2 receptors regulate mouse and human gastric antral epithelial cell homoeostasis. *Gut* 66: 1001-1011, 2017.

47. Bleuming SA, He XC, Kodach LL, Hardwick JC, Koopman FA, Ten Kate FJ, van Deventer SJ, Hommes DW, Peppelenbosch MP, Offerhaus GJ, Li L, and van den Brink GR. Bone morphogenetic protein signaling suppresses tumorigenesis at gastric epithelial transition zones in mice. *Cancer Res* 67: 8149-8155, 2007.

48. Todisco A, Mao M, Keeley TM, Ye W, Samuelson LC, and Eaton KA. Regulation of gastric epithelial cell homeostasis by gastrin and bone morphogenetic protein signaling. *Physiol Rep* 3: 2015.

49. Torihashi S, Hattori T, Hasegawa H, Kurahashi M, Ogaeri T, and Fujimoto T. The expression and crucial roles of BMP signaling in development of smooth muscle progenitor cells in the mouse embryonic gut. *Differentiation* 77: 277-289, 2009.

50. Lombardo Y, Scopelliti A, Cammareri P, Todaro M, Iovino F, Ricci-Vitiani L, Gulotta G, Dieli F, de Maria R, and Stassi G. Bone morphogenetic protein 4 induces differentiation of colorectal cancer stem cells and increases their response to chemotherapy in mice. *Gastroenterology* 140: 297-309, 2011.

51. He XC, Zhang J, Tong WG, Tawfik O, Ross J, Scoville DH, Tian Q, Zeng X, He X, Wiedemann LM, Mishina Y, and Li L. BMP signaling inhibits intestinal stem cell self-renewal through suppression of Wnt-beta-catenin signaling. *Nat Genet* 36: 1117-1121, 2004.

52. Wolffling S, Daddi AA, Imai-Matsushima A, Fritsche K, Goosmann C, Traulsen J, Lisle R, Schmid M, Reines-Benassar MDM, Pfannkuch L, Brinkmann V, Bornschein J, Malfertheiner P, Ordemann J, Link A, Meyer TF, and Boccellato F. EGF and BMPs Govern Differentiation and Patterning in Human Gastric Glands. *Gastroenterology* 161: 623-636 e616, 2021.

53. Qi Z, Li Y, Zhao B, Xu C, Liu Y, Li H, Zhang B, Wang X, Yang X, Xie W, Li B, Han JJ, and Chen YG. BMP restricts stemness of intestinal Lgr5(+) stem cells by directly suppressing their signature genes. *Nat Commun* 8: 13824, 2017.

54. Maloum F, Allaire JM, Gagne-Sansfacon J, Roy E, Belleville K, Sarret P, Morisset J, Carrier JC, Mishina Y, Kaestner KH, and Perreault N. Epithelial BMP signaling is required for proper specification of epithelial cell lineages and gastric endocrine cells. *Am J Physiol Gastrointest Liver Physiol* 300: G1065-1079, 2011.

55. Kapalczynska M, Lin M, Maertzdorf J, Heuberger J, Muellerke S, Zuo X, Vidal R, Shureiqi I, Fischer AS, Sauer S, Berger H, Kidess E, Mollenkopf HJ, Tacke F, Meyer TF, and Sigal M. BMP feed-forward loop promotes terminal differentiation in gastric glands and is interrupted by H. pylori-driven inflammation. *Nat Commun* 13: 1577, 2022.

56. Takabayashi H, Shinohara M, Mao M, Phaosawasdi P, El-Zaatari M, Zhang M, Ji T, Eaton KA, Dang D, Kao J, and Todisco A. Anti-inflammatory activity of bone morphogenetic protein signaling pathways in stomachs of mice. *Gastroenterology* 147: 396-406 e397, 2014.

57. Bragdon B, Moseychuk O, Saldanha S, King D, Julian J, and Nohe A. Bone morphogenetic proteins: a critical review. *Cell Signal* 23: 609-620, 2011.

58. Todisco A. Regulation of Gastric Metaplasia, Dysplasia, and Neoplasia by Bone Morphogenetic Protein Signaling. *Cell Mol Gastroenterol Hepatol* 3: 339-347, 2017.

59. Hsu DR, Economides AN, Wang X, Eimon PM, and Harland RM. The Xenopus dorsalizing factor Gremlin identifies a novel family of secreted proteins that antagonize BMP activities. *Mol Cell* 1: 673-683, 1998.

60. Shinohara M, Mao M, Keeley TM, El-Zaatari M, Lee HJ, Eaton KA, Samuelson LC, Merchant JL, Goldenring JR, and Todisco A. Bone morphogenetic protein signaling regulates gastric epithelial cell development and proliferation in mice. *Gastroenterology* 139: 2050-2060 e2052, 2010.

61. Roy SAB, Allaire JM, Ouellet C, Maloum-Rami F, Pomerleau V, Lemieux E, Babeu JP, Rousseau J, Paquet M, Garde-Granger P, Boudreau F, and Perreault N. Loss

of mesenchymal bone morphogenetic protein signaling leads to development of reactive stroma and initiation of the gastric neoplastic cascade. *Sci Rep* 6: 32759, 2016.

62. Lim J, Burclaff J, He G, Mills JC, and Long F. Unintended targeting of Dmp1-Cre reveals a critical role for Bmpr1a signaling in the gastrointestinal mesenchyme of adult mice. *Bone Res* 5: 16049, 2017.

63. Karam SM, and Leblond CP. Dynamics of epithelial cells in the corpus of the mouse stomach. III. Inward migration of neck cells followed by progressive transformation into zymogenic cells. *Anat Rec* 236: 297-313, 1993.

64. Verzi MP, Khan AH, Ito S, and Shivdasani RA. Transcription factor foxq1 controls mucin gene expression and granule content in mouse stomach surface mucous cells. *Gastroenterology* 135: 591-600, 2008.

65. Wee P, and Wang Z. Epidermal Growth Factor Receptor Cell Proliferation Signaling Pathways. *Cancers (Basel)* 9: 2017.

66. Tarnawski AS, and Ahluwalia A. The Critical Role of Growth Factors in Gastric Ulcer Healing: The Cellular and Molecular Mechanisms and Potential Clinical Implications. *Cells* 10: 2021.

67. Goldenring JR, Ray GS, Soroka CJ, Smith J, Modlin IM, Meise KS, and Coffey RJ, Jr. Overexpression of transforming growth factor-alpha alters differentiation of gastric cell lineages. *Dig Dis Sci* 41: 773-784, 1996.

68. Toubia N, and Schubert ML. Menetrier's Disease. *Curr Treat Options Gastroenterol* 11: 103-108, 2008.

69. Fiske WH, Tanksley J, Nam KT, Goldenring JR, Slebos RJ, Liebler DC, Abtahi AM, La Fleur B, Ayers GD, Lind CD, Washington MK, and Coffey RJ. Efficacy of cetuximab in the treatment of Menetrier's disease. *Sci Transl Med* 1: 8ra18, 2009.

70. Burdick JS, Chung E, Tanner G, Sun M, Paciga JE, Cheng JQ, Washington K, Goldenring JR, and Coffey RJ. Treatment of Menetrier's disease with a monoclonal antibody against the epidermal growth factor receptor. *N Engl J Med* 343: 1697-1701, 2000.

71. Settle SH, Washington K, Lind C, Itzkowitz S, Fiske WH, Burdick JS, Jerome WG, Ray M, Weinstein W, and Coffey RJ. Chronic treatment of Menetrier's disease with Erbitux: clinical efficacy and insight into pathophysiology. *Clin Gastroenterol Hepatol* 3: 654-659, 2005.

72. Choi E, Means AL, Coffey RJ, and Goldenring JR. Active Kras Expression in Gastric Isthmal Progenitor Cells Induces Foveolar Hyperplasia but Not Metaplasia. *Cell Mol Gastroenterol Hepatol* 7: 251-253 e251, 2019.

73. Schiemann U, Konturek J, Assert R, Rembiasz K, Domschke W, Konturek S, and Pfeiffer A. mRNA expression of EGF receptor ligands in atrophic gastritis before and after Helicobacter pylori eradication. *Med Sci Monit* 8: CR53-58, 2002.

74. Keates S, Keates AC, Katchar K, Peek RM, Jr., and Kelly CP. Helicobacter pylori induces up-regulation of the epidermal growth factor receptor in AGS gastric epithelial cells. *J Infect Dis* 196: 95-103, 2007.

75. Keates S, Keates AC, Nath S, Peek RM, Jr., and Kelly CP. Transactivation of the epidermal growth factor receptor by cag+ Helicobacter pylori induces upregulation of the early growth response gene Egr-1 in gastric epithelial cells. *Gut* 54: 1363-1369, 2005.

76. Yan F, Cao H, Chaturvedi R, Krishna U, Hobbs SS, Dempsey PJ, Peek RM, Jr., Cover TL, Washington MK, Wilson KT, and Polk DB. Epidermal growth factor receptor activation protects gastric epithelial cells from Helicobacter pylori-induced apoptosis. *Gastroenterology* 136: 1297-1307, e1291-1293, 2009.

77. Bartfeld S, Bayram T, van de Wetering M, Huch M, Begthel H, Kujala P, Vries R, Peters PJ, and Clevers H. In vitro expansion of human gastric epithelial stem cells and their responses to bacterial infection. *Gastroenterology* 148: 126-136.e126, 2015.

78. Noguchi TK, Ninomiya N, Sekine M, Komazaki S, Wang PC, Asashima M, and Kurisaki A. Generation of stomach tissue from mouse embryonic stem cells. *Nat Cell Biol* 17: 984-993, 2015.

79. Schumacher MA, Aihara E, Feng R, Engevik A, Shroyer NF, Ottemann KM, Worrell RT, Montrose MH, Shivdasani RA, and Zavros Y. The use of murine-derived fundic organoids in studies of gastric physiology. *J Physiol* 593: 1809-1827, 2015.

80. Nitsche H, Ramamoorthy S, Sareban M, Pausawasdi N, and Todisco A. Functional role of bone morphogenetic protein-4 in isolated canine parietal cells. *Am J Physiol Gastrointest Liver Physiol* 293: G607-614, 2007.

81. Speer AL, Al Alam D, Sala FG, Ford HR, Bellusci S, and Grikscheit TC. Fibroblast growth factor 10-fibroblast growth factor receptor 2b mediated signaling is not required for adult glandular stomach homeostasis. *PLoS One* 7: e49127, 2012.

82. Ramsey VG, Doherty JM, Chen CC, Stappenbeck TS, Konieczny SF, and Mills JC. The maturation of mucus-secreting gastric epithelial progenitors into digestive-enzyme secreting zymogenic cells requires Mist1. *Development* 134: 211-222, 2007.

83. Bredemeyer AJ, Geahlen JH, Weis VG, Huh WJ, Zinselmeyer BH, Srivatsan S, Miller MJ, Shaw AS, and Mills JC. The gastric epithelial progenitor cell niche and differentiation of the zymogenic (chief) cell lineage. *Dev Biol* 325: 211-224, 2009.

84. Huh WJ, Esen E, Geahlen JH, Bredemeyer AJ, Lee AH, Shi G, Konieczny SF, Glimcher LH, and Mills JC. XBP1 controls maturation of gastric zymogenic cells by induction of MIST1 and expansion of the rough endoplasmic reticulum. *Gastroenterology* 139: 2038-2049, 2010.

85. Burclaff J, Willet SG, Saenz JB, and Mills JC. Proliferation and Differentiation of Gastric Mucous Neck and Chief Cells During Homeostasis and Injury-induced Metaplasia. *Gastroenterology* 158: 598-609 e595, 2020.

86. Schmidt PH, Lee JR, Joshi V, Playford RJ, Poulsom R, Wright NA, and Goldenring JR. Identification of a metaplastic cell lineage associated with human gastric adenocarcinoma. *Lab Invest* 79: 639-646, 1999.

87. Fox JG, Lee A, Otto G, Taylor NS, and Murphy JC. Helicobacter felis gastritis in gnotobiotic rats: an animal model of Helicobacter pylori gastritis. *Infect Immun* 59: 785-791, 1991.

88. Nam KT, Lee HJ, Sousa JF, Weis VG, O'Neal RL, Finke PE, Romero-Gallo J, Shi G, Mills JC, Peek RM, Jr., Konieczny SF, and Goldenring JR. Mature chief cells are cryptic progenitors for metaplasia in the stomach. *Gastroenterology* 139: 2028-2037.e2029, 2010.

89. Goldenring JR, Ray GS, Coffey RJ, Meunier PC, Haley PJ, Barnes TB, and Car BD. Reversible drug-induced oxyntic atrophy in rats. *Gastroenterology* 118: 1080-1093, 2000.

90. Huh WJ, Khurana SS, Geahlen JH, Kohli K, Waller RA, and Mills JC. Tamoxifen induces rapid, reversible atrophy, and metaplasia in mouse stomach. *Gastroenterology* 142: 21-24 e27, 2012.

91. Leushacke M, Tan SH, Wong A, Swathi Y, Hajamohideen A, Tan LT, Goh J, Wong E, Denil S, Murakami K, and Barker N. Lgr5-expressing chief cells drive epithelial regeneration and cancer in the oxyntic stomach. *Nat Cell Biol* 19: 774-786, 2017.

92. Mills JC, and Goldenring JR. Metaplasia in the Stomach Arises From Gastric Chief Cells. *Cell Mol Gastroenterol Hepatol* 4: 85-88, 2017.

93. Radyk MD, Burclaff J, Willet SG, and Mills JC. Metaplastic Cells in the Stomach Arise, Independently of Stem Cells, via Dedifferentiation or Transdifferentiation of Chief Cells. *Gastroenterology* 154: 839-843.e832, 2018.

94. Bockerstett KA, Lewis SA, Wolf KJ, Noto CN, Jackson NM, Ford EL, Ahn TH, and DiPaolo RJ. Single-cell transcriptional analyses of spasmolytic polypeptide-expressing metaplasia arising from acute drug injury and chronic inflammation in the stomach. *Gut* 69: 1027-1038, 2020.

95. Caldwell B, Meyer AR, Weis JA, Engevik AC, and Choi E. Chief cell plasticity is the origin of metaplasia following acute injury in the stomach mucosa. *Gut* 71: 1068-1077, 2022.

96. Lee JH, Kim S, Han S, Min J, Caldwell B, Bamford AD, Rocha ASB, Park J, Lee S, Wu SS, Lee H, Fink J, Pilat-Carotta S, Kim J, Josserand M, Szep-Bakonyi R, An Y, Ju YS, Philpott A, Simons BD, Stange DE, Choi E, Koo BK, and Kim JK. p57(Kip2) imposes the reserve stem cell state of gastric chief cells. *Cell Stem Cell* 29: 826-839.e829, 2022.

97. Ru Y, Chen XJ, Zhao ZW, Zhang PF, Feng SH, Gao Q, Gao SG, and Feng XS. CyclinD1 and p57(kip2) as biomarkers in differentiation, metastasis and prognosis of gastric cardia adenocarcinoma. *Oncotarget* 8: 73860-73870, 2017.

98. Matsumoto A, Takeishi S, Kanie T, Susaki E, Onoyama I, Tateishi Y, Nakayama K, and Nakayama KI. p57 is required for quiescence and maintenance of adult hematopoietic stem cells. *Cell Stem Cell* 9: 262-271, 2011.

99. Tesio M, and Trumpp A. Breaking the cell cycle of HSCs by p57 and friends. *Cell Stem Cell* 9: 187-192, 2011.

100. Zou P, Yoshihara H, Hosokawa K, Tai I, Shinmyozu K, Tsukahara F, Maru Y, Nakayama K, Nakayama KI, and Suda T. p57(Kip2) and p27(Kip1) cooperate to

maintain hematopoietic stem cell quiescence through interactions with Hsc70. *Cell Stem Cell* 9: 247-261, 2011.

101. Sato T, Vries RG, Snippert HJ, van de Wetering M, Barker N, Stange DE, van Es JH, Abo A, Kujala P, Peters PJ, and Clevers H. Single Lgr5 stem cells build crypt-villus structures in vitro without a mesenchymal niche. *Nature* 459: 262-265, 2009.

102. McCracken KW, Cata EM, Crawford CM, Sinagoga KL, Schumacher M, Rockich BE, Tsai YH, Mayhew CN, Spence JR, Zavros Y, and Wells JM. Modelling human development and disease in pluripotent stem-cell-derived gastric organoids. *Nature* 516: 400-404, 2014.

103. McCracken KW, Aihara E, Martin B, Crawford CM, Broda T, Treguier J, Zhang X, Shannon JM, Montrose MH, and Wells JM. Wnt/beta-catenin promotes gastric fundus specification in mice and humans. *Nature* 541: 182-187, 2017.

104. Fujii M, Clevers H, and Sato T. Modeling Human Digestive Diseases With CRISPR-Cas9-Modified Organoids. *Gastroenterology* 156: 562-576, 2019.

105. Lancaster MA, and Huch M. Disease modelling in human organoids. *Dis Model Mech* 12: 2019.

106. Pompaiah M, and Bartfeld S. Gastric Organoids: An Emerging Model System to Study Helicobacter pylori Pathogenesis. *Curr Top Microbiol Immunol* 400: 149-168, 2017.

107. Tsai YH, Czerwinski M, Wu A, Dame MK, Attili D, Hill E, Colacino JA, Nowacki LM, Shroyer NF, Higgins PDR, Kao JY, and Spence JR. A Method for Cryogenic Preservation of Human Biopsy Specimens and Subsequent Organoid Culture. *Cell Mol Gastroenterol Hepatol* 6: 218-222 e217, 2018.

108. Hinman SS, Wang Y, and Allbritton NL. Photopatterned Membranes and Chemical Gradients Enable Scalable Phenotypic Organization of Primary Human Colon Epithelial Models. *Anal Chem* 91: 15240-15247, 2019.

109. Boccellato F, Woelffling S, Imai-Matsushima A, Sanchez G, Goosmann C, Schmid M, Berger H, Morey P, Denecke C, Ordemann J, and Meyer TF. Polarised epithelial monolayers of the gastric mucosa reveal insights into mucosal homeostasis and defence against infection. *Gut* 68: 400-413, 2019.

110. Baker NE. Molecular cloning of sequences from wingless, a segment polarity gene in Drosophila: the spatial distribution of a transcript in embryos. *EMBO J* 6: 1765-1773, 1987.

111. Rijsewijk F, Schuermann M, Wagenaar E, Parren P, Weigel D, and Nusse R. The Drosophila homolog of the mouse mammary oncogene int-1 is identical to the segment polarity gene wingless. *Cell* 50: 649-657, 1987.

112. Najdi R, Proffitt K, Sprowl S, Kaur S, Yu J, Covey TM, Virshup DM, and Waterman ML. A uniform human Wnt expression library reveals a shared secretory pathway and unique signaling activities. *Differentiation* 84: 203-213, 2012.

113. Kabiri Z, Greicius G, Madan B, Biechele S, Zhong Z, Zaribafzadeh H, Edison, Aliyev J, Wu Y, Bunte R, Williams BO, Rossant J, and Virshup DM. Stroma provides an

intestinal stem cell niche in the absence of epithelial Wnts. *Development* 141: 2206-2215, 2014.

114. Banziger C, Soldini D, Schutt C, Zipperlen P, Hausmann G, and Basler K. Wntless, a conserved membrane protein dedicated to the secretion of Wnt proteins from signaling cells. *Cell* 125: 509-522, 2006.

115. San Roman AK, Jayewickreme CD, Murtaugh LC, and Shivdasani RA. Wnt secretion from epithelial cells and subepithelial myofibroblasts is not required in the mouse intestinal stem cell niche in vivo. *Stem Cell Reports* 2: 127-134, 2014.

116. Davidson G. LRPs in WNT Signalling. *Handb Exp Pharmacol* 269: 45-73, 2021.

117. Niehrs C. The complex world of WNT receptor signalling. *Nat Rev Mol Cell Biol* 13: 767-779, 2012.

118. Clevers H. Wnt/beta-catenin signaling in development and disease. *Cell* 127: 469-480, 2006.

119. Stamos JL, Chu ML, Enos MD, Shah N, and Weis WI. Structural basis of GSK-3 inhibition by N-terminal phosphorylation and by the Wnt receptor LRP6. *Elife* 3: e01998, 2014.

120. Cadigan KM. TCFs and Wnt/beta-catenin signaling: more than one way to throw the switch. *Curr Top Dev Biol* 98: 1-34, 2012.

121. Mosimann C, Hausmann G, and Basler K. Beta-catenin hits chromatin: regulation of Wnt target gene activation. *Nat Rev Mol Cell Biol* 10: 276-286, 2009.

122. Holland JD, Klaus A, Garratt AN, and Birchmeier W. Wnt signaling in stem and cancer stem cells. *Curr Opin Cell Biol* 25: 254-264, 2013.

123. Katoh M, and Katoh M. Molecular genetics and targeted therapy of WNT-related human diseases (Review). *Int J Mol Med* 40: 587-606, 2017.

124. de Lau W, Peng WC, Gros P, and Clevers H. The R-spondin/Lgr5/Rnf43 module: regulator of Wnt signal strength. *Genes Dev* 28: 305-316, 2014.

125. Ruffner H, Sprunger J, Charlat O, Leighton-Davies J, Grosshans B, Salathe A, Zietzling S, Beck V, Therier M, Isken A, Xie Y, Zhang Y, Hao H, Shi X, Liu D, Song Q, Clay I, Hintzen G, Tchorz J, Bouchez LC, Michaud G, Finan P, Myer VE, Bouwmeester T, Porter J, Hild M, Bassilana F, Parker CN, and Cong F. R-Spondin potentiates Wnt/beta-catenin signaling through orphan receptors LGR4 and LGR5. *PLoS One* 7: e40976, 2012.

126. Hao HX, Xie Y, Zhang Y, Charlat O, Oster E, Avello M, Lei H, Mickanin C, Liu D, Ruffner H, Mao X, Ma Q, Zamponi R, Bouwmeester T, Finan PM, Kirschner MW, Porter JA, Serluca FC, and Cong F. ZNRF3 promotes Wnt receptor turnover in an R-spondin-sensitive manner. *Nature* 485: 195-200, 2012.

127. Koo BK, Spit M, Jordens I, Low TY, Stange DE, van de Wetering M, van Es JH, Mohammed S, Heck AJ, Maurice MM, and Clevers H. Tumour suppressor RNF43 is a stem-cell E3 ligase that induces endocytosis of Wnt receptors. *Nature* 488: 665-669, 2012.

128. Seshagiri S, Stawiski EW, Durinck S, Modrusan Z, Storm EE, Conboy CB, Chaudhuri S, Guan Y, Janakiraman V, Jaiswal BS, Guillory J, Ha C, Dijkgraaf GJ, Stinson J, Gnad F, Huntley MA, Degenhardt JD, Haverty PM, Bourgon R, Wang W, Koeppen H, Gentleman R, Starr TK, Zhang Z, Largaespada DA, Wu TD, and de Sauvage FJ. Recurrent R-spondin fusions in colon cancer. *Nature* 488: 660-664, 2012.

129. Wizenty J, Mullerke S, Kolesnichenko M, Heuberger J, Lin M, Fischer AS, Mollenkopf HJ, Berger H, Tacke F, and Sigal M. Gastric stem cells promote inflammation and gland remodeling in response to Helicobacter pylori via Rspo3-Lgr4 axis. *EMBO J* 41: e109996, 2022.

130. Rattner A, Hsieh JC, Smallwood PM, Gilbert DJ, Copeland NG, Jenkins NA, and Nathans J. A family of secreted proteins contains homology to the cysteine-rich ligand-binding domain of frizzled receptors. *Proc Natl Acad Sci U S A* 94: 2859-2863, 1997.

131. Bovolenta P, Esteve P, Ruiz JM, Cisneros E, and Lopez-Rios J. Beyond Wnt inhibition: new functions of secreted Frizzled-related proteins in development and disease. *J Cell Sci* 121: 737-746, 2008.

132. Bafico A, Liu G, Yaniv A, Gazit A, and Aaronson SA. Novel mechanism of Wnt signalling inhibition mediated by Dickkopf-1 interaction with LRP6/Arrow. *Nat Cell Biol* 3: 683-686, 2001.

133. Kuhnert F, Davis CR, Wang HT, Chu P, Lee M, Yuan J, Nusse R, and Kuo CJ. Essential requirement for Wnt signaling in proliferation of adult small intestine and colon revealed by adenoviral expression of Dickkopf-1. *Proc Natl Acad Sci U S A* 101: 266-271, 2004.

134. Pinto D, Gregorieff A, Begthel H, and Clevers H. Canonical Wnt signals are essential for homeostasis of the intestinal epithelium. *Genes Dev* 17: 1709-1713, 2003.

135. Hsieh JC, Kodjabachian L, Rebbert ML, Rattner A, Smallwood PM, Samos CH, Nusse R, Dawid IB, and Nathans J. A new secreted protein that binds to Wnt proteins and inhibits their activities. *Nature* 398: 431-436, 1999.

136. Li X, Zhang Y, Kang H, Liu W, Liu P, Zhang J, Harris SE, and Wu D. Sclerostin binds to LRP5/6 and antagonizes canonical Wnt signaling. *J Biol Chem* 280: 19883-19887, 2005.

137. Zhu W, Shiojima I, Ito Y, Li Z, Ikeda H, Yoshida M, Naito AT, Nishi J, Ueno H, Umezawa A, Minamino T, Nagai T, Kikuchi A, Asashima M, and Komuro I. IGFBP-4 is an inhibitor of canonical Wnt signalling required for cardiogenesis. *Nature* 454: 345-349, 2008.

138. Farin HF, Van Es JH, and Clevers H. Redundant sources of Wnt regulate intestinal stem cells and promote formation of Paneth cells. *Gastroenterology* 143: 1518-1529 e1517, 2012.

139. Sato T, Stange DE, Ferrante M, Vries RG, Van Es JH, Van den Brink S, Van Houdt WJ, Pronk A, Van Gorp J, Siersema PD, and Clevers H. Long-term expansion of epithelial organoids from human colon, adenoma, adenocarcinoma, and Barrett's epithelium. *Gastroenterology* 141: 1762-1772, 2011.

140. Valenta T, Degirmenci B, Moor AE, Herr P, Zimmerli D, Moor MB, Hausmann G, Cantù C, Aguet M, and Basler K. Wnt Ligands Secreted by Subepithelial Mesenchymal Cells Are Essential for the Survival of Intestinal Stem Cells and Gut Homeostasis. *Cell Rep* 15: 911-918, 2016.

141. Stzepourginski I, Nigro G, Jacob JM, Dulauroy S, Sansonetti PJ, Eberl G, and Peduto L. CD34+ mesenchymal cells are a major component of the intestinal stem cells niche at homeostasis and after injury. *Proc Natl Acad Sci U S A* 114: E506-E513, 2017.

142. Greicius G, Kabiri Z, Sigmundsson K, Liang C, Bunte R, Singh MK, and Virshup DM. pericryptal stromal cells are the critical source of Wnts and RSPO3 for murine intestinal stem cells in vivo. *Proc Natl Acad Sci U S A* 115: E3173-E3181, 2018.

143. Aoki R, Shoshkes-Carmel M, Gao N, Shin S, May CL, Golson ML, Zahm AM, Ray M, Wiser CL, Wright CV, and Kaestner KH. Foxl1-expressing mesenchymal cells constitute the intestinal stem cell niche. *Cell Mol Gastroenterol Hepatol* 2: 175-188, 2016.

144. McCarthy N, Manieri E, Storm EE, Saadatpour A, Luoma AM, Kapoor VN, Madha S, Gaynor LT, Cox C, Keerthivasan S, Wucherpfennig K, Yuan GC, de Sauvage FJ, Turley SJ, and Shivdasani RA. Distinct Mesenchymal Cell Populations Generate the Essential Intestinal BMP Signaling Gradient. *Cell Stem Cell* 26: 391-402 e395, 2020.

145. Degirmenci B, Valenta T, Dimitrieva S, Hausmann G, and Basler K. GLI1-expressing mesenchymal cells form the essential Wnt-secreting niche for colon stem cells. *Nature* 558: 449-453, 2018.

146. Shoshkes-Carmel M, Wang YJ, Wangensteen KJ, Toth B, Kondo A, Massasa EE, Itzkovitz S, and Kaestner KH. Subepithelial telocytes are an important source of Wnts that supports intestinal crypts. *Nature* 557: 242-246, 2018.

147. Fischer AS, Mullerke S, Arnold A, Heuberger J, Berger H, Lin M, Mollenkopf HJ, Wizenty J, Horst D, Tacke F, and Sigal M. R-spondin/YAP axis promotes gastric oxyntic gland regeneration and Helicobacter pylori-associated metaplasia in mice. *J Clin Invest* 132: 2022.

148. Kim JE, Fei L, Yin WC, Coquenlorge S, Rao-Bhatia A, Zhang X, Shi SSW, Lee JH, Hahn NA, Rizvi W, Kim KH, Sung HK, Hui CC, Guo G, and Kim TH. Single cell and genetic analyses reveal conserved populations and signaling mechanisms of gastrointestinal stromal niches. *Nat Commun* 11: 334, 2020.

149. Broda TR, McCracken KW, and Wells JM. Generation of human antral and fundic gastric organoids from pluripotent stem cells. *Nat Protoc* 14: 28-50, 2019.

150. Sigal M, Reinés MDM, Müllerke S, Fischer C, Kapalczynska M, Berger H, Bakker ERM, Mollenkopf HJ, Rothenberg ME, Wiedenmann B, Sauer S, and Meyer TF. R-spondin-3 induces secretory, antimicrobial Lgr5. *Nat Cell Biol* 21: 812-823, 2019.

151. Bertaux-Skeirik N, Wunderlich M, Teal E, Chakrabarti J, Biesiada J, Mahe M, Sundaram N, Gabre J, Hawkins J, Jian G, Engevik AC, Yang L, Wang J, Goldenring JR, Qualls JE, Medvedovic M, Helmrath MA, Diwan T, Mulloy JC, and Zavros Y. CD44 variant isoform 9 emerges in response to injury and contributes to the regeneration of the gastric epithelium. *J Pathol* 242: 463-475, 2017.

152. Gracz AD, Fuller MK, Wang F, Li L, Stelzner M, Dunn JC, Martin MG, and Magness ST. Brief report: CD24 and CD44 mark human intestinal epithelial cell populations with characteristics of active and facultative stem cells. *Stem Cells* 31: 2024-2030, 2013.

153. Khurana SS, Riehl TE, Moore BD, Fassan M, Rugge M, Romero-Gallo J, Noto J, Peek RM, Jr., Stenson WF, and Mills JC. The hyaluronic acid receptor CD44 coordinates normal and metaplastic gastric epithelial progenitor cell proliferation. *J Biol Chem* 288: 16085-16097, 2013.

154. Wada T, Ishimoto T, Seishima R, Tsuchihashi K, Yoshikawa M, Oshima H, Oshima M, Masuko T, Wright NA, Furuhashi S, Hirashima K, Baba H, Kitagawa Y, Saya H, and Nagano O. Functional role of CD44v-xCT system in the development of spasmolytic polypeptide-expressing metaplasia. *Cancer Sci* 104: 1323-1329, 2013.

155. Willet SG, Thanintorn N, McNeill H, Huh SH, Ornitz DM, Huh WJ, Hoft SG, DiPaolo RJ, and Mills JC. SOX9 governs gastric mucous neck cell identity and is required for injury-induced metaplasia. *Cell Mol Gastroenterol Hepatol* 2023.

156. Wend P, Runke S, Wend K, Anchondo B, Yesayan M, Jardon M, Hardie N, Loddenkemper C, Ulasov I, Lesniak MS, Wolsky R, Bentolila LA, Grant SG, Elashoff D, Lehr S, Latimer JJ, Bose S, Sattar H, Krum SA, and Miranda-Carboni GA. WNT10B/beta-catenin signalling induces HMGA2 and proliferation in metastatic triple-negative breast cancer. *EMBO Mol Med* 5: 264-279, 2013.

157. Khalaf AM, Fuentes D, Morshid AI, Burke MR, Kaseb AO, Hassan M, Hazle JD, and Elsayes KM. Role of Wnt/beta-catenin signaling in hepatocellular carcinoma, pathogenesis, and clinical significance. *J Hepatocell Carcinoma* 5: 61-73, 2018.

158. Rapp J, Jaromi L, Kvell K, Miskei G, and Pongracz JE. WNT signaling - lung cancer is no exception. *Respir Res* 18: 167, 2017.

159. Ram Makena M, Gatla H, Verlekar D, Sukhavasi S, M KP, and K CP. Wnt/beta-Catenin Signaling: The Culprit in Pancreatic Carcinogenesis and Therapeutic Resistance. *Int J Mol Sci* 20: 2019.

160. Murillo-Garzon V, and Kypta R. WNT signalling in prostate cancer. *Nat Rev Urol* 14: 683-696, 2017.

161. Cancer Genome Atlas N. Comprehensive molecular characterization of human colon and rectal cancer. *Nature* 487: 330-337, 2012.

162. Nathke I. Cytoskeleton out of the cupboard: colon cancer and cytoskeletal changes induced by loss of APC. *Nat Rev Cancer* 6: 967-974, 2006.

163. Christie M, Jorissen RN, Mouradov D, Sakthianandeswaren A, Li S, Day F, Tsui C, Lipton L, Desai J, Jones IT, McLaughlin S, Ward RL, Hawkins NJ, Ruszkiewicz AR, Moore J, Burgess AW, Busam D, Zhao Q, Strausberg RL, Simpson AJ, Tomlinson IP, Gibbs P, and Sieber OM. Different APC genotypes in proximal and distal sporadic colorectal cancers suggest distinct WNT/beta-catenin signalling thresholds for tumourigenesis. *Oncogene* 32: 4675-4682, 2013.

164. Korinek V, Barker N, Morin PJ, van Wichen D, de Weger R, Kinzler KW, Vogelstein B, and Clevers H. Constitutive transcriptional activation by a beta-catenin-Tcf complex in APC-/- colon carcinoma. *Science* 275: 1784-1787, 1997.

165. Galiatsatos P, and Foulkes WD. Familial adenomatous polyposis. *Am J Gastroenterol* 101: 385-398, 2006.

166. Kanth P, Grimmett J, Champine M, Burt R, and Samadder NJ. Hereditary Colorectal Polyposis and Cancer Syndromes: A Primer on Diagnosis and Management. *Am J Gastroenterol* 112: 1509-1525, 2017.

167. Sammour T, Hayes IP, Hill AG, Macrae FA, and Winter DC. Familial colorectal cancer syndromes: an overview of clinical management. *Expert Rev Gastroenterol Hepatol* 9: 757-764, 2015.

168. Kinzler KW, and Vogelstein B. Lessons from hereditary colorectal cancer. *Cell* 87: 159-170, 1996.

169. Groden J, Thliveris A, Samowitz W, Carlson M, Gelbert L, Albertsen H, Joslyn G, Stevens J, Spirio L, Robertson M, and et al. Identification and characterization of the familial adenomatous polyposis coli gene. *Cell* 66: 589-600, 1991.

170. Min BH, Hwang J, Kim NK, Park G, Kang SY, Ahn S, Ahn S, Ha SY, Lee YK, Kushima R, Van Vrancken M, Kim MJ, Park C, Park HY, Chae J, Jang SS, Kim SJ, Kim YH, Kim JI, and Kim KM. Dysregulated Wnt signalling and recurrent mutations of the tumour suppressor RNF43 in early gastric carcinogenesis. *J Pathol* 240: 304-314, 2016.

171. Cancer Genome Atlas Research N. Comprehensive molecular characterization of gastric adenocarcinoma. *Nature* 513: 202-209, 2014.

172. Dinarvand P, Davaro EP, Doan JV, Ising ME, Evans NR, Phillips NJ, Lai J, and Guzman MA. Familial Adenomatous Polyposis Syndrome: An Update and Review of Extraintestinal Manifestations. *Arch Pathol Lab Med* 143: 1382-1398, 2019.

173. Ksiaa F, Ziadi S, Amara K, Korbi S, and Trimeche M. Biological significance of promoter hypermethylation of tumor-related genes in patients with gastric carcinoma. *Clin Chim Acta* 404: 128-133, 2009.

174. Weiss JM, Gupta S, Burke CA, Axell L, Chen LM, Chung DC, Clayback KM, Dallas S, Felder S, Gbolahan O, Giardiello FM, Grady W, Hall MJ, Hampel H, Hodan R, Idos G, Kanth P, Katona B, Lamps L, Llor X, Lynch PM, Markowitz AJ, Pirzadeh-Miller S, Samadder NJ, Shibata D, Swanson BJ, Szymaniak BM, Wiesner GL, Wolf A, Yurgelun MB, Zakhour M, Darlow SD, Dwyer MA, and Campbell M. NCCN Guidelines(R) Insights: Genetic/Familial High-Risk Assessment: Colorectal, Version 1.2021. *J Natl Compr Canc Netw* 19: 1122-1132, 2021.

175. Paszkowski J, Samborski P, Kucharski M, Cwalinski J, Banasiewicz T, and Plawski A. Endoscopic Surveillance and Treatment of Upper GI Tract Lesions in Patients with Familial Adenomatous Polyposis-A New Perspective on an Old Disease. *Genes (Basel)* 13: 2022.

176. Fukuda M, Ishigaki H, Sugimoto M, Mukaisho KI, Matsubara A, Ishida H, Moritani S, Itoh Y, Sugihara H, Andoh A, Ogasawara K, Murakami K, and Kushima R.

Histological analysis of fundic gland polyps secondary to PPI therapy. *Histopathology* 75: 537-545, 2019.

177. Odze RD, Marcial MA, and Antonioli D. Gastric fundic gland polyps: a morphological study including mucin histochemistry, stereometry, and MIB-1 immunohistochemistry. *Hum Pathol* 27: 896-903, 1996.

178. Abraham SC. Fundic gland polyps: common and occasionally problematic lesions. *Gastroenterol Hepatol (N Y)* 6: 48-51, 2010.

179. Genta RM, Schuler CM, Robiou CI, and Lash RH. No association between gastric fundic gland polyps and gastrointestinal neoplasia in a study of over 100,000 patients. *Clin Gastroenterol Hepatol* 7: 849-854, 2009.

180. Sonnenberg A, and Genta RM. Prevalence of benign gastric polyps in a large pathology database. *Dig Liver Dis* 47: 164-169, 2015.

181. Arnason T, Liang WY, Alfaro E, Kelly P, Chung DC, Odze RD, and Lauwers GY. Morphology and natural history of familial adenomatous polyposis-associated dysplastic fundic gland polyps. *Histopathology* 65: 353-362, 2014.

182. Martin FC, Chenevix-Trench G, and Yeomans ND. Systematic review with meta-analysis: fundic gland polyps and proton pump inhibitors. *Aliment Pharmacol Ther* 44: 915-925, 2016.

183. Tanaka M, Kataoka H, and Yagi T. Proton-pump inhibitor-induced fundic gland polyps with hematemesis. *Clin J Gastroenterol* 12: 193-195, 2019.

184. Tran-Duy A, Spaetgens B, Hoes AW, de Wit NJ, and Stehouwer CD. Use of Proton Pump Inhibitors and Risks of Fundic Gland Polyps and Gastric Cancer: Systematic Review and Meta-analysis. *Clin Gastroenterol Hepatol* 14: 1706-1719 e1705, 2016.

185. Kim JS, Chae HS, Kim HK, Cho YS, Park YW, Son HS, Han SW, and Choi KY. [Spontaneous resolution of multiple fundic gland polyps after cessation of treatment with omeprazole]. *Korean J Gastroenterol* 51: 305-308, 2008.

186. Franic TV, Judd LM, Robinson D, Barrett SP, Scarff KL, Gleeson PA, Samuelson LC, and Van Driel IR. Regulation of gastric epithelial cell development revealed in H(+)/K(+)-ATPase beta-subunit- and gastrin-deficient mice. *Am J Physiol Gastrointest Liver Physiol* 281: G1502-1511, 2001.

187. Rubio CA, and Miller ML. Fundic gland cysts in Atp4a-/- mice mimic fundic gland polyps in humans. *In Vivo* 23: 979-981, 2009.

188. Spicer Z, Miller ML, Andringa A, Riddle TM, Duffy JJ, Doetschman T, and Shull GE. Stomachs of mice lacking the gastric H,K-ATPase alpha -subunit have achlorhydria, abnormal parietal cells, and ciliated metaplasia. *J Biol Chem* 275: 21555-21565, 2000.

189. Shiotani A, Katsumata R, Gouda K, Fukushima S, Nakato R, Murao T, Ishii M, Fujita M, Matsumoto H, and Sakakibara T. Hypergastrinemia in Long-Term Use of Proton Pump Inhibitors. *Digestion* 97: 154-162, 2018.

190. Fossmark R, Jianu CS, Martinsen TC, Qvigstad G, Syversen U, and Waldum HL. Serum gastrin and chromogranin A levels in patients with fundic gland polyps caused by long-term proton-pump inhibition. *Scand J Gastroenterol* 43: 20-24, 2008.

191. Radulescu S, Ridgway RA, Cordero J, Athineos D, Salgueiro P, Poulsom R, Neumann J, Jung A, Patel S, Woodgett J, Barker N, Pritchard DM, Oien K, and Sansom OJ. Acute WNT signalling activation perturbs differentiation within the adult stomach and rapidly leads to tumour formation. *Oncogene* 32: 2048-2057, 2013.

192. Hayakawa Y, Ariyama H, Stancikova J, Sakitani K, Asfaha S, Renz BW, Dubeykovskaya ZA, Shibata W, Wang H, Westphalen CB, Chen X, Takemoto Y, Kim W, Khurana SS, Tailor Y, Nagar K, Tomita H, Hara A, Sepulveda AR, Setlik W, Gershon MD, Saha S, Ding L, Shen Z, Fox JG, Friedman RA, Konieczny SF, Worthley DL, Korinek V, and Wang TC. Mist1 Expressing Gastric Stem Cells Maintain the Normal and Neoplastic Gastric Epithelium and Are Supported by a Perivascular Stem Cell Niche. *Cancer Cell* 28: 800-814, 2015.

193. Douchi D, Yamamura A, Matsuo J, Melissa Lim YH, Nuttonmanit N, Shimura M, Suda K, Chen S, Pang S, Kohu K, Abe T, Shioi G, Kim G, Shabbir A, Srivastava S, Unno M, Bok-Yan So J, Teh M, Yeoh KG, Huey Chuang LS, and Ito Y. Induction of Gastric Cancer by Successive Oncogenic Activation in the Corpus. *Gastroenterology* 161: 1907-1923 e1926, 2021.

194. Powell AE, Vlacich G, Zhao ZY, McKinley ET, Washington MK, Manning HC, and Coffey RJ. Inducible loss of one Apc allele in Lrig1-expressing progenitor cells results in multiple distal colonic tumors with features of familial adenomatous polyposis. *Am J Physiol Gastrointest Liver Physiol* 307: G16-23, 2014.

195. Abraham SC, Nobukawa B, Giardiello FM, Hamilton SR, and Wu TT. Sporadic fundic gland polyps: common gastric polyps arising through activating mutations in the beta-catenin gene. *Am J Pathol* 158: 1005-1010, 2001.

196. Sekine S, Shibata T, Yamauchi Y, Nakanishi Y, Shimoda T, Sakamoto M, and Hirohashi S. Beta-catenin mutations in sporadic fundic gland polyps. *Virchows Arch* 440: 381-386, 2002.

197. Dickey W, Kenny BD, and McConnell JB. Prevalence of fundic gland polyps in a western European population. *J Clin Gastroenterol* 23: 73-75, 1996.

198. Mankaney G, Leone P, Cruise M, LaGuardia L, O'Malley M, Bhatt A, Church J, and Burke CA. Gastric cancer in FAP: a concerning rise in incidence. *Fam Cancer* 16: 371-376, 2017.

199. Bianchi LK, Burke CA, Bennett AE, Lopez R, Hasson H, and Church JM. Fundic gland polyp dysplasia is common in familial adenomatous polyposis. *Clin Gastroenterol Hepatol* 6: 180-185, 2008.

200. Jalving M, Koornstra JJ, Boersma-van Ek W, de Jong S, Karrenbeld A, Hollema H, de Vries EG, and Kleibeuker JH. Dysplasia in fundic gland polyps is associated with nuclear beta-catenin expression and relatively high cell turnover rates. *Scand J Gastroenterol* 38: 916-922, 2003.

201. Wood LD, Salaria SN, Cruise MW, Giardiello FM, and Montgomery EA. Upper GI tract lesions in familial adenomatous polyposis (FAP): enrichment of pyloric gland adenomas and other gastric and duodenal neoplasms. *Am J Surg Pathol* 38: 389-393, 2014.

202. Knudson AG. Two genetic hits (more or less) to cancer. *Nat Rev Cancer* 1: 157-162, 2001.

203. McCart AE, Vickaryous NK, and Silver A. Apc mice: models, modifiers and mutants. *Pathol Res Pract* 204: 479-490, 2008.

204. Abraham SC, Nobukawa B, Giardiello FM, Hamilton SR, and Wu TT. Fundic gland polyps in familial adenomatous polyposis: neoplasms with frequent somatic adenomatous polyposis coli gene alterations. *Am J Pathol* 157: 747-754, 2000.

205. Lamlum H, Ilyas M, Rowan A, Clark S, Johnson V, Bell J, Frayling I, Efstathiou J, Pack K, Payne S, Roylance R, Gorman P, Sheer D, Neale K, Phillips R, Talbot I, Bodmer W, and Tomlinson I. The type of somatic mutation at APC in familial adenomatous polyposis is determined by the site of the germline mutation: a new facet to Knudson's 'two-hit' hypothesis. *Nat Med* 5: 1071-1075, 1999.

206. Albuquerque C, Breukel C, van der Luijt R, Fidalgo P, Lage P, Slors FJ, Leitao CN, Fodde R, and Smits R. The 'just-right' signaling model: APC somatic mutations are selected based on a specific level of activation of the beta-catenin signaling cascade. *Hum Mol Genet* 11: 1549-1560, 2002.

207. Lewis A, Segditsas S, Deheragoda M, Pollard P, Jeffery R, Nye E, Lockstone H, Davis H, Clark S, Stamp G, Poulsom R, Wright N, and Tomlinson I. Severe polyposis in Apc(1322T) mice is associated with submaximal Wnt signalling and increased expression of the stem cell marker Lgr5. *Gut* 59: 1680-1686, 2010.

208. Lähde M, Heino S, Högström J, Kaijalainen S, Anisimov A, Flanagan D, Kallio P, Leppänen VM, Ristimäki A, Ritvos O, Wu K, Tammela T, Hodder M, Sansom OJ, and Alitalo K. Expression of R-Spondin 1 in Apc. *Gastroenterology* 160: 245-259, 2021.

209. Langlands AJ, Carroll TD, Chen Y, and Nathke I. Chir99021 and Valproic acid reduce the proliferative advantage of Apc mutant cells. *Cell Death Dis* 9: 255, 2018.

210. Yan KS, Janda CY, Chang J, Zheng GXY, Larkin KA, Luca VC, Chia LA, Mah AT, Han A, Terry JM, Ootani A, Roelf K, Lee M, Yuan J, Li X, Bolen CR, Wilhelmy J, Davies PS, Ueno H, von Furstenberg RJ, Belgrader P, Ziraldo SB, Ordonez H, Henning SJ, Wong MH, Snyder MP, Weissman IL, Hsueh AJ, Mikkelsen TS, Garcia KC, and Kuo CJ. Non-equivalence of Wnt and R-spondin ligands during Lgr5(+) intestinal stem-cell self-renewal. *Nature* 545: 238-242, 2017.

211. Leedham SJ, Rodenas-Cuadrado P, Howarth K, Lewis A, Mallappa S, Segditsas S, Davis H, Jeffery R, Rodriguez-Justo M, Keshav S, Travis SP, Graham TA, East J, Clark S, and Tomlinson IP. A basal gradient of Wnt and stem-cell number influences regional tumour distribution in human and mouse intestinal tracts. *Gut* 62: 83-93, 2013.

212. Albuquerque C, Baltazar C, Filipe B, Penha F, Pereira T, Smits R, Cravo M, Lage P, Fidalgo P, Claro I, Rodrigues P, Veiga I, Ramos JS, Fonseca I, Leitao CN, and Fodde R. Colorectal cancers show distinct mutation spectra in members of the canonical WNT

signaling pathway according to their anatomical location and type of genetic instability. *Genes Chromosomes Cancer* 49: 746-759, 2010.

CHAPTER II

Differential Sensitivity to Wnt Signaling Gradients in Human Gastric Organoids Derived from Corpus and Antrum

This chapter is adapted from the following published manuscript:
McGowan, KM, Delgado, E, Hibdon, ES, Samuelson, LC. Differential sensitivity to Wnt signaling gradients in human gastric organoids derived from corpus and antrum. *Am J Physiol Gastrointest Liver Physiol* 325: G0-G0, 2023

2.1 Summary

Wnt signaling regulates gastric stem cell proliferation and differentiation. While similar Wnt gradients exist within the corpus and antrum of the human stomach, there are striking differences in gland architecture and disease manifestation that suggest Wnt may differentially regulate progenitor cell function in each compartment. In this study we tested sensitivities to Wnt activation in human gastric corpus and antral organoids to determine whether progenitor cells have region-specific differences in Wnt responsiveness. Human patient-matched corpus and antral organoids were grown in the presence of varying concentrations of the Wnt pathway activator CHIR99021 to assess regional sensitivity to Wnt signaling on growth and proliferation. Corpus organoids were further studied to understand how high Wnt affected cellular differentiation and progenitor cell function. A lower concentration of CHIR99021 stimulated peak growth in corpus organoids compared to patient-matched antral organoids. Supramaximal Wnt signaling levels in corpus organoids suppressed

proliferation, altered morphology, reduced surface cell differentiation, and increased differentiation of deep glandular neck and chief cells. Surprisingly, corpus organoids grown in high CHIR99021 had enhanced organoid forming potential, indicating that progenitor cell function was maintained in these non-proliferative, deep glandular cell-enriched organoids. Passaging high-Wnt quiescent organoids into low Wnt rescued normal growth, morphology, and surface cell differentiation. Our findings suggest that human corpus progenitor cells have a lower threshold for optimal Wnt signaling than antral progenitor cells. We demonstrate that Wnt signaling in the corpus regulates a bimodal axis of differentiation, with high Wnt promoting deep glandular cell differentiation and suppressing proliferation while simultaneously promoting progenitor cell function.

2.2 Introduction

The human glandular stomach is separated into two anatomically and physiologically distinct regions. The proximal region, termed the corpus or body, is defined by elongated epithelial glands containing acid-secreting parietal cells and protease-secreting chief cells. The distal region, the antrum or pylorus, has shorter epithelial glands composed primarily of alkaline mucous-producing cells and a unique population of endocrine cells secreting the hormone gastrin (1). In adults, local populations of progenitor cells fuel constant epithelial cell turnover and renewal to maintain tissue homeostasis. This orchestrated equilibrium of self-renewal and differentiation is tightly regulated by a specialized microenvironment of signaling factors and cell-to-cell interactions known as the stem cell niche (2). Studies in mouse models have identified key niche signaling pathways that regulate gastric epithelial homeostasis

for corpus and antral compartments, including Notch, BMP, mTOR, and Wnt (3-11). However, few studies have examined how these basic developmental pathways regulate human gastric epithelial cell homeostasis and disease.

The canonical Wnt signaling pathway regulates gastrointestinal stem cell function through controlling translocation of the transcriptional activator β-catenin into the nucleus (12). In the presence of Wnt ligand, nuclear β-catenin activates target genes involved in growth, proliferation, and stemness. Notably, Wnt/β-catenin signaling is enhanced by secreted proteins called R-spondins (Rspo) which stabilize Wnt receptors (13). In the absence of Wnt ligand, a destruction complex suppresses β-catenin levels through phosphorylation-mediated ubiquitination and cytosolic degradation. Inhibition or mutation of the major destruction complex component APC leads to aberrant activation of the pathway, resulting in hyperproliferative gastrointestinal disease, including cancer (12, 14).

Evidence for intragastric regionality in Wnt signaling appears during stomach development. Wnt drives early corpus specification in mice, and addition of the small molecule Wnt pathway activator and GSK3β inhibitor CHIR99021 (CHIR) pushes human induced pluripotent stem cells towards gastric corpus versus antral organoid identity (15, 16). Furthermore, the disease familial adenomatous polyposis (FAP), which is caused by Wnt-activating loss-of-function mutations to APC, results in abundant yet benign gastric polyposis. Interestingly, these polyps, called fundic gland polyps (FGPs), are generally restricted to the corpus while the antrum is largely spared (17-19). Therefore, there is clear evidence of a region-specific role for Wnt signaling in the

stomach, and further work is needed to elucidate why Wnt has a different effect on epithelial cells of the gastric corpus compared to the antrum.

Studies in adult mouse stomach have shown that WNT and RSPO ligands are primarily supplied by submucosal stromal cell populations at the gastric gland base (7, 13, 20). This localization establishes a Wnt signaling gradient along the basal-luminal gland axis, with the highest Wnt signaling present at the base and diminishing towards the luminal surface. Despite having similar Wnt gradients, the corpus and antrum have strikingly different gland architecture that suggests regional differences in progenitor cell Wnt sensitivity (Figure 2.1A). The structure of antral glands mimics that of the intestine with self-renewing stem cells residing at the base where Wnt signaling and proliferation are the highest (3, 21). The first marker identified for self-renewing antral stem cells was *Lgr5*, a Wnt target gene encoding a receptor that binds RSPO ligands (3). In contrast, the zone of proliferation in the corpus is closer to the lumen, distant from the maximal Wnt signaling zone (1, 22). Recent work has demonstrated that expression of Wnt target genes *Lgr5*, *Axin2*, and *Tnfrsf19* (*Troy*) are expressed in mature chief cells located in the high Wnt zone at the gland base (7, 23-25). This suggests that, in contrast to the antrum, Wnt signaling in the corpus is highest in non-proliferating differentiated cell types.

Despite their identity as zymogenic cells secreting digestive enzymes, studies suggest that chief cells at the gland base possess facultative stem cell capability. Although quiescent during homeostasis, long-term lineage tracing studies using Cre-LoxP mouse models demonstrated low-level turnover and generation of local pools of chief cell-derived epithelial cell clones in the gland base (26, 27). Importantly, upon

gastric epithelial injury, chief cells can remodel to a metaplastic lineage known as spasmolytic polypeptide-expressing metaplasia (SPEM) (27-29). Furthermore, single Troy-expressing mouse chief cells have been shown to generate long-lived gastric organoids in culture (23). However, it is unknown what role Wnt signaling plays in maintaining chief cell identity during homeostasis or in enabling metaplastic transformation during SPEM.

In mice, a bipotential axis of differentiation has been defined during homeostasis in which undifferentiated gastric corpus isthmus progenitors can differentiate towards a luminal surface cell lineage or, alternatively, towards deep glandular neck and chief cells (22). However, it is poorly understood what key signaling pathways direct fate determination along this axis in humans. Given the position of chief cells and neck cells at the highest end of the Wnt gradient, Wnt signaling likely plays a key role in directing deep glandular cell type differentiation. This mechanism is supported by a recent study demonstrating that human organoids grown in WNT/RSPO-rich media consist of populations of deep glandular neck and chief cells, while Wnt withdrawal leads to rapid surface cell differentiation (30, 31).

In this study, we investigated how activation of Wnt signaling in human gastric organoids regionally regulates epithelial cell proliferation, differentiation, and progenitor cell maintenance. Our findings show that corpus-derived organoids have a lower threshold for Wnt signaling to induce peak growth than patient-matched antral organoids. Increased Wnt signaling beyond peak growth-inducing conditions suppressed proliferation of corpus organoids and pushed cellular differentiation towards a deep glandular neck and chief cell fate as opposed to a surface cell fate. Despite this,

high Wnt growth conditions promoted stemness as cells are maintained in a quiescent yet primed state with increased organoid establishment efficiency observed upon return to moderate Wnt levels, as well as a resumption of normal organoid growth and surface cell differentiation.

2.3 Results

Corpus-derived human organoids have a lower threshold for optimal Wnt than antral organoids

The proximal and distal stomach have differing gland architecture and localization of proliferating progenitor cells relative to the basal-luminal Wnt gradient, suggesting different Wnt signaling sensitivity and threshold for progenitor cell proliferation between gastric corpus and antrum (Figure 2.1A). To test how Wnt signaling regulates human corpus and antral progenitor cells, we used organoids derived from patients with no known underlying gastric disease. From each individual patient (H58, H59, and H109), independent corpus and antral-derived organoid lines were established from primary biopsy tissue and cultured for at least three passages in growth media containing WNT, RSPO, and Noggin (WRN media) before analysis. We measured the impact of variable Wnt signaling on the growth of each organoid line to determine if progenitor cells from the two gastric compartments have different thresholds for optimal growth. Established human organoid lines were passaged into WNT/RSPO depleted media containing recombinant Noggin and varying concentrations of the Wnt activator CHIR (CN media) (Figure 2.1B). CHIR promotes canonical Wnt signaling by inhibiting GSK3β mediated phosphorylation and destruction of β-catenin. Organoids demonstrated a stepwise increase in mRNA abundance of the Wnt target

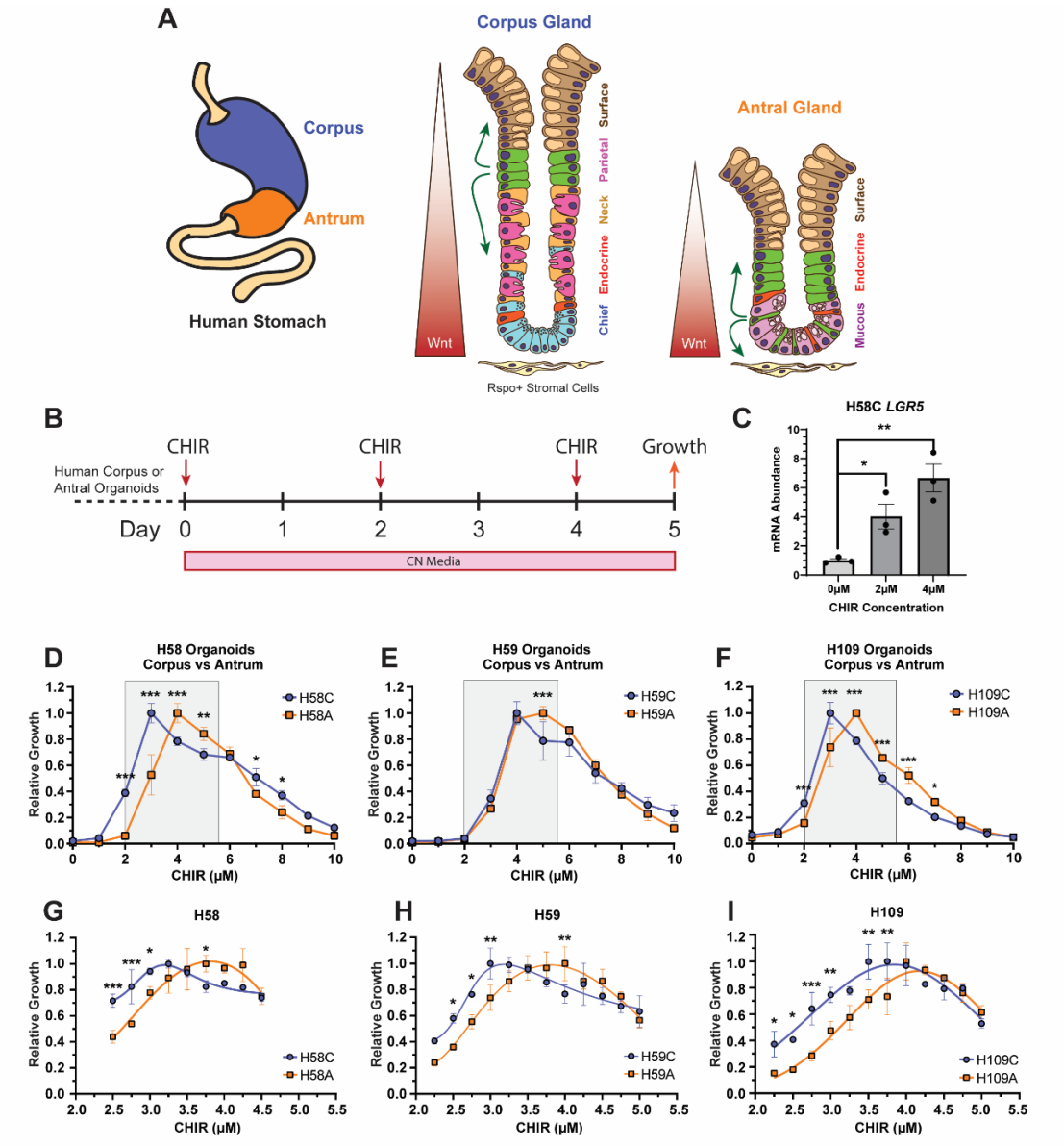

Figure 2.1: Human corpus organoids have a reduced optimal level of Wnt signaling than patient-matched antral organoids.

(A) Glands in the corpus and antrum have unique architectures, progenitor zones (labeled in green), and cellular compositions in relation to the basal-luminal Wnt gradient created by R-spondin secreted by stromal cells at the gland base. (B) Corpus and antral organoids from three patients (H58, H59 and H109) were grown in CN Media containing recombinant Noggin and various concentrations of CHIR99021 (CHIR), and growth was measured through ATP-dependent luminescence on Day 5. (C) mRNA abundance of the Wnt target gene *LGR5* was measured 48 hours after growth in CN media by qRT-PCR. Gene expression was normalized to *HPRT* and shown as fold change relative to 0 μM CHIR (mean ± SD; n = 3 wells/condition; *p<0.05, **p<0.005). (D-I) Relative growth of corpus and antral organoid cultures after 5 days growth in various CHIR concentrations. Growth rates were normalized to the maximal growth rate observed for each line and data are presented as mean ± SD (n = 3 wells/condition; *p<0.05, **p<0.005, ***p<0.001 between corpus and antrum at each respective concentration).

gene *LGR5* in response to increasing CHIR, confirming that CHIR dose-dependently regulates Wnt signaling in human gastric organoid cultures (Figure 2.1C).

We initially measured human gastric organoid growth in a wide range of CHIR concentrations, from 0 to 10 μM, in 1 μM increments. In each patient organoid pair, we than in matched antral organoids (Figure 2.1D-F). To define optimal CHIR concentrations more precisely, we repeated the growth analysis with a narrower range of CHIR covering the growth peaks (grey shading) in 0.25 μM increments (Figure 2.1G-I). The analysis confirmed our initial findings and established that corpus organoids reached maximal growth on average in 0.67 ± 0.24 μM lower CHIR than the concentration needed for peak growth in antral organoids. Interestingly, although corpus lines uniformly had peak growth at lower CHIR concentrations than matched antral lines, there was patient-to-patient variation in optimal CHIR conditions, with H58C peaking at 3.25 μM, H59C peaking at 3.00 μM, and H109C peaking at 3.75 μM.

To further understand differences in Wnt-regulated organoid growth, we assessed organoid morphology and measured cellular proliferation 48 hours after renewal with CN media containing 1–5 μM CHIR (Figure 2.2A). Unlike the previously described experiments, organoids were initially seeded with standardized WRN media to enable controlled establishment and growth of organoids prior to transition at day 4. At this time, organoids are still within a growth phase, which allowed analysis of acute effects of different CHIR concentrations on growth and proliferation.

After two days in CN media, organoid morphology showed dynamic CHIR concentration-dependent changes, particularly in corpus organoids. Corpus organoids

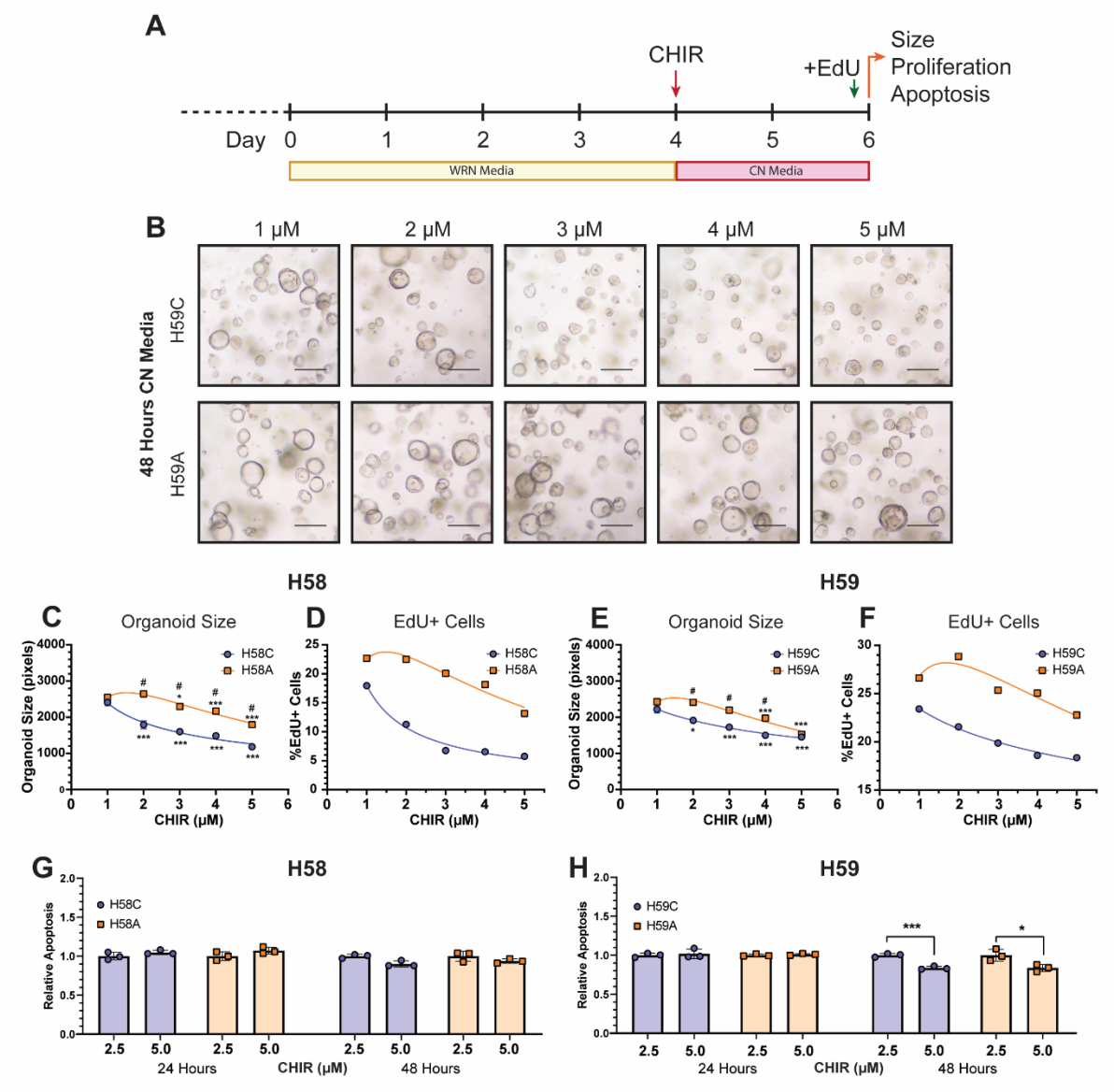

Figure 2.2: Increased Wnt suppresses corpus organoid growth and proliferation without inducing apoptosis.

(A) Paired organoid lines H58C/A and H59C/A were grown in WRN media for four days, then transitioned to CN media for two days before measuring growth, proliferation, and apoptosis. (B) Representative images of H59C and H59A organoids after culture for 48 hours in CN media containing indicated CHIR concentrations (size bars = 200 μm). (C, E) Organoid size at Day 6 in respective CHIR concentrations. Size in pixels is shown as mean ± SEM (n ≥ 250 organoids/condition; *p<0.05, ***p<0.001 compared to organoid line size at 1 μM; #p<0.05 between patient-matched corpus and antral organoids at each concentration). (D, F) Percentage of EdU+ cells in each organoid culture as determined by flow cytometry (n = 3 independent wells pooled per concentration, approx. 50k-100k cells). (G-H) Apoptosis was measured in organoid cultures 24- or 48-hours post-transition into CN media by caspase 3/7-dependent luminescence. Data are shown as mean ± SD (n = 3 individual wells/condition; *p<0.05, ***p<0.001 compared to 2.5 μM).

transitioned from a cystic morphology with an open lumen to a closed morphology with increasing Wnt signaling (Figure 2.2B). Measurement of organoid size in two independent patients showed a significant reduction in corpus organoid size at CHIR concentrations ≥2 μM, while paired antral lines required higher CHIR concentrations (>3 μM) to see a size reduction (Figure 2.2C, E). Measurement of proliferation by flow cytometric analysis of EdU incorporation showed a similar profile. Proliferation in corpus organoids decreased with CHIR concentrations ≥2 μM, while antral proliferation remained stable and began to decline only at the highest concentrations (Figure 2.2D, F).

To ensure that changes to organoid size and proliferation were not a consequence of cell death, we measured apoptosis 24 and 48 hours after transition from WRN media to CN media containing 2.5 or 5.0 μM CHIR in H58 and H59 patient organoid lines (Figure 2.2G, H). This analysis showed that apoptosis was not induced by high CHIR concentration, suggesting that organoids remained viable even when Wnt signaling levels exceeded that required for the maximal growth response, and that the reduced organoid size was driven by changes to proliferation and/or differentiation.

High Wnt signaling promotes deep glandular cell differentiation in corpus organoids

Given that high CHIR reduced corpus organoid proliferation and size, we next examined how increasing Wnt signaling affected cellular differentiation in corpus organoids. Established human corpus organoids from a fourth patient, H60C, were cultured in WRN media for one day and then transitioned for 6 additional days to CN media containing 2.5 μM (Moderate), 5 μM (High), 7.5 μM (Very High), or 10 μM

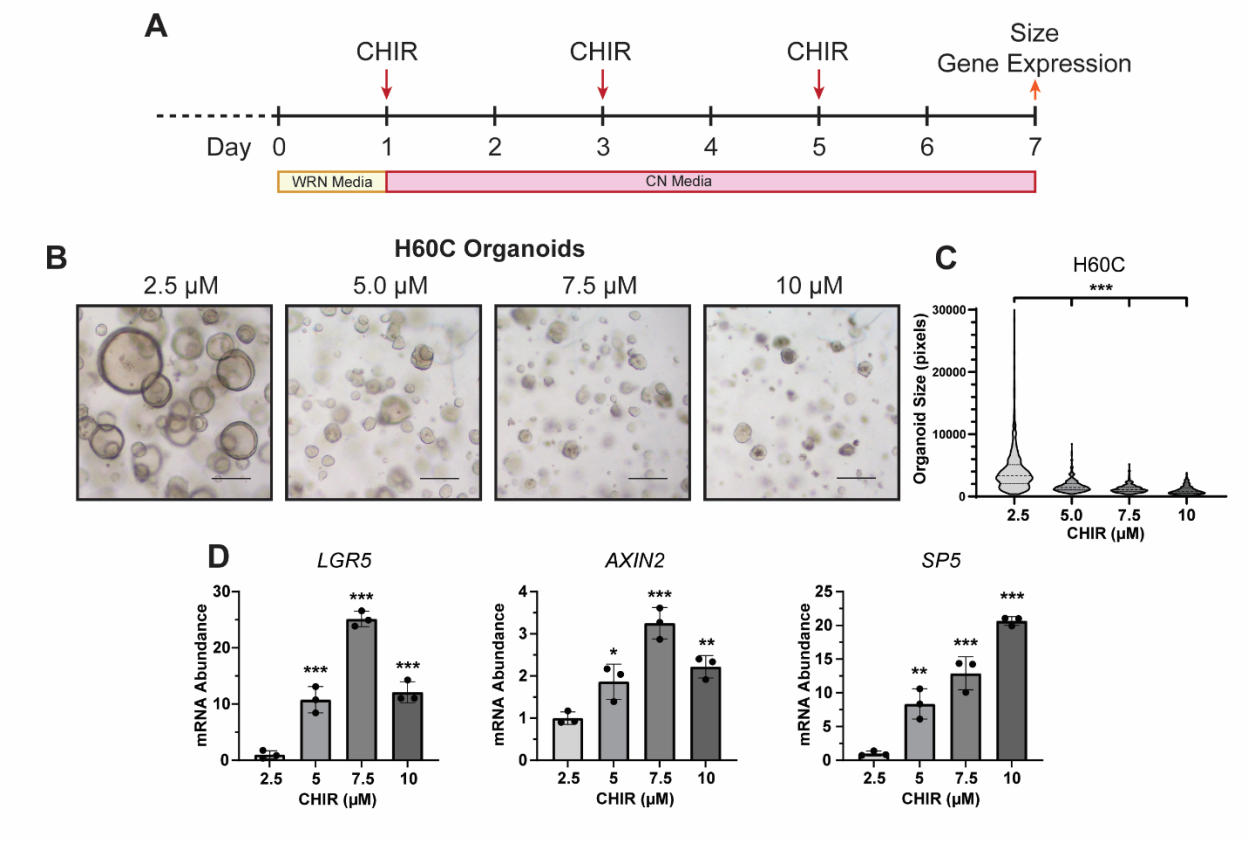

Figure 2.3: High Wnt signaling leads to reduced growth and abnormal corpus organoid morphology.

(A) Normal human corpus-derived organoids (line H60C) were established for one day in WRN media, then transferred to CN media with varying CHIR for six days. Organoids were analyzed at Day 7. (B) Representative images of corpus organoids grown in different CHIR concentrations (size bars = 200 µm). (C) Organoid size was quantified using ImageJ (n ≥ 500 organoids/condition; ***p<0.001 compared to 2.5 µM). (D) mRNA abundance of Wnt target genes for Day 7 organoids, represented as fold change to 2.5 µM (n = 3 individual wells/condition; *p<0.05, **p<0.005, ***p<0.001).

(Extreme) CHIR (Figure 2.3A). Similar to our previous findings, corpus organoids grown in higher levels of CHIR (5, 7.5, and 10 μM) did not exhibit normal cystic morphology but were organized as cell clusters with a reduced lumen (Figure 2.3B). Increasing CHIR concentrations directly led to a stepwise decrease in organoid size, consistent with our previous finding of reduced proliferation (Figure 2.3C). Gene expression analysis demonstrated a dose-dependent increase in the abundance of Wnt targets *LGR5*, *AXIN2*, and *SP5*, indicating that high CHIR concentrations successfully induced elevated Wnt signaling (Figure 2.3D).

We tested how varying Wnt signaling levels affected cellular differentiation through analysis of gastric cell type specific markers. mRNA abundance of surface mucous cell-specific transcripts *MUC5AC*, *TFF1*, and *TFF2*, as well as the lineage-driving transcription factor *FOXQ1*, were dependent on CHIR dose, with reduced surface cell marker expression observed in organoids grown in increasing Wnt levels (Figure 2.4A). Immunohistochemical analysis of MUC5AC protein in whole-mount organoid preparations confirmed that expression of this surface cell marker was reduced in high-Wnt organoids (Figure 2.4B).

Having observed that increasing Wnt signaling reduced differentiation towards the luminal surface cell lineage, we next tested differentiation to deep glandular mucous neck and chief cells. We found that mRNA abundance of the neck cell markers *MUC6*, *CD44*, and *AQP5* was significantly increased in organoids grown in increasing concentrations of CHIR (Figure 2.5A). Immunohistochemical staining of organoids confirmed that high Wnt conditions induced expression of MUC6 and CD44, with most cells appearing to be CD44+ in 7.5 μM CHIR (Figure 2.5B). Expression of the chief cell

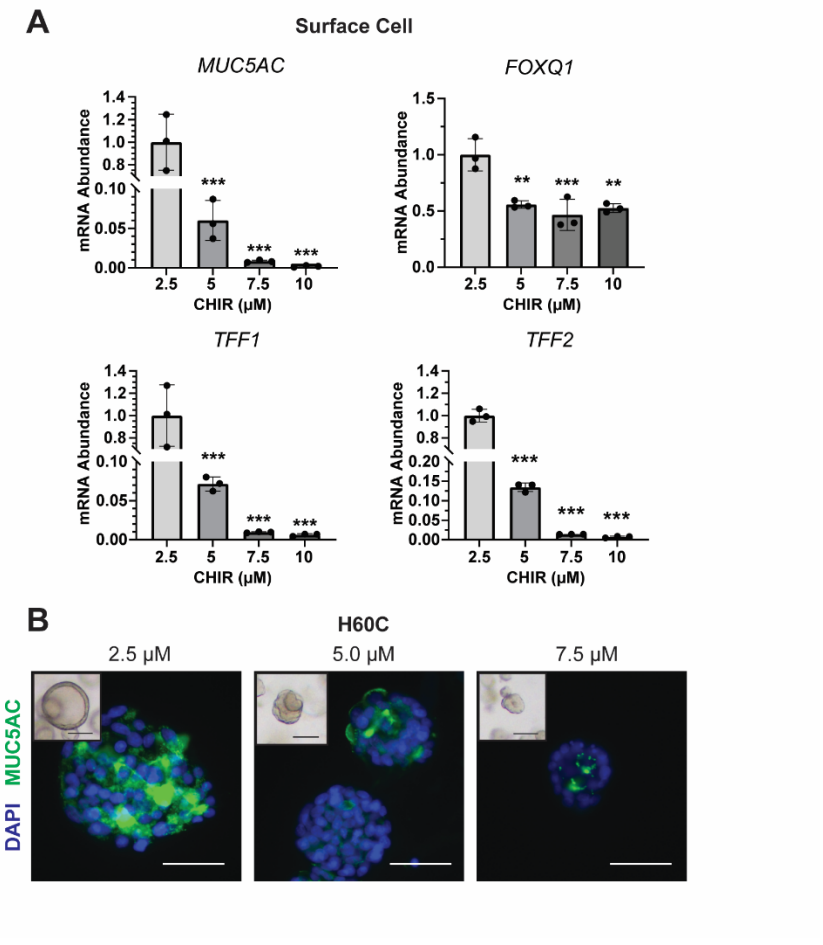

Figure 2.4: Increasing Wnt signaling in human corpus organoids reduces surface cell marker expression.

(A) mRNA abundance of surface cell marker genes in H60C organoids grown for 6 days in different CHIR concentrations (Figure 2.3A). Data are shown as mean ± SD fold change relative to 2.5 μM CHIR (n = 3 individual wells/condition; *p<0.05, **p<0.005, ***p<0.001). (B) Immunostaining of whole-mount organoids for MUC5AC (green) and DAPI (blue) (size bars = 80 μm). Insets represent high-power images of corpus organoids grown for 6 days in different CHIR concentrations (size bars = 100 μm).

markers *LIPF*, *PGC*, and *TNFRSF19* was also significantly increased in high-Wnt organoids (Figure 2.5C).

Overall, the data revealed a Wnt-dependent bi-modal axis of differentiation in human corpus organoids, with surface cell differentiation occurring in low Wnt conditions while neck and chief cell differentiation was promoted by high Wnt conditions. This axis follows the cellular architecture of the corpus gland relative to the Wnt gradient, where chief and neck cells reside at the gland base where Wnt signaling is the highest, while surface cells are in the lowest Wnt zone along the gland axis (Figure 2.1A).

We also examined parietal cell and endocrine cell marker expression to determine if Wnt directly impacted their development and differentiation in human corpus organoids. Interestingly, we observed significantly elevated expression of parietal cell markers *ATP4A* and *GIF* in high-Wnt conditions (Figure 2.6A). This follows the normal localization of most parietal cells in an intermediate Wnt signaling region below the proliferating progenitors (Figure 2.1A). However, mRNA abundance, especially for *ATP4A*, was very low, consistent with previous observations that parietal cells are typically absent in corpus organoids grown in normal culture conditions (23, 30). We saw no change in the expression of endocrine markers *CHGA* and *GHRL*, which were also expressed at very low levels in the corpus organoids (Figure 2.6B).

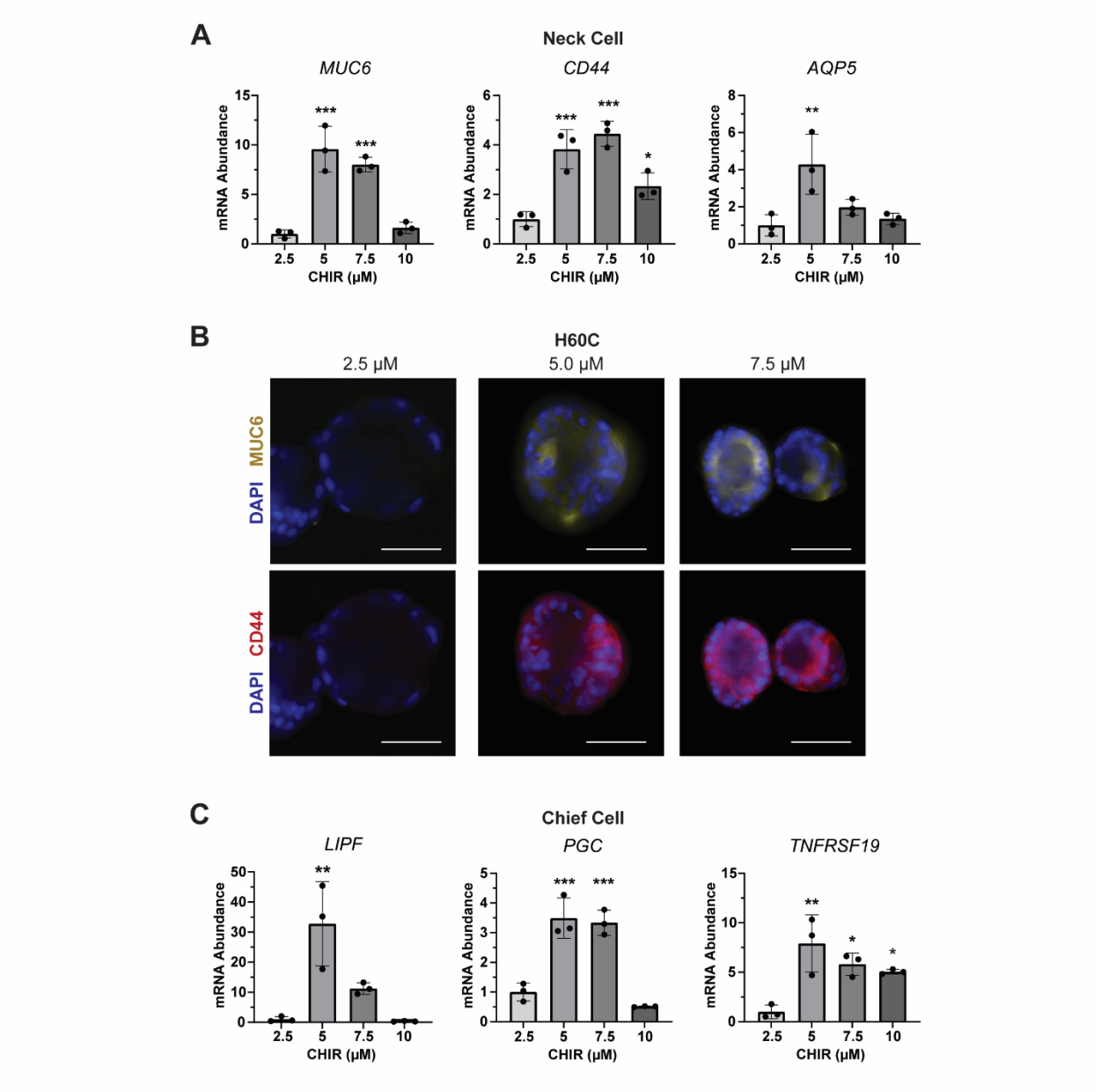

Figure 2.5: Increasing Wnt signaling in human corpus organoids promotes deep glandular neck and chief cell marker expression.

(A) mRNA abundance of neck cell marker genes in H60C organoids grown for 6 days in different CHIR concentrations (Figure 2.3A). Data are shown as mean ± SD fold change relative to 2.5 μM CHIR (n =3 individual wells/condition; *p<0.05, **p<0.005, ***p<0.001). (B) Immunostaining of whole-mount organoids for neck cell markers MUC6 (yellow) or CD44 (red), and DAPI (blue) (size bars = 80 μm). (C) mRNA abundance of chief cell marker genes in corpus organoids grown for 6 days in different CHIR concentrations. Data are shown as mean ± SD fold change relative to 2.5 μM CHIR (n = 3 individual wells/condition; *p<0.05, **p<0.005, ***p<0.001).

High Wnt conditions enhance stemness despite reduced growth and proliferation

Wnt signaling is known to maintain stemness and self-renewal of gastrointestinal progenitor cells (32). We tested for stem/progenitor cell activity in organoids cultured in different CHIR concentrations by measuring organoid forming efficiency after passage into WRN media. Corpus organoids cultured in CN media containing 2.5 μM, 5 μM, or 7.5 μM CHIR for 6 days were dispersed to single cells and plated in WRN media at identical densities (Figure 2.7A). Organoid numbers were counted after 6 days of growth in WRN media and plating efficiency was calculated (Figure 2.7B). Surprisingly, organoids grown in High (5 μM) and Very High (7.5 μM) CHIR had on average an 82% increase in organoid-forming ability compared to organoids grown in Moderate Wnt levels (2.5 μM CHIR). This finding suggests a dynamic response to Wnt signaling in which activation of Wnt signaling maintains and enhances stem/progenitor cell potential while simultaneously suppressing proliferation and inducing deep glandular cell differentiation. Interestingly, the organoid formation efficiency of organoids grown in 5 μM and 7.5 μM CHIR was strikingly similar (37%), indicating a threshold Wnt signaling level for increasing stemness.

Increased organoid formation efficiency from organoids with reduced proliferation suggests that cells were held in a quiescent yet primed state (G1) rather than removed from the cell cycle (G0), which is normally associated with cellular differentiation. To test this, we measured cell cycle status by staining cells with Hoechst 33342 (DNA) and Pyronin Y (RNA) to distinguish between these two states, as G1 cells have increased RNA content relative to G0 (33). We measured the proportion of cells in G0, G1, S, and

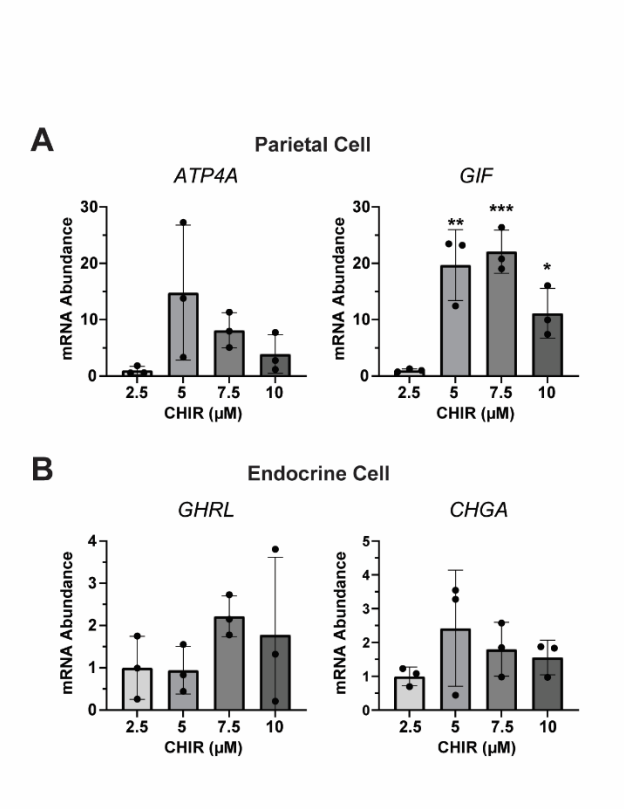

Figure 2.6: Increasing Wnt signaling promotes parietal cell marker expression but not endocrine cell marker expression.

(A, B) mRNA abundance of (A) parietal cell marker genes and (B) endocrine cell marker genes in corpus organoids grown for 6 days in different CHIR concentrations (Figure 3A). Data are shown as mean ± SD fold change relative to 2.5 μM CHIR (n = 3 individual wells/condition; *p<0.05, **p<0.005, ***p<0.001).

G2 by flow cytometry in corpus organoids cultured for 6 days in CN media containing 2.5 μM, 5 μM, or 7.5 μM CHIR (Figure 2.7A). This analysis showed that organoids grown in higher Wnt conditions increased the proportion of cells in G1, with a corresponding decrease in G2 cells (Figure 2.7C). In the 5.0 μM CHIR cell population 58% of cells were in G1 ($Hoechst^{Low}$:$Pyronin\ Y^{High}$), a 20% increase from the 2.5 μM CHIR cell population with 48% of cells in G1. Cells grown in 7.5 μM CHIR had an even greater increase with 65% of the population in G1. This increase came predominately at the expense of the G2 population which measured 26%, 21%, and 13% of cells grown in 2.5 μM, 5.0 μM, and 7.5 μM CHIR, respectively. The percentage of cells in G0 (16%, 14%, and 13%) remained stable across all three populations. These findings provide evidence that high-Wnt induced G1 arrest rather than cell cycle exit.

The cyclin-dependent kinase inhibitor p57 (CDKN1C) regulates cell cycle progression at the G1-S transition. In mouse stomach, p57 is expressed in chief cells at homeostasis where it functions as a molecular break to regulate proliferative responses to SPEM-inducing injury (34). Expression of *CDKN1C* has also been mapped to chief cells in the human stomach, and low expression is associated with poor prognosis of gastric cancer (35, 36). To test whether *CDKN1C* expression was upregulated in high-Wnt organoids, we measured mRNA abundance in corpus organoids grown in various CHIR concentrations for 6 days. We observed that organoids grown in High (5 μM) or Very High (7.5 μM) CHIR had increased expression of *CDKN1C* (Figure 2.7D), suggesting a possible mechanism for increased cell numbers in the G1 population.

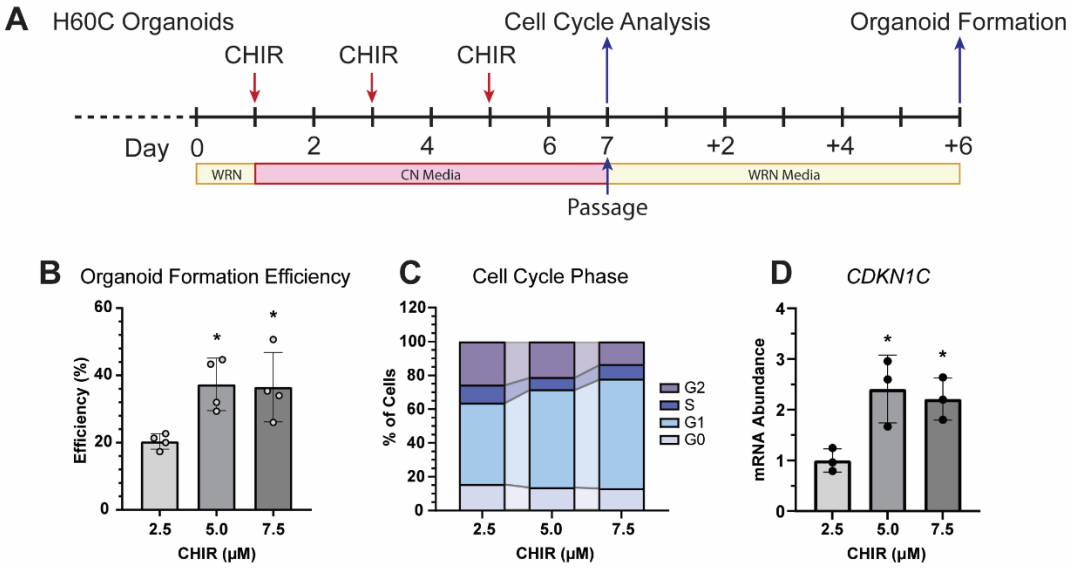

Figure 2.7: Enhanced stemness and alterations in cell cycle in high-Wnt organoids. (A) H60C organoids grown for 6 days in different CHIR concentrations were analyzed for organoid initiation efficiency, cell cycle status, and expression of the cell cycle inhibitor *CDKN1C.* (B) Organoid formation efficiency was measured by plating 150 cells per well and counting organoid numbers after growth in WRN media for 6 days. The proportion of cells from the different CHIR growth conditions that formed organoids is shown as mean ± SD (n = 4 wells/condition; *p<0.05, **p<0.005 relative to 2.5 μM CHIR). (C) Cell cycle status of H60C organoids grown for 6 days in different CHIR concentrations was measured by flow cytometry analysis of single cells stained with Hoechst 33342 and Pyronin Y as described in Methods. (D) mRNA abundance of p57 (*CDKN1C*) in Day 7 organoids is shown as mean ± SD fold change relative to 2.5 μM (n = 3 individual wells/condition; *p<0.05)

High-Wnt organoids re-establish normal growth and cellular differentiation after passage into low Wnt conditions

Given that high-Wnt organoids were viable and formed new organoids at increased rates, we tested whether they were committed to the deep glandular cell fate or if they retained plasticity to transition to a surface cell phenotype after passaging into low Wnt conditions. Organoids grown for 6 days in 2.5 μM, 5.0 μM, 7.5 μM, or 10 μM were passaged, plated into WRN media for one day, and cultured for six days in CN media with 2.5 μM CHIR (Figure 2.8A). We observed that all organoids, regardless of their initial CHIR concentration, regained normal cystic morphology (Figure 2.8B). In accordance with our previous finding that organoids grown in High and Very High CHIR levels exhibited increased organoid initiation efficiency, we observed increased numbers of organoids in those cultures as all cultures were plated with identical starting cell numbers. Despite the marked organoid size difference before passage (Figure 2.3C), there was no difference in organoid size once they re-established into Moderate CHIR, indicating similar growth rates across all conditions (Figure 2.8C). Comparison of mRNA abundance of Wnt target genes from pre-passage to the conclusion of 6 days of growth in Moderate CHIR showed loss of the enhanced Wnt signaling that was induced by the previous high CHIR concentrations (Figure 2.8D).

With normal organoid growth and morphology restored after transition to Moderate CHIR, we tested whether this restored surface cell differentiation. Remarkably, we observed that organoids derived from high-Wnt conditions regained expression of surface cell markers *MUC5AC*, *FOXQ1, TFF1, and TFF2* after passage into culture conditions stimulating moderate Wnt signaling (Figure 2.9A). Whole mount

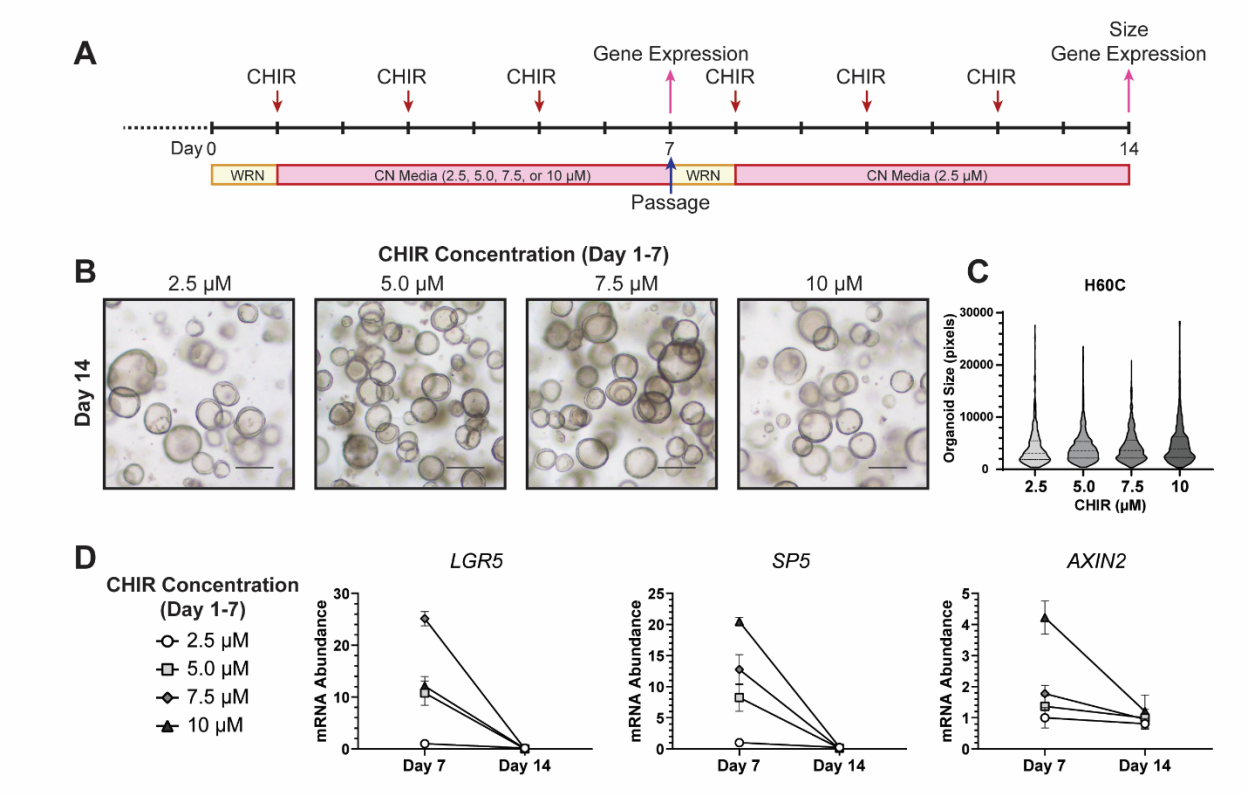

Figure 2.8: Normal organoid growth and morphology are restored after high-Wnt organoids are transitioned to moderate Wnt conditions.

(A) H60C organoids grown in 2.5 µM, 5.0 µM, 7.5 µM, or 10 µM CHIR were passaged to WRN Media for one day and then transitioned to CN media with 2.5 µM CHIR for six additional days. (B) Representative images of organoids grown in different CHIR concentrations after recovery growth in 2.5 µM CHIR (size bars = 200 µm). (C) Organoid size at the end of the recovery growth in 2.5 µM CHIR is shown (n ≥ 500 organoids/condition). (D) mRNA abundance of Wnt target genes after 6 days growth in different concentrations of CHIR and then after passage and recovery growth in 2.5 µM CHIR. Data are shown as mean ± SD fold change relative to gene expression for organoids grown in 2.5 µM CHIR for 6 days (n = 3 wells/condition).

immunostaining confirmed widespread expression of the surface marker MUC5AC (Figure 2.9B). Analysis of deep glandular cell markers showed that high-Wnt organoids (5 μM and 7.5 μM) had reduced expression of neck cell markers *MUC6*, *CD44*, and *AQP5* after growth in moderate CHIR (2.5 μM) (Figure 2.9C). Similarly, the abundance of chief cell markers *LIPF*, *PGC*, and *TNFRSF19* was also reduced after transition into Moderate Wnt (Figure 2.9D). Overall, we demonstrate a dynamic and plastic response of human corpus organoids transitioning into different Wnt signaling environments, with differentiation towards surface cells versus deep glandular cells determined by the level of Wnt signaling.

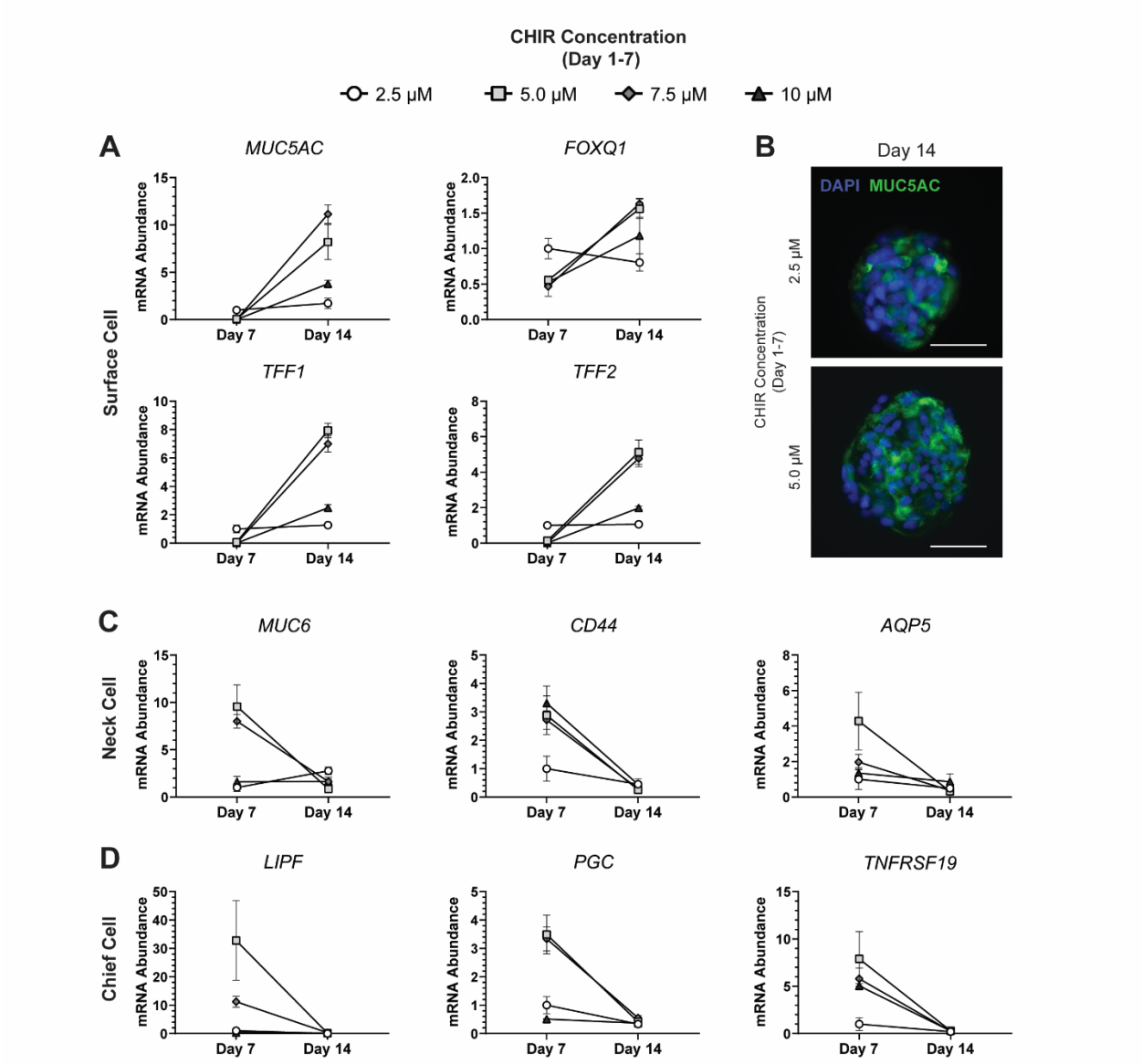

Figure 2.9: Transition of high Wnt organoids into moderate Wnt conditions causes loss of the deep-glandular phenotype in favor of enhanced surface cell differentiation.

mRNA abundance for (A) surface cell markers, (C) neck cell markers, and (D) chief cell markers in H60C organoids harvested at Day 7 (the end of 6 days growth in 2.5 µM, 5.0 µM, 7.5 µM, or 10 µM CHIR) or Day 14 (the end of recovery growth in 2.5 µM CHIR), as shown in Figure 2.8A. Data are shown as mean ± SD fold change relative to the measured abundance at Day 7 for organoids grown in 2.5 µM CHIR (n = 3 wells/condition). (B) Immunostaining of whole-mount organoids for MUC5AC (green) and DAPI (blue) (size bars = 80 µm).

2.4 Discussion

This study tested how the Wnt signaling gradient along the gastric gland axis affects proliferation and differentiation of human stem/progenitor cells. Like the intestinal crypt-villus axis, a basal-luminal Wnt signaling gradient is created by secretion of RSPOs from the underlying mesenchyme at the gland base (7, 13, 20). The stark difference in the location of proliferating progenitors in the corpus compared to the antrum suggests regional differences in the sensitivity of stem/progenitor cells to Wnt levels (Figure 2.1A). We used patient-matched corpus-antrum organoid lines established from human gastric tissue biopsies and tested their responses to a wide range of Wnt levels by using different concentrations of the Wnt pathway activator CHIR. This analysis demonstrated that the maximal growth and proliferation rate of corpus organoids occurs at lower Wnt signaling levels than in patient-matched antral organoids. This observation follows the *in vivo* architecture of corpus versus antral glands, mirroring the relationship of the location of the primary zones of proliferation to the Wnt signaling gradient.

The difference in gastric stem/progenitor cell responses to Wnt becomes clinically relevant with disease-associated Wnt activating mutations. Familial adenomatous polyposis (FAP) is a genetic disease resulting from loss-of-function mutations in the *APC* gene which leads to hyperactivation of the Wnt signaling pathway. FAP patients are burdened with polyp growth throughout the gastrointestinal tract. Outside of the colon, which exhibits the most serious disease manifestations with the development of cancer, FAP patients also commonly exhibit gastric polyposis. However, in contrast to aggressive, pre-cancerous colorectal polyps, the gastric fundic gland polyps (FGPs) which emerge are abundant, yet typically sessile, benign, and rarely progress into cancer (17, 37). Remarkably, FAP gastric polyposis is primarily restricted

to the corpus while the antrum is mostly spared. The rare polyps that do emerge in the antrum are often adenomatous and carry a higher cancer risk than FGPs indicating a more severe mutational landscape underscoring their formation. Interestingly, sporadic FGPs have also been associated with increased Wnt signaling due to activating mutations in the *CTNNB1* gene, which encodes β-catenin (38). Furthermore, FGPs have also been linked with *H pylori* infection, which has been demonstrated to increase Wnt signaling through induced expression of Rspo (7, 39). Therefore, activation of Wnt signaling has a clear association with hyperproliferation in the corpus epithelium, and the regionality of these polyps suggests that the corpus and antrum have different sensitivities and/or thresholds for Wnt signaling to promote proliferation.

Previous studies have explored the association of Wnt tone with the regional patterns of polyp development in the intestine and proposed a Goldilocks zone of Wnt signaling that fuels polyposis in a region-specific manner in a model dubbed the 'Just-Right' Hypothesis (40-42). Here, we demonstrate intragastric regionality that suggests corpus and antral cells have different intrinsic Wnt sensitivities that may shift their respective Goldilocks zone for optimal growth and proliferation. Our findings also contextualize the patterns of gastric polyp manifestation within FAP patients, and ongoing work in our lab is being conducted to further understand the etiology of gastric polyp formation in these patients.

The other major finding of our study is that Wnt signaling regulated the axis of cellular differentiation in human corpus organoids, consistent with cell type location along the base-lumen gland axis (Figure 2.1A). Low Wnt signaling promoted surface mucous cell differentiation, while high Wnt conditions enriched for deep glandular cell

types, including neck and chief cells, while simultaneously depleting surface cells. Our observations align with a recent mouse study showing that subepithelial Rspo regulated corpus epithelial cell differentiation. Loss of *Rspo3* enhanced surface cell differentiation and *Rspo3* overexpression shifted differentiation towards chief and parietal cells (31). Further, this study showed that mouse corpus organoid cultures supplemented with WNT and RSPO promoted chief and neck cell character, while withdrawal stimulated surface cell expression. Another study which focused on defining ideal growth conditions for human corpus organoids discovered that Wnt signaling was essential to maintain chief and neck cell lineages, while Wnt withdrawal promoted surface cell marker expression (30). Our work corroborates and expands upon these findings, showing that Wnt levels direct human corpus differentiation in a dose-dependent manner and contextualizes how Wnt activation rather than silencing impacts differentiation. Interestingly, high Wnt signaling in the human corpus drives differentiation rather than promoting progenitor cell proliferation. This association has also been demonstrated in the hematopoietic stem cell (HSC) system, where the dosage of canonical Wnt signaling tightly regulates cell identity and high Wnt conditions can lead to loss of hematopoietic stemness (43-45).

Remarkably, despite enhanced deep gland cell differentiation, slow growth, and altered morphology of corpus organoids grown in high Wnt conditions, they effectively establish new organoids when passaged, suggesting enhanced stem cell function. It is unknown which specific cells in the high-Wnt organoids (i.e., chief, neck, or other) were primarily responsible for the establishment of new organoids following passaging. Notably, chief cells have been demonstrated to possess ‘reserve’ stem cell capability.

Single chief cells derived from mouse stomach based on expression of the cell-specific marker and Wnt target gene *Troy* have been shown to form long-lived organoids (23, 27). Perhaps the human chief cells formed in the high-Wnt corpus organoids exhibit similar reserve stem cell activity.

Once high-Wnt organoids were passaged into moderate Wnt growth conditions they resumed a normal cystic morphology and growth rate observed in organoids maintained in moderate Wnt, suggesting that high-Wnt induced a quiescent yet primed state that enabled cells to re-initiate active cycling. This result bares striking similarity to observations from a study of mouse small intestine which demonstrated that overexpression of Rspo led to reduced lineage tracing and crypt-trapping of Lgr5+ stem cells (46). Accordingly, we showed that high Wnt organoids did not exit the cell cycle, but instead increased the proportion of cells in G1. The high-Wnt organoids also showed higher expression of *CDKN1C*, which inhibits G1 cyclin-CDK complexes to arrest the cell cycle in the G1 phase. Interestingly, p57 was recently shown in mice to play an essential role in regulating the activation of chief cell proliferation in response to injury (34). After gastric tissue injury, chief cells rapidly remodel to form a proliferating metaplastic lineage, termed spasmolytic peptide-expressing metaplasia (SPEM) (25, 47). SPEM appears to function as a regenerative lineage to repair the epithelium and re-establish cellular homeostasis. Post-injury, chief cells have been shown to lineage trace into different corpus cell types, including actively cycling progenitor cells, thus exhibiting features of reserve stem cells. Importantly, post-injury, chief cells rapidly lose p57 before they start proliferating (34). Furthermore, this study showed that mice engineered to overexpress p57 exhibited impaired chief cell responses to injury. The

data suggest that p57 acts as a molecular switch to maintain quiescence during homeostasis, with injury-induced p57 loss responsible for activation of proliferation.

Basal expression of p57 in chief cells suggests that they exist in a non-proliferative G1 state, poised to rapidly respond to injury. Interestingly, p57 has also been demonstrated to play an important role in maintaining quiescence and self-renewal capacity in HSCs (48, 49). Like chief cells, HSCs have a low basal rate of proliferation but can enter the cell cycle in response to stress or injury (50). Transcript profiling of murine chief cells after SPEM-inducing injury showed decreased expression of genes commonly upregulated in quiescent HSCs, including p57 (34). However, it remains unclear if p57, or other cell cycle checkpoint regulators, are directly regulated by Wnt signaling.

Although we confirm that CHIR dose-dependently activates Wnt signaling in gastric organoid cultures, we cannot rule out potential confounding effects of GSK3β inhibition. GSK3 has broader kinase activity in pathways including glycogen synthase, NFκB, AP-1, and CREB (51). Despite this, CHIR has been extensively used in *in vitro* models to activate Wnt signaling in a variety of applications within dose ranges similar to the ones described within this study (16, 42, 52, 53). Furthermore, our observations on inducing differentiation with CHIR follow the current body of literature demonstrated within the proximal stomach, therefore providing confidence that Wnt is the primary force influencing cellular changes within our system.

To conclude, our study highlights the key role Wnt signaling plays in defining human gastric progenitor cell function and cellular homeostasis. We suggest that Wnt is a key regulator of differentiation, and that activation of this signaling pathway in

progenitor cells leads to the formation of deep glandular neck and chief cells while simultaneously arresting cell cycle at the G1 checkpoint. Active Wnt signaling is essential to maintain these lineages in organoid models, and there are dose-dependent thresholds that dictate cellular identity. The role of Wnt signaling in fate determination in the corpus contrasts with the gastric antrum which does not contain an expansive sub-progenitor differentiated cell compartment. Furthermore, the gland architecture is consistent with our observation of different thresholds for Wnt signaling in corpus versus antral progenitor cells which provides perspective for gastric epithelial cell fate and the manifestation of Wnt-activation diseases that affect the stomach.

2.5 Materials and Methods

Establishment of human gastric organoids.

Human gastric tissue biopsies were collected from patients undergoing endoscopy under Institutional Review Board-approved protocols at the University of Michigan. Biopsies were placed in 15 mL conical tubes containing 5 mL of ice-cold DPBS (Gibco, 14190144) with Antibiotic-Antimycotic (100 U/mL Pen/Strep + 250 ng/mL Amphotericin B, Gibco, 15240062) for transport to the research lab. Biopsies were minced into small fragments (~1mm), transferred to 5 mL of ice-cold DPBS + Antibiotic-Antimycotic in 15 mL conical tubes, and rocked in the cold room for 1 hour. Organoids were established from either isolated epithelium or directly from minced tissue that was embedded in Matrigel (Corning, 354234). For the isolated epithelium approach, 15 mM EDTA (Invitrogen, 15575038) was included during rocking. Tissue fragments were transferred to a new 15 mL conical containing 8 mL of ice-cold DPBS and gastric glandular epithelium was released by vortexing at maximum speed for 2 minutes. The

suspended epithelial glands were transferred to a new 15 mL conical tube, taking care to avoid remaining tissue fragments. Glands were pelleted at 600xg for 5 minutes at 4°C. The supernatant was aspirated, and glands were resuspended in Matrigel for plating. For the minced tissue approach, tissue was directly embedded within Matrigel. Epithelial outgrowth emerged from minced tissue fragments within 2-3 days of plating. All organoids were grown for at least three passages prior to experimentation in order to remove stromal contamination and obtain pure epithelial cultures.

Human gastric organoid culture.

Organoids were maintained in WRN (WNT, RSPO, Noggin) media or CN (CHIR99021, Noggin) media as specified. 50 mL of WRN media was generated with 20 mL (40%) L-WRN conditioned media (University of Michigan Translational Tissue Modeling Laboratory), 6 mL Fetal Bovine Serum (20% v/v including contribution from L-WRN media) (Sigma, F0926), 22.5 mL DMEM/F12 (Gibco, 12634010), 500 µL GlutaMAX (2 mM, Gibco, 35050061), 500 µL Antibiotic-Antimycotic (100 U/mL Pen/Strep + 250 ng/mL Amphotericin B, Gibco, 15240062), 500 µL HEPES (10 mM, Gibco, 15630080), 10 µM Y-27632 (Tocris, 1254), 10 µM SB431542 (Tocris, 1614), and 50 µg/mL Gentamycin (Gibco, 15750060). 50 mL of CN Media consisted of 10 mL Fetal Bovine Serum (20%), 37.5 mL DMEM/F12, GlutaMAX, Antibiotic-Antimycotic, HEPES, Y-27632, SB431532, and Gentamycin in the same concentrations as above, and was supplemented with 100 nM recombinant Noggin (R&D, 6057-NG) and CHIR99021 (CHIR, Tocris, 4423) as specified. DMSO added through stock solutions of CHIR and SB431542 was maintained at a final concentration of 0.3% in CN Media.

Organoid cultures were maintained by replenishing with fresh media every two days and passaging every six days. To passage organoids, media was aspirated from wells and Matrigel patties containing mature organoids were overlaid with 500 µL of cold PBS. Patties were mechanically disrupted through scraping with a P1000 pipet tip, and then transferred to a 1.5 mL Eppendorf tube. Organoids were centrifuged at 250xg for 5 minutes at 4°C, the supernatant was aspirated, and the pellet was resuspended in 500 µL of TrypLE Express (Gibco, 12604013), and incubated in a 37°C water bath for 10 minutes. Using a P1000, organoids were vigorously pipetted approximately 40 times to mechanically break organoids down into single cells. 700 µL of cold DPBS was added, and cells were spun at 250xg for 5 minutes at 4°C to pellet. The supernatant was aspirated, and cells were resuspended in 30-100 µL of DMEM and cell concentration was quantified using a hemocytometer. For all experiments, cells were plated at a density of 300 cells/µL of Matrigel patty. Matrigel patties were given 30-45 minutes to solidify at 37°C, then overlayed with the appropriate warmed media.

RNA extraction from organoids and qPCR analysis.

Organoids were dispersed to single cells using TrypLE, washed, pelleted, and RNA was isolated using the Qiagen Mini Kit (Qiagen, 74106) according to the manufacturer's instructions. The cell pellet was resuspended in RLT Buffer + 1% βME and vortexed at max speed for 30 seconds before RNA extraction. cDNA was synthesized from 250ng of RNA using the iScript™ cDNA Synthesis Kit (BioRad, 1708891). qPCR reactions used the iTaq™ Universal SYBR Green Supermix (BioRad, 1725124) and respective primers (Table 1). qRT-PCR was performed with samples in

triplicates, and average cycle threshold values were quantified relative to the reference mRNA *HPRT* using the ΔΔCT method to determine mRNA abundance.

Analysis of organoid growth, apoptosis, and establishment efficiency.

Organoids were dispersed to single cells and plated into a 96-well round-bottom plate in 5 µL patties of Matrigel at a density of 1,500 cells/well. For measurement of growth, media was aspirated and 150 µL of a room temperature 50:50 mixture of DMEM (75 µL) and CellTiter-Glo 3D (75 µL) (Promega, G9681) was added to each well. Plates were incubated for 30 minutes at room temperature in the dark, the Matrigel patty was broken down by rapid pipetting, and the total contents of each well were transferred to individual wells of a white, opaque 96-well plate. Luminescence was measured using a plate reader with an integration time of 500ms.

For measurement of apoptosis, wells were washed with 200 µL of warm DPBS to remove residual media as FBS contains low baseline activity that results in a high background signal. The DPBS was aspirated, and 200 µL of room temperature 50:50 DMEM (100 µL) and CaspaseGlo 3/7 3D reagent (100 µL) (Promega, G8981) was added to each well. Plates were incubated at room temperature in the dark for one hour, the Matrigel patty was broken down by rapid pipetting, and the total contents of each well were transferred to individual wells of a white, opaque 96-well plate. Luminescence was measured using a plate reader with an integration time of 500ms.

For measurement of organoid formation efficiency, organoids were dispersed to single cells and plated at concentrations of 150 single cells in 5 µL Matrigel patties in a 96-well plate. Media was replenished every two days. On day 6, the number of formed

organoids was counted in each well. A formed organoid was counted as a cell cluster with a defined luminal interior to account for growth and exclude single cells. Percent organoid formation efficiency was determined by dividing the number of formed organoids by the 150 cell starting quantity.

Flow cytometric analysis of proliferation and cell cycle.

The Click-iT™ EdU Flow Cytometry Assay Kit (Invitrogen, C10419) was used to measure proliferation. EdU (provided in kit) was added to each well from 10mM stock solutions to a final concentration of 10 μM. After culturing for 30 minutes at 37°C, organoids were dispersed into single cells, washed in PBS + 1% BSA, pelleted, and single cells were resuspended in 100 μL of Click-iT™ fixative. Cells were incubated for 15 minutes at room temperature in the dark to fix. After fixation, 1 mL of PBS + 1% BSA was added, cells were pelleted at 500xg for 5 minutes at 4°C, washed with cold PBS, resuspended in 100 μL of saponin-based permeabilization buffer (provided in kit), and incubated for 15 minutes at room temperature. 500 μL of Click-iT™ cocktail was added, mixed, and incubated for 30 minutes at room temperature in the dark. Cells were spun at 500xg for 5 minutes, washed with 1X permeabilization buffer, pelleted, resuspended in 500 μL of 1X permeabilization buffer containing DAPI (0.5 μg/mL, Invitrogen, D1306), and filtered through a 40 μM filter. Single cells were analyzed via flow cytometry on a Sony MA900 Multi-Application Cell Sorter in the University of Michigan Flow Cytometry Core Facility.

For cell cycle analysis, cells were fixed and permeabilized as above. Following permeabilization, cells were suspended in 500 μL of 4 μg/mL Hoechst 33342

(Invitrogen, H3570) in 1X permeabilization buffer and incubated for 15 minutes at room temperature. 500 µL of 8 µg/mL Pyronin Y (Sigma, P9172) in 1X permeabilization buffer was then added, resulting in a final concentration of 2 µg/mL Hoechst 33342 and 4 µg/mL Pyronin Y. Cells were incubated for 30 minutes, washed twice in 1X permeabilization buffer, resuspended in 1X permeabilization buffer, filtered through a 40 µm filter, and analyzed by flow cytometry. Cells were analyzed on a Sony MA900 Multi-Application Cell Sorter in the University of Michigan Flow Cytometry Core Facility.

Organoid immunostaining.

Culture media was aspirated, and wells were overlayed with ice-cold DPBS. Matrigel patties containing organoids were transferred to 1.5 mL Eppendorf tubes with a P1000 and broken down with gentle pipetting. Organoids were incubated on ice for 15 minutes, pelleted at 250xg, and washed four times in ice-cold DPBS to remove the Matrigel. After the fourth wash, organoids were resuspended in 200 µL of 4% paraformaldehyde in PBS (PFA). After incubation for 30 minutes at room temperature, organoids were washed with ice-cold PBS three times to remove PFA and stored in PBS at 4°C for up to one month prior to staining.

For whole-mount staining, fixed organoids were pelleted at 250xg and resuspended in blocking solution (10% BSA and 10% Goat Serum (Sigma, G9023)) in PBS containing 0.3% TritonX-100, incubated for 2 hours at room temperature, followed by pelleting and resuspended in blocking solution containing primary antibody: anti-MUC5AC (1:50, Invitrogen, mouse monoclonal, MA1-35707), anti-MUC6 (1:50, Vector Labs, mouse monoclonal, VP-M658), CD44 (1:50, Thermo Scientific, rat monoclonal,

MA1-10229). After overnight incubation, organoids were washed and resuspended in blocking solution containing conjugated secondary antibody, Goat-anti-Mouse Alexa 488 (1:1000, Invitrogen, A-10680) or Goat-anti-Mouse Alexa 555 (1:1000, Invitrogen, A-21137). Organoids were incubated for 1 hour at room temperature, washed three times in PBS, resuspended in PBS containing DAPI (0.5 µg/mL, Invitrogen, D1306), washed, pelleted, resuspended in 50 µL of PBS, and transferred to a slide in a single droplet. The organoid droplet was circled with ProLong™ Gold Antifade Mountant (Invitrogen, P36930) and cover-slipped for microscopy. Images were captured on a Nikon E800 (Tokyo, Japan) microscope with Olympus DP (Tokyo, Japan) controller software. Image analysis and processing was performed using Image J (National Institutes of Health, Bethesda, MD), and any processing was equally applied to all images.

Statistical analysis.

GraphPad Prism (version 9.0, Software, San Diego, CA) was used for statistical analysis. Student's *t* test was used to compare two groups. For comparison of three or more conditions within one organoid line, a 1-way analysis of variance (ANOVA) was used with a Dunnett's post-hoc analysis. For comparison of corpus versus antral organoids grown across multiple similar conditions, a two-way analysis of variance (ANOVA) was used with a Šídák's post-hoc analysis. *$p<0.05$, #$p<0.05$, **$p<0.005$, and ***$p<0.001$ were used to denote significance. All authors had access to the study data and had reviewed and approved the final manuscript.

2.6 Acknowledgements

The authors are grateful to D. Kim Turgeon, MD, and Colin Burnett for coordinating the collection of patient tissue biopsies, to Jason Spence, PhD and Michael Dame, PhD in the Translational Tissue Modeling Laboratory for WRN media and microscopes, and to members of the Samuelson Laboratory for their helpful comments on the manuscript.

Table 2.1: Oligonucleotide primer sequences used for qRT-PCR gene expression analysis.

Gene	Amplicon size (bp)	Forward Primer (5' – 3')	Reverse Primer (5' – 3')
HPRT	131	CCTGGCGTCGTGATTAGTGAT	AGACGTTCAGTCCTGTCCATAA
AQP5	139	TACGGTGTGGCACCGCTCAATG	AGTCAGTGGAGGCGAAGATGCA
AXIN2	103	CTGGTGCAAAGACATAGCCA	AGTGTGAGGTCCACGGAAAC
CD44	151	CCAGAAGGAACAGTGGTTTGGC	ACTGTCCTCTGGGCTTGGTGTT
CHGA	117	GGTTCTTGAGAACCAGAGCAGC	GCTTCACCACTTTTCTCTGCCTC
FOXQ1	159	ATTTCTTGCTATTGACCGATGC	CCCAAGGAGACCACAGTTAGAG
GHRL	256	CTGAGCCCTGAACACCAGAG	CCTCTTTGGCCTCTTCCCAG
GIF	150	TGCCCCAGGTCACTTGTAGT	TGGTCTCGTTGAAGAGCAGC
ATP4A	265	ACAGATTGGTCAACGAGCCC	TGGCACACCTCAATGCTGAT
LGR5	159	CCTATCGTCCAACCTCCTGTCG	GCACAGCACTGGTAAGCATAAGG
LIPF	127	TGACCTTCCAGCCACAATCGAC	TTTAGCCAGGCTGGGATTGGTG
MUC5AC	103	GGAACTGTGGGGACAGCTCTT	GTCACATTCCTCAGCGAGGTC
MUC6	122	GGACTGTGAGTGTCTGTGCGAT	GCGTGTTGTAGAAGCCGCAGTA
CDKN1C	138	AGATCAGCGCCTGAGAAGTCGT	TCGGGGCTCTTTGGGCTCTAAA
PGC	128	ACCTACTCCACCAATGGGCAG	TCACTCAAGCCGAACTCCTGGT
SP5	147	CTCGCTGCAGGCCTTTCT	TAGGGCACCTGCAGGAAGT
TFF1	179	CCCAGTGTGCAAATAAGGGC	GCTCTGGGACTAATCACCGT
TFF2	228	GACAATGGATGCTGTTTCG	GTAATGGCAGTCTTCCACAGA
TNFRSF19	114	CAGGCATCTGAAAACTCGCCAC	GGTGCATTCTGCAGCCAGTCTT

2.7 References

1. Choi E, Roland JT, Barlow BJ, O'Neal R, Rich AE, Nam KT, Shi C, and Goldenring JR. Cell lineage distribution atlas of the human stomach reveals heterogeneous gland populations in the gastric antrum. *Gut* 63: 1711-1720, 2014.

2. Mills JC, and Shivdasani RA. Gastric epithelial stem cells. *Gastroenterology* 140: 412-424, 2011.

3. Barker N, Huch M, Kujala P, van de Wetering M, Snippert HJ, van Es JH, Sato T, Stange DE, Begthel H, van den Born M, Danenberg E, van den Brink S, Korving J, Abo A, Peters PJ, Wright N, Poulsom R, and Clevers H. Lgr5(+ve) stem cells drive self-renewal in the stomach and build long-lived gastric units in vitro. *Cell Stem Cell* 6: 25-36, 2010.

4. Demitrack ES, Gifford GB, Keeley TM, Carulli AJ, VanDussen KL, Thomas D, Giordano TJ, Liu Z, Kopan R, and Samuelson LC. Notch signaling regulates gastric antral LGR5 stem cell function. *EMBO J* 34: 2522-2536, 2015.

5. Demitrack ES, Gifford GB, Keeley TM, Horita N, Todisco A, Turgeon DK, Siebel CW, and Samuelson LC. NOTCH1 and NOTCH2 regulate epithelial cell proliferation in mouse and human gastric corpus. *Am J Physiol Gastrointest Liver Physiol* 312: G133-G144, 2017.

6. Gifford GB, Demitrack ES, Keeley TM, Tam A, La Cunza N, Dedhia PH, Spence JR, Simeone DM, Saotome I, Louvi A, Siebel CW, and Samuelson LC. Notch1 and Notch2 receptors regulate mouse and human gastric antral epithelial cell homoeostasis. *Gut* 66: 1001-1011, 2017.

7. Sigal M, Logan CY, Kapalczynska M, Mollenkopf HJ, Berger H, Wiedenmann B, Nusse R, Amieva MR, and Meyer TF. Stromal R-spondin orchestrates gastric epithelial stem cells and gland homeostasis. *Nature* 548: 451-455, 2017.

8. Ye W, Takabayashi H, Yang Y, Mao M, Hibdon ES, Samuelson LC, Eaton KA, and Todisco A. Regulation of Gastric Lgr5+ve Cell Homeostasis by Bone Morphogenetic Protein (BMP) Signaling and Inflammatory Stimuli. *Cell Mol Gastroenterol Hepatol* 5: 523-538, 2018.

9. Li K, Wu H, Wang A, Charron J, Mishina Y, Habib SL, Liu H, and Li B. mTOR signaling regulates gastric epithelial progenitor homeostasis and gastric tumorigenesis via MEK1-ERKs and BMP-Smad1 pathways. *Cell Rep* 35: 109069, 2021.

10. Horita N, Keeley TM, Hibdon ES, Delgado E, Lafkas D, Siebel CW, and Samuelson LC. Delta-like 1-Expressing Cells at the Gland Base Promote Proliferation of Gastric Antral Stem Cells in Mouse. *Cell Mol Gastroenterol Hepatol* 13: 275-287, 2022.

11. Kapalczynska M, Lin M, Maertzdorf J, Heuberger J, Muellerke S, Zuo X, Vidal R, Shureiqi I, Fischer AS, Sauer S, Berger H, Kidess E, Mollenkopf HJ, Tacke F, Meyer TF, and Sigal M. BMP feed-forward loop promotes terminal differentiation in gastric glands and is interrupted by H. pylori-driven inflammation. *Nat Commun* 13: 1577, 2022.

12. Clevers H. Wnt/beta-catenin signaling in development and disease. *Cell* 127: 469-480, 2006.

13. Fischer AS, and Sigal M. The Role of Wnt and R-spondin in the Stomach During Health and Disease. *Biomedicines* 7: 44, 2019.

14. Barker N, Ridgway RA, van Es JH, van de Wetering M, Begthel H, van den Born M, Danenberg E, Clarke AR, Sansom OJ, and Clevers H. Crypt stem cells as the cells-of-origin of intestinal cancer. *Nature* 457: 608-611, 2009.

15. McCracken KW, Aihara E, Martin B, Crawford CM, Broda T, Treguier J, Zhang X, Shannon JM, Montrose MH, and Wells JM. Wnt/beta-catenin promotes gastric fundus specification in mice and humans. *Nature* 541: 182-187, 2017.

16. Broda TR, McCracken KW, and Wells JM. Generation of human antral and fundic gastric organoids from pluripotent stem cells. *Nat Protoc* 14: 28-50, 2019.

17. Burt RW. Gastric fundic gland polyps. *Gastroenterology* 125: 1462-1469, 2003.

18. Bianchi LK, Burke CA, Bennett AE, Lopez R, Hasson H, and Church JM. Fundic gland polyp dysplasia is common in familial adenomatous polyposis. *Clin Gastroenterol Hepatol* 6: 180-185, 2008.

19. Islam RS, Patel NC, Lam-Himlin D, and Nguyen CC. Gastric polyps: a review of clinical, endoscopic, and histopathologic features and management decisions. *Gastroenterol Hepatol (N Y)* 9: 640-651, 2013.

20. Kim JE, Fei L, Yin WC, Coquenlorge S, Rao-Bhatia A, Zhang X, Shi SSW, Lee JH, Hahn NA, Rizvi W, Kim KH, Sung HK, Hui CC, Guo G, and Kim TH. Single cell and genetic analyses reveal conserved populations and signaling mechanisms of gastrointestinal stromal niches. *Nat Commun* 11: 334, 2020.

21. Barker N, van Es JH, Kuipers J, Kujala P, van den Born M, Cozijnsen M, Haegebarth A, Korving J, Begthel H, Peters PJ, and Clevers H. Identification of stem cells in small intestine and colon by marker gene Lgr5. *Nature* 449: 1003-1007, 2007.

22. Karam SM, and Leblond CP. Dynamics of epithelial cells in the corpus of the mouse stomach. I. Identification of proliferative cell types and pinpointing of the stem cell. *Anat Rec* 236: 259-279, 1993.

23. Stange DE, Koo BK, Huch M, Sibbel G, Basak O, Lyubimova A, Kujala P, Bartfeld S, Koster J, Geahlen JH, Peters PJ, van Es JH, van de Wetering M, Mills JC, and Clevers H. Differentiated Troy+ chief cells act as reserve stem cells to generate all lineages of the stomach epithelium. *Cell* 155: 357-368, 2013.

24. Bartfeld S, and Koo BK. Adult gastric stem cells and their niches. *Wiley Interdiscip Rev Dev Biol* 6: e261, 2017.

25. Leushacke M, Tan SH, Wong A, Swathi Y, Hajamohideen A, Tan LT, Goh J, Wong E, Denil S, Murakami K, and Barker N. Lgr5-expressing chief cells drive epithelial regeneration and cancer in the oxyntic stomach. *Nat Cell Biol* 19: 774-786, 2017.

26. Han S, Fink J, Jorg DJ, Lee E, Yum MK, Chatzeli L, Merker SR, Josserand M, Trendafilova T, Andersson-Rolf A, Dabrowska C, Kim H, Naumann R, Lee JH, Sasaki N, Mort RL, Basak O, Clevers H, Stange DE, Philpott A, Kim JK, Simons BD, and Koo BK. Defining the Identity and Dynamics of Adult Gastric Isthmus Stem Cells. *Cell Stem Cell* 25: 342-356.e347, 2019.

27. Caldwell B, Meyer AR, Weis JA, Engevik AC, and Choi E. Chief cell plasticity is the origin of metaplasia following acute injury in the stomach mucosa. *Gut* 71: 1068-1077, 2022.

28. Meyer AR, and Goldenring JR. Injury, repair, inflammation and metaplasia in the stomach. *J Physiol* 596: 3861-3867, 2018.

29. Radyk MD, Burclaff J, Willet SG, and Mills JC. Metaplastic Cells in the Stomach Arise, Independently of Stem Cells, via Dedifferentiation or Transdifferentiation of Chief Cells. *Gastroenterology* 154: 839-843.e832, 2018.

30. Bartfeld S, Bayram T, van de Wetering M, Huch M, Begthel H, Kujala P, Vries R, Peters PJ, and Clevers H. In vitro expansion of human gastric epithelial stem cells and their responses to bacterial infection. *Gastroenterology* 148: 126-136.e126, 2015.

31. Fischer AS, Mullerke S, Arnold A, Heuberger J, Berger H, Lin M, Mollenkopf HJ, Wizenty J, Horst D, Tacke F, and Sigal M. R-spondin/YAP axis promotes gastric oxyntic gland regeneration and Helicobacter pylori-associated metaplasia in mice. *J Clin Invest* 132: 2022.

32. Clevers H, Loh KM, and Nusse R. Stem cell signaling. An integral program for tissue renewal and regeneration: Wnt signaling and stem cell control. *Science* 346: 1248012, 2014.

33. Eddaoudi A, Canning SL, and Kato I. Flow Cytometric Detection of G0 in Live Cells by Hoechst 33342 and Pyronin Y Staining. *Methods Mol Biol* 1686: 49-57, 2018.

34. Lee JH, Kim S, Han S, Min J, Caldwell B, Bamford AD, Rocha ASB, Park J, Lee S, Wu SS, Lee H, Fink J, Pilat-Carotta S, Kim J, Josserand M, Szep-Bakonyi R, An Y, Ju YS, Philpott A, Simons BD, Stange DE, Choi E, Koo BK, and Kim JK. p57(Kip2) imposes the reserve stem cell state of gastric chief cells. *Cell Stem Cell* 29: 826-839.e829, 2022.

35. Ru Y, Chen XJ, Zhao ZW, Zhang PF, Feng SH, Gao Q, Gao SG, and Feng XS. CyclinD1 and p57(kip2) as biomarkers in differentiation, metastasis and prognosis of gastric cardia adenocarcinoma. *Oncotarget* 8: 73860-73870, 2017.

36. Busslinger GA, Weusten BLA, Bogte A, Begthel H, Brosens LAA, and Clevers H. Human gastrointestinal epithelia of the esophagus, stomach, and duodenum resolved at single-cell resolution. *Cell Rep* 34: 108819, 2021.

37. Abraham SC, Nobukawa B, Giardiello FM, Hamilton SR, and Wu TT. Fundic gland polyps in familial adenomatous polyposis: neoplasms with frequent somatic adenomatous polyposis coli gene alterations. *Am J Pathol* 157: 747-754, 2000.

38. Abraham SC, Nobukawa B, Giardiello FM, Hamilton SR, and Wu TT. Sporadic fundic gland polyps: common gastric polyps arising through activating mutations in the beta-catenin gene. *Am J Pathol* 158: 1005-1010, 2001.

39. Elhanafi S, Saadi M, Lou W, Mallawaarachchi I, Dwivedi A, Zuckerman M, and Othman MO. Gastric polyps: Association with Helicobacter pylori status and the pathology of the surrounding mucosa, a cross sectional study. *World J Gastrointest Endosc* 7: 995-1002, 2015.

40. Albuquerque C, Breukel C, van der Luijt R, Fidalgo P, Lage P, Slors FJ, Leitao CN, Fodde R, and Smits R. The 'just-right' signaling model: APC somatic mutations are selected based on a specific level of activation of the beta-catenin signaling cascade. *Hum Mol Genet* 11: 1549-1560, 2002.

41. Leedham SJ, Rodenas-Cuadrado P, Howarth K, Lewis A, Mallappa S, Segditsas S, Davis H, Jeffery R, Rodriguez-Justo M, Keshav S, Travis SP, Graham TA, East J, Clark S, and Tomlinson IP. A basal gradient of Wnt and stem-cell number influences regional tumour distribution in human and mouse intestinal tracts. *Gut* 62: 83-93, 2013.

42. Langlands AJ, Carroll TD, Chen Y, and Nathke I. Chir99021 and Valproic acid reduce the proliferative advantage of Apc mutant cells. *Cell Death Dis* 9: 255, 2018.

43. Luis TC, Naber BA, Fibbe WE, van Dongen JJ, and Staal FJ. Wnt3a nonredundantly controls hematopoietic stem cell function and its deficiency results in complete absence of canonical Wnt signaling. *Blood* 116: 496-497, 2010.

44. Luis TC, Naber BA, Roozen PP, Brugman MH, de Haas EF, Ghazvini M, Fibbe WE, van Dongen JJ, Fodde R, and Staal FJ. Canonical wnt signaling regulates hematopoiesis in a dosage-dependent fashion. *Cell Stem Cell* 9: 345-356, 2011.

45. Famili F, Brugman MH, Taskesen E, Naber BEA, Fodde R, and Staal FJT. High Levels of Canonical Wnt Signaling Lead to Loss of Stemness and Increased Differentiation in Hematopoietic Stem Cells. *Stem Cell Reports* 6: 652-659, 2016.

46. Yan KS, Janda CY, Chang J, Zheng GXY, Larkin KA, Luca VC, Chia LA, Mah AT, Han A, Terry JM, Ootani A, Roelf K, Lee M, Yuan J, Li X, Bolen CR, Wilhelmy J, Davies PS, Ueno H, von Furstenberg RJ, Belgrader P, Ziraldo SB, Ordonez H, Henning SJ, Wong MH, Snyder MP, Weissman IL, Hsueh AJ, Mikkelsen TS, Garcia KC, and Kuo CJ. Non-equivalence of Wnt and R-spondin ligands during Lgr5(+) intestinal stem-cell self-renewal. *Nature* 545: 238-242, 2017.

47. Nam KT, Lee HJ, Sousa JF, Weis VG, O'Neal RL, Finke PE, Romero-Gallo J, Shi G, Mills JC, Peek RM, Jr., Konieczny SF, and Goldenring JR. Mature chief cells are cryptic progenitors for metaplasia in the stomach. *Gastroenterology* 139: 2028-2037.e2029, 2010.

48. Matsumoto A, Takeishi S, Kanie T, Susaki E, Onoyama I, Tateishi Y, Nakayama K, and Nakayama KI. p57 is required for quiescence and maintenance of adult hematopoietic stem cells. *Cell Stem Cell* 9: 262-271, 2011.

49. Zou P, Yoshihara H, Hosokawa K, Tai I, Shinmyozu K, Tsukahara F, Maru Y, Nakayama K, Nakayama KI, and Suda T. p57(Kip2) and p27(Kip1) cooperate to maintain hematopoietic stem cell quiescence through interactions with Hsc70. *Cell Stem Cell* 9: 247-261, 2011.

50. Tesio M, and Trumpp A. Breaking the cell cycle of HSCs by p57 and friends. *Cell Stem Cell* 9: 187-192, 2011.

51. Gotschel F, Kern C, Lang S, Sparna T, Markmann C, Schwager J, McNelly S, von Weizsacker F, Laufer S, Hecht A, and Merfort I. Inhibition of GSK3 differentially modulates NF-kappaB, CREB, AP-1 and beta-catenin signaling in hepatocytes, but fails to promote TNF-alpha-induced apoptosis. *Exp Cell Res* 314: 1351-1366, 2008.

52. Huang J, Guo X, Li W, and Zhang H. Activation of Wnt/beta-catenin signalling via GSK3 inhibitors direct differentiation of human adipose stem cells into functional hepatocytes. *Sci Rep* 7: 40716, 2017.

53. Wang B, Khan S, Wang P, Wang X, Liu Y, Chen J, and Tu X. A Highly Selective GSK-3beta Inhibitor CHIR99021 Promotes Osteogenesis by Activating Canonical and Autophagy-Mediated Wnt Signaling. *Front Endocrinol (Lausanne)* 13: 926622, 2022.

CHAPTER III

Region-Specific Wnt Signaling Responses Promote Gastric Polyp Formation in Familial Adenomatous Polyposis Patients

This chapter is adapted from the following manuscript in preparation:

McGowan, KM, Delgado, E, Keeley TM, Hibdon, ES, Turgeon DK, Stoffel E, Samuelson, LC. Region-specific Wnt signaling responses promote gastric polyp formation in familial adenomatous polyposis patients. 2023

3.1 Summary

Germline *APC* mutation in familial adenomatous polyposis (FAP) patients promotes gastrointestinal polyposis, including the formation of frequent gastric fundic gland polyps (FGPs). In this study, we investigated how dysregulated Wnt signaling promotes FGPs and why they localize to the corpus region of the stomach. We developed a biobank of FGP and surrounding non-polyp corpus biopsies and organoids from FAP patients for comparative studies. Polyp biopsies and polyp-derived organoids exhibited enhanced Wnt target gene expression. Polyp-derived organoids with intrinsic upregulated Wnt signaling showed poor tolerance to further induction, suggesting that high Wnt restricts growth. Targeted genomic sequencing revealed that most gastric polyps did not arise via *APC* loss-of-heterozygosity. Studies in genetic mouse models demonstrated that heterozygous *Apc* loss increased epithelial cell proliferation in the corpus but not the antrum, while homozygous *Apc* loss was not maintained in the corpus yet induced hyperproliferation in antrum. Our findings suggest that heterozygous *APC* mutation in FAP patients may be sufficient to drive polyp formation in the corpus

region while subsequent loss-of-heterozygosity to further enhance Wnt signaling is not tolerated. This finding contextualizes the abundant yet benign nature of gastric polyps in FAP patient corpus compared to the rare, yet adenomatous polyps in the antrum.

3.2 Introduction

Familial adenomatous polyposis (FAP) is an autosomal dominant disease resulting from an inherited loss-of-function mutation to the tumor suppressor adenomatous polyposis coli (*APC*). *APC* mutation leads to activation of the Wnt signaling pathway, and thus FAP patients are predisposed to developing disease in numerous tissues (1, 2). The most significant disease burden occurs within the gastrointestinal tract where, in the absence of endoscopic or surgical intervention, FAP patients have a >90% effective risk of developing colorectal cancer throughout their lifetime (2-4).

FAP patients are also at an increased risk for polyposis within the stomach. The abundance of gastric polyps within FAP patients varies, with some patients developing 100 to 1000's of lesions and often leading to carpeting of the gastric corpus (5). These polyps predominately arise as fundic gland polyps (FGPs) which are sessile lesions characterized by cystically dilated glands (6-9). FGPs in FAP patients sometimes present with features of low-grade dysplasia, but rarely demonstrate high-grade dysplasia and are typically considered benign (5, 10-12). These polyps are also regionally restricted to the corpus, with gastric polyps in FAP patients only rarely found within the antral region. The rare antral polyps that emerge typically exhibit

adenomatous change and have increased potential to progress to cancer in line with colorectal polyps (13).

The mechanisms through which Wnt signaling underscores FGP emergence remain unclear as little is known about how Wnt regulates corpus epithelial homeostasis in humans. Furthermore, it is unknown why FGPs rarely progress to cancer while colorectal cancer in these patients is so prevalent. Although *APC* mutations have been detected in 7-34% of gastric cancer, FAP patients are only at a 0.5-1.3% lifetime risk of developing gastric cancer (13-17). The mechanism of polyp emergence within the colon would suggest that additional somatic hits to *APC*, including loss-of-heterozygosity, initiates formation; however, few studies have investigated the mutational landscape of FGPs in FAP patients (18).

The ‘just-right’ hypothesis describes an optimal range of Wnt signaling to drive cellular growth and proliferation in the context of polyposis. This principle has been used to describe regional distribution of cancer throughout the colon but has not been explored within the stomach (19-23). We have recently demonstrated that human corpus organoids have a lower threshold for Wnt signaling to drive optimal growth relative to patient-matched antral organoids (24). This finding predicts that corpus stem/progenitor cells may be more susceptible to develop hyperplasia upon Wnt activation compared to antral stem cells, but this concept and the subsequent application of the ‘just-right’ hypothesis underscoring FGP development has not been defined.

In this study, we investigated the etiology of FGP formation resulting from germline *APC* mutations in FAP patients. We established a biobank of patient-matched

FGP and surrounding non-polyp samples to conduct comparative analyses of genomic DNA sequencing, mRNA expression analysis, and *in vitro* organoid growth experiments. We demonstrate that FGPs have increased expression of Wnt target genes relative to their patient-matched non-polyp samples, indicating upregulation of the Wnt signaling pathway. However, additional somatic alterations to *APC* indicating loss-of-heterozygosity were infrequent, demonstrating that this mechanism does not underscore enhanced Wnt signaling and is not required for polyp emergence. Ultimately, we demonstrate through human FAP organoids and genetic mouse models that heterozygous loss of *APC* optimally drives corpus proliferation while homozygous loss is not tolerated.

3.3 Results

Enhanced Wnt target gene expression in FAP-associated fundic gland polyps

APC mutation activates Wnt signaling through unregulated translocation of β-catenin to the nucleus resulting from compromised function of the destruction complex (Figure 3.1A). To investigate the molecular and cellular etiology of gastric FGP formation in FAP patients, we established a biobank of patient-paired FGP (P) and surrounding non-polyp (NP) gastric corpus tissue samples (Figure 3.1B). From biopsy sample pairs, we extracted genomic DNA, RNA, and/or developed paired organoid cultures for further analyses. Our biobank consisted of samples from 34 individual FAP patients across a spectrum of germline *APC* mutations (Figure 3.1C, Table 1).

We first analyzed the gene expression profile of patient-matched P versus NP biopsies to determine whether upregulated Wnt signaling underscored FGP emergence.

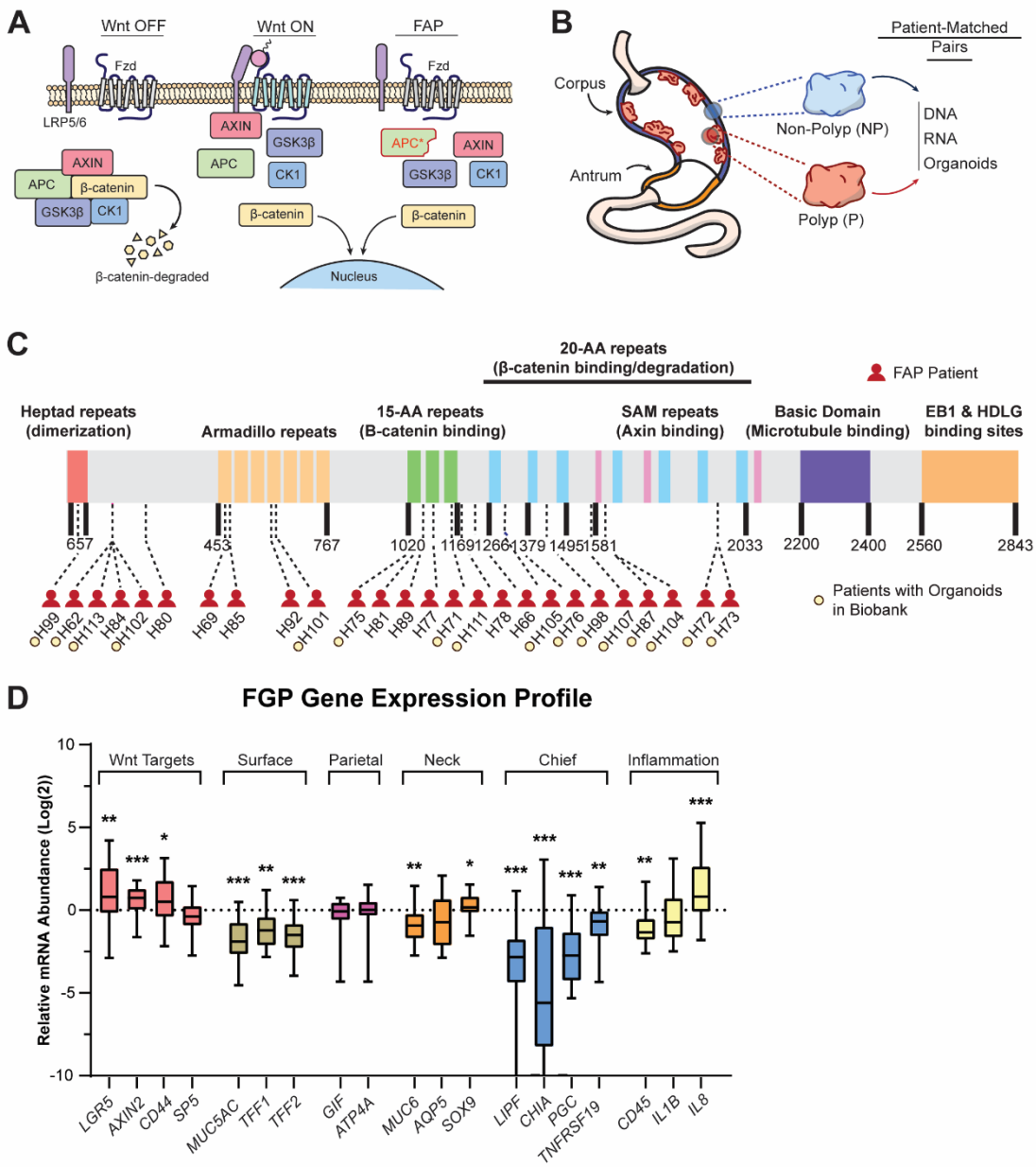

Figure 3.1: Fundic gland polyp biopsy samples from FAP patients have increased Wnt target gene expression.

A) Schematic of Wnt signaling in Wnt OFF, Wnt ON, and in FAP patients with mutated APC (APC*) demonstrating nuclear localization of β-catenin in the absence of Wnt ligand. B) Biopsies from paired fundic gland polyps (P) and surrounding non-polyp (NP) corpus tissue were collected to establish an FAP patient biobank of RNA, DNA, and organoids. C) Schematic of the APC protein labeled with specific familial mutation sites for the patients in our biobank. Patients with established polyp and non-polyp organoids are designated. Only patients with known germline mutations are included on this schematic (Table 1). D) Relative mRNA abundance of select genes in FAP patient biopsies. qRT-PCR analysis of Wnt target, cell marker, and inflammation-related transcripts, with *HPRT* used as an internal reference transcript. Data are displayed as Log(2) fold change relative to patient-matched non-polyp tissue ($n_{non\text{-}polyp}$ = 27 biopsies, n_{polyp} = 30 biopsies; *p<0.05, **p<0.005, ***p<0.001 by unpaired parametric *t* test).

qPCR analysis of transcript abundance revealed that Wnt target genes *LGR5*, *AXIN2*, and *CD44* were upregulated in FGP biopsies relative to patient-matched non-polyp tissue (Figure 3.1D, 3.2A). Analysis of differentiated cell markers showed that FGP biopsies were deficient in markers for surface cells, which is consistent with studies showing that upregulation of Wnt signaling alters corpus epithelial cell differentiation (Figure 3.1D, 3.2B) (24-26). FGP biopsies also showed markedly reduced expression of chief cell markers *LIPF*, *CHIA*, *PGC*, and *TNFRSF19* along with a more subdued decrease in the mucous neck cell marker *MUC6* (Figure 3.1D, 3.2D-E). It is unknown whether these changes in cell marker expression are a consequence of biopsy extraction or due to altered stem/progenitor cell differentiation secondary to Wnt activation in FGPs. Notably, parietal cell markers *GIF* and H/K ATPase subunit *ATP4A* were unchanged (Figure 3.1D, 3.2C). Analysis of inflammatory markers showed a surprising reduction in *CD45*, suggesting that FGP formation was not associated with inflammatory cell influx, although some polyps exhibited a pro-inflammatory environment suggested by increased expression of *IL8* (Figure 3.1D, 3.2F).

Wnt tone is intrinsically elevated in high Wnt FGP-derived organoids

Given our observations that Wnt target gene expression was upregulated in FGPs, we tested whether Wnt signaling is intrinsically elevated in corpus progenitors by generating P- and NP-derived organoids. We passaged FAP patient-derived organoids at least three times before analysis to remove non-epithelial cells and to establish stable self-renewing cultures. Wnt target gene expression was measured in nine patient-matched organoid pairs after growth in normal media containing exogenous Wnt

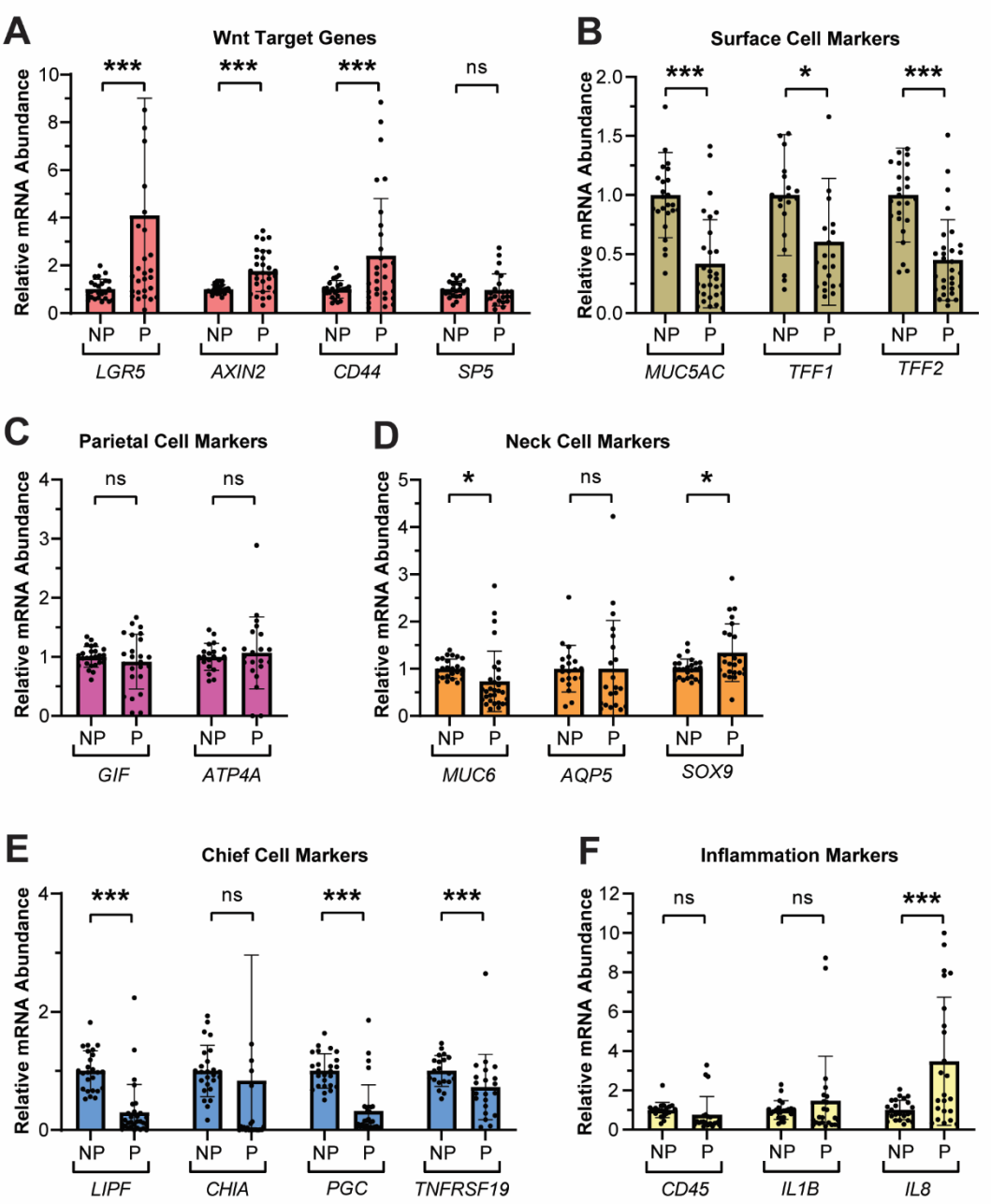

Figure 3.2: mRNA expression analysis of primary FGP and surrounding non-polyp biopsies from FAP patients.

A-F) Relative mRNA abundance of (A) Wnt target genes, (B) surface mucous cell markers, (C) parietal cell markers, (D) mucous neck cell markers, (E) chief cell markers, and (F) immune cells/inflammatory markers was measured by qRT-PCR analysis of polyp (P) and non-polyp (NP) biopsies from 10 FAP patients. mRNA abundance was calculated as fold-change relative to the mean patient-matched non-polyp mRNA abundance and normalized within each patient data set, with *HPRT* used for a reference. Data are shown as mean ± SD ($n_{non\text{-}polyp}$ = 27 biopsies, n_{polyp} = 30 biopsies; *p<0.05, **p<0.005, ***p<0.001 by unpaired parametric *t* test).

signaling ligands (WNT, RSPO; WR media) and following transition into WNT/RSPO depleted media (WR-Free) (Figure 3.3A). Comparison of *LGR5* mRNA abundance in FAP patient-matched P- and NP-derived organoids revealed variability in intrinsic Wnt tone, with polyp organoids falling into two subgroups (Figure 3.3B). In some patient pairs, such as H62 and H71, we noted either no difference in *LGR5* expression between P and NP organoids, or even decreased *LGR5* in P organoids grown in WR media (Figure 3.3B). Other patients, such as H72 and H73, demonstrated enhanced *LGR5* expression in P organoids. In all lines, we observed that *LGR5* expression was drastically reduced following acute WNT/RSPO withdrawal, thus demonstrating that all lines remained sensitive to exogenous Wnt. Broadening our analysis to include *AXIN2* and *SP5* demonstrated consistent trends in Wnt target gene expression (Figure 3.3C). Based on this analysis, we sub-grouped the organoids into High Wnt polyps with enhanced Wnt target gene expression relative to patient-matched non-polyp organoids (H72, H73, H61, H87), and Low Wnt polyps with similar or reduced target gene expression (H76, H71, H62, H82, H75) (Figure 3.3D).

We further assessed intrinsic Wnt tone by growing organoids for two passages in WR-Free media. Consistent with previous studies reporting that corpus organoids require both exogenous WNT and RSPO to be maintained over time, none of the non-polyp or Low Wnt polyp lines were capable of sustained growth in Wnt-depleted media (25). In contrast, all four High Wnt polyp lines grew long-term in WR-Free media, thus demonstrating long-term Wnt independent growth (Figure 3.3E). Therefore, enhanced

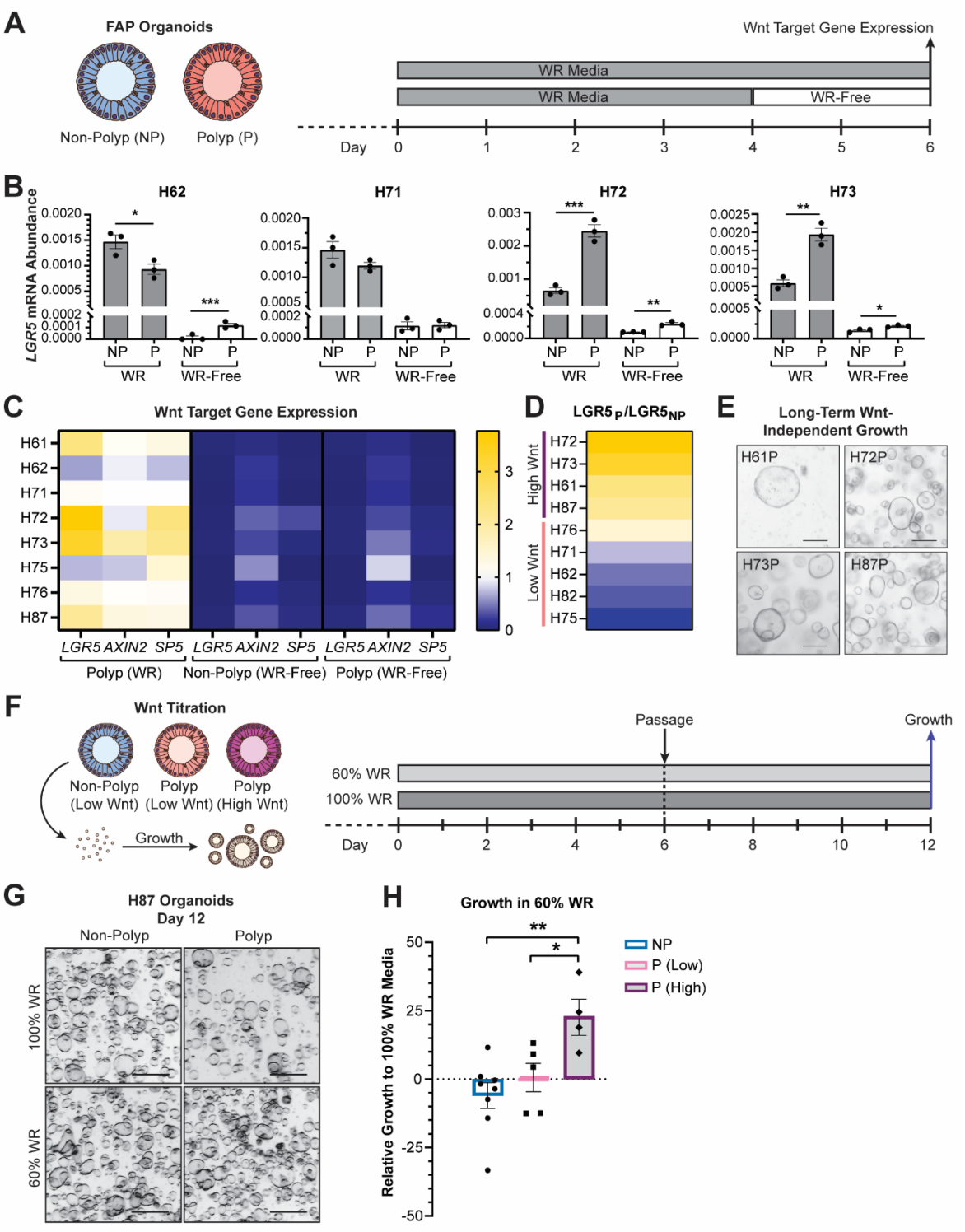

Figure 3.3: Enhanced Wnt signaling in a subset of FAP gastric polyp-derived organoids.

A) Wnt target gene expression was measured in patient-matched polyp (P)/non-polyp (NP) organoid pairs following six days of growth in WR media, or following four days of growth in WR and two days of growth in WR-Free media. B) *LGR5* mRNA abundance of FAP organoids grown

in WR or WR-Free media. Data are shown as mean ± SD mRNA abundance relative to the reference gene *ACTB* (n = 3 individual wells; *p<0.05, **p<0.005, ***p<0.001 by one-way ANOVA with Tukey's multiple-comparison test). C) Heatmap of relative Wnt target gene expression in polyp organoids. Data are shown as mean fold-change relative to the expression of each target gene in matched non-polyp organoids grown in WR media for six days. D) Heatmap of *LGR5* mRNA expression in polyp organoids, shown as mean fold-change relative to patient-matched non-polyp organoids and ordered from highest to lowest expression. High Wnt and Low Wnt denote the classification of polyp-derived lines with increased or similar/decreased Wnt target gene expression. E) Images of polyp organoids grown for two passages (12 days) in WR-Free media, demonstrating Wnt-independent growth (size bars = 100 μm). F) Growth of organoids cultured for 12 days in 100% or 60% WR media was measured through ATP-dependent luminescence. G) Images of H87 organoids at day 12 following growth in 100% or 60% WR (size bars = 200 μm). H) Relative growth of non-polyp and polyp organoids clustered by Wnt target gene expression characteristics (High Wnt and Low Wnt) in 60% compared to 100% WR media. Each point represents an individual organoid line shown as the average of triplicate wells. Each bar graph shows the average ± SD of the organoids in that group (n=4-9 individual organoid lines; *p<0.05, **p<0.005 by one-way ANOVA with Tukey's multiple-comparison test).

Wnt target gene expression and growth in Wnt-depleted media suggests an intrinsic increase in Wnt signaling in these FAP polyps.

To test whether High Wnt polyp organoids grow in WR-Free media because they secrete endogenous WNT ligand, we measured growth after treatment with the PORCN inhibitor LGK974, which suppresses Wnt ligand secretion (Figure 3.4A). We observed that LGK974 treatment had no impact on growth of High Wnt polyp lines H72P, H73P, or H87P (Figure 3.4B-C). We further observed that neither co-culture of High Wnt organoids growing in WR-Free media with non-polyp organoids, nor feeding non-polyp organoids with conditioned media from these High Wnt lines could rescue non-polyp organoid growth in the absence of exogenous WNT/RSPO (Figure 3.4D-G). Therefore, we demonstrate through both pharmacologic inhibition and co-culture experiments that High Wnt polyp organoids are sustained long-term in WR-Free media through an intrinsic signaling mechanism rather than by secreting Wnt or other growth factors into their environment.

Increased growth of High Wnt FGP-derived organoids in reduced Wnt media

Wnt signaling in the gastrointestinal tract has been proposed to follow a principle known as the ‘just-right’ hypothesis where excessive growth leading to polyposis is driven by an optimal level of Wnt. While too little Wnt signaling induces differentiation, hypermorphic upregulation of Wnt signaling, such as through total loss of APC function, can also be prohibitive to growth. This principle has previously been demonstrated to underscore regional patterns of colorectal cancer emergence in FAP patients where second-hit mutations to *APC* leading to further dysregulation of Wnt signaling are

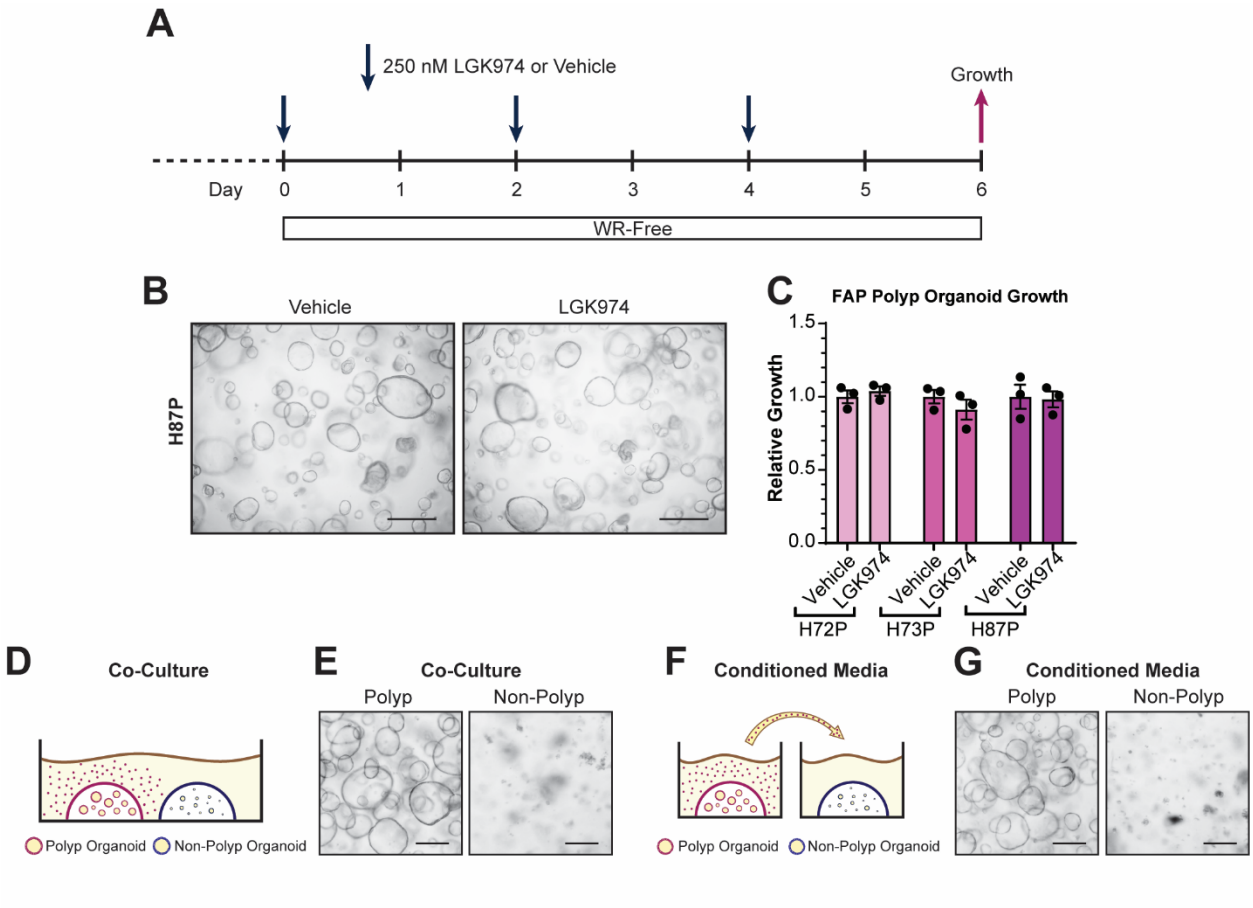

Figure 3.4: High Wnt FAP organoids are not sustained through secreted ligands.

A) High Wnt polyp organoids demonstrating long-term Wnt independent growth in WR-Free media were treated with the porcupine inhibitor LGK974 (250 nM) or DMSO (Vehicle). Growth was measured through ATP-dependent luminescence on day 6. B) Representative images of H87P organoids grown in WR-Free media on day 6 following treatment with Vehicle or LGK974 (size bars = 200 μm). C) Relative growth of Vehicle- or LGK974-treated H72P, H73P, or H87P organoids (n = 3 triplicate wells). D) Schematic of co-culture experiment of non-polyp organoids within the same well as polyp organoids from High Wnt lines that had been growing for several passages in WR-Free media. E) Representative images of H87P and H87NP organoids after six days of co-culture in WR-Free media (size bars = 100 μm). F) Schematic demonstrating treatment of non-polyp organoids with conditioned media derived from High Wnt polyp organoids grown six days in WR-Free media. G) Representative images of H87P and H87NP organoids following growth for six days in High Wnt polyp conditioned media (size bars = 100 μm).

selected to preserve some residual APC function (20-23, 27). We were interested in whether this principle also holds true for growth of FAP gastric polyp organoids. We hypothesized that High Wnt polyp organoids would have a reduced tolerance for extrinsic Wnt due to elevated intrinsic Wnt signaling, and therefore would exhibit maximal growth at lower concentrations of exogenous Wnt than non-polyp or Low Wnt polyp organoids. To test sensitivity to extrinsic Wnt, we grew organoids over two passages (12 days total) in either normal (100%) WR or reduced (60%) WR media to define the optimal Wnt environment for growth for each organoid line (Figure 3.3F). At day 12, organoids were imaged to assess overall appearance, and growth was measured using an ATP-dependent cell viability assay.

Using organoids from patient H87 as an example, we observed that non-polyp organoids grew at similar densities in 100% and 60% WR media (Figure 3.3G). In contrast, H87 polyp organoids, which are in the High Wnt subgroup, grew denser in 60% WR. Extending this analysis to all nine patient lines, we observed that non-polyp organoids exhibited similar growth in 60% WR media as they did in 100% WR (Figure 3.3H). While Low Wnt polyp-derived organoids had, on average, no change in growth between the two conditions, polyp organoids from the High Wnt group exhibited significantly enhanced growth in 60% WR. These results align with the ‘just-right’ hypothesis and demonstrates an interplay between intrinsic Wnt tone and extrinsic Wnt signaling for optimal growth.

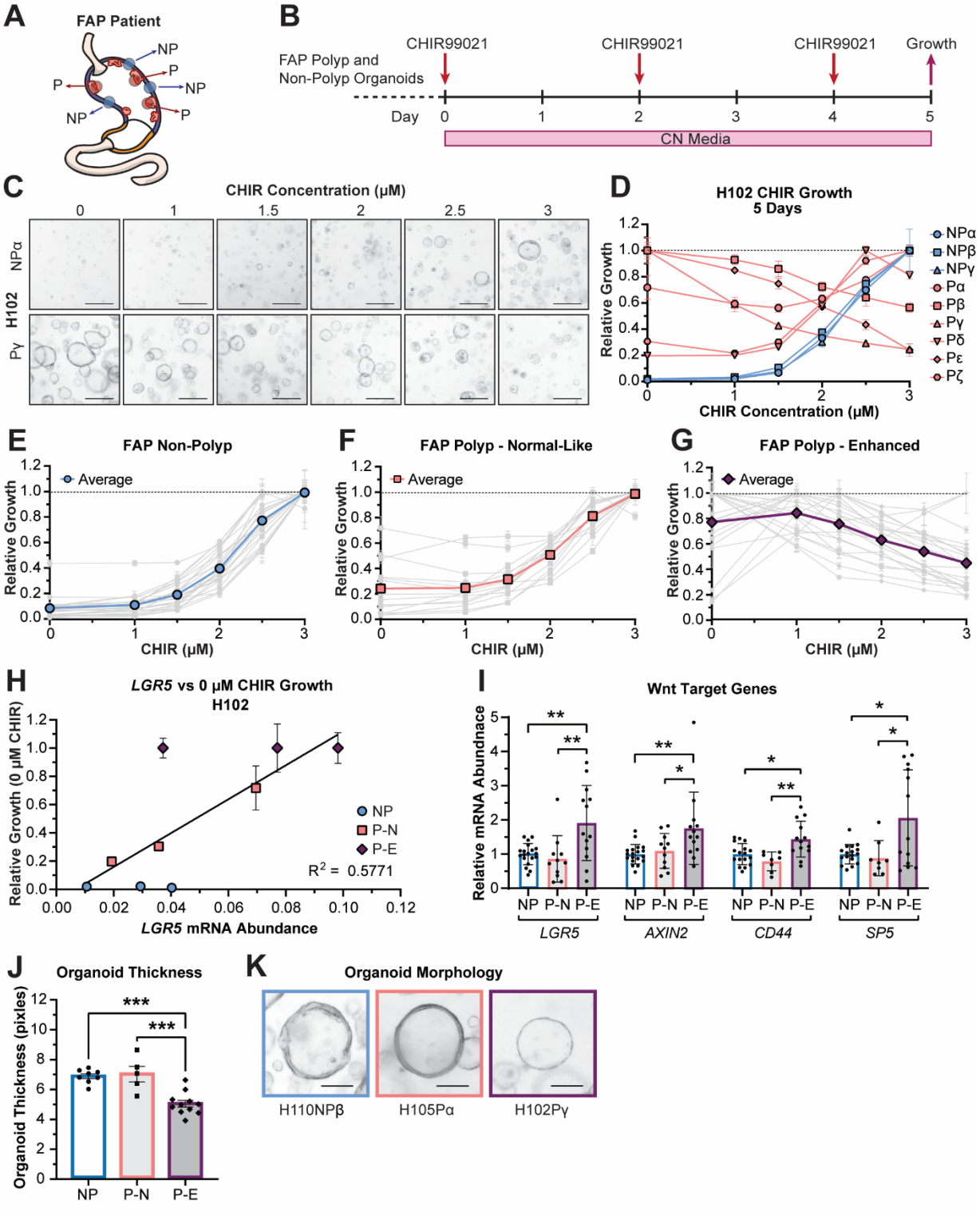

Figure 3.5: Intrinsic Wnt tone patterns intra-patient FGP variability.

A) Polyp (P) and non-polyp (NP) biopsies were harvested to analyze multiple polyps from each FAP patient. B) Established patient-matched organoids were grown in CN Media containing recombinant noggin and varying concentrations of CHIR99021 (CHIR) and growth was

measured through ATP-dependent luminescence on day 5. C) Representative images of H102NPα and H102Pγ following culture in 0-3 μM CHIR (size bars = 100 μm). D) Relative growth of all H102 organoid lines plotted as a function of CHIR concentration. Growth rates were normalized to the maximal growth rate observed for each line and data are presented as mean ± SD of triplicate wells for each line. E-G) Relative growth of FAP organoid lines from 12 FAP patients plotted as a function of CHIR concentration. Individual organoid lines are shown in grey, and the average of all lines is shown in color. E) FAP non-polyp organoid lines (blue, n = 23 lines). F) FAP polyp organoid lines demonstrating normal-like growth (pink, n = 14 lines). G) FAP polyp organoid lines demonstrating enhanced Wnt-independent growth (purple, n = 21 lines). H) Relative growth of H102 organoid lines after five days growth in 0 μM CHIR (WR-Free media) versus *LGR5* mRNA abundance after six days growth in 60% WR media. The trendline was calculated via linear regression analysis. I) Relative mRNA abundance of Wnt target genes in FAP organoids after six days growth in 60% WR media. Data are shown as mean ± SD fold change relative to patient-matched non-polyp. *HPRT* was used as an internal reference transcript. NP = non-polyp (n = 19); P-N = polyp normal-like (n = 11); P-E = polyp, enhanced (n = 13) (*$p<0.05$, **$p<0.005$ by one-way ANOVA with Tukey's multiple-comparison test). J) Average NP, P-N, or P-E organoid thickness (in pixels) after six days growth in 60% WR (***$p<0.001$). K) Representative images of organoid from non-polyp group (H110NPβ), normal-like polyp group (H105Pα), and enhanced polyp group (H102Pγ) after six days growth in 60% WR (size bars = 50 μm).

Intra-patient variability in FGP-derived organoid growth

We sought to further investigate the relationship between intrinsic Wnt tone and Wnt sensitivity through an analysis of additional FAP patient-derived organoids. We were also interested in whether individual polyps from the same patient would exhibit polyp-to-polyp variability or similar characteristics, which might suggest genotype-dependent mechanisms. To study this, we expanded our organoid biobank to include multiple independent polyp and non-polyp samples from 17 additional patients (Figure 3.5A, Figure 3.1C, Table 1). Organoids were established by directly embedding minced biopsy tissue in Matrigel, which improved establishment efficiency compared to our previous gland isolation approach. Based on our growth analysis, we established these organoids in 60% WR media to prevent selection bias or suppression of growth in lines with elevated Wnt tone. Epithelial outgrowth was observed after 2-4 days in culture, and subsequent passaging resulted in purification of epithelial organoids (Figure 3.6A). We noted that most polyp-derived biopsies developed organoids at faster rates than non-polyp biopsies, suggesting that polyps had increased progenitor potential (Figure 3.6B-C). Organoids were passaged at least three times before analysis to establish pure epithelial cultures.

We evaluated Wnt sensitivity by passaging these FAP organoids into media containing the pharmacologic Wnt activator CHIR99021 (CHIR) to dose-dependently activate Wnt signaling in the absence of exogenous WNT/RSPO ligands (Figure 3.5B) (24). Organoids were cultured for five days in media with 0 – 3 μM CHIR, as well as equal concentrations of recombinant Noggin (CN Media), to assess Wnt-dependent growth.

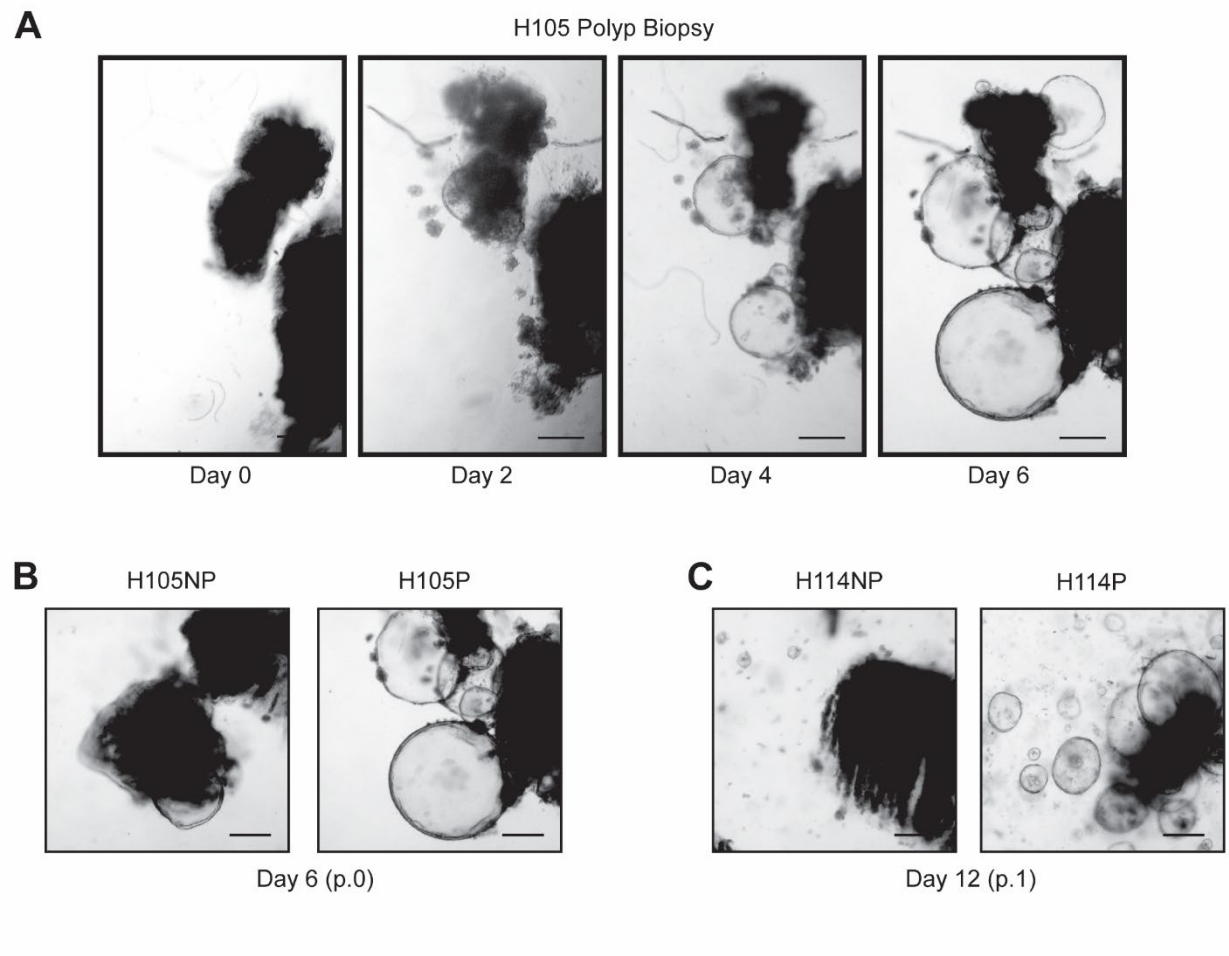

Figure 3.6: Establishment of human FAP gastric organoids from biopsies.

FAP patient biopsies were minced, embedded in Matrigel and cultured in 60% WR media. A) Representative images of epithelial outgrowth from primary FGP biopsy from patient H105 embedded in Matrigel (size bars = 100 μm). B) Representative images of epithelial outgrowth from non-polyp (H105NP) and polyp (H105P) biopsies six days after initial embedding in Matrigel (size bars = 100 μm). C) Representative images of epithelial outgrowth from non-polyp (H114NP) and polyp (H114P) biopsies six days after the first passage (12 days from initial seeding) (size bars = 100 μm).

In each patient sample set, we observed polyp-to-polyp variability in Wnt sensitivity (Figure 3.5, Figure 3.7). For example, from patient H102 we established organoids from six unique fundic gland polyps and three distinct non-polyp regions. Images taken on day 5 of CN media showed that while non-polyp line H102NPα has a positive growth response to increasing Wnt, polyp line H102Pγ is Wnt-averse, with reduced growth in response to increased CHIR (Figure 3.5C). While all H102 non-polyp lines followed the growth patterns of H102NPα, we observed that some polyp lines, including Pβ, Pγ, and Pε, showed enhanced Wnt-independent growth and reduced growth with increased Wnt signaling (Figure 3.5D). In contrast, increased CHIR stimulated growth in lines Pα, Pδ, and Pζ, similar to non-polyp lines.

This CHIR growth analysis stratified the expanded patient organoids into two subgroups. Regardless of patient, we found that all non-polyp organoids followed a near identical dose-response pattern with growth peaking at ~3 μM CHIR (Figure 3.5E). One subgroup of polyp organoids (termed Normal-Like or P-N) had a similar growth pattern with increased CHIR leading to increased growth (Figure 3.5F). The second subgroup (Enhanced or P-E) demonstrated Wnt independence and high sensitivity to increased CHIR (Figure 3.5G). From 35 polyp lines, 14 (40%) were P-N and 21 (60%) were P-E. While some patients' polyps exhibited either P-N or P-E growth characteristics, others exhibited both types (Figure 3.7). This variability suggests that polyp growth characteristics are not strictly genotype determined, although the small numbers of polyps analyzed from each patient makes it difficult to reach conclusions.

To determine if P-E organoids had higher Wnt signaling tone, we cultured organoids for six days in 60% WR media and measured Wnt target gene expression

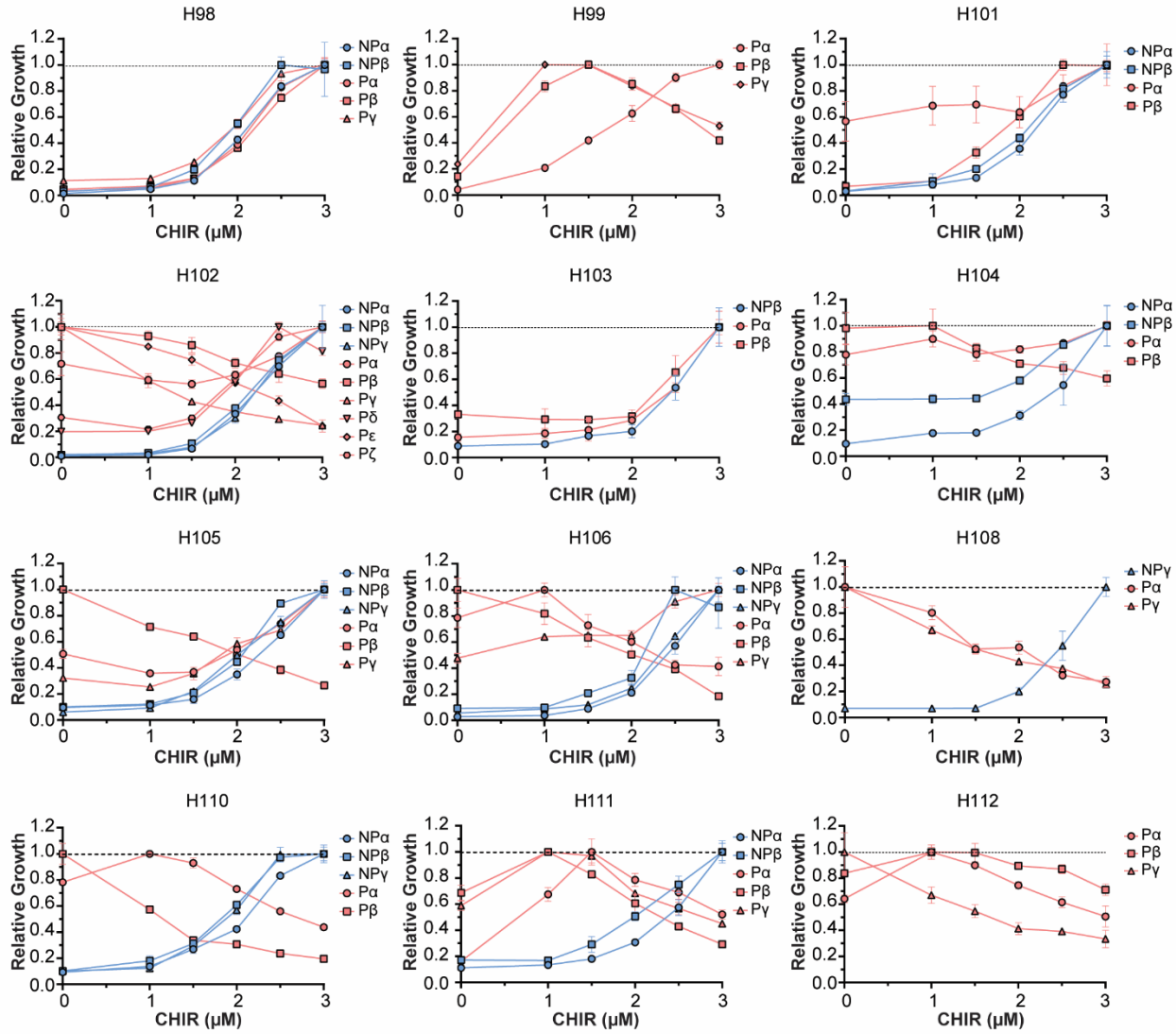

Figure 3.7: Polyp-derived FAP organoids exhibit significant intra-patient variability in Wnt dependence.

Relative growth of established polyp and non-polyp organoid lines from respective FAP patients measured on day 5 after growth in CHIR99021 (experimental design shown in Figure 3B). Growth rates were normalized to the maximum observed growth rate observed for each individual line. Data are presented as mean ± SD of triplicate wells for each line. Blue lines represent non-polyp organoids. Red lines represent polyp organoids. These data complement the summary data shown in Figure 3.

(Figure 3.5H-I, 3.8A). Using H102 organoids as an example, we determined that *LGR5* expression was positively correlated with enhanced Wnt-independent growth, suggesting that upregulated Wnt tone corresponded with increased Wnt sensitivity (Figure 3.5H). Expanding this analysis showed that P-E organoids significantly upregulated Wnt target genes relative to paired non-polyp and P-N organoids, consistent with our previous findings and the 'just-right' hypothesis (Figure 3.5I).

We also analyzed cell differentiation markers in these three organoid types (Figure 3.8B-E). We and others have shown that Wnt regulates a bimodal axis of differentiation in human and mouse corpus organoids, with low Wnt promoting surface mucous cell differentiation and high Wnt promoting neck and chief cell differentiation (24-26). Analysis of cell marker expression showed that P-E organoids had the lowest expression of surface cell markers *MUC5AC, TFF1,* and *TFF2*, consistent with enhanced Wnt signaling (Figure 3.8B). This finding also aligns with our analysis of gene expression in primary biopsy samples (Figure 3.1D). Interestingly, while our biopsy analysis showed a decrease in chief cell markers, analysis of P-E organoids demonstrated increased expression of some (*LIPF* and *TRFRSF19*) but not all (*PGC)* chief cell markers (Figure 3.8D). However, *PGC* can also localize to human gastric neck cells, and we did not observe alterations in neck cell marker expression (Figure 3.8C) (28). The organoid types also exhibited morphological differences. While non-polyp and normal-like polyp organoids were similar, P-E organoids were significantly thinner (Figure 3.5J, K). We speculate that this may be due to the altered differentiation characteristics.

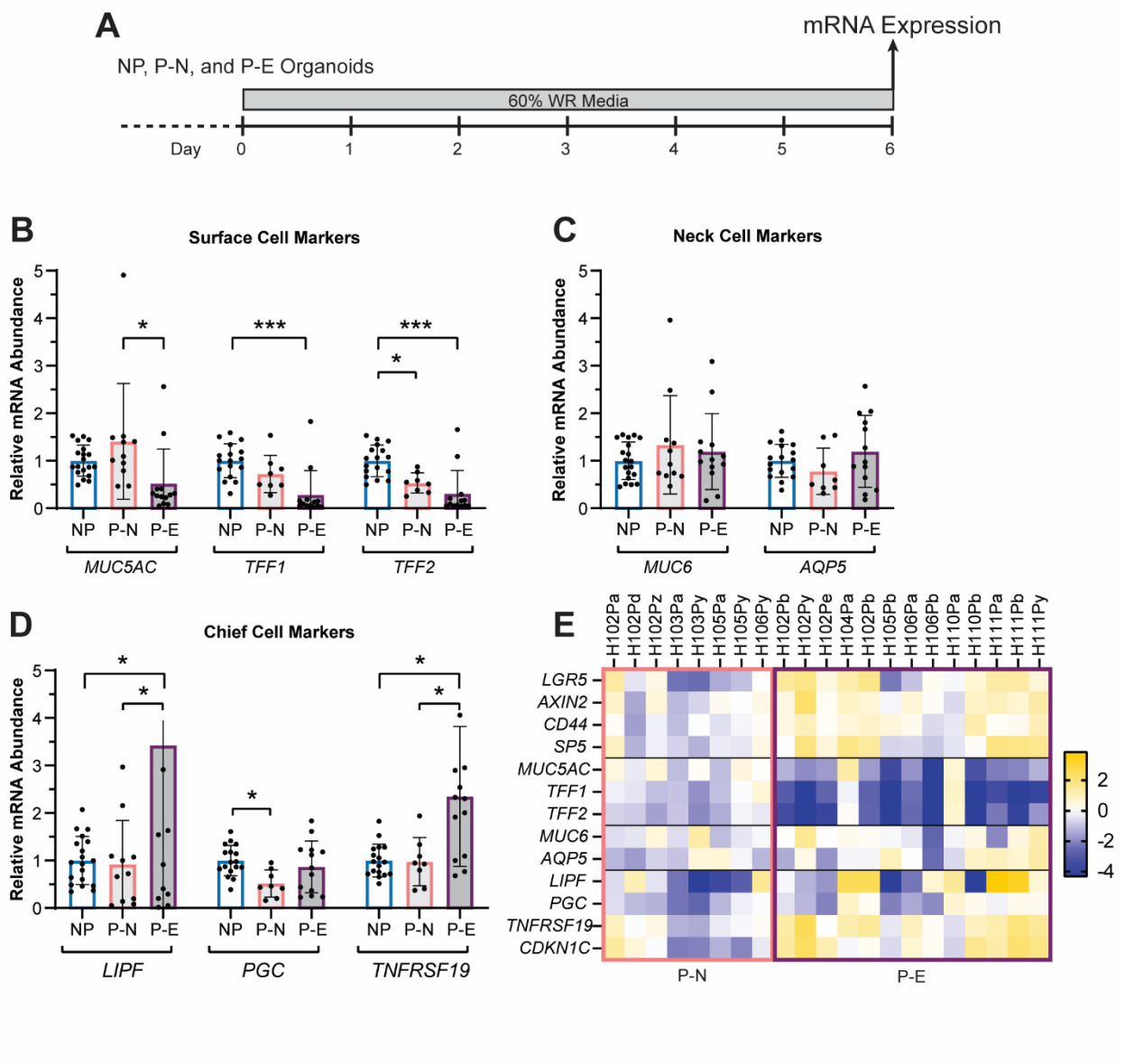

Figure 3.8: Gene expression in FAP organoids.

A) RNA was extracted from established polyp and non-polyp FAP organoids following six days growth in 60% WR media. Organoids were categorized as non-polyp (NP, n = 19); normal-like polyp (P-N, n = 11), and enhanced polyp (P-E, n = 13) as described in the text and Figure 3. B-D) Relative mRNA abundance of (B) surface, (C) neck, and (D) chief cell markers. Data are shown as mean ± SD fold change relative to patient-matched non-polyp organoids and normalized across all lines, with *HPRT* used as a reference. (*p<0.05, ***p<0.001 by one-way ANOVA with Tukey's multiple-comparison test). E) Heatmap of mRNA expression for individual polyp organoid lines. Data are presented as Log(2) fold-change expression in polyp organoids relative to average of non-polyp organoids from the same patient. Lines outlined in pink (left box) are normal-like polyps (P-N). Lines outlined in purple (right box) are enhanced polyps (P-E).

FAP fundic gland polyps develop without requirement for APC loss-of-heterozygosity

We sought to understand the mutational landscape that led to enhanced Wnt signaling in biopsies and organoids that may underscore FGP formation. One likely mechanism would be somatic *APC* mutation leading to loss-of-heterozygosity and further dysregulation of the Wnt signaling pathway, as this underscores FAP polyp emergence in the colon. DNA was extracted from our initial 19 patient biopsies or organoids for genomic analysis of tumor suppressors and oncogenes using a Qiagen Comprehensive Cancer Gene Panel, which included *APC* (Table 2). In each paired patient set (P vs. NP) we confirmed the familial *APC* mutation. Our analysis revealed that only one patient of the 19 studied (H85) had a novel somatic loss-of-function *APC* mutation (Figure 3.9A, Table 2). Further intra-patient comparisons revealed that about a third (6/19) of polyp samples harbored *APC*-specific copy number variations, although sequencing did not provide insight into whether the mutant or functional (normal) allele was affected (Figure 3.9B, Table 2). Looking broadly at the mutational landscape, we also observed chromosomal changes ranging from no observed copy number variations to extensive (50+) incidences in polyps (Figure 3.9C, Table 2).

A low Wnt environment selects for Wnt-activating mutations to sustain organoid growth

We tested whether there was transcriptional silencing of the wild-type *APC* allele during polyp organoid culture as another mechanism to enhance Wnt tone. *APC* is commonly hypermethylated in gastric cancer (52.9%) relative to normal tissue (37.7%) (29). Although High Wnt polyp organoids from H72, H73, and H87 demonstrated few genomic mutations or copy-number variations, transcriptional silencing of the wild-type

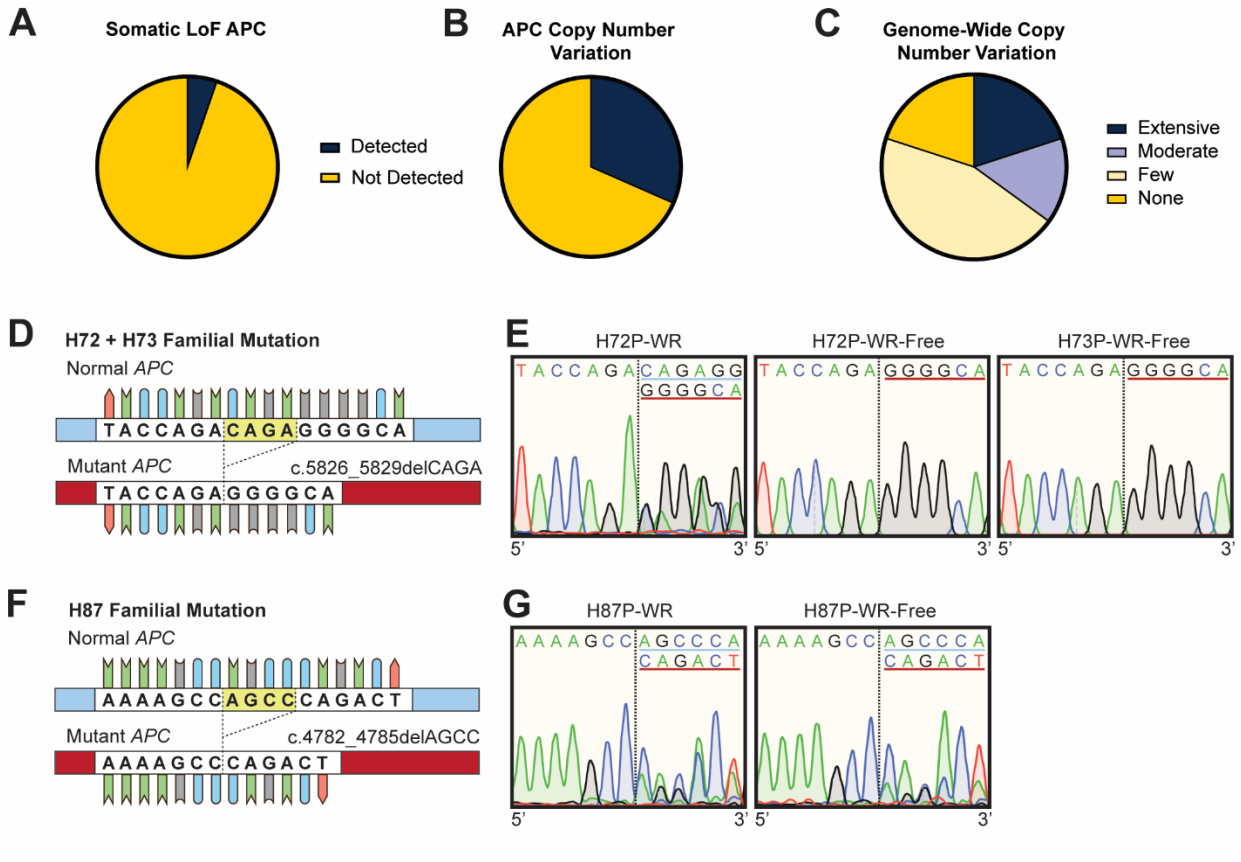

Figure 3.9: Infrequent somatic *APC* mutation in FAP patient FGPs.

A) Targeted sequencing of 19 FAP patient polyp and non-polyp samples using a Qiagen Comprehensive Target Cancer Panel detected one patient (H85) polyp with a novel somatic *APC* loss-of-function mutation. B) Six patients, including H85, demonstrated *APC* specific copy number variation (duplication or deletion) in their sequenced polyp DNA. C) Copy number variations detected through sequencing across the panel of 283 target genes by patient: None = 0 CNVs (4/19), Few = 1-4 (9/19), Moderate = 5-25 (3/19), Extensive = >26+ (4/19). D) *APC* mRNA sequence of normal and mutant allele in patients H72 and H73 at the familial mutation site (c.5826_5829). The highlighted CAGA sequence is deleted in the germline mutant *APC* allele. E) Chromatogram of sequenced *APC* cDNA harvested from H72 polyp organoids grown in 100% WR media, H72 polyp organoids grown for 2+ passages in WR-Free media, and H73 polyp organoids grown for 3+ passages in WR-Free media, depicting 7 bp 5' of the mutation site and 6 bp 3' of the mutation site. The blue underlined sequence aligned with the wild-type sequence. The red underlined sequence aligned with the mutant sequence. F) *APC* mRNA sequence of the wild-type and mutant allele in patient H87 at the familial mutation site (c.4782_4785). The highlighted AGCC sequence is deleted in the germline mutant *APC* allele. G) Chromatogram of sequenced *APC* cDNA harvested from H87 polyp organoids grown either in WR media or for 2+ passages in WR-Free media. The blue underlined sequence aligned with the wild-type sequence. The red underlined sequence aligned with the mutant sequence.

allele could explain their elevated Wnt tone. We tested whether High Wnt organoids grown in WR or WR-Free media exhibited loss of the wild-type *APC* transcript by sequencing mRNA harvested from these three organoid lines at their respective *APC* familial mutation.

Patients H72 and H73, a parent-child pair sharing a common familial mutation, and patient H87 had inherited four base-pair deletions at c.5826_5829 and c.4782_4785, respectively (Figure 3.9D, F). Sequencing *APC* mRNA at the familial mutation site for H72 polyp-derived organoids grown in WR culture conditions confirmed transcription of both normal and mutant alleles (Figure 3.9E). This was determined by bifurcation of sequencing products 3' to the mutation site. However, after growth for three passages in WR-Free media, H72P and H73P organoids only expressed the mutant allele (Figure 3.9E). In contrast, H87P organoids retained the wild-type *APC* transcript in both growth conditions (Figure 3.9G).

To further understand the dynamics of loss of wildtype *APC* in H73P organoids grown in WR-Free media, we utilized organoids from the earliest available passage post initial biopsy seeding to minimize the influence of genetic drift in culture. H73P organoid RNA was harvested at passage 2 in WR media, and then at passage 3 after six days growth in 100%, 50%, or 0% WR media (Figure 3.10A). As before, we detected both wild-type and mutant transcripts in WR conditions (Figure 3.10B). However, after passage, while organoids grown in 100% or 50% WR media maintained expression of both alleles (Figure 3.10C), growth in WR-Free conditions rapidly led to loss of the wild-type transcript. Thus, growth in a WR-Free environment can select for loss of expression of the wildtype *APC* allele.

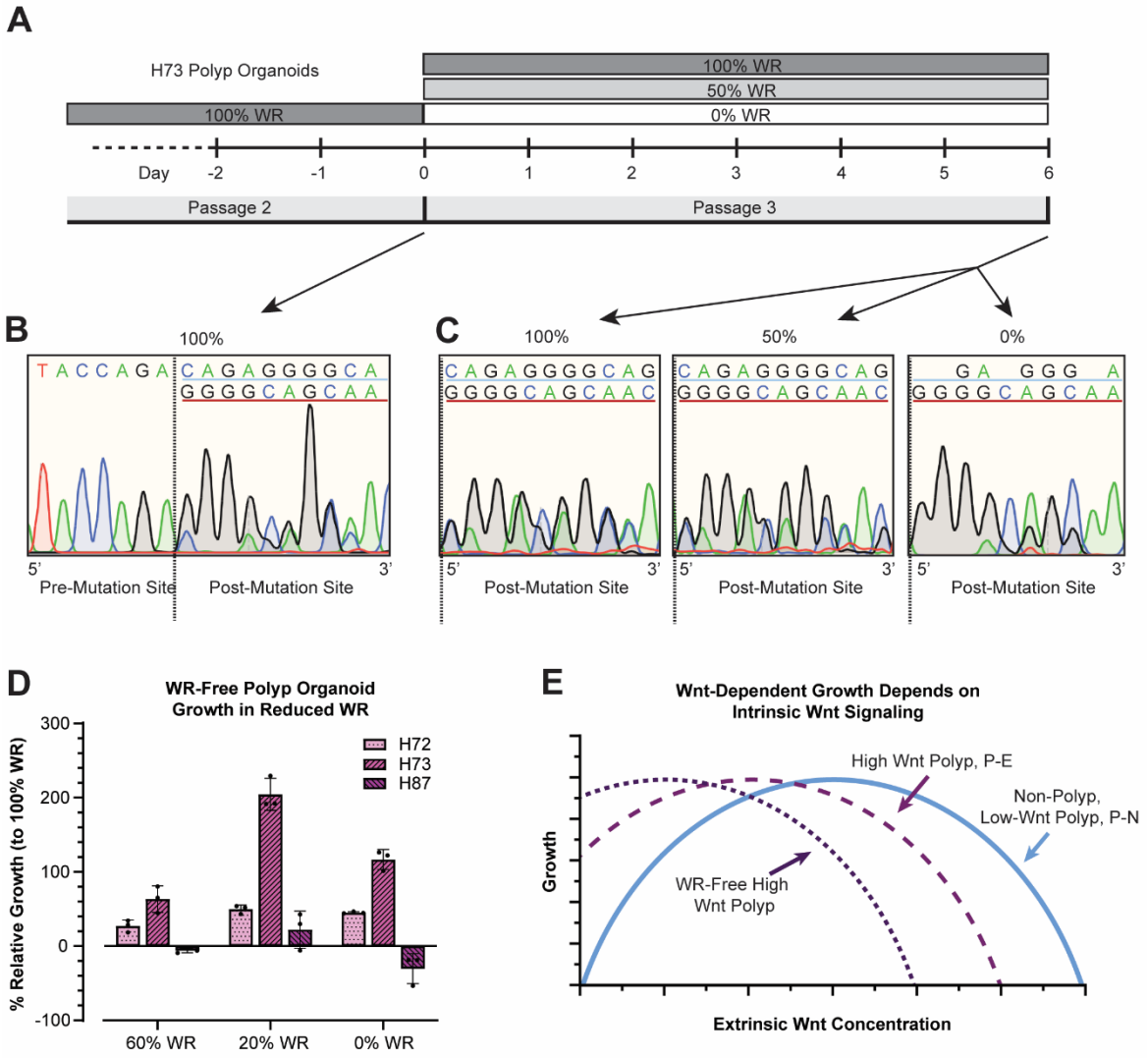

Figure 3.10: WR-Free media selects for organoids with transcriptional loss of wildtype *APC* expression.

A) H73 polyp organoids (passage 2) were grown from initial *in vitro* establishment in 100% WR, then transitioned to 100%, 50%, or 0% WR media during passage 3. mRNA was harvested at the conclusion of passage 2, or on day 6 of passage 3. B) Chromatogram of sequenced *APC* cDNA harvested from H73 polyp organoids at the conclusion of passage 2. The blue underlined sequence aligned with the normal sequence. The red underline sequence aligned with the mutant sequence. C) Chromatogram of sequenced *APC* cDNA harvested from H73 polyp organoids following growth for passage 3 in 100%, 50%, or 0% WR. The sequence shown includes the 10 base pairs immediately downstream of the familial mutation site (see Figure 3.9D). The blue underlined sequence aligned with the normal sequence. The red underlined sequence aligned with the mutant sequence. D) H72, H73, and H87 polyp organoids were grown for 3+ passages in WR-Free media to establish long-term Wnt independent growth, then grown for 12 days in 100%, 60%, 20%, or 0% WR. Values are polyp organoid growth at day 12 in 60%, 20%, or 0% WR relative to growth in 100% WR, following the same procedure outlined in Figure 3.3F. E) Schematic of relationship between intrinsic Wnt characteristics and extrinsic Wnt ligand in driving growth in accordance with the 'just-right' hypothesis.

Following the ‘just-right’ hypothesis, we hypothesized that the optimal growth of WR-Free polyp organoids would occur in media with minimal exogenous Wnt. We titrated each of the WR-Free lines to their optimal Wnt signaling environment and determined that optimal growth occurred in 20% WR media (Figure 3.10D). Ultimately, this establishes a relationship between extrinsic and intrinsic Wnt in accordance with the ‘just-right’ hypothesis for gastric corpus organoids. As intrinsic Wnt tone is increased through mutation or otherwise, tolerance to extrinsic Wnt is reduced (Figure 3.10E).

Mice demonstrate region-specific gastric proliferation in response to Apc mutation

Our data suggests that genomic *APC* loss-of-heterozygosity is not required for FAP polyp emergence. Further, FAP organoid growth suggests that polyp organoids do not tolerate high levels of extrinsic or pharmacologic Wnt activation in accordance with the ‘just-right’ hypothesis. These findings, in combination with the low clinical prevalence of cancer progression from FAP polyps, suggest that additional somatic mutations to *APC,* such as *APC*-null, may not be tolerated within the corpus epithelium. Rather, in the corpus, the *APC* heterozygous state may be sufficient to promote growth. We sought to test these concepts *in vivo* in a mouse FAP model to determine the effect of genomic *Apc* loss on corpus epithelial cell proliferation compared to the antrum where, in FAP patients, infrequent polyps are typically adenomatous.

Apc^{fl} mice with *loxP* sites surrounding exon 14 were crossed to *Sox2-CreER*^{T2} mice. *Apc* mutation was induced in adults by treatment with tamoxifen and gastric tissue was harvested from control (*Apc*$^{fl/+}$ or *Apc*$^{fl/fl}$), heterozygous (*Sox2CreER*^{T2}; *Apc*$^{fl/+}$), and homozygous (*Sox2CreER*^{T2}*; Apc*$^{fl/fl}$) mice one month later (Figure 3.11A). We confirmed

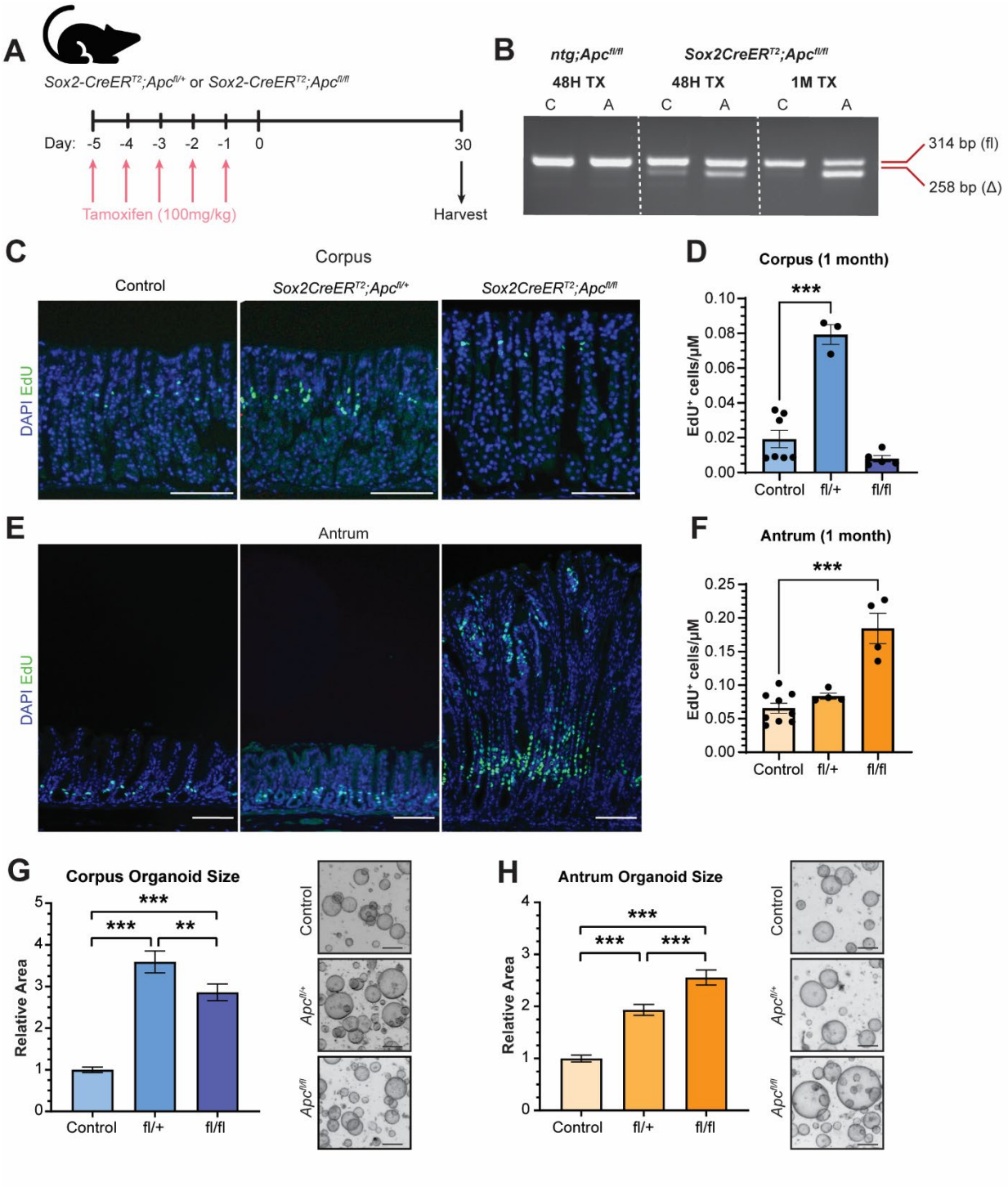

Figure 3.11: Gastric region-specific proliferation in FAP mouse model.

A) Adult *Sox2CreER^{T2}; Apc$^{fl/+}$* (heterozygous), *Sox2CreER^{T2}; Apc$^{fl/fl}$* (homozygous), and control (*Apc$^{fl/+}$* or *Apc$^{fl/fl}$*) mice were treated with tamoxifen (TX) to delete *Apc* exon 14, and tissue was harvested one month later. B) Agarose gel showing PCR products amplified from genomic DNA with primers flanking a *loxP* site in the *Apc* gene to identify either the unrecombined allele (fl,

314bp) or recombined allele (Δ, 258 bp). DNA was isolated from full thickness corpus (C) or antral (A) tissue from control (*Apc*$^{fl/fl}$) mice one-month post-TX, or from homozygous *Sox2CreER*^{T2}*; Apc*$^{fl/fl}$ mice 48 hours or one-month post-TX. C, E) Representative images of control, *Sox2CreER*^{T2}*; Apc*$^{fl/+}$, and *Sox2CreER*^{T2}*; Apc*$^{fl/fl}$ mice one-month post-TX corpus (C) and antral (E) tissue stained for EdU (green) to mark proliferating cells (size bar = 100 μm). D, F) Morphometric quantification of proliferating EdU^{+} cells per μm of corpus (D) or antral (F) tissue in control, heterozygous (fl/+), and homozygous (fl/fl) mice at one-month post-TX. Data are presented as mean ± SEM (n=3-9 mice per group, ***p<0.001 by one-way ANOVA with Tukey's multiple comparison test). G, H) Size and representative images of corpus (G) or antrum (H) organoids derived from control (*Sox2CreER*^{T2}), heterozygous (fl/+), and homozygous (fl/fl) mice. Data are presented as mean ± SEM (n=171-278 organoids; **p<0.05, ***p<0.005 by one-way ANOVA with Tukey's multiple-comparison test). Growth analysis: *Sox2CreER*^{T2} (n= 3 mice, 208 corpus organoids; 217 antrum organoids), *Sox2-CreERT2; Apc*$^{fl/+}$ (n=3 mice, 171 corpus organoids; 256 antrum organoids) and *Sox2-CreERT2; Apc*$^{fl/fl}$ (n=3 mice, 218 corpus organoids; 278 antrum organoids).

Apc exon 14 deletion in DNA isolated from corpus and antrum by PCR amplification 48 hours post-tamoxifen (Figure 3.11B). Further analysis demonstrated that heterozygous *Apc* deletion was maintained one-month post deletion in both corpus and antrum, while homozygous deletion of *Apc* was poorly maintained in the corpus (Figure 3.11B, 3.12).

Analysis of proliferation showed stark differences in response to *Apc* mutation in the corpus and antrum. Corpus tissue at one-month post-tamoxifen revealed no change in tissue morphology or proliferation after *Apc* homozygous deletion (Figure 3.11C-D). However, we observed a significant (~4x) increase in corpus epithelial proliferation in heterozygous mice. In contrast, there was no observed change in antral proliferation in heterozygous *Apc* mice, while complete loss of *Apc* in homozygotes resulted in profound hyperproliferation and the formation of polyp-like structures (Figure 3.11E-F).

We further tested the effect of *Apc* mutation on mouse gastric organoid growth. Organoids were initiated from gastric glands isolated from control, heterozygous, and homozygous *Apc* mutant mice 48 hours post-tamoxifen treatment, and organoid size was measured four days later. Consistent with the *in vivo* findings, heterozygous *Apc* mutant corpus organoids (*Sox2CreER*^{T2}; *Apc*$^{fl/+}$) grew larger than control, with homozygous *Apc* organoids (*Sox2CreER*^{T2}*; Apc*$^{fl/fl}$) exhibiting diminished growth (Figure 3.11G). In contrast, antral organoids demonstrated a stepwise growth advantage in response to heterozygous and homozygous *Apc* deletion (Figure 3.11H).

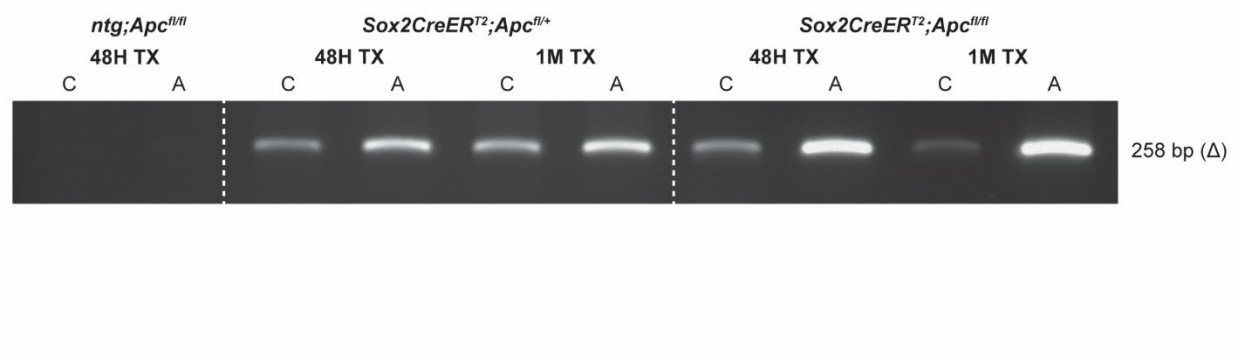

Figure 3.12: Heterozygous loss of *Apc* is maintained long-term within the corpus epithelium.

Agarose gel showing PCR products for the recombined Apc^{fl} allele (258 bp) at 48 hours (48H) and one month (1M) post-tamoxifen. DNA was isolated from full-thickness corpus (C) or antrum (A) of $Apc^{fl/fl}$ (control), $Sox2CreER^{T2}; Apc^{fl/+}$ (heterozygous), or $Sox2CreER^{T2}; Apc^{fl/fl}$ (homozygous) mice.

3.4 Discussion

This study investigated how dysregulation of Wnt signaling in FAP patients leads to abundant yet benign FGPs in the gastric corpus. We initially hypothesized that polyp emergence in the FAP patient corpus was due to somatic mutation resulting in *APC* loss-of-heterozygosity. This would align with the general understanding of colorectal polyposis in which a second hit to *APC* is considered a requirement and the first step in the mutational cascade inevitably leading to colorectal cancer (18, 30). Surprisingly, we determined that *APC* loss-of-heterozygosity is not a requirement for gastric FGP formation within FAP patients as underlying somatic *APC* alteration was rare. There have been few comparative studies observing the mutational landscape underscoring FGP formation from FAP patients. One study demonstrated that 51% (21/41) of FAP-associated polyps obtained from 17 patients had acquired a somatic *APC* gene alteration through either a loss-of-function mutation (15/41) or allelic loss (6/41) resulting in loss-of-heterozygosity (31). While this study did demonstrate a higher proportion of FGPs arising from somatic *APC* gene alterations than ours, it confirms our finding that *APC* loss-of-heterozygosity is not a requirement for their emergence.

Despite an absence of second-hit somatic *APC* alteration within our FAP patient biobank, we observed that Wnt signaling was generally upregulated in FGP biopsy samples as well as within a subset of our polyp-derived organoids. This underscores the role of Wnt activation in driving polyp formation and that other second-hit mutations in the form of subtle genetic or epigenetic changes may have occurred to increase Wnt signaling. Studies have shown that sporadic FGPs in otherwise healthy patients often contain activating mutations in *CTNNB1*, encoding beta-catenin, which would increase

Wnt signaling (32, 33). Despite the difference in underlying genetic mutation between sporadic and FAP FGPs, there is no apparent histopathological difference between the two subtypes (34). Although, *APC*-associated FGPs have a greater tendency to present with low-grade dysplasia, as well as high-grade dysplasia in rare cases (5, 10-12). This commonly occurs with features of surface cell dysplasia, which could relate to elevated Wnt tone. We did note features of altered differentiation, such as low expression of surface cell markers, within some of our polyp biopsies as well as within corresponding polyp-derived organoids.

A remaining subset of polyp-derived organoids across our FAP biobank did not demonstrate increased Wnt signaling, but instead demonstrated similar expression and Wnt tolerance as non-polyp organoids. This subgroup was observed across our patient set without a clear genotype-phenotype association. It is plausible that outgrowth of cells with more normal-like Wnt characteristics could be selected for because all organoids were established in media containing WNT/RSPO. However, primary biopsies also demonstrated heterogeneity in Wnt target gene expression as well as a lack of somatic *APC* alteration, suggesting that selection in culture does not necessarily underly this subgroup. Therefore, additional Wnt-independent mechanisms, such as environmental factors or upregulation of other pathways, could also underscore FGP emergence in FAP patients.

Studies in colorectal cancer cell lines have demonstrated that loss of APC function leads to chromosomal instability (35). We observed copy number variation in our targeted genomic analysis and speculate that heterozygous loss of *APC* may also confer instability that could sensitize tissue to polyposis in lieu of a second-hit *APC*

mutation. Notably, FGP biopsies established organoids at faster rates than non-polyp biopsies, indicating enhanced progenitor cell function. However, it remains unclear how upregulated Wnt in the *APC* heterozygous mutant corpus leads to robust polyp formation while the antrum is spared, despite having the same underlying germline mutation.

A recent study from our lab demonstrated that human corpus-derived organoids generated from patients without underlying disease have a reduced threshold for Wnt to induce growth compared to patient-matched antral organoids (24). Combined with the present study, our findings suggest that corpus polyposis in FAP patients may result from an intrinsic heightened sensitivity for Wnt to drive proliferation in corpus progenitor cells. That is, the familial, heterozygous *APC* mutation may prime corpus progenitors to hyperproliferate, while antral progenitors require further second-hit *APC* mutations to induce proliferation, thus underscoring the increased risk of adenoma. This aligns with the abundance of FGPs (100's to 1000's of lesions) in some FAP patients as there would be no requirement for the rare genomic occurrence of a second hit. This theory was supported by analysis of an FAP mouse model, where we showed stark differences in response to *Apc* mutation in the corpus and antrum. We observed that the murine stomach displayed a similar regional pattern to human FAP, with heterozygous *Apc* mutation ($Apc^{+/-}$) promoting corpus proliferation and homozygous deletion ($Apc^{-/-}$) promoting profound antral hyperplasia while the corpus is spared; thus, demonstrating that loss-of-heterozygosity is not tolerated in the corpus.

Previous studies in mouse also showed that homozygous deletion of *Apc* in differentiated chief cells did not promote corpus hyperplasia (36, 37). Our study

contextualizes these findings by demonstrating that *Apc*$^{-/-}$ cells are either not retained in the corpus epithelium long term or do not contribute to cellular turnover. Conversely, *Apc*$^{+/-}$ cells are maintained and contribute to enhanced corpus proliferation. Importantly, another study of heterozygous *Apc* mutant mice (*Lrig1CreER*^{T2}*;Apc*$^{fl/+}$) showed evidence of hyperplasia and increased proliferation in the corpus and antrum 100+ days following recombination (38). Overall, the body of available literature in combination with our results suggest that heterozygous loss of *Apc* in mice mimicking the FAP condition promotes a favorable environment for corpus hyperplasia while additional *Apc* gene mutation is not tolerated unless combined with additional oncogenic mutations.

Our findings align with a principle of Wnt signaling known as the 'just-right' hypothesis which describes a Goldilocks zone of signaling tone to drive excessive growth in the context of FAP polyposis. Studies exploring this concept have demonstrated that there are regional differences in Wnt signaling tone throughout the small intestine and colon that contribute to region-specific Wnt sensitivity and tumorigenesis (20, 23, 27, 39). We have now expanded this understanding to the stomach by demonstrating that regional differences in Wnt signaling in the corpus versus the antrum may contribute to the emergence of polyps.

On the other extreme, the 'just-right' hypothesis predicts an upper limit to Wnt signaling that becomes growth prohibitive (22, 40). An intermediate level of Wnt signaling therefore best promotes hyperproliferation and tumorigenesis, with the optimal level differing along the GI tract (20, 22, 40). Our study confirms these findings in polyp organoids and demonstrates that increased intrinsic Wnt signaling sensitizes organoids to additional upregulation of the Wnt pathway. This, again, suggests that somatic *APC*

mutation may not be tolerated *in vivo* as Wnt signaling would be elevated beyond an upper threshold of tolerability. Furthermore, these principles would underscore the benign nature of FGPs relative to polyps of the antrum and colon.

In conclusion, our study translates the 'just-right' hypothesis of Wnt signaling to the clinical manifestation of gastric disease caused by pathway dysregulation and develops two unique conclusions related to FGP emergence and pathogenesis in FAP patients. First, we demonstrate that Wnt signaling is predominately upregulated in polyp tissues as well as polyp-derived organoids and therefore confirm that enhanced intrinsic Wnt signaling is a key characteristic of FGPs. The lack of requirement for a second hit to *APC* may explain the abundant nature through which FGPs emerge. Second, we establish a definitive relationship between intrinsic and extrinsic Wnt signaling in gastric corpus organoids and demonstrate that additional Wnt signaling in cells with intrinsically upregulated Wnt tone prohibits growth. The corpus environment may therefore selectively prohibit high intrinsic Wnt signaling, such as through *APC* loss-of-heterozygosity. These thresholds may therefore underscore the benign nature of fundic gland polyps as well as the regionality of their emergence.

3.5 Materials and Methods

FAP patient biopsy collection and processing

Human gastric tissue biopsies were collected from patients undergoing endoscopy at Michigan Medicine. Biopsies were placed in 15 mL conical tubes containing 5 mL of ice-cold DPBS (Gibco, 14190144) with antibiotic-antimycotic (100

U/mL Pen/Strep + 250 ng/mL Amphotericin B, Gibco, 15240062) for transport to the research lab.

Biopsies were minced into small fragments (~1mm) and divided for nucleotide (DNA or RNA) extraction or organoid formation. Fragments set aside for nucleotide extraction were placed into 1.5 mL Eppendorf tubes and snap-frozen in liquid N_2. Fragments for organoid formation were transferred to 5 mL ice-cold DPBS + antibiotic-antimycotic for subsequent processing. In some instances, minced biopsies were frozen for later organoid development by resuspending in DMEM/F12 (Gibco, 12634010) with 10% DMSO and 10% Fetal Bovine Serum (Sigma, F0926) and frozen in cryovials for long-term storage in liquid N_2 (41).

Establishment and culture of human gastric organoids

Organoids were established from either isolated gastric glands or directly from minced tissue that was embedded in 40 µL Matrigel (Corning, 354234). For the isolated glands approach, 15 mM EDTA (Invitrogen, 15575038) was added to minced biopsies in 5 mL DPBS + antibiotic-antimycotic in 15 mL conical tubes and rocked at 4°C for 1 hour. Tissue fragments were transferred to a new tube containing 8 mL of ice-cold DPBS and gastric glands were released by vortexing at maximum speed for 2 minutes. The suspended gastric glands were transferred to a new tube, pelleted at 600xg for 5 minutes at 4°C, and resuspended in Matrigel for plating. Alternatively, minced tissue was directly embedded in Matrigel, with epithelial outgrowths emerging within 2-3 days of plating (Figure 3.6). Organoid lines were established by passaging at least three times before analysis.

Organoids were maintained in WR (WNT, RSPO, Noggin), WR-Free (Noggin), or CN (CHIR99021, Noggin) media as specified. 100% WR media was generated with 50% L-WRN conditioned media (University of Michigan Translational Tissue Modeling Laboratory), 10% Fetal Bovine Serum (Sigma, F0926), 37% DMEM/F12 (Gibco, 12634010), 2mM GlutaMAX (Gibco, 35050061), Antibiotic-Antimycotic (100 U/mL Pen/Strep + 250 ng/mL Amphotericin B, Gibco, 15240062), 10 μM Y-27632 (Tocris, 1254), 10 μM SB431542 (Tocris, 1614), and 50 μg/mL Gentamycin (Gibco, 15750060). WR-Free media consisted of 20% Fetal Bovine Serum, 77% DMEM/F12, GlutaMAX, Antibiotic-Antimycotic, Y-27632, SB431532, and Gentamycin in the same concentrations as above, and was supplemented with 100 nM recombinant Noggin (R&D, 6057-NG). For WR media formulations, normal (100%) WR and WR-Free media were mixed at appropriate ratios to obtain the desired final WR concentration. For CN media, CHIR99021 (CHIR, Tocris, 4423) was added to WR-Free media to obtain the final concentration as specified. DMSO added through stock solutions of CHIR and SB431542 was maintained at a final concentration of 0.3% in CN Media.

Organoid cultures were maintained by replenishing with fresh media every two days and passaging every six days. To passage organoids, media was aspirated and Matrigel patties containing organoids were overlaid with 500 μL of cold DPBS, mechanically disrupted through scraping with a P1000 pipet tip and transferred to a 1.5 mL Eppendorf tube. Organoids were pelleted at 250xg for 5 minutes at 4°C, resuspended in 500 μL of TrypLE Express (Gibco, 12604013), and incubated at 37°C for 10 minutes. Organoids were vigorously pipetted approximately 40 times with a P1000 to dissociate into single cells. 700 μL of cold DPBS was added, cells were

pelleted at 250xg for 5 minutes at 4°C, resuspended in 30-100 µL of DMEM, and cell concentration was quantified using a hemocytometer. For all experiments, cells were plated at a density of 300 cells/µL of Matrigel patty. Matrigel patties were given 30-45 minutes to solidify at 37°C, then overlayed with the appropriate warmed media.

DNA Library Preparation

DNA was extracted from FAP patient biopsies using the Qiagen Blood & Tissue DNA kit (Qiagen #69504), with the following modification: samples were eluted in 100-200 µL Buffer TE. For DNA extraction from paired non-polyp and polyp organoid samples, culture media was aspirated from each Matrigel patty (3 wells pooled/sample), organoids were suspended in DPBS, pelleted at 300xg for 5 min, resuspended in 200 µL DPBS, and DNA extracted.

For preparation of DNA libraries, genomic DNA samples were indexed using the QIAseq 96-Index I Set A kit (Qiagen #333727) and libraries were constructed for sequencing using the QIAseq targeted Human Comprehensive Cancer Panel (Qiagen #333515, catalog #DHS-3501Z-96). NextGen DNA sequencing was performed using a HiSeq 4000 (Illumina), with sequencing and analysis conducted in collaboration with the University of Michigan Advanced Genomics Core.

RNA extraction, qPCR analysis, and mRNA sequencing

RNA was isolated using the Qiagen Mini Kit (Qiagen, 74106) according to the manufacturer's instructions. Frozen minced tissue from biopsies was transferred to RLT Buffer + 1% βME and homogenized, and centrifuged at 14,000xg for 3 minutes to pellet

particulates. Supernatant was collected, transferred to a new tube, and mixed with an equal volume of 70% EtOH. For organoid RNA extraction, organoids were dispersed to single cells using TrypLE, washed, resuspended in RLT Buffer + 1% βME and vortexed at max speed for 30 seconds before RNA extraction.

cDNA was synthesized from 250ng RNA using the iScript™ cDNA Synthesis Kit (BioRad, 1708891). qPCR reactions used the iTaq™ Universal SYBR Green Supermix (BioRad, 1725124) and respective primers (Supplementary Table 1). qRT-PCR was performed with samples in triplicates, and average cycle threshold values were quantified relative to the reference mRNA *ACTB* or *HPRT* using the ΔΔCT method to determine mRNA abundance.

For *APC* mRNA sequencing, RNA was extracted from organoids, cDNA was synthesized, and qPCR reactions were performed using primers encompassing the *APC* mutation site (Supplementary Table 2). PCR products were purified using the QIAquick PCR Purification Kit according to the manufacturer's instructions, sent to Eurofins Genomics (Louisville, KY) for sequencing, and sequences were analyzed using SnapGene (San Diego, CA) software.

Co-culture and conditioned media experiments

Polyp organoids from lines H72, H73, and H87, as well as non-polyp organoids from H87, were dispersed to single cells. For co-culture experiments, single cells from polyp and non-polyp organoids were plated in independent 10 µL patties of Matrigel at a density of 3,000 cells/patty within the same well of a 24-well plate, taking care to ensure patties did not touch. For conditioned media experiments, the three high Wnt organoid

lines were each plated in independent 10 µL patties of Matrigel at a density of 3,000 cells/patty within the same well of a 24-well plate. Cells were overlayed with WR-Free media. On day 4, media from High Wnt polyp organoids was transferred to patties containing freshly passaged single cells from non-polyp organoids. WR-Free media was replenished, and this was repeated every two days for a total of six days.

Human organoid growth experiments

For Wnt titration experiments, organoids were dispersed to single cells, plated into triplicate wells of a 24-well plate in 40 µL patties of Matrigel at a density of 12,000 cells/well, and overlayed with the appropriate media. On day 6, triplicate wells of each media condition were consolidated, organoids were dispersed to single cells, and cells were resuspended at the same split ratio across all conditions. The concentration of cells in 100% WR was calculated, and cells from each condition were plated at the split ratio calculated to reach 12,000 cells/well in 40 µL Matrigel patties for the 100% WR condition. For measurement of growth, media was aspirated, and patties were overlayed with a room temperature 50:50 mixture of DMEM (200 µL) and Cell-Titer-Glo 3D (200 µL) (Promega, G9681). Plates were incubated for 30 minutes at room temperature in the dark, the Matrigel patty was broken down by rapid pipetting, and the total contents of each well were transferred to individual wells of a white, opaque 96-well plate. Luminescence was measured using a plate reader with an integration time of 500ms.

For CHIR growth experiments, organoids were dispersed to single cells and plated into a 96-well round-bottom plate in 5 µL patties of Matrigel at a density of 1,500

cells/well. For measurement of growth, media was aspirated and 150 µL of a room temperature 50:50 mixture of DMEM (75 µL) and CellTiter-Glo 3D (75 µL) (Promega, G9681) was added to each well. Plates were incubated for 30 minutes at room temperature in the dark, the Matrigel patty was broken down by rapid pipetting, and the total contents of each well were transferred to individual wells of a white, opaque 96-well plate. Luminescence was measured using a plate reader with an integration time of 500ms.

Mouse Experiments

Adult mice of both sexes 2-3 months old were housed under specific pathogen-free conditions. *Sox2-CreER^{T2}* (Jackson Labs #017593) (42) and *Apc580^{fl}* (*Apc^{fl}*) (43) mice have been previously described. *Apc^{fl}* mice contain a floxed exon 14, which upon Cre-mediated deletion encodes an APC protein truncated at codon 580. *Apc^{fl}* mice were on a 129/SvJae background and *Sox2-CreER^{T2}* mice were on a mixed C57BL/6 x 129/SvJae background. *Sox2-CreER^{T2}* and *Apc^{fl}* mice were bred to generate the following genotypes: *Sox2CreER^{T2}*; *Apc$^{fl/+}$* (heterozygous), *Sox2CreER^{T2}; Apc$^{fl/fl}$* (homozygous), and control (*Apc$^{fl/+}$* and *Apc$^{fl/fl}$*).

To induce Cre-mediated recombination of the floxed *Apc* allele, mice were treated with 100 mg/kg tamoxifen (TX) via intraperitoneal injection once daily for 5 days. For analysis of *Apc* recombination, full thickness tissue was homogenized, and DNA was isolated using the DNeasy Blood & Tissue Kit (Qiagen, 69504) per the manufacturer's instructions. Recombination was analyzed via PCR amplification using the following primers (43): P3: 5'-GTT CTG TAT CAT GGA AAG ATA GGT GGT C-3', P4:

5′-CAC TCA AAA CGC TTT TGA GGG TTG ATT C-3′, P5: 5′-GAG TAC GGG GTC TCT GTC TCA GTG AA-3′. P3 and P4 generate a 314 bp product encompassing the unrecombined loxP site, while P3 and P5 generate a 258 bp product encompassing the recombined region.

For analysis of proliferation, mice were injected with 5-ethynyl-2'-deoxyuridine (EdU, 25 mg/kg, Invitrogen, A10044) two hours prior to tissue collection. For morphometric quantification of EdU incorporation, the entire length of the corpus and antrum for each animal was imaged (n = 3–9 animals per group) and blinded cell counts were normalized to epithelial length (μm) using ImageJ software (National Institutes of Health, Bethesda, MD).

Analysis of murine gastric organoids

Mouse gastric organoids were established from corpus and antrum tissue collected from *Sox2-CreER^{T2}* (control), *Sox2-CreER^{T2}; Apc$^{fl/+}$*(heterozygous), and *Sox2-CreER^{T2}; Apc$^{fl/fl}$* (homozygous) mice 48 hours post final TX injection. Gastric tissue was washed in ice-cold DPBS and minced into 2-3 mm fragments. Tissue fragments were transferred to DPBS containing 8 mM EDTA and rocked at 4 °C for 1 hour. To isolate glands, tissue fragments were transferred to a fresh DPBS solution containing 10 mM EDTA (Invitrogen, 15575038) and rocked at 4 °C for 2 hours. During the last 10 minutes of incubation, samples were placed on ice to allow glands to settle, and the EDTA-DPBS solution was replaced with DPBS and gently mixed 3-5 times using an FBS-coated p1000 tip with the opening enlarged to prevent breaking or sticking of isolated glands. Once the mixture was cloudy, glands were transferred to a 1.5 mL Eppendorf

tube and centrifuged at 150xg for 10 minutes at 4ºC. After aspirating the supernatant, glands were resuspended in 40 µL Matrigel (Corning, 354234) and plated. Murine gastric organoids were maintained in culture using the same procedures outlined for human organoid growth, but without TGF-β inhibitor SB431542.

For size measurement, mouse organoids were imaged at day 4 of culture using an Olympus Stereomicroscope at 1.7X magnification. The area of growth was calculated from digital images using the Orgaquant software (44). Three technical replicates were used for each group and were pooled for analysis, with >170 organoids measured from each condition.

Statistics

GraphPad Prism (version 9.0, Software, San Diego, CA) was used for statistical analysis. Student's *t* test was used to compare two groups. For comparison of 3 or more groups, a One-Way Analysis of Variance (ANOVA) was used followed by a Turkey post-hoc test. *$p<0.05$, **$p<0.005$, and ***$p<0.001$ were used to denote significance.

Study Approval

Collection of human tissue was conducted under Institutional Review Board-approved protocol (HUM00102771) at the University of Michigan. Written informed consent was provided by individual patients prior to collection of biopsies. Mouse studies were conducted under University of Michigan Institutional Animal Care & Use Committee (IACUC) approved protocols (PRO00010803).

3.6 Acknowledgements

The authors are grateful to Colin Burnett and Michael Santiago-Castro for coordinating the collection of patient tissue biopsies, to Jason Spence, PhD and Michael Dame, PhD in the Translational Tissue Modeling Laboratory for LWRN media and microscopes, to members of the Samuelson Laboratory for their helpful comments on the manuscript, and to the patients who generously provided tissue samples to enable this research. K.P.M was supported by National Institutes of Health T32-DK094775 and T32-HD007505. E.D. was supported by National Institutes of Health R25-GM086262. E.S.H. was supported by National Institutes of Health K01-DK111710. The research was funded by National Institutes of Health R01-DK126451 awarded to L.C.S and core support from the Michigan Gastrointestinal Research Center grant (National Institutes of Health P30-DK34933).

Table 3.1: FAP Patient Biobank

	Patient	Familial *APC* Mutation	Age**	Sex	Ethnicity	Organoids	
						NP	P
Genomic DNA, Organoids	**H61**	Deletion Promotor 1B	70	F	White, Non-Hispanic	1	1
	H62	c.426_427delAT, p.L143AfsX4	50	F	White, Non-Hispanic	1	1
	H66	exon 15 c.3668C>T, p.Q1230X	40	F	White, Non-Hispanic		
	H69	c.1417C>T, p.Q473X	40	F	White, Non-Hispanic		
	H71	c.3439dupT; p.Tyr1147LeufsX3	60	F	White, Non-Hispanic	1	1
	H72	c.5826_5829delCAGA; p.D1942EfsX27	50	M	White, Non-Hispanic	1	1
	H73	c.5826_5829delCAGA; p.D1942EfsX27	20	M	White, Non-Hispanic	1	1
	H75	c.3183_3187delACAAA; p.Lys1061_Gln1062insTer	50	M	African American	1	1
	H76	Possibly: c.3921_3925delAAAAG; p.Glu1309fs	70	F	White, Non-Hispanic	1	1
	H77	c.3260_3261delTC; p.L1087QfsX31	30	F	White, Non-Hispanic		
	H78	c.3472A>T; p.R1158X	70	M	White, Non-Hispanic		
	H80	c.694C>T; p.R232X	40	F	White, Non-Hispanic		
	H81	c.3183_3187delACAAA; p.Gln1062X	30	F	White, Non-Hispanic		
	H82	No germline mutations	50	F	White, Non-Hispanic	1	1
	H84	c.426_427delAT; p.Leu143fs	50	F	White, Non-Hispanic		
	H85	c.1458T>G; p.Tyr486Ter	50	F	White, Non-Hispanic		
	H87	c.4782_4785delAGCC; p.Ala1595Argfs	30	F	White, Non-Hispanic	1	1
	H89	c.3183_3187delACAAA; p.Q1062X	50	M	White, Non-Hispanic		
	H92	deletion of exons 11-13	30	F	White, Non-Hispanic		
	H93	*Same as H73**	20	M	White, Non-Hispanic		
RNA, Multiple Organoids	**H98**	c.4046delA; p.His1439ProfsX66	40	F	Unknown	3	3
	H99	c.118_119insSVA (SVA retrotransposon)	50	F	White, Non-Hispanic		3
	H100	Unknown	70	M	White, unknown		
	H101	c.1866C>G;p.Tyr622X	50	F	Korean, Non-Hispanic	2	2
	H102	c.426_427delAT, p.L143AfsX4	70	M	White, Non-Hispanic	3	6
	H103	Deletion Exons 3-4	20	F	White, Non-Hispanic	2	2
	H104	c.4782_4785delAGCC; p.Ala1595Argfs	50	F	White, Non-Hispanic	2	2
	H105	c.3927_3931delAAAGA; p.Glu1309AspfsX4	30	M	White, Non-Hispanic	3	3
	H106	No germline mutations	50	F	White, Non-Hispanic	3	3
	H107	c.4705_4706delGA	70	F	White, Non-Hispanic	1	1
	H108	*Same as H102**	70	M	White, Non-Hispanic	1	2
	H110	Unknown	70	F	White, Non-Hispanic	3	2
	H111	c.3472A>T; p.R1158X	40	F	White, Non-Hispanic	2	3
	H112	c.426_427delAT, p.L143AfsX4	31	F	White, Non-Hispanic		3
	H113	c.426_427delAT, p.L143AfsX4	60	F	White, Non-Hispanic		
	H114	Unknown	30	M	White, Non-Hispanic	2	3
	H115	*Same as H104**	50	F	White, Non-Hispanic		3

* Repeat sample collection from indicated patient

** Age listed to nearest decade

Table 3.2: Qiagen Comprehensive Cancer Panel sequencing results

Patient	Tissue Sequenced	Somatic *APC* Mutation	*APC* CNV	Total CNVs
H61	Organoids	-	-	2
H62	Organoids	-	-	3
H66	Biopsy	-	-	58
H69	Biopsy	-	Deletion	23
H71	Organoids	-	-	0
H72	Organoids	-	-	25
H73	Organoids	-	-	0
H75	Organoids	-	Deletion	36
H76	Organoids	-	-	8
H77	Biopsy	-	Duplication	47
H78	Biopsy	-	-	1
H80	Biopsy	-	Deletion	3
H81	Biopsy	-	-	1
H82	Organoids	-	-	1
H84	Biopsy	-	-	1
H85	Biopsy	c.263delG; p.Ser89fs	Duplication	160
H87	Organoids	-	-	0
H89	Biopsy	-	Deletion	16
H92	Biopsy	-	-	0
H93	Biopsy	-	-	3

-: not detected

Table 3.3: Oligonucleotide primer sequences used for qRT-PCR gene expression analysis.

Gene	Amplicon size (bp)	Forward Primer (5' – 3')	Reverse Primer (5' – 3')
HPRT	131	CCTGGCGTCGTGATTAGTGAT	AGACGTTCAGTCCTGTCCATAA
AQP5	139	TACGGTGTGGCACCGCTCAATG	AGTCAGTGGAGGCGAAGATGCA
ATP4A	265	ACAGATTGGTCAACGAGCCC	TGGCACACCTCAATGCTGAT
AXIN2	103	CTGGTGCAAAGACATAGCCA	AGTGTGAGGTCCACGGAAAC
CD44	151	CCAGAAGGAACAGTGGTTTGGC	ACTGTCCTCTGGGCTTGGTGTT
CD45	126	ACCACAAGTTTACTAACGCAAGT	TTTGAGGGGGATTCCAGGTAAT
CDKN1C	138	AGATCAGCGCCTGAGAAGTCGT	TCGGGGCTCTTTGGGCTCTAAA
CHIA	143	AAGGCTACACTGGAGAGAACAG	GGTAGGGAATCCAACGATGAGC
IL-1B	159	ATTTCTTGCTATTGACCGATGC	CCCAAGGAGACCACAGTTAGAG
IL-8	256	CTGAGCCCTGAACACCAGAG	CCTCTTTGGCCTCTTCCCAG
GIF	150	TGCCCCAGGTCACTTGTAGT	TGGTCTCGTTGAAGAGCAGC
LGR5	159	CCTATCGTCCAACCTCCTGTCG	GCACAGCACTGGTAAGCATAAGG
LIPF	127	TGACCTTCCAGCCACAATCGAC	TTTAGCCAGGCTGGGATTGGTG
MUC5AC	103	GGAACTGTGGGGACAGCTCTT	GTCACATTCCTCAGCGAGGTC
MUC6	122	GGACTGTGAGTGTCTGTGCGAT	GCGTGTTGTAGAAGCCGCAGTA
PGC	128	ACCTACTCCACCAATGGGCAG	TCACTCAAGCCGAACTCCTGGT
SP5	147	CTCGCTGCAGGCCTTTCT	TAGGGCACCTGCAGGAAGT
SOX9	116	TGCAGGAGGAGAAGAGAAGG	GTGGCCAGTTCACAGCTGC
TFF1	179	CCCAGTGTGCAAATAAGGGC	GCTCTGGGACTAATCACCGT
TFF2	228	GACAATGGATGCTGTTTCG	GTAATGGCAGTCTTCCACAGA
TNFRSF19	114	CAGGCATCTGAAAACTCGCCAC	GGTGCATTCTGCAGCCAGTCTT

Table 3.4: Oligonucleotide sequences for *APC* mRNA amplification

***APC* Mutation Site**	**Patients**	**Amplicon size (bp)**	**Sequence (5' – 3')**
D1942	H72, H73	279	F: AACCTCCAACCAACAATCAGC
			R: GGGGGCTCAGTCTCTTTGATAG
A1585	H87	295	F: TGAAAACCAAGAGAAAGAGGCAG
			R: AACACAATACACCCGTGGCA

3.7 References

1. Korinek V, Barker N, Morin PJ, et al. Constitutive transcriptional activation by a beta-catenin-Tcf complex in APC-/- colon carcinoma. *Science.* 1997;275(5307):1784-7.
2. Galiatsatos P, and Foulkes WD. Familial adenomatous polyposis. *Am J Gastroenterol.* 2006;101(2):385-98.
3. Groden J, Thliveris A, Samowitz W, et al. Identification and characterization of the familial adenomatous polyposis coli gene. *Cell.* 1991;66(3):589-600.
4. Kinzler KW, and Vogelstein B. Lessons from hereditary colorectal cancer. *Cell.* 1996;87(2):159-70.
5. Arnason T, Liang WY, Alfaro E, et al. Morphology and natural history of familial adenomatous polyposis-associated dysplastic fundic gland polyps. *Histopathology.* 2014;65(3):353-62.
6. Odze RD, Marcial MA, and Antonioli D. Gastric fundic gland polyps: a morphological study including mucin histochemistry, stereometry, and MIB-1 immunohistochemistry. *Hum Pathol.* 1996;27(9):896-903.
7. Genta RM, Schuler CM, Robiou CI, et al. No association between gastric fundic gland polyps and gastrointestinal neoplasia in a study of over 100,000 patients. *Clin Gastroenterol Hepatol.* 2009;7(8):849-54.
8. Abraham SC. Fundic gland polyps: common and occasionally problematic lesions. *Gastroenterol Hepatol (N Y).* 2010;6(1):48-51.
9. Sonnenberg A, and Genta RM. Prevalence of benign gastric polyps in a large pathology database. *Dig Liver Dis.* 2015;47(2):164-9.
10. Wu TT, Kornacki S, Rashid A, et al. Dysplasia and dysregulation of proliferation in foveolar and surface epithelia of fundic gland polyps from patients with familial adenomatous polyposis. *Am J Surg Pathol.* 1998;22(3):293-8.
11. Jalving M, Koornstra JJ, Boersma-van Ek W, et al. Dysplasia in fundic gland polyps is associated with nuclear beta-catenin expression and relatively high cell turnover rates. *Scand J Gastroenterol.* 2003;38(9):916-22.
12. Bianchi LK, Burke CA, Bennett AE, et al. Fundic gland polyp dysplasia is common in familial adenomatous polyposis. *Clin Gastroenterol Hepatol.* 2008;6(2):180-5.
13. Paszkowski J, Samborski P, Kucharski M, et al. Endoscopic Surveillance and Treatment of Upper GI Tract Lesions in Patients with Familial Adenomatous Polyposis-A New Perspective on an Old Disease. *Genes (Basel).* 2022;13(12).
14. Cancer Genome Atlas Research N. Comprehensive molecular characterization of gastric adenocarcinoma. *Nature.* 2014;513(7517):202-9.

15. Min BH, Hwang J, Kim NK, et al. Dysregulated Wnt signalling and recurrent mutations of the tumour suppressor RNF43 in early gastric carcinogenesis. *J Pathol.* 2016;240(3):304-14.

16. Dinarvand P, Davaro EP, Doan JV, et al. Familial Adenomatous Polyposis Syndrome: An Update and Review of Extraintestinal Manifestations. *Arch Pathol Lab Med.* 2019;143(11):1382-98.

17. Weiss JM, Gupta S, Burke CA, et al. NCCN Guidelines(R) Insights: Genetic/Familial High-Risk Assessment: Colorectal, Version 1.2021. *J Natl Compr Canc Netw.* 2021;19(10):1122-32.

18. Knudson AG. Two genetic hits (more or less) to cancer. *Nat Rev Cancer.* 2001;1(2):157-62.

19. Lamlum H, Ilyas M, Rowan A, et al. The type of somatic mutation at APC in familial adenomatous polyposis is determined by the site of the germline mutation: a new facet to Knudson's 'two-hit' hypothesis. *Nat Med.* 1999;5(9):1071-5.

20. Albuquerque C, Breukel C, van der Luijt R, et al. The 'just-right' signaling model: APC somatic mutations are selected based on a specific level of activation of the beta-catenin signaling cascade. *Hum Mol Genet.* 2002;11(13):1549-60.

21. Albuquerque C, Baltazar C, Filipe B, et al. Colorectal cancers show distinct mutation spectra in members of the canonical WNT signaling pathway according to their anatomical location and type of genetic instability. *Genes Chromosomes Cancer.* 2010;49(8):746-59.

22. Lewis A, Segditsas S, Deheragoda M, et al. Severe polyposis in Apc(1322T) mice is associated with submaximal Wnt signalling and increased expression of the stem cell marker Lgr5. *Gut.* 2010;59(12):1680-6.

23. Leedham SJ, Rodenas-Cuadrado P, Howarth K, et al. A basal gradient of Wnt and stem-cell number influences regional tumour distribution in human and mouse intestinal tracts. *Gut.* 2013;62(1):83-93.

24. McGowan KP, Delgado E, Hibdon ES, et al. Differential sensitivity to Wnt signaling gradients in human gastric organoids derived from corpus and antrum. *Am J Physiol Gastrointest Liver Physiol.* 2023.

25. Bartfeld S, Bayram T, van de Wetering M, et al. In vitro expansion of human gastric epithelial stem cells and their responses to bacterial infection. *Gastroenterology.* 2015;148(1):126-36.e6.

26. Fischer AS, Mullerke S, Arnold A, et al. R-spondin/YAP axis promotes gastric oxyntic gland regeneration and Helicobacter pylori-associated metaplasia in mice. *J Clin Invest.* 2022;132(21).

27. Christie M, Jorissen RN, Mouradov D, et al. Different APC genotypes in proximal and distal sporadic colorectal cancers suggest distinct WNT/beta-catenin signalling thresholds for tumourigenesis. *Oncogene.* 2013;32(39):4675-82.

28. Busslinger GA, Weusten BLA, Bogte A, et al. Human gastrointestinal epithelia of the esophagus, stomach, and duodenum resolved at single-cell resolution. *Cell Rep.* 2021;34(10):108819.

29. Ksiaa F, Ziadi S, Amara K, et al. Biological significance of promoter hypermethylation of tumor-related genes in patients with gastric carcinoma. *Clin Chim Acta.* 2009;404(2):128-33.

30. Ichii S, Horii A, Nakatsuru S, et al. Inactivation of both APC alleles in an early stage of colon adenomas in a patient with familial adenomatous polyposis (FAP). *Hum Mol Genet.* 1992;1(6):387-90.

31. Abraham SC, Nobukawa B, Giardiello FM, et al. Fundic gland polyps in familial adenomatous polyposis: neoplasms with frequent somatic adenomatous polyposis coli gene alterations. *Am J Pathol.* 2000;157(3):747-54.

32. Abraham SC, Nobukawa B, Giardiello FM, et al. Sporadic fundic gland polyps: common gastric polyps arising through activating mutations in the beta-catenin gene. *Am J Pathol.* 2001;158(3):1005-10.

33. Sekine S, Shibata T, Yamauchi Y, et al. Beta-catenin mutations in sporadic fundic gland polyps. *Virchows Arch.* 2002;440(4):381-6.

34. Levy MD, and Bhattacharya B. Sporadic Fundic Gland Polyps With Low-Grade Dysplasia: A Large Case Series Evaluating Pathologic and Immunohistochemical Findings and Clinical Behavior. *Am J Clin Pathol.* 2015;144(4):592-600.

35. Fodde R, Kuipers J, Rosenberg C, et al. Mutations in the APC tumour suppressor gene cause chromosomal instability. *Nat Cell Biol.* 2001;3(4):433-8.

36. Hayakawa Y, Ariyama H, Stancikova J, et al. Mist1 Expressing Gastric Stem Cells Maintain the Normal and Neoplastic Gastric Epithelium and Are Supported by a Perivascular Stem Cell Niche. *Cancer Cell.* 2015;28(6):800-14.

37. Douchi D, Yamamura A, Matsuo J, et al. Induction of Gastric Cancer by Successive Oncogenic Activation in the Corpus. *Gastroenterology.* 2021;161(6):1907-23 e26.

38. Powell AE, Vlacich G, Zhao ZY, et al. Inducible loss of one Apc allele in Lrig1-expressing progenitor cells results in multiple distal colonic tumors with features of familial adenomatous polyposis. *Am J Physiol Gastrointest Liver Physiol.* 2014;307(1):G16-23.

39. Adam RS, van Neerven SM, Pleguezuelos-Manzano C, et al. Intestinal region-specific Wnt signalling profiles reveal interrelation between cell identity and oncogenic pathway activity in cancer development. *Cancer Cell Int.* 2020;20(1):578.

40. Langlands AJ, Carroll TD, Chen Y, et al. Chir99021 and Valproic acid reduce the proliferative advantage of Apc mutant cells. *Cell Death Dis.* 2018;9(3):255.

41. Tsai YH, Czerwinski M, Wu A, et al. A Method for Cryogenic Preservation of Human Biopsy Specimens and Subsequent Organoid Culture. *Cell Mol Gastroenterol Hepatol.* 2018;6(2):218-22 e7.

42. Arnold K, Sarkar A, Yram MA, et al. Sox2(+) adult stem and progenitor cells are important for tissue regeneration and survival of mice. *Cell Stem Cell.* 2011;9(4):317-29.

43. Shibata H, Toyama K, Shioya H, et al. Rapid colorectal adenoma formation initiated by conditional targeting of the Apc gene. *Science.* 1997;278(5335):120-3.

44. Borten MA, Bajikar SS, Sasaki N, et al. Automated brightfield morphometry of 3D organoid populations by OrganoSeg. *Sci Rep.* 2018;8(1):5319.

3.8 Appendix

Mutational Landscape of Sequenced Polyps

H61

Copy Number Variations

Chr	vs A	vs C
2 LRP1B.1		Duplication
13 BRCA2		Duplication

Patient	Tissue/Orgs	Clinical Mutation	Type	Present?	CNV - APC	Somatic	Val1822Asp	Tyr486Ter
H61	Organoids	Del 1B Promotor					Yes	

Additional Rare APC Germline Mutations

None					

Somatic Mutations

	vs A	vs C							
SF3B1		55.54%	2:198260895	T	A	Missense	NM_012433.2	NM_012433.2:c.3424A>T	NP_036565.2:p.Asn1142Tyr
FANCD2		50%	3:10081677	A	-	Other	NM_033084.3	NM_033084.3:c.695+148delA	
ERG		29.24%	21:39775625	G	A	Missense	NM_001136154.1	NM_001136154.1:c.416C>T	NP_001129626.1:p.Thr139Met

Loss of Heterozygosity

	vs A	vs C							
GEN1	71.03%	84.29%	2:17959421	AC	-	Other	NM_182625.3	NM_182625.3:c.1264+91_1264+92delAC	
MSH2	46.81%	80%	2:47709704	T	C	Other	NM_000251.2	NM_000251.2:c.2635-214T>C	
MSH6	53.97%	79.17%	2:48018479	G	T	Other	NM_000179.2	NM_000179.2:c.457+217G>T	
ATR	29.62%	17.27%	3:142259707	A	-	Other	NM_001184.3	NM_001184.3:c.3581+39delT	
BCL6	22.45%	0%	3:187440506	C	A	Other	NM_001706.4	NM_001706.4:c.1978-1176>T	
TERT	56.52%	90.91%	5:1282319	C	A	Other	NM_198253.2	NM_198253.2:c.1769+225G>T	
JAK2	51.09%	76%	9:5055015	C	T	Other	NM_004972.3	NM_004972.3:c.936+131C>T	
GNAQ	42.86%	88.89%	9:80409138	C	G	Other	NM_002072.3	NM_002072.3:c.735+241G>C	

Germline Mutation			vs A		vs C		Location		
APC	Missense	Tolerated			49.67%	49.01%	5:112176756	T	A

Total Germline Mutations	94		
Damaging Mutations	25	Tolerated Mutations	59

H62

Copy Number Variations

Chr	vs A	vs C
2 LRP1B.1/2	Deletion	
2 SF3B1	Deletion	
13 BRCA2	Deletion	

Patient	Tissue/Orgs	Clinical Mutation	Type	Present?	CNV - APC	Somatic	Val1822Asp	Tyr486Ter
H62	Organoids	c.426_427delAT, p.L143Af	frameshift	Yes				

Additional Rare APC Germline Mutations

None					

Somatic Mutations

	vs A	vs C							
MITF	38.46%		3:69986098	C	T	Other	NM_000248.3	NM_000248.3:c.33+192C>T	
KMT2C	60%		7:151944708	T	-	Other	NM_170606.2	NM_170606.2:c.2532+279delA	
PAK3	26.99%		X:110366605	G	A	Other	NM_001128168.1	NM_001128168.1:c.175+99G>A	

Loss of Heterozygosity

	vs A	vs C							
ACVR1B	74.15%	83.19%	12:52345498	GCG	-	Other	NM_020328.3	NM_020328.3:c.-30_-28delGCG	
CDK4	42.86%	0%	12:58145598	C	A	Other	NM_000075.3	NM_000075.3:c.-19-79G>T	
BRCA1	54.55%	75.47%	17:41251646	T	A	Other	NM_007294.3	NM_007294.3:c.547+146A>T	
KMT2B	27.79%	0%	19:36215884	C	T	Other	NM_014727.1	NM_014727.1:c.3430-6C>T	
ARAF	67.65%	89.13%	X:47430615	T	G	Other	NM_001256196.1	NM_001256196.1:c.1696-107T>G	
ARAF	56.76%	81.25%	X:47430617	T	G	Other	NM_001256196.1	NM_001256196.1:c.1696-105T>G	

Germline Mutation			vs A		vs C		Location		
APC	LoF	Damaging	46.57%	48.25%			5:112111329	AT	-

Total Germline Mutations	97		
Damaging Mutations	25	Tolerated Mutations	64

H66

Copy Number Variations

Chr	vs A	vs C
1 MTOR+ANGP	Deletion	Deletion
1 NOTCH2	Duplication	Duplication
1 DDR2	Duplication	
2 XPO1	Deletion	Deletion
2 SF3B1	Deletion	Deletion
2 LRP1B.1/2	Duplication	Duplication
2 ERBB4.2	Duplication	
2 ERBB4..1	Duplication	
3 FANCD2/VHL	Deletion	Deletion
3 SETD2	Deletion	Deletion
3 CBLB	Duplication	
3 EPHA3	Duplication	Duplication
4 KDR	Duplication	
4 EPHA5	Duplication	Duplication
5 FGFR4+NSD1	Deletion	Deletion
6 ROS1	Duplication	Duplication
7 KMT2C	Duplication	Duplication
7 MET	Duplication	Duplication
7 EGFR	Duplication	Duplication
7 HGF	Duplication	Duplication
7 KMT2C+XRC	Duplication	Duplication
7 EZH2	Duplication	Duplication
7 IKZF1	Duplication	Duplication
7 INHBA	Duplication	
7 BRAF		Duplication
9 NOTCH1	Deletion	Deletion
9 NTRK2	Duplication	
11 KMT2A		Deletion
12 ERBB3	Deletion	
12 KMT2D.2	Deletion	
12 POLE		Deletion
13 FLT3		Deletion
14 HSP90AA1	Deletion	Deletion
15 BLM	Deletion	Deletion
15 NTRK3	Duplication	
16 CTCF	Deletion	
16 FANCA	Deletion	Deletion
16 PALB2	Deletion	Deletion
16 CDH1	Deletion	Deletion
16 TSC2	Deletion	
16 CREBBP		Deletion
17 NF1/EVI2A	Duplication	Duplication
17 RNF43	Duplication	Duplication
17 BRIP1	Duplication	Duplication
17 MAP2K4	Duplication	
17 AXIN2		Duplication
19 KEAP1	Deletion	Deletion
19 CBLC	Deletion	
19 DNM2	Deletion	Deletion
19 TCF3	Deletion	Deletion
19 DOT1L	Deletion	Deletion
19 JAK3	Deletion	Deletion
19 NOTCH3	Deletion	Deletion
19 SMARCA4	Deletion	Deletion
22 EP300	Deletion	Deletion
22 BCR		Deletion
X AR	Duplication	
X PAK3	Duplication	

Patient	Tissue/Orgs	Clinical Mutation	Type	Present?	CNV - APC	Somatic	Val1822Asp	Tyr486Ter
H66	Tissue	exon 15 c.3668C>T, p.Q12	stop	Yes			Yes	Yes

Additional Rare APC Germline Mutations				
missense_va: c.5009C>T; p.Ala1670Val				

Somatic Mutations

	vs A	vs C							
XPO1	41.67%	51.58%	2:61713321	T	-	Other	NM_003400.3	NM_003400.3:c.2314-224delA	
MLH1	37.5%		3:37067097	ATA	-	Other	NM_000249.3	NM_000249.3:c.1039-31_1039-29delATA	
FGFR1	20.83%	37.5%	8:38298094	TT	-	Other	NM_001174067.1	NM_001174067.1:c.191-10629_191-10628delAA	
PRKDC	29.41%		8:48848624	A	-	Other	NM_006904.6	NM_006904.6:c.1279-164delT	
JAK2	69.23%		9:5080892	C	T	Other	NM_004972.3	NM_004972.3:c.2434+209C>T	
CD79A	20%		19:42383918	G	T	Other	NM_001783.3	NM_001783.3:c.498+195G>T	
MAPK1	42.86%		22:22142389	A	-	Other	NM_002745.4	NM_002745.4:c.856+157delT	
BCR			22:23614057	T	-	Other	NM_004327.3	NM_004327.3:c.1921+278delT	

Loss of Heterozygosity

	vs A	vs C						
CSF3R		66.67%	1:36935128	G	A	Other	NM_156039.3	NM_156039.3:c.1474+125C>T
PDGFRB		35.29%	5:149501803	C	T	Other	NM_002609.3	NM_002609.3:c.2184-200G>A
IKZF1	68.97%		7:50455346	C	T	Other	NM_006060.4	NM_006060.4:c.555+178C>T
IDH2	35.71%		15:90632237	C	G	Other	NM_002168.2	NM_002168.2:c.374-258G>C

Germline Mutation			vs A		vs C		Location		
APC	LoF	Damaging	50.43%	50.79%	52.43%	50.79%	5:112162854	T	G
APC	LoF	Damaging	50.69%	50.96%	47.5%	50.96%	5:112174979	C	T
APC	Missense	Tolerated	50.23%	51.07%			5:112176300	C	T
APC	Missense	Tolerated	100%	100%			5:112176756	T	A

Total Germline Mutations	104		
Damaging Mutations	31	**Tolerated Mutations**	67

H69

Copy Number Variations

Chr	vs A	vs C
2 SF3B1	Deletion	Deletion
2 ALK	Duplication	
2 XPO1		Deletion
2 LRP1B.1		Deletion
3 ATRX		Deletion
5 APC		Deletion
5 FLT4		Duplication
8 PRKDC		Deletion
9 NOTCH1		Duplication
10 SMC3		Deletion
11 CHEK1		Deletion
11 ATM		Deletion
12 POLE		Duplication
13 BRCA2		Deletion
13 FLT3		Deletion
14 AKT1		Duplication
16 GRIN2A	Duplication	
16 TSC2		Duplication
16 FANCA		Duplication
19 JAK3	Deletion	
19 DOT1L		Duplication
20 GNAS		Duplication
X ATRX		Deletion

Patient	Tissue/Orgs	Clinical Mutation	Type	Present?	CNV - APC	Somatic	Val1822Asp	Tyr486Ter
H69	Tissue	c.1417C>T, p.Q473X	stop	Yes	Deletion		Yes, two copie	Yes

Additional Rare APC Germline Mutations				
None				

Somatic Mutations

	vs A	vs C							
ARID1B	26.67%		6:157150706	T	-	Other	NM_020732.3	NM_020732.3:c.1737+151delT	
FGFR1	33.33%	33.33%	8:38298094	TT	-	Other	NM_001174067.1	NM_001174067.1:c.191-10629_191-10628delAA	
PRKDC		40%	8:48869537	C	-	Other	NM_006904.6	NM_006904.6:c.324+194delG	
PRKDC		60%	8:48869538	CAA	-	Other	NM_006904.6	NM_006904.6:c.324+191_324+193delTTG	
CDH1	62.5%		16:68863862	C	-	Other	NM_004360.3	NM_004360.3:c.2439+162delC	
MAP2K4	27.27%		17:11999213	-	TGTG	Other	NM_001281435.1	NM_001281435.1:c.546+201_546+202insTGTG	
NOTCH3	40%		19:15273584	T	G	Other	NM_000435.2	NM_000435.2:c.5816-211A>C	
ERG		27.27%	21:39870560	T	-	Other	NM_001136154.1	NM_001136154.1:c.40-53016delA	
CRLF2		26.67%	X:1327466	A	-	Other	NM_022148.2	NM_022148.2:c.182+233delT	
AR		23.91%	X:66766357	-	GGC	Missense	NM_000044.3	NM_000044.3:c.1368_1369insGGC	NP_000035.2:p.Gly473_Glu474insGly

Loss of Heterozygosity

	vs A	vs C						
FAM46C		58.82%	7.69%	1:118166900	AT	-	Other	NM_017709.3	NM_017709.3:c.*234_*235delAT
FAM46C		62.5%	10%	1:118166902	G	T	Other	NM_017709.3	NM_017709.3:c.*236G>T
FAM46C		62.5%	11.11%	1:118166905	CT	-	Other	NM_017709.3	NM_017709.3:c.*239_*240delCT
RAC1	47.06%	11.11%		7:6414545	C	T	Other	NM_018890.3	NM_018890.3:c.35+144C>T
Intergenic		28.41%	11.25%	7:50444182	T	-	Other		
EED		36.84%	76.92%	11:85979270	T	G	Other	NM_003797.3	NM_003797.3:c.861-228T>G
BIRC3		24.24%	2.7%	11:102207319	A	-	Other	NM_001165.4	NM_001165.4:c.1580-172delA
KRAS	44.44%	85.71%	36.36%	85.71%	12:25362552	A	C	Other	NM_033360.2	NM_033360.2:c.*298T>G
BRCA1			50%	11.54%	17:41219854	T	-	Other	NM_007294.3	NM_007294.3:c.4987-142delA
MED12	59.02%	78.5%	66.67%	78.5%	X:70352516	A	G	Other	NM_005120.2	NM_005120.2:c.4415+128A>G

Germline Mutation			vs A		vs C		Location		
APC	LoF	Damaging	52.45%	48.21%	48.77%	48.21%	5:112162813	C	T
APC	LoF	Damaging	58.85%	61.25%	58.84%	61.25%	5:112162854	T	G
APC	Missense	Tolerated	100%	99.69%	99.08%	99.69%	5:112176756	T	A

Total Germline Mutations	106		
Damaging Mutations	27	**Tolerated Mutations**	79

H71

Copy Number Variations

Chr	vs A	vs C
None		

Patient	Tissue/Orgs	Clinical Mutation	Type	Present?	CNV - APC	Somatic	Val1822Asp	Tyr486Ter
H71	Organoids	c.3439dupT; p.Tyr1147Leu	frameshift	Yes			Yes, two copi	Yes

Additional Rare APC Germline Mutations				
None				

Somatic Mutations

	vs A	vs C							
SETD2		40%	3:47088350	T	-	Other	NM_014159.6	NM_014159.6:c.6964-239delA	
GATA3		33.33%	10:8106274	C	-	Other	NM_001002295.1	NM_001002295.1:c.924+173delC	
BCR		21.05%	22:23634615	T	-	Other	NM_004327.3	NM_004327.3:c.2783-113delT	
MED12		26.42%	X:70353187	T	-	Other	NM_005120.2	NM_005120.2:c.4617+125delT	

Loss of Heterozygosity

	vs A	vs C							
GEN1	21.74%	0%	2:17959526	-	CG	Other	NM_182625.3	NM_182625.3:c.1264+195_1264+196insCG	
LRP1B	40%	83.33%	2:141812434	C	T	Other	NM_018557.2	NM_018557.2:c.1552+251G>A	
PDGFRA	22.39%	0.18%	4:55155218	G	A	Other	NM_006206.4	NM_006206.4:c.2817G>A	NP_006197.1:p.=
PIK3R1	25%	0.11%	5:67589576	-	A	LoF	NM_181523.2	NM_181523.2:c.1338_1339insA	NP_852664.1:p.Leu449fs

Germline Mutation			vs A	vs C			Location		
APC	LoF	Damaging		53.58%	50.81%	5:112162854	T	G	
APC	LoF	Damaging		50.28%	47.68%	5:112174729	-	T	
APC	Missense	Tolerated		99.83%	100%	5:112176756	T	A	

Total Germline Mutations	99		
Damaging Mutations	29	**Tolerated Mutations**	62

H72

Copy Number Variations

Chr	vs A	vs C
1 FUBP1		Duplication
2 DNMT3A		Deletion
2 LRP1B.1/2		Duplication
2 MSH6		Duplication
2 PMS1		Duplication
3 BAP1		Deletion
3 CBLB		Duplication
4 FGFR3		Deletion
5 CSF1R+PDGFRB		Deletion
7 HGF		Duplication
9 NOTCH1		Deletion
9 JAK2		Duplication
11 ATM		Duplication
12 KMT2D.1/2		Deletion
12 POLE		Deletion
13 BRCA2		Duplication
16 TSC2		Deletion
19 DOT1L		Deletion
19 JAK3		Deletion
19 POLD1		Deletion
19 SMARCA4		Deletion
19 CIC		Deletion
19 NOTCH3		Deletion
20 PLCG1		Deletion
X ATRX		Duplication

Patient	Tissue/Orgs	Clinical Mutation	Type	Present?	CNV - APC	Somatic	Val1822Asp	Tyr486Ter
H72	Organoids	c.5826_5829delCAGA; p.D	frameshift	Yes			Yes	

Additional Rare APC Germline Mutations						
5_prime_UTR NM_001127	intron_varian NM_000038.	intron_varian NM_000038.	intron_varian NM_000038.	3_prime_UTR NM_000038.5:c.*86C>A		

Somatic Mutations

	vs A	vs C							
ARID1A		25%	1:27087178	A	-	Other	NM_006015.4	NM_006015.4:c.1921-169delA	
BLM		22.58%	15:91295411	T	-	Other	NM_000057.2	NM_000057.2:c.959+235delT	
ZR5R2		25%	X:15822073	A	-	Other	NM_005089.3	NM_005089.3:c.312+154delA	

Loss of Heterozygosity

	vs A	vs C							
ATR	28.07%	8.57%	3:142279407	T	-	Other	NM_001184.3	NM_001184.3:c.1350-111delA	
NSD1	40.43%	16.22%	5:176636530	A	-	Other	NM_022455.4	NM_022455.4:c.1237-107delA	
CARD11	21.32%	0.15%	7:2968294	G	A	Other	NM_032415.4	NM_032415.4:c.1692C>T	NP_115791.3:p.=
KAT6A	25%	100%	8:41906694	A	T	Other	NM_006766.3	NM_006766.3:c.-199T>A	
GNAS	22.83%	0%	20:57429286	C	T	Missense	NM_080425.2	NM_080425.2:c.966C>T	NP_536350.2:p.=
CRLF2	38.24%	82.61%	X:1321079	G	C	Other	NM_022148.2	NM_022148.2:c.483+193C>G	

Germline Mutation			vs A	vs C			Location		
APC	LoF	Damaging		46.52%	48.25%	5:112177113	CAGA	-	
APC	Missense	Tolerated		51.11%	48.29%	5:112176756	T	A	

Total Germline Mutations	99		
Damaging Mutations	22	**Tolerated Mutations**	66

H73

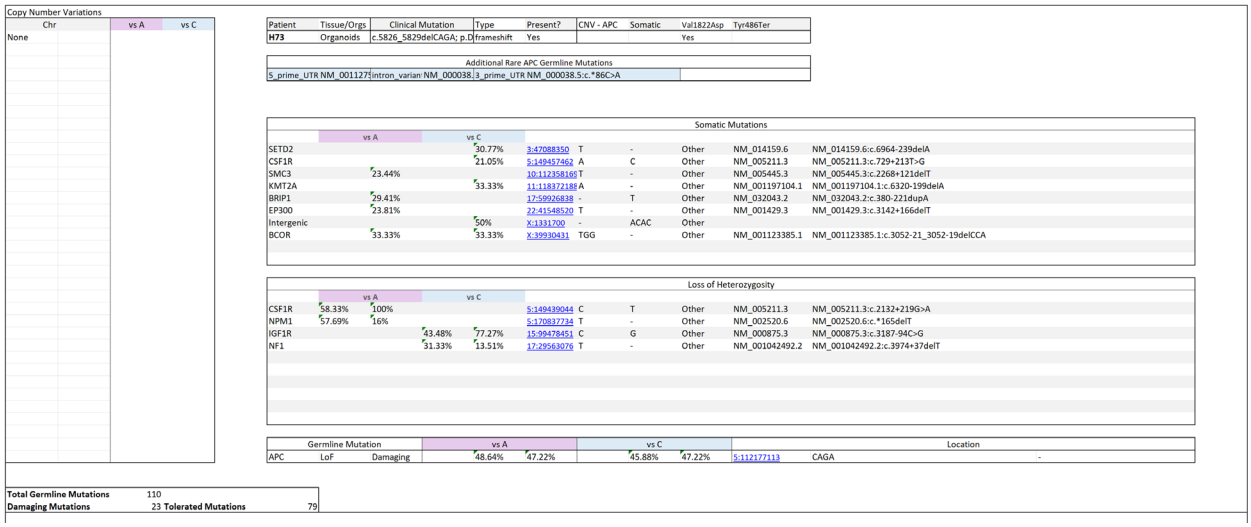

Copy Number Variations

Chr	vs A	vs C
None		

Patient	Tissue/Orgs	Clinical Mutation	Type	Present?	CNV - APC	Somatic	Val1822Asp	Tyr486Ter
H73	Organoids	c.5826_5829delCAGA; p.D	frameshift	Yes			Yes	

Additional Rare APC Germline Mutations				
5_prime_UTR NM_001127	intron_varian	NM_000038.	3_prime_UTR	NM_000038.5:c.*86C>A

Somatic Mutations

	vs A	vs C						
SETD2		30.77%	3:47088350	T	-	Other	NM_014159.6	NM_014159.6:c.6964-239delA
CSF1R		21.05%	5:149457462	A	C	Other	NM_005211.3	NM_005211.3:c.729+213T>G
SMC3	23.44%		10:112358166	T	-	Other	NM_005445.3	NM_005445.3:c.2268+121delT
KMT2A		33.33%	11:118372188	A	-	Other	NM_001197104.1	NM_001197104.1:c.6320-199delA
BRIP1	29.41%		17:59926838	-	T	Other	NM_032043.2	NM_032043.2:c.380-221dupA
EP300	23.81%		22:41548520	T	-	Other	NM_001429.3	NM_001429.3:c.3142+166delT
Intergenic		50%	X:1331700	-	ACAC	Other		
BCOR	33.33%	33.33%	X:39930431	TGG	-	Other	NM_001123385.1	NM_001123385.1:c.3052-21_3052-19delCCA

Loss of Heterozygosity

	vs A	vs C						
CSF1R	58.33%	100%	5:149439044	C	T	Other	NM_005211.3	NM_005211.3:c.2132+219G>A
NPM1	57.69%	16%	5:170837734	T	-	Other	NM_002520.6	NM_002520.6:c.*165delT
IGF1R		43.48%	15:99478451	C	G	Other	NM_000875.3	NM_000875.3:c.3187-94C>G
NF1		31.33%	17:29563076	T	-	Other	NM_001042492.2	NM_001042492.2:c.3974+37delT

Germline Mutation			vs A		vs C		Location		
APC	LoF	Damaging	48.64%	47.22%	45.88%	47.22%	5:112177113	CAGA	-

Total Germline Mutations	110		
Damaging Mutations	23	**Tolerated Mutations**	79

H75

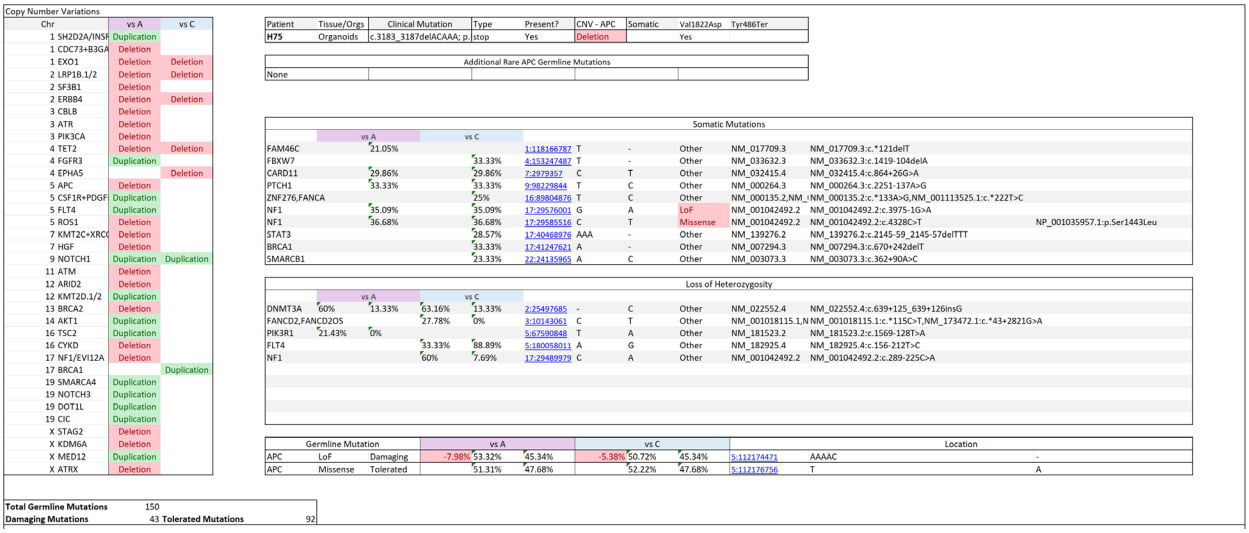

Copy Number Variations

Chr	vs A	vs C
1 SH2D2A/INSR	Duplication	
1 CDC73+B3GA	Deletion	
1 EXO1	Deletion	Deletion
1 LRP1B.1/2	Deletion	Deletion
2 SF3B1	Deletion	
2 ERBB4	Deletion	Deletion
3 CBLB	Deletion	
3 ATR	Deletion	
3 PIK3CA	Deletion	
4 TET2	Deletion	Deletion
4 FGFR3	Duplication	
4 EPHA5		Deletion
5 APC	Deletion	
5 CSF1R+PDGF	Duplication	
5 FLT4	Duplication	
5 ROS1	Deletion	
7 KMT2C+XRC	Deletion	
7 HGF	Deletion	
9 NOTCH1	Duplication	Duplication
11 ATM	Deletion	
12 ARID2	Deletion	
12 KMT2D.1/2	Duplication	
13 BRCA2	Deletion	
14 AKT1	Duplication	
16 TSC2	Duplication	
16 CYKD	Deletion	
17 NF1/EVI12A	Deletion	
17 BRCA1		Duplication
19 SMARCA4	Duplication	
19 NOTCH3	Duplication	
19 DOT1L	Duplication	
19 CIC	Duplication	
X STAG2	Deletion	
X KDM6A	Deletion	
X MED12	Duplication	
X ATRX	Deletion	

Patient	Tissue/Orgs	Clinical Mutation	Type	Present?	CNV - APC	Somatic	Val1822Asp	Tyr486Ter
H75	Organoids	c.3183_3187delACAAA; p.	stop	Yes	Deletion		Yes	

Additional Rare APC Germline Mutations
None

Somatic Mutations

	vs A	vs C						
FAM46C	21.05%		1:118166787	T	-	Other	NM_017709.3	NM_017709.3:c.*121delT
FBXW7		33.33%	4:153247487	T	-	Other	NM_033632.3	NM_033632.3:c.1419-104delA
CARD11	29.86%	29.86%	7:2979357	C	T	Other	NM_032415.4	NM_032415.4:c.864+26G>A
PTCH1	33.33%	33.33%	9:98229844	T	C	Other	NM_000264.3	NM_000264.3:c.2251-137A>G
ZNF276,FANCA		25%	16:89804876	T	C	Other	NM_000135.2,NM_	NM_000135.2:c.*133A>G,NM_001113525.1:c.*222T>C
NF1	35.09%	35.09%	17:29576001	G	A	LoF	NM_001042492.2	NM_001042492.2:c.3975-1G>A
NF1	36.68%	36.68%	17:29585516	C	T	Missense	NM_001042492.2	NM_001042492.2:c.4328C>T NP_001035957.1:p.Ser1443Leu
STAT3		28.57%	17:40468976	AAA	-	Other	NM_139276.2	NM_139276.2:c.2145-59_2145-57delTTT
BRCA1		33.33%	17:41247621	A	-	Other	NM_007294.3	NM_007294.3:c.670+242delT
SMARCB1		23.33%	22:24135965	A	C	Other	NM_003073.3	NM_003073.3:c.362+90A>C

Loss of Heterozygosity

	vs A	vs C						
DNMT3A	60%	13.33%	63.16%	13.33%	2:25497685	-	C	Other	NM_022552.4	NM_022552.4:c.639+125_639+126insG
FANCD2,FANCD2OS			27.78%	0%	3:10143061	C	T	Other	NM_001018115.1,N	NM_001018115.1:c.*115C>T,NM_173472.1:c.*43+2821G>A
PIK3R1	21.43%	0%			5:67590848	T	A	Other	NM_181523.2	NM_181523.2:c.1569-128T>A
FLT4			33.33%	88.89%	5:180058011	A	G	Other	NM_182925.4	NM_182925.4:c.156-212T>C
NF1			60%	7.69%	17:29489979	C	A	Other	NM_001042492.2	NM_001042492.2:c.289-225C>A

Germline Mutation			vs A		vs C		Location		
APC	LoF	Damaging	-7.98%	53.32%	45.34%	-5.38%	50.72%	45.34%	5:112174471	AAAAC	-
APC	Missense	Tolerated		51.31%	47.68%		52.22%	47.68%	5:112176756	T	A

Total Germline Mutations	150		
Damaging Mutations	43	**Tolerated Mutations**	92

H76

Copy Number Variations

Chr	vs A	vs C
5 RAD50		Duplication
7 MET		Duplication
8 PRKDC		Duplication
9 NOTCH1		Deletion
13 BRCA2		Duplication
13 RB1+LPAR6		Duplication
X AR		Deletion
X BCORL1		Deletion

Patient	Tissue/Orgs	Clinical Mutation	Type	Present?	CNV - APC	Somatic	Val1822Asp	Tyr486Ter
H76	Organoids	Possibly: c.3921_3925delA	frameshift	Yes			Yes, two copi	Yes, two copies

Additional Rare APC Germline Mutations
5_prime_UTR NM_001127 intron_varian NM_000038. intron_varian NM_000038. synonymous_NM_000038. 5:c.7201C>T

Somatic Mutations

	vs A	vs C							
FGFR4		33.33%	5:176523877	TCC	-	Other	NM_002011.3	NM_002011.3:c.2153+135_2153+137delTCC	
STK11		20%	19:1206807	C	-	Other	NM_000455.4	NM_000455.4:c.-106delC	

Loss of Heterozygosity

	vs A	vs C							
ARID1A	27.49%	0.18%	1:27100207	C	T	LoF	NM_006015.4	NM_006015.4:c.4003C>T	NP_006006.3:p.Arg1335Ter
TNFAIP3	38.42%	0.65%	6:138196182	T	C	Other	NM_006290.3	NM_006290.3:c.486+10T>C	
NOTCH1	58.62%	18.52%	9:139404895	C	T	Other	NM_017617.3	NM_017617.3:c.2740+210G>A	
ATM	27.78%	0%	11:108224298	-	AC	Other	NM_000051.3	NM_000051.3:c.8786+190_8786+191insAC	
POLE	43.48%	75%	12:133258088	C	T	Other	NM_006231.2	NM_006231.2:c.63-223G>A	
BLM	45.45%	4.76%	15:91337178	A	-	Other	NM_000057.2	NM_000057.2:c.3020-219delA	
NOTCH3	42.11%	76.19%	19:15278374	-	TTTG	Other	NM_000435.2	NM_000435.2:c.5200-155_5200-152dupCAAA	
AURKA	30.77%	0%	20:54959533	G	A	Other	NM_003600.2	NM_003600.2:c.320-153C>T	

Germline Mutation			vs A		vs C		Location		
APC	LoF	Damaging			99.2%	98.89%	5:112162854	T	G
APC	LoF	Damaging			44.49%	44.93%	5:112175212	AAAAG	-
APC	Missense	Tolerated			100%	99.75%	5:112176756	T	A

Total Germline Mutations	94		
Damaging Mutations	25	**Tolerated Mutations**	62

H77

Copy Number Variations

Chr	vs A	vs C
1 MTOR+ANGF	Deletion	Deletion
1 NOTCH2	Duplication	
1 FUBP1		Duplication
2 LRP1B.1/2	Duplication	
2 ERBB4.1/2	Duplication	
2 PMS1		Duplication
3 FANCD2/VHL	Deletion	
3 SETD2	Deletion	
3 PBRM1	Deletion	
3 CBLB	Duplication	
3 EPHA3	Duplication	
3 ATRX		Duplication
3 PIK3CA		Duplication
4 KDR	Duplication	
4 TET2		Duplication
4 EPHA5		Duplication
5 FGFR4+NSD1	Deletion	Deletion
5 FLT4		Deletion
5 APC		Duplication
6 ROS1	Duplication	
7 PMS2	Deletion	Deletion
7 EGFR		Duplication
7 HGF		Duplication
9 NOTCH1		Deletion
9 NTRK2		Duplication
11 KMT2A	Deletion	Deletion
11 ATM		Duplication
12 POLE	Deletion	Deletion
16 CDH1	Deletion	
16 FANCA	Deletion	Deletion
16 TSC2		Deletion
16 CREBBP		Deletion
17 BRCA1	Deletion	Deletion
17 CDK12	Deletion	Deletion
17 ERBB2/IKZF4		Deletion
18 SETBP1	Duplication	
19 NOTCH3	Deletion	Deletion
19 JAK3	Deletion	Deletion
19 SMARCA4	Deletion	Deletion
19 CBLC		Deletion
19 TVF3		Deletion
19 POLD1		Deletion
20 PLCG1	Duplication	
22 EP300	Deletion	Deletion
22 BCR		Deletion
X ATRX		Duplication
X STAG2		Duplication

Patient	Tissue/Orgs	Clinical Mutation	Type	Present?	CNV - APC	Somatic	Val1822Asp	Tyr486Ter
H77	Tissue	c.3260_3261delTC; p.L108	frameshift	Yes	Duplication		Yes	

Additional Rare APC Germline Mutations
None

Somatic Mutations

	vs A	vs C						
PMS1		44.44%	2:190720063	T	-	Other	NM_000534.4	NM_000534.4:c.1856+209delT
NTRK3		30.77%	15:88459541	A	G	Other	NM_001012338.2	NM_001012338.2:c.2133+12881T>C
MAPK1	38.46%		22:22159929	-	A	Other	NM_002745.4	NM_002745.4:c.492+210dupT
MAPK1	38.46%		22:22159929	A	-	Other	NM_002745.4	NM_002745.4:c.492+210delT
BCORL1		22.22%	X:129162912	T	G	Other	NM_021946.4	NM_021946.4:c.4305+76T>G

Loss of Heterozygosity

	vs A	vs C						
CUX1		27.27%	100%	7:101838533	T	-	Other	NM_001202543.1	NM_001202543.1:c.1159-254delT
SMC1A	26.32%	78.57%		X:53421574	CT	-	Other	NM_006306.3	NM_006306.3:c.2973+123_2973+124delAG

Germline Mutation			vs A		vs C		Location		
APC	LoF	Damaging	19.06%	22.33%	20.82%	22.33%	5:112174550	CT	-
APC	Missense	Tolerated	49.54%	51.85%	51.04%	51.85%	5:112176756	T	A

Total Germline Mutations	97		
Damaging Mutations	23	**Tolerated Mutations**	66

H78

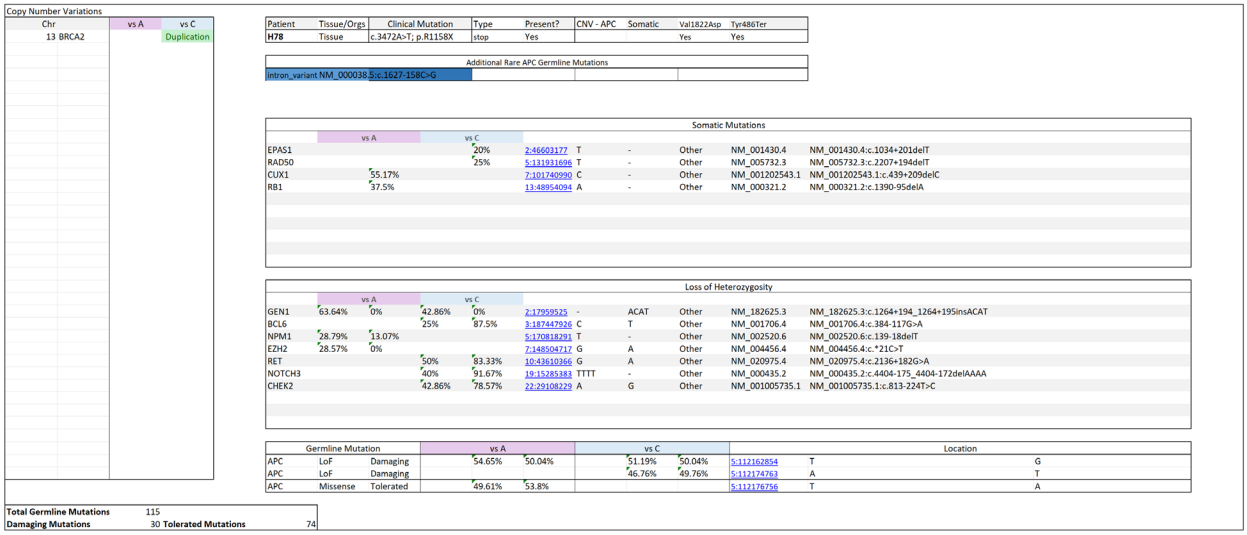

Copy Number Variations

Chr	vs A	vs C
13 BRCA2		Duplication

Patient	Tissue/Orgs	Clinical Mutation	Type	Present?	CNV - APC	Somatic	Val1822Asp	Tyr486Ter
H78	Tissue	c.3472A>T; p.R1158X	stop	Yes			Yes	Yes

Additional Rare APC Germline Mutations				
intron_variant	NM_000038.5:c.1627-158C>G			

Somatic Mutations

	vs A	vs C						
EPAS1		20%	2:46603177	T	-	Other	NM_001430.4	NM_001430.4:c.1034+201delT
RAD50		25%	5:131931696	T	-	Other	NM_005732.3	NM_005732.3:c.2207+194delT
CUX1	55.17%		7:101740990	C	-	Other	NM_001202543.1	NM_001202543.1:c.439+209delC
RB1	37.5%		13:48954094	A	-	Other	NM_000321.2	NM_000321.2:c.1390-95delA

Loss of Heterozygosity

	vs A		vs C							
GEN1	63.64%	0%	42.86%	0%	2:17959525	-	ACAT	Other	NM_182625.3	NM_182625.3:c.1264+194_1264+195insACAT
BCL6			25%	87.5%	3:187447926	C	T	Other	NM_001706.4	NM_001706.4:c.384-117G>A
NPM1	28.79%	13.07%			5:170818291	T	-	Other	NM_002520.6	NM_002520.6:c.139-1delT
EZH2	28.57%	0%			7:148504717	G	A	Other	NM_004456.4	NM_004456.4:c.*21C>T
RET			50%	83.33%	10:43610366	G	A	Other	NM_020975.4	NM_020975.4:c.2136+182G>A
NOTCH3			40%	91.67%	19:15285383	TTTT	-	Other	NM_000435.2	NM_000435.2:c.4404-175_4404-172delAAAA
CHEK2			42.86%	78.57%	22:29108229	A	G	Other	NM_001005735.1	NM_001005735.1:c.813-224T>C

Germline Mutation			vs A		vs C		Location		
APC	LoF	Damaging	54.65%	50.04%	51.19%	50.04%	5:112162854	T	G
APC	LoF	Damaging			46.76%	49.76%	5:112174763	A	T
APC	Missense	Tolerated	49.61%	53.8%			5:112176756	T	A

Total Germline Mutations	115		
Damaging Mutations	30	**Tolerated Mutations**	74

H80

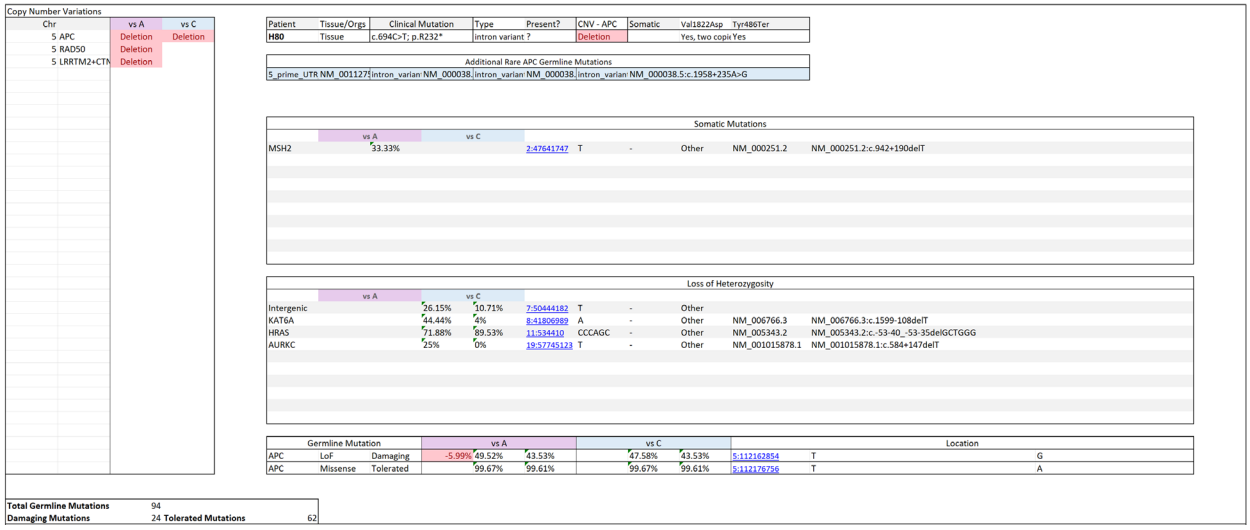

Copy Number Variations

Chr	vs A	vs C
5 APC	Deletion	Deletion
5 RAD50	Deletion	
5 LRRTM2+CTN	Deletion	

Patient	Tissue/Orgs	Clinical Mutation	Type	Present?	CNV - APC	Somatic	Val1822Asp	Tyr486Ter
H80	Tissue	c.694C>T; p.R232*	intron variant ?		Deletion		Yes, two copie	Yes

Additional Rare APC Germline Mutations			
5_prime_UTR	NM_001127	intron_varian	NM_000038.
intron_varian	NM_000038.	intron_varian	NM_000038.5:c.1958+235A>G

Somatic Mutations

	vs A	vs C						
MSH2	33.33%		2:47641747	T	-	Other	NM_000251.2	NM_000251.2:c.942+190delT

Loss of Heterozygosity

	vs A	vs C						
Intergenic		26.15%	10.71%	7:50444182	T	-	Other	
KAT6A		44.44%	4%	8:41806989	A	-	Other	NM_006766.3	NM_006766.3:c.1599-108delT
HRAS		71.88%	89.53%	11:534410	CCCAGC	-	Other	NM_005343.2	NM_005343.2:c.-53-40_-53-35delGCTGGG
AURKC		25%	0%	19:57745123	T	-	Other	NM_001015878.1	NM_001015878.1:c.584+147delT

Germline Mutation			vs A		vs C		Location		
APC	LoF	Damaging	-5.99%	49.52%	43.53%	47.58%	43.53%	5:112162854	T	G
APC	Missense	Tolerated		99.67%	99.61%	99.67%	99.61%	5:112176756	T	A

Total Germline Mutations	94		
Damaging Mutations	24	**Tolerated Mutations**	62

H81

Copy Number Variations

Chr	vs A	vs C
13 BRCA2	Deletion	Deletion

Patient	Tissue/Orgs	Clinical Mutation	Type	Present?	CNV - APC	Somatic	Val1822Asp	Tyr486Ter
H81	Tissue	c.3183_3187delACAAA; p.	stop	Yes			Yes	

Additional Rare APC Germline Mutations
None

Somatic Mutations

	vs A	vs C						
DDR2	43.75%		1:162750211	TT	-	Other	NM_006182.2	NM_006182.2:c.*175_*176delTT
GATA3	41.67%		10:8106275	TT	-	Other	NM_001002295.1	NM_001002295.1:c.924+174_924+175delTT
MDM2	27.78%	27.78%	12:69230723	C	T	Other	NM_002392.5	NM_002392.5:c.918+194C>T
CREBBP	37.5%		16:3788316	-	A	Other	NM_004380.2	NM_004380.2:c.4394+244dupT

Loss of Heterozygosity

	vs A	vs C						
XPO1	50%	80.95%	2:61727215	G	A	Other	NM_003400.3	NM_003400.3:c.409-186C>T
TET2	54.55%	100%	4:106193588	A	G	Other	NM_001127208.2	NM_001127208.2:c.4183-133A>G
FLT4	54.55%	7.14%	5:180051228	T	-	Other	NM_182925.4	NM_182925.4:c.1422-167delA
ABL1		42.86%	9:133711139	-	TTTCTC	Other	NM_007313.2	NM_007313.2:c.137-18313_137-18312insTTTCTC
ASXL1		22.22%	20:30946480	C	-	Other	NM_015338.5	NM_015338.5:c.-99delC
ARAF	73.9%	82.3%	X:47430621	T	G	Other	NM_001256196.1	NM_001256196.1:c.1696-101T>G
KDM5C		23.97%	11.3% X:53222044	-	C	Other	NM_004187.3	NM_004187.3:c.*105dupG

Germline Mutation			vs A		vs C		Location		
APC	LoF	Damaging	48.29%	46.6%	45.64%	46.6%	5:112174471	AAAAC	-
APC	Missense	Tolerated	46.1%	48.71%	52.72%	48.71%	5:112176756	T	A

Total Germline Mutations	97		
Damaging Mutations	24	**Tolerated Mutations**	66

H82

Copy Number Variations

Chr	vs A	vs C
14 DICER1		Deletion

Patient	Tissue/Orgs	Clinical Mutation	Type	Present?	CNV - APC	Somatic	Val1822Asp	Tyr486Ter
H82	Organoids	No germline mutations						

Additional Rare APC Germline Mutations
None

Somatic Mutations

	vs A	vs C
None		

Loss of Heterozygosity

	vs A	vs C						
KAT6A		23.08%	0%	8:41801609	TTCCTTCC	-	Other	NM_006766.3	NM_006766.3:c.1997-119_1997-112delGGAAGGAA
KMT2D		40%	75%	12:49421427	G	A	Other	NM_003482.3	NM_003482.3:c.14643+159C>T

Germline Mutation	vs A	vs C	Location
None			

Total Germline Mutations	90		
Damaging Mutations	25	**Tolerated Mutations**	60

H84

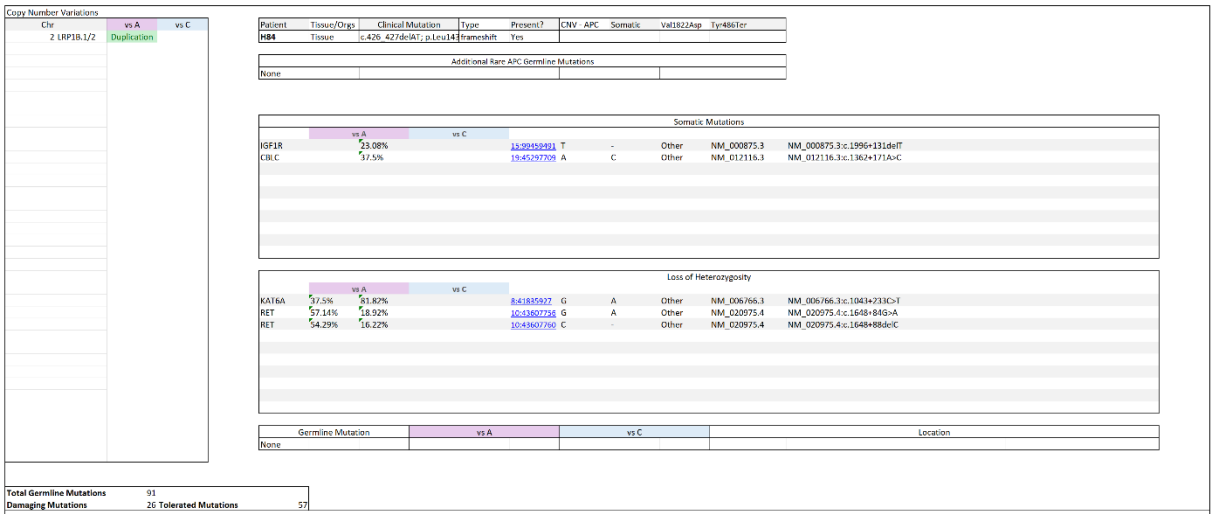

Copy Number Variations

Chr	vs A	vs C
2 LRP1B.1/2	Duplication	

Patient	Tissue/Orgs	Clinical Mutation	Type	Present?	CNV - APC	Somatic	Val1822Asp	Tyr486Ter
H84	Tissue	c.426_427delAT; p.Leu143fs	frameshift	Yes				

Additional Rare APC Germline Mutations

None

Somatic Mutations

	vs A	vs C						
IGF1R	23.08%		15:99459491	T	-	Other	NM_000875.3	NM_000875.3:c.1996+131delT
CBLC	37.5%		19:45297709	A	C	Other	NM_012116.3	NM_012116.3:c.1362+171A>C

Loss of Heterozygosity

	vs A	vs C						
KAT6A	37.5%	81.82%	8:41835927	G	A	Other	NM_006766.3	NM_006766.3:c.1041+233C>T
RET	57.14%	18.92%	10:43607758	G	A	Other	NM_020975.4	NM_020975.4:c.1648+84G>A
RET	54.29%	16.22%	10:43607760	C	-	Other	NM_020975.4	NM_020975.4:c.1648+88delC

Germline Mutation	vs A	vs C	Location
None			

Total Germline Mutations	91		
Damaging Mutations	26	Tolerated Mutations	57

H85

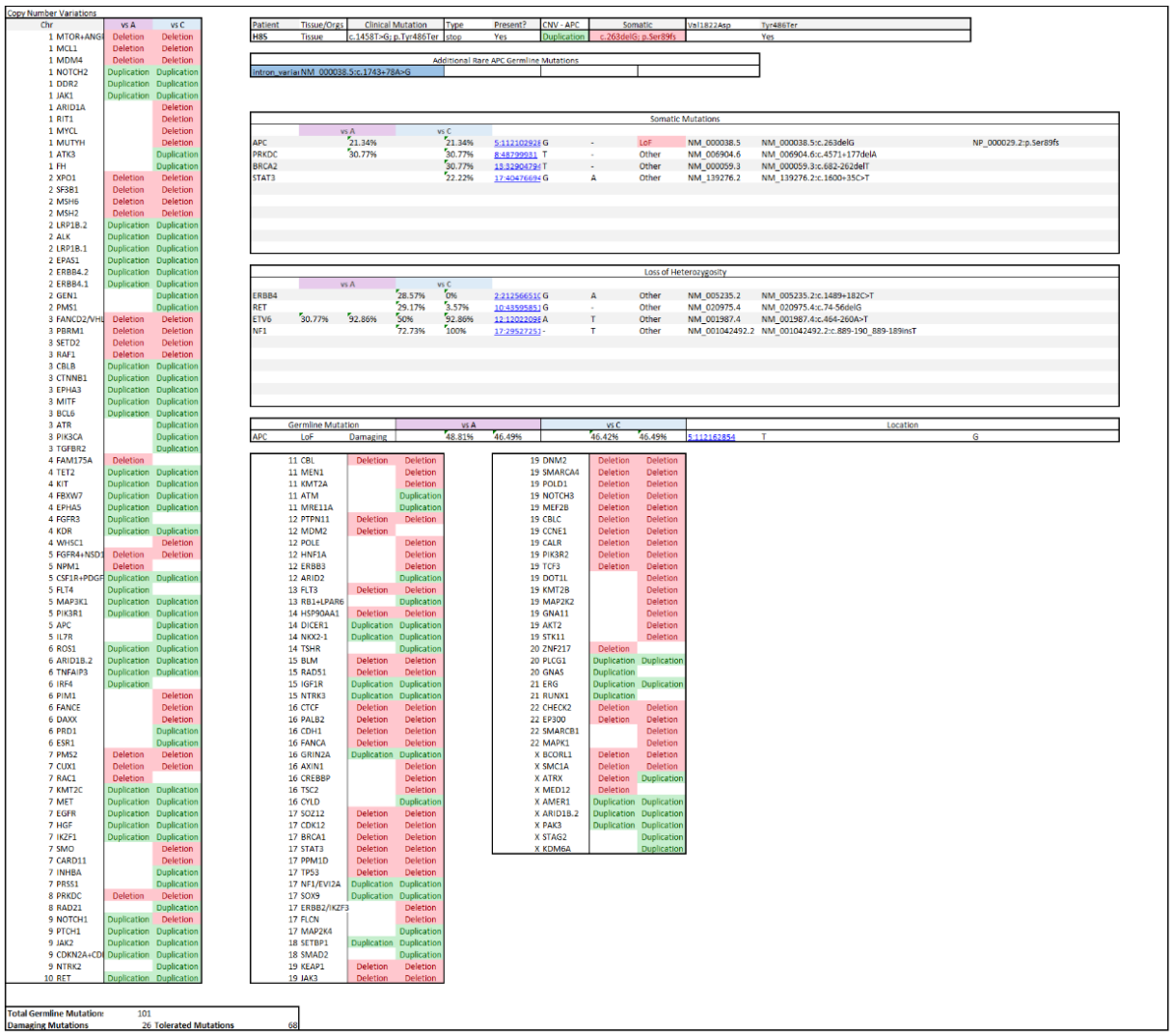

Copy Number Variations

Chr	vs A	vs C
1 MTOR+ANG	Deletion	Deletion
1 MCL1	Deletion	Deletion
1 MDM4	Deletion	Deletion
1 NOTCH2	Duplication	Duplication
1 DDR2	Duplication	Duplication
1 JAK1	Duplication	Duplication
1 ARID1A		Deletion
1 RIT1		Deletion
1 MYCL		Deletion
1 MUTYH		Deletion
1 ATK3		Duplication
1 FH		Duplication
2 XPO1	Deletion	Deletion
2 SF3B1	Deletion	Deletion
2 MSH6	Deletion	Deletion
2 MSH2	Deletion	Deletion
2 LRP1B.2	Duplication	Duplication
2 ALK	Duplication	Duplication
2 LRP1B.1	Duplication	Duplication
2 EPAS1	Duplication	Duplication
2 ERBB4.2	Duplication	Duplication
2 ERBB4.1	Duplication	Duplication
2 GEN1		Duplication
2 PMS1		Duplication
3 FANCD2/VHL	Deletion	Deletion
3 PBRM1	Deletion	Deletion
3 SETD2	Deletion	Deletion
3 RAF1	Deletion	Deletion
3 CBLB	Duplication	Duplication
3 CTNNB1	Duplication	Duplication
3 EPHA3	Duplication	Duplication
3 MITF	Duplication	Duplication
3 BCL6	Duplication	Duplication
3 ATR		Duplication
3 PIK3CA		Duplication
3 TGFBR2		Duplication
4 FAM175A	Deletion	
4 TET2	Duplication	Duplication
4 KIT	Duplication	Duplication
4 FBXW7	Duplication	Duplication
4 EPHA5	Duplication	Duplication
4 FGFR3	Duplication	
4 KDR	Duplication	Duplication
4 WHSC1		Deletion
5 FGFR4+NSD1	Deletion	Deletion
5 NPM1	Deletion	
5 CSF1R+PDGF	Duplication	Duplication
5 FLT4	Duplication	
5 MAP3K1	Duplication	Duplication
5 PIK3R1	Duplication	Duplication
5 APC		Duplication
5 IL7R		Duplication
6 ROS1	Duplication	Duplication
6 ARID1B.2	Duplication	Duplication
6 TNFAIP3	Duplication	Duplication
6 IRF4	Duplication	
6 PIM1		Deletion
6 FANCE		Deletion
6 DAXX		Deletion
6 PRD1		Duplication
6 ESR1		Duplication
7 PMS2	Deletion	Deletion
7 CUX1	Deletion	Deletion
7 RAC1	Deletion	
7 KMT2C	Duplication	Duplication
7 MET	Duplication	Duplication
7 EGFR	Duplication	Duplication
7 HGF	Duplication	Duplication
7 IKZF1	Duplication	Duplication
7 SMO		Deletion
7 CARD11		Deletion
7 INHBA		Duplication
7 PRSS1		Duplication
8 PRKDC	Deletion	Deletion
8 RAD21		Duplication
9 NOTCH1	Duplication	Deletion
9 PTCH1	Duplication	Duplication
9 JAK2	Duplication	Duplication
9 CDKN2A+CDI	Duplication	Duplication
9 NTRK2		Duplication
10 RET	Duplication	Duplication
11 CBL	Deletion	Deletion
11 MEN1		Deletion
11 KMT2A		Deletion
11 ATM		Duplication
11 MRE11A		Duplication
12 PTPN11	Deletion	Deletion
12 MDM2	Deletion	
12 POLE		Deletion
12 HNF1A		Deletion
12 ERBB3		Deletion
12 ARID2		Duplication
13 FLT3	Deletion	Deletion
13 RB1+LPAR6		Duplication
14 HSP90AA1	Deletion	Deletion
14 DICER1	Duplication	Duplication
14 NKX2-1	Duplication	Duplication
14 TSHR		Duplication
15 BLM	Deletion	Deletion
15 RAD51	Deletion	Deletion
15 IGF1R	Duplication	Duplication
15 NTRK3	Duplication	Duplication
16 CTCF	Deletion	Deletion
16 PALB2	Deletion	Deletion
16 CDH1	Deletion	Deletion
16 FANCA	Deletion	Deletion
16 GRIN2A	Duplication	Duplication
16 AXIN1		Deletion
16 CREBBP		Deletion
16 TSC2		Deletion
16 CYLD		Duplication
17 SOZ12	Deletion	Deletion
17 CDK12	Deletion	Deletion
17 BRCA1	Deletion	Deletion
17 STAT3	Deletion	Deletion
17 PPM1D	Deletion	Deletion
17 TP53	Deletion	Deletion
17 NF1/EVI2A	Duplication	Duplication
17 SOX9	Duplication	Duplication
17 ERBB2/IKZF3		Deletion
17 FLCN		Deletion
17 MAP2K4		Duplication
18 SETBP1	Duplication	Duplication
18 SMAD2		Duplication
19 KEAP1	Deletion	Deletion
19 JAK3	Deletion	Deletion
19 DNM2	Deletion	Deletion
19 SMARCA4	Deletion	Deletion
19 POLD1	Deletion	Deletion
19 NOTCH3	Deletion	Deletion
19 MEF2B	Deletion	Deletion
19 CBLC	Deletion	Deletion
19 CCNE1	Deletion	Deletion
19 CALR	Deletion	Deletion
19 PIK3R2	Deletion	Deletion
19 TCF3	Deletion	Deletion
19 DOT1L		Deletion
19 KMT2B		Deletion
19 MAP2K2		Deletion
19 GNA11		Deletion
19 AKT2		Deletion
19 STK11		Deletion
20 ZNF217	Deletion	
20 PLCG1	Duplication	Duplication
20 GNAS	Duplication	
21 ERG	Duplication	Duplication
21 RUNX1	Duplication	
22 CHEOX2	Deletion	Deletion
22 EP300	Deletion	Deletion
22 SMARCB1		Deletion
22 MAPK1		Deletion
X BCORL1	Deletion	Deletion
X SMC1A	Deletion	Deletion
X ATRX	Deletion	Duplication
X MED12	Deletion	
X AMER1	Duplication	Duplication
X ARID1B.2	Duplication	Duplication
X PAK3	Duplication	Duplication
X STAG2		Duplication
X KDM6A		Duplication

Patient	Tissue/Orgs	Clinical Mutation	Type	Present?	CNV - APC	Somatic	Val1822Asp	Tyr486Ter
H85	Tissue	c.1458T>G; p.Tyr486Ter	stop	Yes	Duplication	c.263delG; p.Ser89fs		Yes

Additional Rare APC Germline Mutations

Intron_variant NM_000038.5:c.1743+78A>G

Somatic Mutations

	vs A	vs C							
APC	21.34%	21.34%	5:112102924	G	-	LoF	NM_000038.5	NM_000038.5:c.263delG	NP_000029.2:p.Ser89fs
PRKDC	30.77%	30.77%	8:48799031	T	-	Other	NM_006904.6	NM_006904.6:c.4571+177delA	
BRCA2		30.77%	13:32906729	T	-	Other	NM_000059.3	NM_000059.3:c.682-262delT	
STAT3		22.22%	17:40476694	G	A	Other	NM_139276.2	NM_139276.2:c.1600+35C>T	

Loss of Heterozygosity

	vs A	vs C						
ERBB4		28.57%	0%	2:212566651	G	A	Other	NM_005235.2	NM_005235.2:c.1489+182C>T
RET		29.17%	3.57%	10:43595851	G	-	Other	NM_020975.4	NM_020975.4:c.74-56delG
ETV6	30.77%	92.86%	50%	92.86%	12:12022098	A	T	Other	NM_001987.4	NM_001987.4:c.464-260A>T
NF1		72.73%	100%	17:29527251	-	T	Other	NM_001042492.2	NM_001042492.2:c.889-190_889-189insT

Germline Mutation			vs A		vs C		Location		
APC	LoF	Damaging	48.81%	46.49%	46.42%	46.49%	5:112162854	T	G

Total Germline Mutation:	101	
Damaging Mutations	26	Tolerated Mutations 68

H87

Copy Number Variations

Chr	vs A	vs C
None		

Patient	Tissue/Orgs	Clinical Mutation	Type	Present?	CNV - APC	Somatic	Val1822Asp	Tyr486Ter
H87	Organoids	c.4782_4785delAGCC; p.A	frameshift	Yes			Yes, two copies	

Additional Rare APC Germline Mutations				
intron_varian	NM_000038.5:c.136-53T>C			

Somatic Mutations

	vs A	vs C						
FLT4		42.86%	5:180051228	T	-	Other	NM_182925.4	NM_182925.4:c.1422-167delA
ERG		37.5%	21:39870560	T	-	Other	NM_001136154.1	NM_001136154.1:c.40-53016delA

Loss of Heterozygosity

	vs A	vs C						
GEN1	45.45%	93.33%	2:17947623	G	A	Other	NM_182625.3	NM_182625.3:c.526-223G>A
BCL6	21.56%	6.29%	3:187443226	CTCCGCTCG	-	Other	NM_001706.4	NM_001706.4:c.1839+45_1839+61delCGGGCAGGCGAGCGGAG
ERBB3	40.74%	77.78%	12:56491880	T	G	Other	NM_001982.3	NM_001982.3:c.2616+15T>G

Germline Mutation			vs A		vs C		Location		
APC	LoF	Damaging			48.79%	46.01%	5:112176069	AGCC	-
APC	Missense	Tolerated			99.79%	100%	5:112176756	T	A

Total Germline Mutations	97		
Damaging Mutations	27	**Tolerated Mutations**	62

H89

Copy Number Variations

Chr	vs A	vs C
2 LRP1B.1/2	Deletion	
4 FBXW7	Deletion	
5 APC	Deletion	
5 CSF1R+PDGF	Duplication	
6 ROS1	Deletion	
7 HGF	Deletion	
7 MET	Deletion	
8 RAD21	Deletion	
9 JAK2	Deletion	
9 NOTCH1	Duplication	Deletion
11 ATM	Deletion	
12 KMT2D.1/2	Duplication	
13 BRCA2	Deletion	
16 TSC2	Duplication	
17 NF1/EVI2A	Deletion	
19 DOT1L	Duplication	

Patient	Tissue/Orgs	Clinical Mutation	Type	Present?	CNV - APC	Somatic	Val1822Asp	Tyr486Ter
H89	Tissue	c.3183_3187delACAAA; p.	stop	Yes	Deletion		Yes, two copi	Yes, two copies

Additional Rare APC Germline Mutations				
None				

Somatic Mutations

	vs A	vs C						
NOTCH2		63.64%	1:120611715	A	G	Other	NM_024408.3	NM_024408.3:c.73+233T>C
NPM1		40%	5:170819591	TTT	-	Other	NM_002520.6	NM_002520.6:c.353-123_353-121delTTT
GNAQ		37.5%	9:80645804	-	TG	Other	NM_002072.3	NM_002072.3:c.136+211_136+212dupCA
BLM	23.53%		15:91337178	A	-	Other	NM_000057.2	NM_000057.2:c.3020-219delA
CBLC	21.74%		19:45284852	A	G	Other	NM_012116.3	NM_012116.3:c.657+232A>G

Loss of Heterozygosity

	vs A	vs C						
PMS2	53.57%	87.5%	7:6045385	T	C	Other	NM_000535.5	NM_000535.5:c.163+138A>G
RAC1	50%	81.25%	7:6442156	C	A	Other	NM_018890.3	NM_018890.3:c.*79C>A
BCL2L1	43.75%	75%	20:30309262	G	-	Other	NM_138578.1	NM_138578.1:c.564+196delC

Germline Mutation			vs A		vs C		Location		
APC	LoF	Damaging	99.74%	99.24%	99.14%	99.24%	5:112162854	T	G
APC	LoF	Damaging	50.26%	48.9%	46.48%	48.9%	5:112174471	AAAAC	-
APC	Missense	Tolerated	99.69%	99.83%	99.8%	99.83%	5:112176756	T	A

Total Germline Mutations	108		
Damaging Mutations	30	**Tolerated Mutations**	71

H92

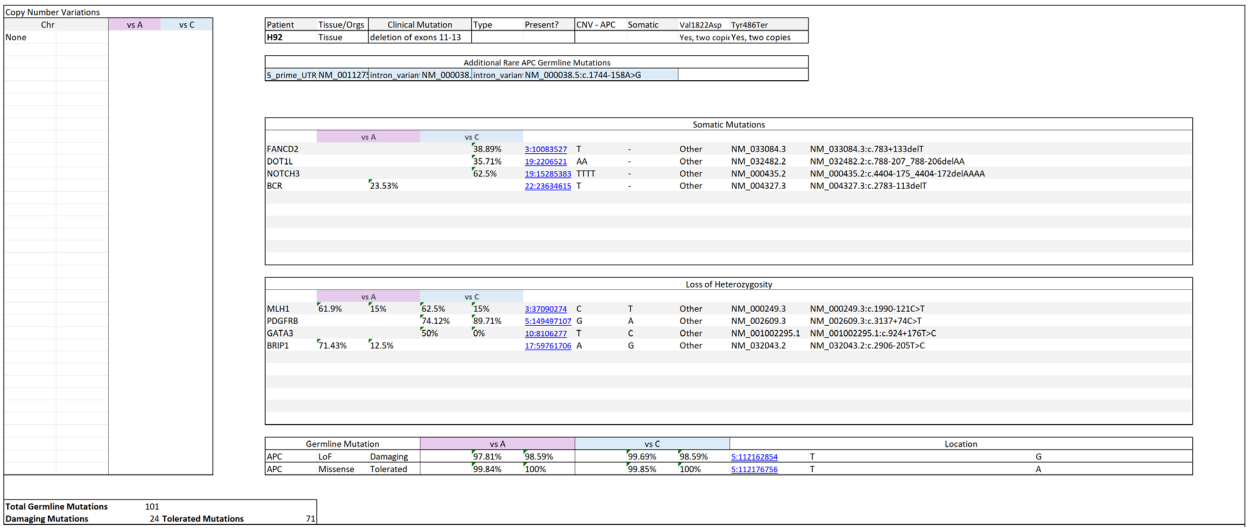

Copy Number Variations

Chr	vs A	vs C
None		

Patient	Tissue/Orgs	Clinical Mutation	Type	Present?	CNV - APC	Somatic	Val1822Asp	Tyr486Ter
H92	Tissue	deletion of exons 11-13					Yes, two copi	Yes, two copies

Additional Rare APC Germline Mutations

5_prime_UTR	NM_001127	intron_varian	NM_000038.	intron_varian

NM_000038.5:c.1744-158A>G	

Somatic Mutations

	vs A		vs C							
FANCD2			38.89%		3:10083527	T	-	Other	NM_033084.3	NM_033084.3:c.783+133delT
DOT1L			35.71%		19:2206521	AA	-	Other	NM_032482.2	NM_032482.2:c.788-207_788-206delAA
NOTCH3			62.5%		19:15285383	TTTT	-	Other	NM_000435.2	NM_000435.2:c.4404-175_4404-172delAAAA
BCR		23.53%			22:23634615	T	-	Other	NM_004327.3	NM_004327.3:c.2783-113delT

Loss of Heterozygosity

	vs A		vs C							
MLH1	61.9%	15%	62.5%	15%	3:37090274	C	T	Other	NM_000249.3	NM_000249.3:c.1990-121C>T
PDGFRB			74.12%	89.71%	5:149497107	G	A	Other	NM_002609.3	NM_002609.3:c.3137+74C>T
GATA3			50%	0%	10:8106277	T	C	Other	NM_001002295.1	NM_001002295.1:c.924+176T>C
BRIP1	71.43%	12.5%			17:59761706	A	G	Other	NM_032043.2	NM_032043.2:c.2906-205T>C

Germline Mutation			vs A		vs C		Location		
APC	LoF	Damaging	97.81%	98.59%	99.69%	98.59%	5:112162854	T	G
APC	Missense	Tolerated	99.84%	100%	99.85%	100%	5:112176756	T	A

Total Germline Mutations	101		
Damaging Mutations	24	**Tolerated Mutations**	71

H93

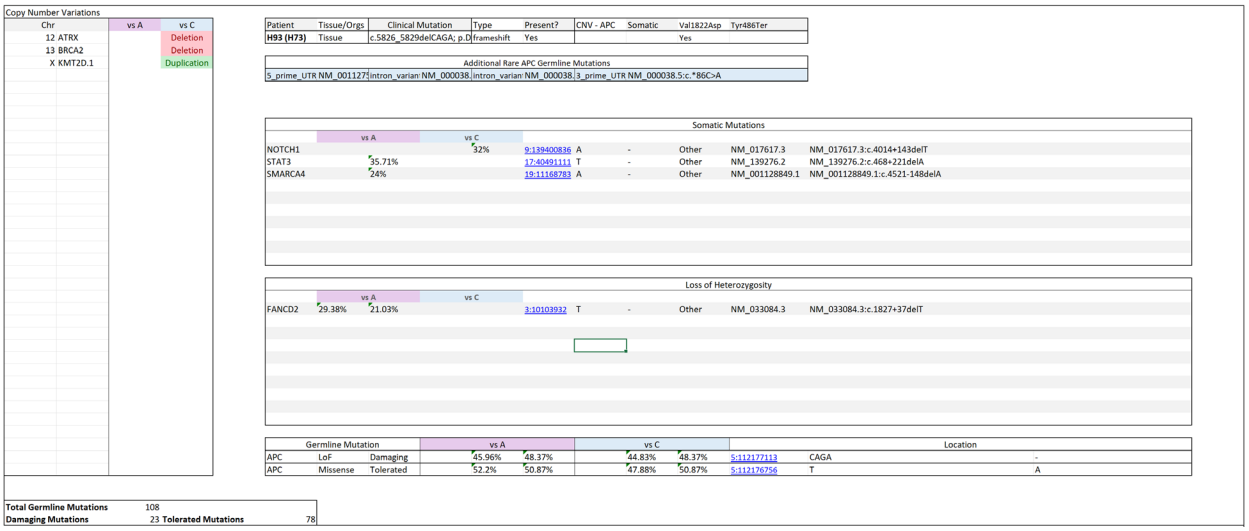

Copy Number Variations

Chr	vs A	vs C
12 ATRX		Deletion
13 BRCA2		Deletion
X KMT2D.1		Duplication

Patient	Tissue/Orgs	Clinical Mutation	Type	Present?	CNV - APC	Somatic	Val1822Asp	Tyr486Ter
H93 (H73)	Tissue	c.5826_5829delCAGA; p.D	frameshift	Yes			Yes	

Additional Rare APC Germline Mutations

5_prime_UTR	NM_001127	intron_varian	NM_000038.	intron_varian	NM_000038.	3_prime_UTR	NM_000038.5:c.*86C>A	

Somatic Mutations

	vs A		vs C							
NOTCH1			32%		9:139400836	A	-	Other	NM_017617.3	NM_017617.3:c.4014+143delT
STAT3		35.71%			17:40491111	T	-	Other	NM_139276.2	NM_139276.2:c.468+221delA
SMARCA4		24%			19:11168783	A	-	Other	NM_001128849.1	NM_001128849.1:c.4521-148delA

Loss of Heterozygosity

	vs A		vs C							
FANCD2	29.38%	21.03%			3:10103932	T	-	Other	NM_033084.3	NM_033084.3:c.1827+37delT

Germline Mutation			vs A		vs C		Location		
APC	LoF	Damaging	45.96%	48.37%	44.83%	48.37%	5:112177113	CAGA	-
APC	Missense	Tolerated	52.2%	50.87%	47.88%	50.87%	5:112176756	T	A

Total Germline Mutations	108		
Damaging Mutations	23	**Tolerated Mutations**	78

CHAPTER IV
Conclusions and Perspectives

The role of Wnt signaling in regulating the corpus epithelium has long remained unclear. The earliest studies on mouse models utilizing Wnt target gene *Lgr5* as a marker for intestinal and antral stem cells failed to identify *Lgr5*+ stem cells within the adult gastric corpus. This led to the belief that Wnt signaling may be dispensable for normal corpus epithelial turnover and homeostasis. However, we now know that chief cells are Wnt signaling cells in the corpus, and activation of Wnt signaling has been implicated in the clinical manifestation of gastric hyperproliferative disease and in tissue renewal following injury. Most studies of the gastric corpus thus far have focused on mouse models to identify the mechanisms through which various pathways, such as Wnt signaling, orchestrate gastric homeostasis. In my studies, I sought to expand upon these findings and establish a role for Wnt signaling in regulating epithelial homeostasis and disease manifestation within the human gastric corpus.

In this dissertation, I used human corpus epithelial organoids to demonstrate that Wnt signaling regulates proliferation, differentiation, and stem cell renewal. Furthermore, I show that there are regional differences in Wnt signaling between the gastric corpus and antrum that underscore the abundant yet benign manifestation of polyps in Wnt activation diseases. Throughout this chapter, I comment on some of the key findings of my studies, put them in perspective of currently published literature, and

suggest future experiments to continue investigating the role of Wnt in regulating corpus epithelial cell function.

4.1 Regional Wnt Signaling Tone

Increased Wnt sensitivity in corpus epithelial cells

One of the key findings of my studies was that patient-matched corpus and antral organoids have different thresholds for Wnt signaling to drive optimal growth (Figure 4.1). We demonstrate *in vitro* that corpus organoids from three independent patients reach optimal growth rates at a lower concentration of Wnt pathway activator CHIR99021 relative to patient-matched antral organoids. This indicates that the corpus epithelium may intrinsically be more sensitive than the antral epithelium to Wnt activation. These studies were conducted using pure epithelial organoid cultures, therefore eliminating the presence of an *in vivo* signaling microenvironment that may influence cellular identity and behavior. As a result, the findings of our studies reflect cell intrinsic qualities that are specific to the region from which the organoids are derived.

The mechanism through which the corpus epithelium has increased Wnt sensitivity remains unclear. However, this property makes sense physiologically in the context of the corpus epithelial architecture as the main proliferative compartment within the corpus is further from the high Wnt base than in the antrum or intestines. Therefore, these progenitors are likely to reside in a comparatively reduced Wnt niche, and thus may have heightened sensitivity to pathway activation.

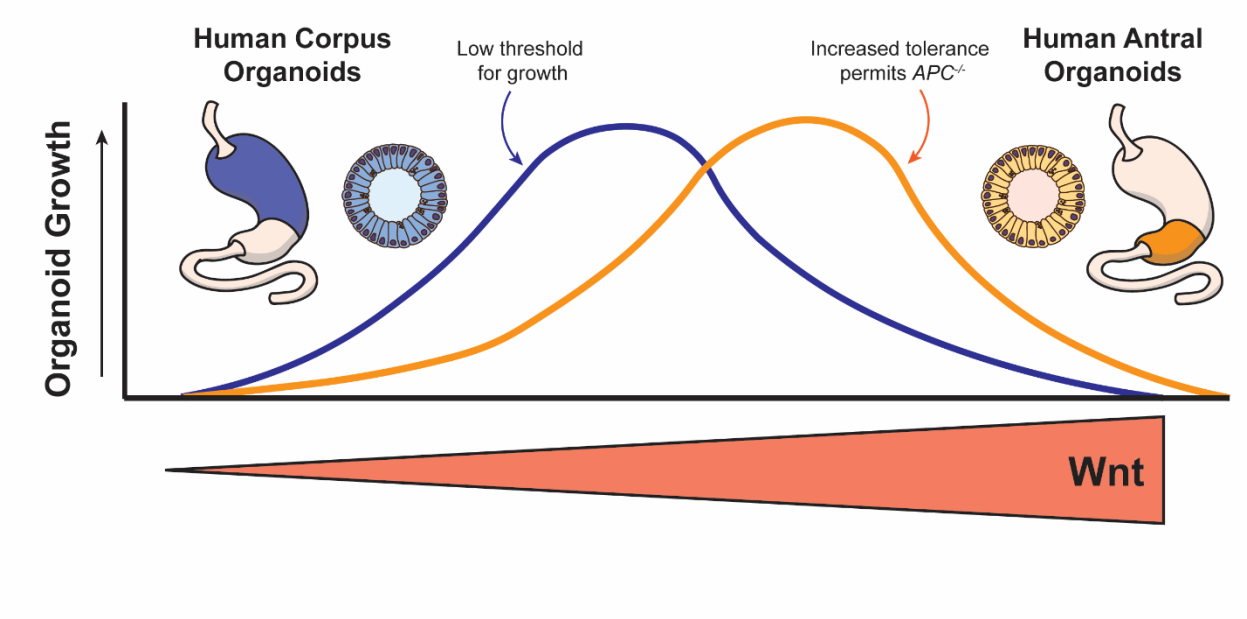

Figure 4.1: Wnt signaling sensitivity in the gastric corpus versus antrum.

Conclusions based on human organoid studies from Chapter 2. Human corpus organoids have a reduced threshold for Wnt to drive proliferation and organoid growth. Paradoxically, high levels of Wnt signaling rapidly reduces organoid corpus organoid growth. Patient-matched antral organoid growth is optimally driven by higher levels of Wnt signaling. These findings potentially translate to the manifestation of gastric disease in FAP patients as increased Wnt sensitivity may drive FGP development but not permit additional loss of *APC*. On the other hand, the increased Wnt tolerance of the antrum permits *APC* loss-of-heterozygosity and enables adenomatous change with increased potential for cancer.

One possible mechanism underscoring this is that the corpus epithelium may have elevated expression of Wnt pathway components, such as FZD receptors. Single cell studies have demonstrated that FZD proteins are expressed throughout the corpus epithelium, however expression levels between gastric regions have not been evaluated (1). FZD7 has been studied in mouse stomach to show that its expression is required for gastric tumorigenesis irrespective of *Apc* mutation status (2). RSPO ligands and their LGR receptors also play a key role in regulating Wnt signaling through preventing Wnt receptor recycling and could be involved in heightened Wnt sensitivity as well (3-5). In this regard, the Samuelson laboratory has unpublished qPCR data showing elevated expression of *Rspo* ligands in mouse corpus compared to antrum and intestine (Figure 4.2).

However, my experiments in human organoids were conducted by manipulating Wnt signaling in the absence of exogenous WNT/RSPO through use of a GSK3β inhibitor to pharmacologically induce β-catenin nuclear translocation downstream of receptor activity. As commented on in the discussion of Chapter 2, although we confirm that CHIR99021 dose-dependently activates Wnt signaling in gastric organoid cultures, we cannot rule out Wnt-independent effects of GSK3β inhibition within other pathways such as glycogen synthase or NFκB. Despite this, CHIR99021 has been extensively used as an activator of Wnt signaling in *in vitro* models within dose ranges similar to the ones described within my study. Furthermore, our observations align with current literature regarding Wnt-dependent regulation of differentiation and growth, therefore providing confidence that Wnt is the primary force influencing cellular changes within our system. While the use of exogenous WNT and RSPO ligands would be another

approach to test Wnt sensitivity, the interplay between WNT and RSPO ligands in regulating Wnt tone has been poorly explored and would lead to potentially confounding variables in describing a dose-response. Furthermore, as *APC* mutations inflict cell-intrinsic changes to Wnt pathway activation, it becomes appropriate to utilize a cell-intrinsic mechanism of pathway activation to explore regional responses.

The results of my studies using CHIR99021 suggest that regional differences in Wnt sensitivity are driven by intrinsic Wnt tone. Therefore, while we cannot rule out FZD, RSPO, or LGRs as a contributing factor *in vivo*, our results demonstrate that increased Wnt sensitivity occurs independent of receptor activity and instead reflects a different mechanism of cell intrinsic regulation. This could include potential changes to APC expression, such as epigenetic transcriptional regulation, or in various additional elements of the Wnt signaling pathway such as regulation of β-catenin.

Beyond Wnt signaling, β-catenin has additional functions at adherens junctions, where it interacts with α-catenin to modulate the actin cytoskeleton, and the centrosome (72). Therefore, free β-catenin is regulated by these interactions as well as the interplay between transcription, synthesis, and destruction complex activity. It is plausible that cell-specific differences in β-catenin regulation through any of these mechanisms could impact intrinsic Wnt sensitivity.

Within the nucleus, β-catenin relies on interactions with TCF/Lef as well as various transcriptional co-activators to RNA polymerase II, such as CBP, SWI, MED12, and Paf-1, to drive Wnt target gene expression (72, 73). Therefore, sensitivity to Wnt signaling may also be conferred through expression of these terminal regulators of β-catenin function. Future studies exploring cell-specific Wnt sensitivity could focus on

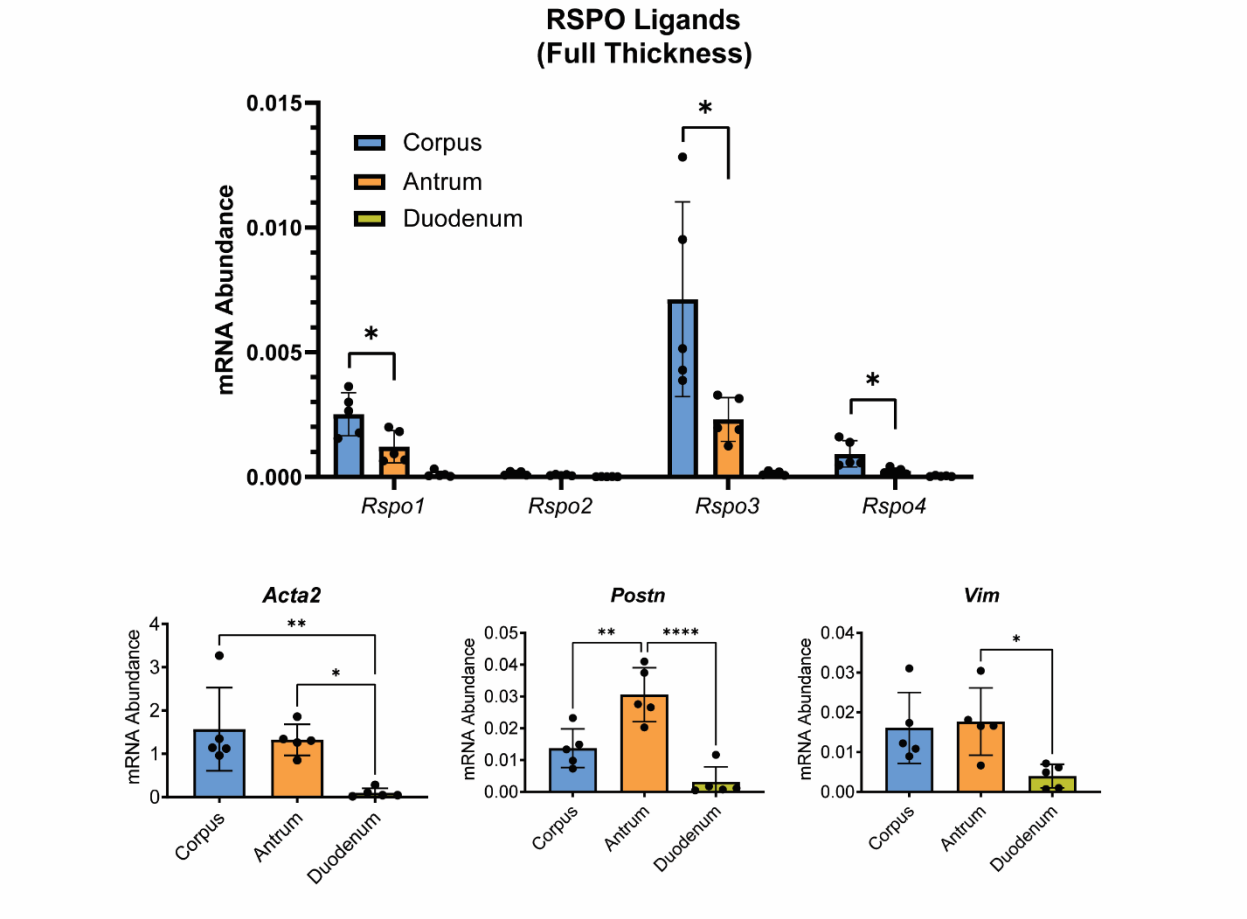

Figure 4.2: Expression of *Rspo1-4* in full thickness mouse gastric tissue.

mRNA expression of *Rspo1-4* from full thickness wild-type mouse corpus, antrum, and duodenum demonstrates enhanced expression of *Rspo1*, *3*, and *4* in the corpus potentially underscoring a high Wnt signaling environment. Stromal markers *Acta2*, *Postn*, and *Vim* are similar within the corpus and antrum, thus indicating that *Rspo* expression is enhanced within consistent populations of cells.

these various mechanisms of downstream β-catenin regulation by exploring how pathway activation drives nuclear import, and by analyzing nuclear β-catenin affinity for transcriptional regulators to drive target gene expression.

Fundic gland polyp emergence and the 'Just-Right' Hypothesis

The differences in Wnt signaling tone between the corpus and antrum likely relate to the regional patterns of disease manifestation to increased Wnt signaling tone within the stomach. Fundic gland polyps in FAP patients appear predominately within the corpus of the stomach while the antrum remains spared. Importantly, the rare antral polyps that do emerge typically harbor adenomatous change, indicating a more severe mutational background (such as *APC* loss-of-heterozygosity) and increased cancer potential. Notably, the rarity of antral polyps coupled with their potential pathological significance limited our access to FAP antral tissue samples to address this question.

My studies showed that despite increased expression of Wnt target genes in primary FGP-derived biopsies, *APC* mutations leading to loss-of-heterozygosity are infrequent and not-required for their emergence. Altogether, my observations from Chapter 2 and 3 suggest that the increased Wnt sensitivity within the corpus may predispose epithelial cells to hyperproliferation in the presence of minor signaling increases. Therefore, a heterozygous *APC* genotype, as is inherited by FAP patients, would prime the cells to more easily drive optimal growth within the corpus and lead to the abundant nature of FGPs while sparing the antrum.

While increased Wnt sensitivity of the corpus epithelium may enable abundant polyp formation, an important question remains as to why FGPs don't develop loss-of-

heterozygosity to further drive proliferation and eventually cancer. Our studies demonstrate that Wnt tone within organoids is regulated by cell intrinsic qualities (the mutational status of cells) and extrinsic qualities (the signaling environment). Previous studies have explored Wnt tone throughout the small intestine and colon and concluded that regional signaling environments may underscore patterns of *APC*-related cancer in mice and humans (6-10). While no previous studies have analyzed Wnt tone in the corpus versus the antrum, there is some evidence that suggests the corpus mucosa is a high Wnt signaling environment.

Wnt signaling is essential during corpus development, and suppression of the canonical signaling pathway leads to antral tissue specification rather than corpus (11). Additionally, studies generating corpus organoids from pluripotent stem cells demonstrated that increased Wnt signaling through the addition of CHIR99021 was necessary to drive corpus specification over an antral phenotype (11, 12). In further support of an elevated Wnt signaling environment within the corpus, unpublished data from our lab showed that expression of *Rspo1* and *Rspo3* is significantly higher in full thickness mouse corpus tissue relative to the antrum and duodenum (Figure 4.2). Stromal markers of cells which release RSPOs, such as *POSTN*, *ACTA2*, and *VIM*, were similar between the corpus and antrum, therefore indicating elevated expression within consistent populations of cells. Altogether, this suggests that high Wnt signaling may be a characteristic of the corpus and could define regionality in Wnt tone and polyp etiology within the stomach.

In Chapter 3, I demonstrate that polyp organoids with elevated intrinsic Wnt signaling are averse to further upregulation of the pathway through either the presence

of exogenous Wnt or through the addition of Wnt pathway activator CHIR99021. A high Wnt signaling environment within the corpus mucosa would therefore contextualize the clinical manifestation of FGPs in FAP patients in line with the 'just-right' hypothesis. *APC* loss-of-heterozygosity within the corpus may not be tolerated as the combination of extrinsic and intrinsic Wnt tone would activate the pathway beyond a tolerable threshold. We observed this in adult mice, where corpus cells with homozygous deletion of *Apc* are lost by one-month post-recombination (Figure 3.11). This is further supported by published mouse studies using *PgcCreER^{T2}* and *Mist1CreER^{T2}* drivers to conditionally delete *Apc* failing to drive corpus hyperplasia unless combined with additional oncogenic mutation (13, 14). On the contrary, in the antrum, homozygous deletion of *Apc* is tolerated, and these cells hyperproliferate to rapidly drive tumorigenesis.

These observations further align with the benign phenotype of FGPs noted within FAP patients. FAP patients have an effective 100% chance of developing colorectal cancer within their lifetime (15-17). This is often triggered by a somatic second hit mutation to *APC* followed by a mutational cascade leading to adenocarcinoma ((18). On the other hand, despite the abundance of FGPs in some patients, gastric cancer, although elevated, is still rare in FAP patients with only a lifetime risk of 0.5-1.3% (19, 20). Furthermore, while low-grade dysplasia is common in APC-associated FGPs, high grade dysplasia and adenomatous change are unlikely, indicating a lack of disease progression (21).

Our findings suggest that this benign nature may be due to second-hit somatic *APC* mutations generally not being tolerated within the corpus. Studies in the colon

have demonstrated that loss of *APC* leads to chromosomal instability and predisposes cells to additional mutation (22). By not tolerating complete *APC* loss, FGPs would therefore not be predisposed to the same level of additional mutational challenge which may enable progression to cancer. Our sequencing data supports this notion as analysis of somatic mutation and copy number variation across all assayed cancer-related genes demonstrated that most polyps were genetically similar to non-polyp regions. The one polyp that did have an *APC* somatic mutation (H85) had 160 copy-number variations detected, by far the most in the data set, as well as a somatic mutation to *NF1*, which is commonly associated with cancer (23) (Table 3.1).

Overall, my studies propose a relationship between Wnt signaling and the corpus epithelium to define the etiology of FGP formation in FAP patients (Figure 4.3). Increased Wnt sensitivity in corpus cells enables abundant polyp formation without a requirement for *APC* loss-of-heterozygosity. However, increased intrinsic sensitivity, and potentially an increased extrinsic signaling environment, reduces the tolerance of corpus cells to further upregulation of the pathway. Therefore, *APC* loss-of-heterozygosity somatic mutations are infrequent as those cells will not contribute to renewal or are lost. This also likely limits the viability of cells with carcinogenic mutations within FGPs to maintain their benign nature. On the contrary, the antrum does permit *APC* loss-of-heterozygosity and leads to rarer polyps with a higher risk for cancer.

Future Studies

Future studies on the physiologic differences in Wnt tone between the corpus and antrum could focus more precisely on the consequences of Wnt activation within a

specific cell. This could be accomplished in mice through lineage tracing cells with homozygous or heterozygous deletion. These models would also help identify the cell-of-origin for FGP emergence and determine which cells primarily respond to *Apc* loss to drive hyperproliferation.

Unfortunately, no good mouse models to study *APC*-associated FGPs exist. While we demonstrate that an *Apc* heterozygous deletion drives increased proliferation, we don't observe cystically dilated glands within the corpus. Powell et al. demonstrated that an *Lrig1CreER^{T2}; Apc$^{fl/+}$* mouse model exhibits corpus hyperplasia, but the histological images they show don't appear to demonstrate features of FGPs either (24). It is possible that the inability of *Apc*-deficient mouse models to demonstrate FGP-like features could be due to the different thresholds of Wnt sensitivity between the human and mouse stomach. In Wnt activation mouse models, such as conditional deletion of *Apc*, the predominant disease burden occurs within the small intestine. However, FAP patients rarely develop small intestinal lesions, thus demonstrating species-specific regional differences in Wnt tone and the required 'just-right' levels of signaling to induce hyperproliferation (10). This concept may also pattern differences between the human and mouse stomach and limit the ability for genetic models to faithfully recapitulate a human clinical phenotype.

To analyze this concept, the CHIR growth experiments discussed within Chapter 2 could be repeated to compare human and mouse corpus organoids. Furthermore, mouse

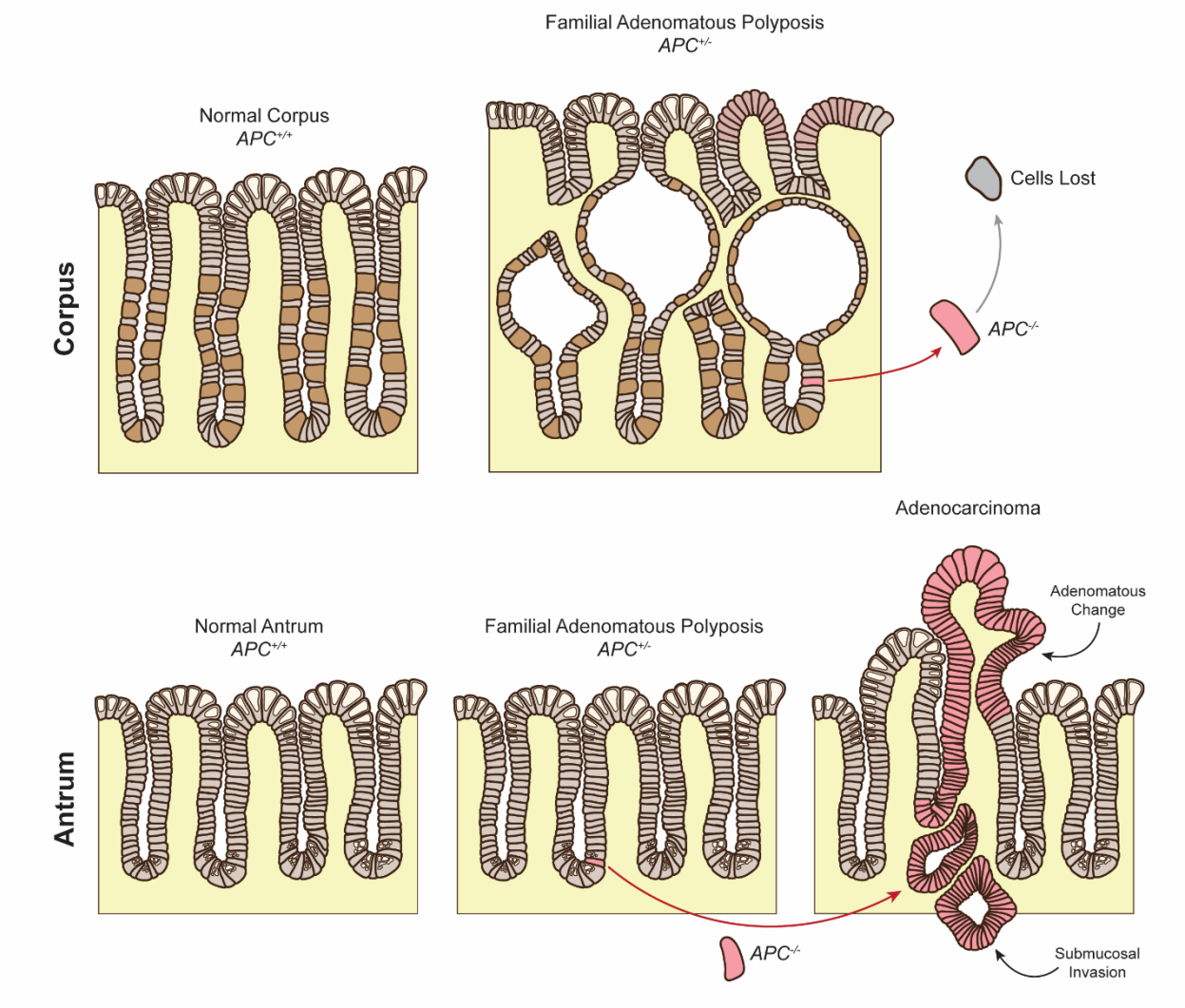

Figure 4.3: Manifestation of gastric disease by APC genotype.

Proposed model of disease manifestation within gastric tissue arising from heterozygous or homozygous loss of *APC*. In the corpus, heterozygous loss of *APC* (the FAP condition) permits increased proliferation and leads to FGPs with a potential for low grade dysplasia, but low risk for progression to cancer. Cells which lose the second *APC* allele following somatic alteration are lost as the corpus epithelium does not tolerate that level of Wnt upregulation. In the antrum, heterozygous loss of *APC* does not lead to any major phenotypic change. However, second-hit mutations to *APC* are tolerated and drive adenomatous change leading the formation of adenocarcinoma.

studies could be readily expanded to observe organoids derived from the intestines as well to assess Wnt tone across the entirety of the gastrointestinal tract. However, as previously mentioned, these experiments only analyze cell-intrinsic Wnt sensitivity and are unable to assay differences in the signaling microenvironment that may also contribute to regional signaling tone.

One mouse model that does demonstrate an FGP-like phenotype are *H/K ATPase*-deficient mice (25, 26). While the mechanism of FGP formation in these mice was not clarified in these studies, it was proposed that glandular cysts form due to a build-up of glandular secretions caused by blockage of glandular outflow by eosinophilic granules likely derived from anucleated parietal cells. These mice, or models with similar functionality, could be utilized alongside lineage tracing models and/or Wnt activation models to determine how FGPs develop on a cellular level. For example, $Apc^{\Delta/+}$ mice could be given a proton-pump inhibitor or DMP-777 to mimic *H/K ATPase* loss and determine if this converts hyperplasia into a FGP phenotype.

Furthermore, to test the hypothesis that a high Wnt signaling environment precludes acquisition of *APC* loss-of-heterozygosity within the corpus, *Apc*-KO studies could be done in combination with WNT or RSPO inhibition/deletion. Our studies suggest that cells with complete *APC* loss may be retained in the corpus epithelium within a reduced Wnt environment and could potentially contribute to the formation of neoplasia.

4.2 Wnt Regulation of Isthmus Progenitors

Early studies of the gastric corpus epithelium observed a bidirectional pattern of differentiation originating from the undifferentiated isthmus progenitors (27). Investigating the pathways regulating this outflow is critical to understanding mechanisms of gastric disease affecting epithelial cell census, such as atrophic gastritis, *H pylori* infection, and cancer. We demonstrated using human organoids that Wnt signaling plays a key role in directing cell fate (Figure 4.4). While low Wnt signaling induces surface cell differentiation, activation of the pathway leads to the establishment of deep glandular neck and chief cells. While it has been demonstrated that Wnt signaling regulates the chief cell compartment *in vivo* as well, the specific consequences of Wnt activation within an isthmus progenitor remain unclear.

Isthmus corpus progenitors in mice and humans don't express known Wnt target genes and don't appear to have a proliferative response to either *Rspo3* knockout or knock-in in *Myh11*+ cells at the gland base (28). However, unpublished data from the Samuelson laboratory shows that acute inhibition of Wnt signaling in adult mice using the PORCN inhibitor C59 reduces isthmus proliferation, suggesting that isthmus progenitors are regulated by Wnt. The studies detailed in this thesis, as well as from other published work, clearly demonstrate that Wnt signaling plays a key role in fate determination *in vitro*. Furthermore, our organoid growth studies indicate that corpus proliferation, which primarily occurs within the isthmus compartment *in vivo*, is Wnt dependent. Finally, my studies in mouse transgenic models showed that corpus progenitors are sensitive to moderate but not high increases in intrinsic Wnt signaling, with increased proliferation observed in *Apc+/-* but not *Apc-/-* stomach (Figure 3.11).

Therefore, it is likely that isthmus progenitors are regulated by Wnt in the adult stomach; however, this may occur through a different mechanism, signaling threshold, or receptor apparatus than in active stem cells of the antrum and intestines.

Potential mechanism for isthmus cell response to Wnt

While LGR5 has long been considered the major RSPO receptor modulating Wnt signaling in stem cells of the gastrointestinal tract, recent studies in mice have implicated LGR4 as another key receptor in homeostasis and injury. These studies showed that LGR4 labeled a broad category of antral cells including base mucous cells, isthmus cells, and mature pit cells (5). Interestingly, *Lgr4*+/*Lgr5*- cells of the antrum appear to be rapidly cycling and more sensitive to RSPO3-induced proliferation following pathologic induction of RSPO3 with *H pylori* infection (29). Thus, Wnt signaling can regulate proliferation and stemness within cells outside of the traditional *Lgr5*+ stem cell pool.

While these studies were focused on the antrum, the role of LGR4 in regulating Wnt within the corpus remains unexplored. It is plausible that isthmus progenitors of the corpus also respond to RSPO in an LGR4-dependent manner. scRNAseq studies of the murine corpus demonstrated expression of *Lgr4* within surface cells and co-localized expression with *Stmn1*+ isthmus cells (30). Human single cell RNAseq studies have confirmed a similar expression pattern as in mice by localizing *LGR4* primarily to isthmus and surface cells throughout the stomach (1). However, this study combined corpus and antral epithelial cells for their analysis, so it is unknown how LGR4 expression is specifically patterned within the human corpus. A potential future

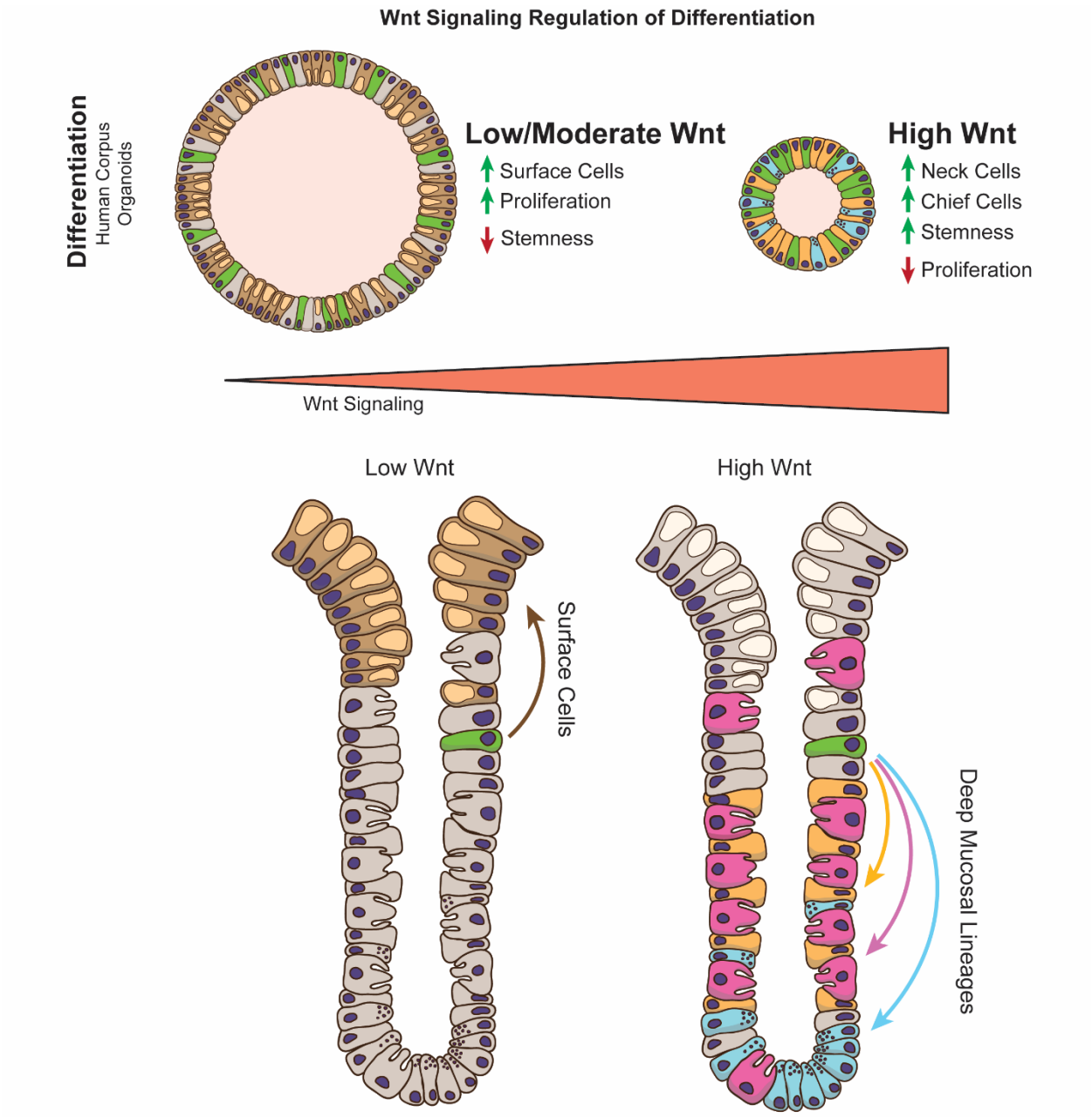

Figure 4.4: Wnt signaling regulation of differentiation

Proposed model of Wnt signaling regulation of differentiation in the human gastric corpus. In organoids, low Wnt signaling induces surface cell differentiation along with high rates of turnover driving organoid growth. High levels of Wnt signaling induce deep glandular neck, parietal, and chief cell differentiation, reduce cell turnover, but increase progenitor potential (stemness). This would suggest that *in vivo*, Wnt signaling directs the bimodal axis of differentiation towards either surface cells or deep glandular lineages.

approach to test the role of LGR4 in the stomach would be to analyze the consequences of gene knockout within the mouse corpus using a *Stmn1-CreER*^{T2} driver along with the published *Lgr4*$^{fl/fl}$ mouse model (29). If the RSPO-LGR4 axis is essential to regulating isthmus progenitor cells, then I would expect loss of LGR4 to lead to reduced proliferation and preferential lineage tracing towards surface cells. Importantly, *Lgr4-cKO* cells may only be transiently maintained within the epithelium as these cells would potential differentiate towards surface cells and be turned over after a few days. Therefore, early lineage tracing would be essential to defining this mechanism of regulation.

Additional future experiments could focus on lineage tracing isthmus cells following either Wnt activation or depletion in vivo to determine the role of Wnt in regulating this proliferative compartment. However, lineage tracing studies from isthmus progenitors in the corpus have long been difficult as there are no distinct markers for this population. While *Sox2*, *Runx1*, *Lrig1*, and *Bmi1* have all been localized to cells with progenitor potential, none of these markers appear to be faithful to an undifferentiated isthmus cell type (1, 31-34). A recent study however has identified *Stmn1* as a cellular marker distinctly labeling proliferating cells of the isthmus, and its expression has been confirmed within single cell studies in mice and humans (35). Wnt activation studies using this new mouse model could provide novel insights into isthmus cell response to Wnt signaling and determine whether the patterns of differentiation we observe *in vitro* are observed *in vivo*.

Opportunities for single cell studies

A limitation of our human organoid studies is that our findings focus on wholistic changes in cell identity and behavior but do not account for cell specific changes. Organoids lack compartmentalization as they are suspended within a 3D pro-proliferative environment, so morphological changes provide less understanding than *in vivo*. While immunohistochemistry can provide insight into the presence of various differentiated lineages, this only provides a snapshot of activity and identity. mRNA analysis can also demonstrate changes in identity and overall expression profile but cannot determine the precise quantity or status of cell types within our human organoids. This is especially true for undifferentiated progenitors within organoids as few markers exist for them. Therefore, although we can assay for markers of isthmus cells such as *STMN1*, we cannot confirm that the progenitor cells within our organoids are similar to the isthmus progenitors *in vivo*.

Single cell RNAseq could be a powerful tool to further study the cellular identity of our organoids. This would enable us to confirm the identity of each differentiated cell type compared to published *in vivo* data, and also track how cell identity changes as a result of increased Wnt signaling. This would be especially insightful to determine how Wnt influences cell fate. Bioinformatic velocity analysis would help understand lineage relationships between different cells types and analysis of different time points could demonstrate how differentiated lineages arise over time.

Single cell studies could also help determine the progenitor potential of various cell types within our corpus organoids. We showed that single cells derived from high Wnt organoids establish new organoids at an increased efficiency (Figure 2.7). This

finding indicates that high Wnt induced increased stemness and progenitor potential within our deep glandular cell enriched organoids. However, we were not able to determine which cells were primarily responsible for establishing new organoids. Undifferentiated isthmus progenitor-like cells are a likely source as progenitors in the intestine have the highest rates of organoid formation efficiency. However, chief cells have also been demonstrated to contain organoid formation potential and can establish organoids comprised of all differentiated lineages (36).

Single cell lineage tracing studies could be conducted to determine which cells are primarily responsible for this formation potential. These studies might be more suited for mouse organoids as genetic labeling techniques, such as with a GFP reporter (e.g. *Gif-GFP*), could label cells *in vitro*. Labeled cells from high Wnt organoids could be sorted and replated to determine the formation potential of each specific cell type following growth in various Wnt conditions. Mature organoids derived from these cells could also be measured for differentiation to assay how specific cell types may contribute to reconstituting various differentiated lineages upon return to a moderate Wnt environment.

In human organoids, such experiments would be more difficult as cells wouldn't be able to be labeled genetically unless they were virally transfected or genetically engineered via CRISPR/Cas9, which has been effectively demonstrated within human organoids (37). These techniques could enable cellular barcoding, which is a method to genetically label individual cells with unique nucleic acid sequences and lineage trace cells over time (38). The use of barcoding would then utilize single cell sequencing to construct fate maps and determine how lineages arose over time. Still, that technique

would occur downstream of initial seeding, and would not be able to identify the specifics of the initial plated cell. The use of a constitutive Cre driver, such as *PGC-CreER^{T2}*, could label cells that were at one point mature chief cells. Further, a fluorescent marker, such as *PGC-GFP*, could also be inserted via CRISPR techniques to label a specific population of differentiated cells. Labeled cells could then be sorted to determine how each population contributes to maintenance and differentiation within organoid cultures. Additional sorting strategies utilizing cell antigens, such as from the cluster of differentiation (CD) group, could also help differentiate the various groups. Single cell sequencing would thus be a powerful tool to use in combination to determine the most representative markers for sorting surface, isthmus, neck, and chief cells.

4.3 Wnt Regulation of Chief Cells

Chief cells being the predominant Wnt signaling cell within the corpus epithelium is a conundrum. Throughout the antrum, small intestine, and colon, cells expressing Wnt target genes are typically active progenitors undergoing regular turnover to renew differentiated lineages (5, 39, 40). Chief cells, on the other hand, are quiescent during homeostasis and only undergo rare instances of turnover. However, in response to injury, chief cells can dedifferentiate and give rise to metaplastic cell lineages, thus demonstrating their innate progenitor potential (28, 41-44). It has been unclear how Wnt directs chief cell differentiation and maintenance, as well as whether Wnt regulates their progenitor potential.

Traditionally it has been believed that chief cells primarily arise from transdifferentiating mucous neck cells. This would connect the chief cell pool to the isthmus compartment and establish a continual outflow of cells originating from isthmus progenitors. Following our studies, this would suggest activation of Wnt signaling as a key signal leading to the fate decision of an isthmus progenitor to a neck and then chief cell. Few studies have been successful in demonstrating this concept *in vivo* as Wnt activation models in the corpus typically fail to demonstrate phenotypic changes. Recently, Fischer et al. showed in mice that *Rspo3* expression by *Myh11*+ cells at the base of glands regulates the chief cell compartment (45). Overexpression of *Rspo3* in transgenic mice led to a significant expansion of the *Gif*+ chief cell compartment, while knock-out reduced the number of *Gif*+ chief cells. This aligns with our *in vitro* findings where we demonstrated that subjecting organoids to high levels of Wnt signaling led to a chief cell phenotype through significantly increased expression of *LIPF*, *PGC*, and *TNFRSF19*, which itself is a Wnt target gene. Overall, this establishes that Wnt signaling regulates the chief cell compartment at the base of glands. However, neither our study nor the study by Fischer et al. define where chief cells arise from in the presence of increased Wnt signaling.

Recent studies have suggested that the gastric corpus epithelium is comprised of two distinct self-renewing compartments with only minor overlap (35, 46). While isthmus progenitors definitively give rise to surface, neck, and parietal cells, chief cells may self-maintain at the base of glands. Although this remains controversial, it would establish a new paradigm for how epithelial renewal occurs within the corpus epithelium. Adding lineage tracing to the Fischer et al. *Rspo3* expression experiments could help determine

whether the expanded chief cell compartment arises from isthmus progenitors or from chief cells themselves (Figure 4.5). It would furthermore be interesting to determine whether loss of Wnt signaling causes chief cells to differentiate *in vivo*, as is suggested by our organoid experiments where high Wnt organoids passaged into low Wnt conditions had restored patterns of differentiation.

Wnt regulation of chief cell proliferation and stemness

The identity of chief cells as a quiescent differentiated cell with high Wnt target gene expression potentially ties into the role of Wnt signaling in regulating stemness and proliferation throughout the gastrointestinal tract. While *LGR5*+ cells are the source of renewal within the antrum and intestines, the highest rates of proliferation occur within transit amplifying cells which exist just outside of the base region (Figure 4.6). Therefore, a high proliferative index appears to be conferred by transitioning from a high to a lower Wnt environment. This has previously been demonstrated in the intestine *in vivo* where loss of Wnt signaling leads to a burst of proliferation as stem cells enter a transit amplifying phenotype (47). However, this is rapidly followed by deterioration of the crypt stem cell compartment and epithelial collapse as cells with proliferative potential are lost. Anecdotally, I have also observed that removal of WNT/RSPO from culture media leads to rapid yet short-lived growth of organoids.

These observations align with the findings described in Chapter 2 where I show that in human corpus organoids high Wnt signaling induces low proliferation rate and slow organoid growth (Figure 2.2, 2.3). Instead, the maximal proliferation occurred in organoids maintained within low to moderate Wnt conditions. However, surprisingly,

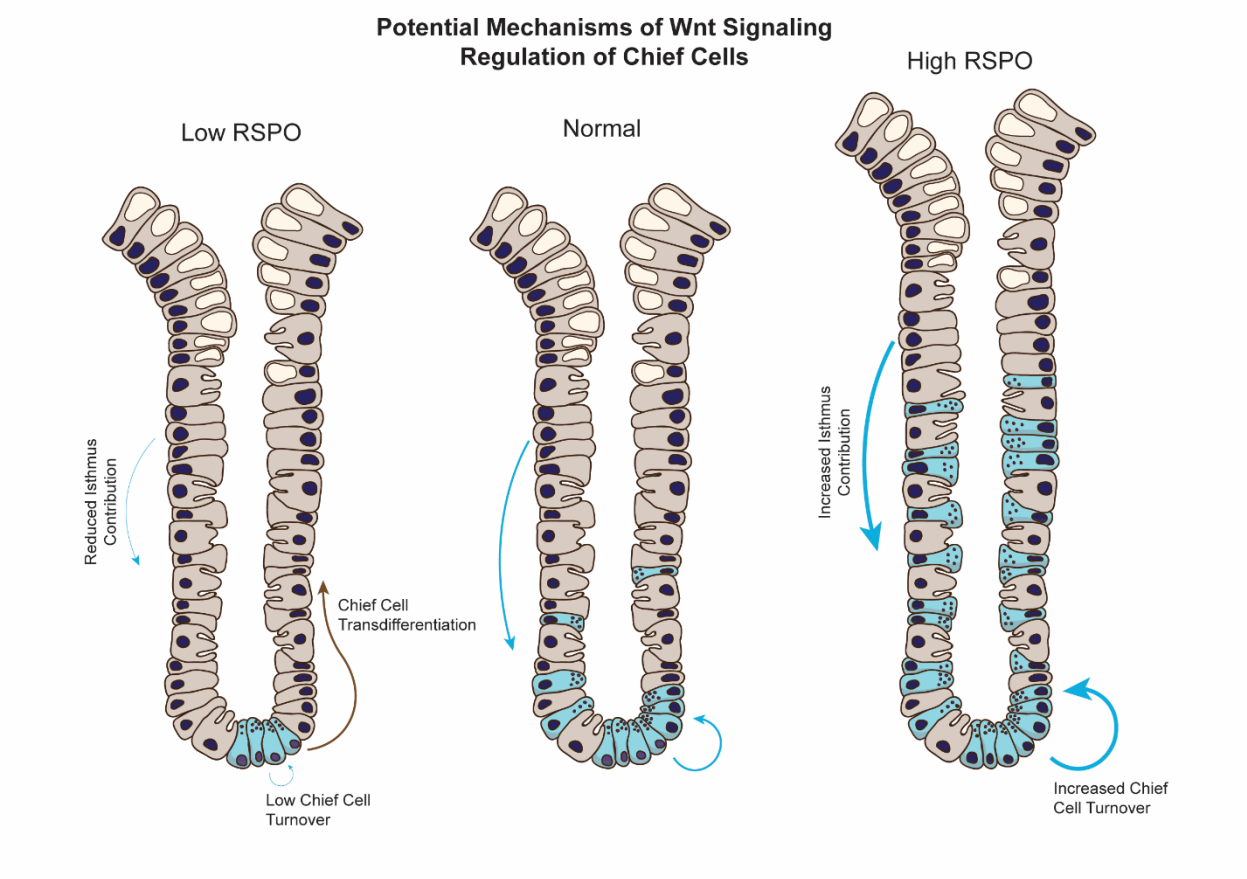

Figure 4.5: Potential mechanisms of Wnt regulation of chief cells

Wnt signaling has been demonstrated to regulate the chief cell compartment within mice through *RSPO3*-deletion or overexpression (45). Low of chief cells in a low WNT/RSPO environment may be due to a reduced contribution from isthmus progenitor cells or a reduced rate of chief cell self-renewal at the gland base. The expanded chief cell compartment following RSPO3 overexpression may be due to increased differentiation arising from isthmus progenitors or increased chief cell self-renewal.

single cells derived from high Wnt organoids established new organoids at enhanced rates (Figure 2.7). Altogether, these findings suggest that Wnt signaling is primarily responsible for inducing stemness and proliferative potential within a cell but does not necessarily drive active proliferation. A few studies have suggested a similar relationship between high Wnt signaling and reduced proliferation *in vivo*. In the antrum and intestine, overexpression of R-spondin ligands leads to *Lgr5*+ stem cells becoming lineage trapped at the gland/crypt base (5, 48). In the intestinal study, Yan et al. conversely demonstrate that LGR5 ECD treatment, which inhibits Wnt signaling by ectopically trapping RSPO ligands, leads to premature lineage tracing of *LGR5*+ cells, indicating that loss of Wnt induced proliferation and an exit from a stem cell state (48). Therefore, in multiple independent contexts, high levels of Wnt signaling induced by high levels of RSPO leads to a quiescent stem cell population, while loss of Wnt signaling causes stem cells to actively proliferate and lose their stemness. It is possible that this mechanism exists to preserve stem cells pools within the mucosal base, although no studies have explored this concept.

In the corpus, *LGR5*+ chief cells appear to follow a similar pattern of lineage trapping with high extrinsic Wnt. My studies suggest that Wnt signaling may be responsible for this patterning as high Wnt, low proliferating organoids are enriched for chief cells. This was also demonstrated by the aforementioned Fischer et al. study where high Wnt signaling leads to an enlarged chief cell compartment at the gland base *in vivo* (28). To maintain the presence of quiescent cells at the base of glands where active progenitors typically reside, the corpus mucosa would have to be a high Wnt signaling environment. As previously discussed, there is evidence for high Wnt signaling

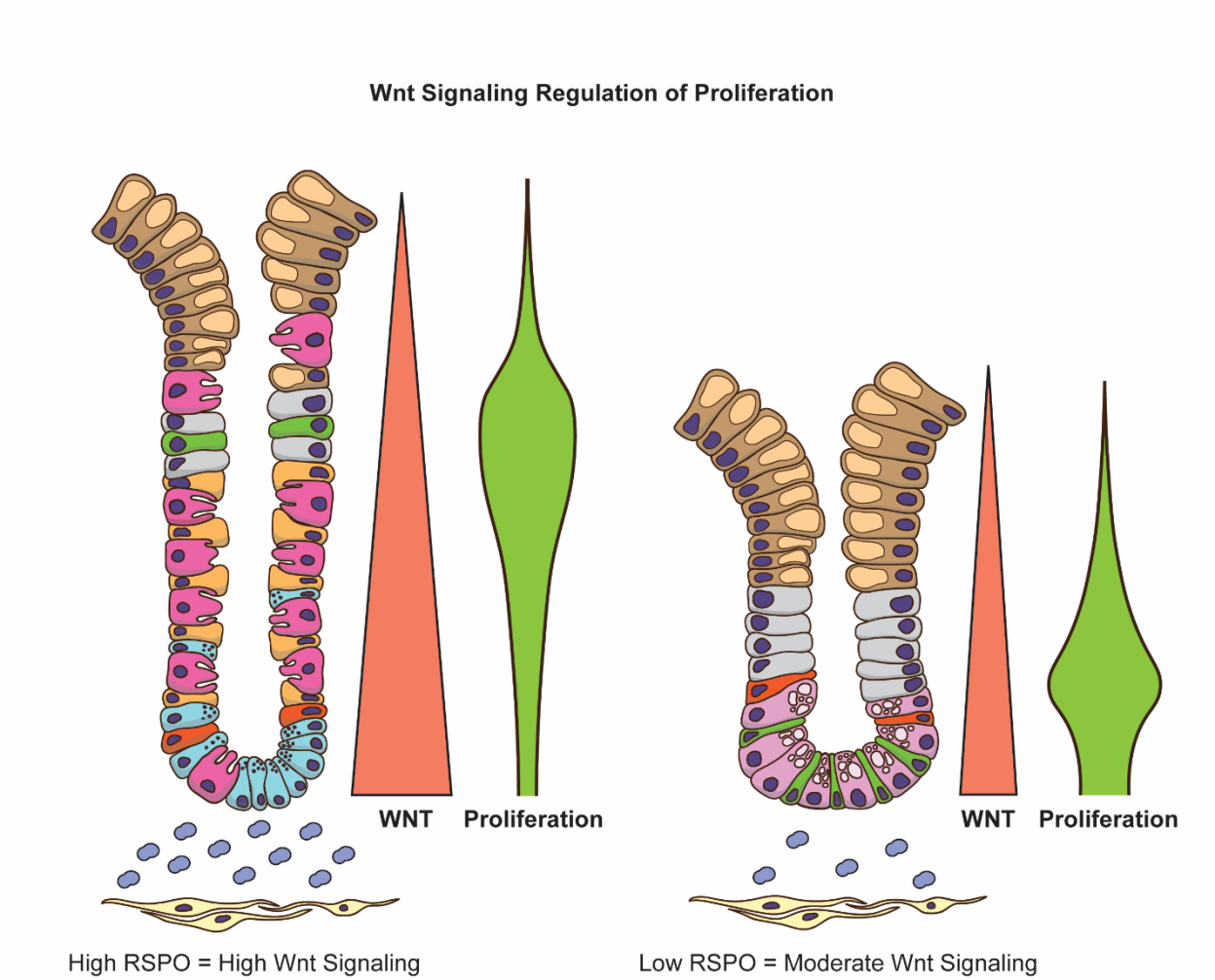

Figure 4.6: Wnt signaling regulation of epithelial zones of proliferation

The corpus and antrum epithelium have defined Wnt signaling gradients constructed by *RSPO3* expression by stromal cells at the base of glands. The highest rates of proliferation within each compartment do not align with the highest level of Wnt signaling; rather, proliferation is greatest in transit isthmus progenitors of the corpus and transit amplifying cells of the antrum within transition zone between high and low Wnt tone. High expression of RSPO within the corpus could underscore the enlarged, quiescent base compartment relative to the antrum where RSPO expression is lower.

within the corpus as the murine corpus has high expression of *Rspo1* and *Rspo3* ligands relative to more distal regions of the GI tract, and with the observation that corpus specification requires enhanced Wnt/β-catenin signaling (11, 12). Thus, increased Wnt signaling may induce the chief cell trapping at the gland base while retaining their progenitor potential.

As an alternative hypothesis, chief cells may possess unique qualities relative to other progenitor cells which enable them to maintain quiescence in a high Wnt environment. A recent study has identified the G1-S cell cycle regulator $p57^{kip2}$ (CDKN1C) as a key protein inducing cell cycle arrest within chief cells during homeostasis (49). Lee et al. demonstrate that upon gastric injury, p57 loss enables chief cells to re-enter the cell cycle. On the other hand, overexpression of *p57* maintains chief cell cycle arrest and prevents this action. Organoid studies demonstrated that p57 is distinctly suited to regulate progenitor cell potential, as overexpression of other cell cycle inhibitors, including p16, p19, p21, and p28 led to poor stem cell maintenance, differentiation, or even organoid death (49). Altogether, these findings suggest that chief cells are maintained in a primed, G1 cell cycle state through induction of p57 during homeostasis, which allows them to respond rapidly to activate proliferation upon tissue injury.

A similar mechanism of cell cycle regulation by p57 is observed within the hematopoietic stem cell (HSC) system. Wnt dose-dependently regulates HSC identity, and p57 has been shown to be essential to maintain stemness (50-53). Furthermore, p57 has recently been demonstrated to be expressed in mice within *Bmi1*+ facultative stem cells of the intestinal crypt (54). Therefore, p57 expression may be a conserved

mechanism to maintain quiescence within pro-proliferative environments, and thus enables cells to maintain progenitor potential as a differentiated cell type through inducing cell cycle arrest at the G1 checkpoint.

We observed that activation of Wnt signaling induces a similar phenotype of quiescence within human corpus organoids. Activation of Wnt signaling dose-dependently induced G1 cell cycle arrest, leading to lower rates of proliferation while maintaining progenitor potential (Figure 2.7). Furthermore, *CDKN1C* expression was upregulated in high Wnt organoids, therefore proposing a mechanism through which G1 arrest occurred. However, it is unknown whether Wnt signaling directly regulates *CDKN1C* or if this is a consequence of altered differentiation towards chief cells which specifically express this protein. Future studies could focus on identifying whether Wnt induces this expression profile, or if there is a different underlying mechanism. This could potentially being accomplished utilizing assays such as ATAC-seq to determine if high Wnt signaling increases chromatin accessibility for p57 transcription, or through determining whether Wnt transcription factor (TCF/LEF) binding domains exist near the promoter regions for p57. The p57-knockout study also demonstrated that p57 loss led to rapid organoid growth (49). Combination of these p57 depleted organoids with high Wnt conditions could help elucidate if Wnt-dependent regulation of proliferation or stemness could be p57 dependent, or if a separate mechanism exists.

Chief cell histology within FGPs

Following the observation that Wnt signaling regulates chief cell differentiation, we might expect high Wnt FGPs in FAP patients to be enriched for chief cells. Histological

analysis of FGPs demonstrated that chief cells are present within cystically dilated glands, although no studies have conducted morphometrics to assess the quantity or expression profile of these cells (55-57). Surprisingly, we observed that polyp biopsies demonstrated remarkably low expression of chief cell markers *LIPF*, *CHIA*, *PGC*, and *TNFRSF19* relative to non-polyp regions (Figure 3.2). However, we cannot rule out technical limitations involving differences in biopsy extraction between non-polyp and polyp regions. This result was surprising as our observations from Chapter 2 would suggest that increased Wnt signaling should direct chief cell differentiation (Figure 2.5). Accordingly, we observe that polyp-derived organoids with increased Wnt signaling do have increased expression of chief cell markers *in vitro* (Figure 3.8). Therefore, there is a potential discrepancy between the axis of differentiation *in vivo* and *in vitro* (Figure 4.7). Future analysis of FGPs could focus on histologically identifying the presence of chief cells within patient tissue. Previously discussed mouse models leading to a FGP phenotype could also provide further insights into how chief cells may contribute to polyposis through the use of lineage tracing studies.

4.4 Wnt Regulation of Parietal Cells

Another important question remains how Wnt signaling influences parietal cell function and differentiation. Parietal cell function in humans is definitively tied to FGP emergence in the oxyntic mucosa as polyposis is associated with acid suppression therapy such as proton pump inhibitors (58, 59). Given that sporadic proton pump inhibitor-associated FGPs have a similar histology to FAP patient FGPs, there may be a

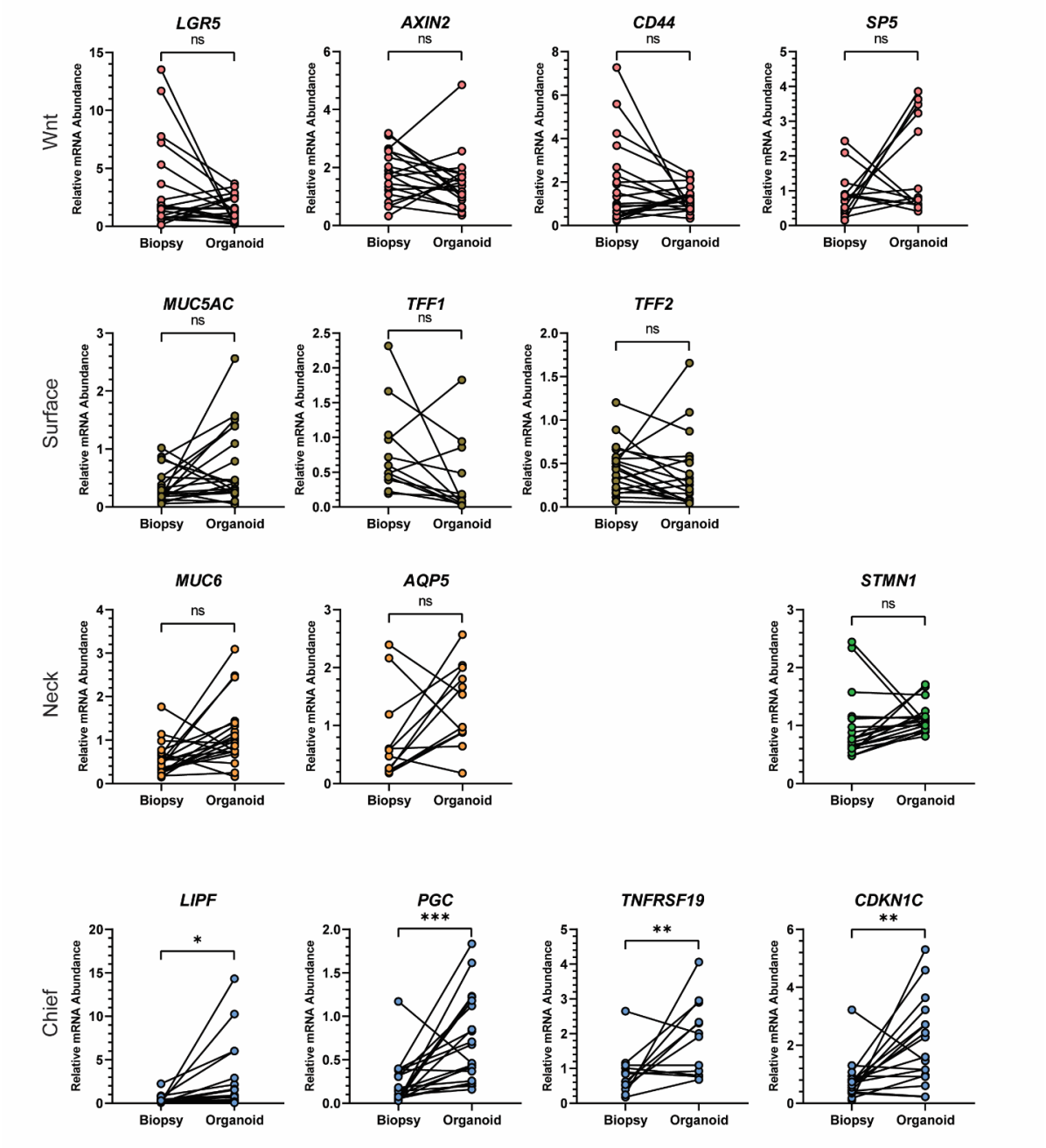

Figure 4.7: Relative mRNA expression of polyp biopsies versus matched organoids.

mRNA expression of Wnt target genes and differentiated markers of individual primary biopsies and the corresponding organoid lines, relative to patient-matched non-polyp samples. Expression of chief cell markers *LIPF*, *PGC*, and *TNFRSF19* was significantly reduced in polyp biopsies relative to non-polyp biopsies, but significantly increased in polyp organoids relative to non-polyp organoids.

similar mechanism rooted in parietal cell development or maturity that underscores both types. Parietal cells are present within the cystically dilated glands of fundic gland polyps; however, they are often attenuated in appearance (55-57, 60). When I analyzed mRNA expression of non-polyp and polyp primary biopsies, I did not note any change in expression of parietal cell marker genes *ATP4A* and *GIF* indicating that their differentiation was not significantly altered (Figure 3.2).

This falls in line with *in vivo* mouse studies which have failed to show that activation of Wnt signaling directly alters parietal cell development. Radulescu et al. demonstrated that Wnt activation via loss of *Apc* or *Gsk3* led to rapid parietal cell loss; however, in this study, there was a potential confounding effect of tamoxifen administration, which itself leads to oxyntic atrophy (61, 62). Numerous other studies, including our own with a *Sox2CreER^{T2}; APC$^{fl/fl}$* mouse model, have failed to demonstrate a similar phenotype following homozygous *Apc* deletion within the corpus epithelium unless challenged with additional oncogenic mutations (13, 14). Using a different Wnt activation approach with *Rspo3* overexpression *in vivo*, Fischer et al. demonstrated that Wnt activation increased parietal cell numbers (28). However, parietal cells remained equally distributed throughout the expanded glands, and therefore this increase could have been due to an overall increase in cell number rather than increased parietal cell differentiation. Therefore, a consensus has not been reached on how activation of Wnt signaling affects parietal cell development or maturity.

In vitro parietal cell analysis

The lack of parietal cells within typical organoid cultures is another confounding variable preventing study of mechanisms regulating their development. This phenomenon has been well documented since the first attempts to establish human corpus organoids and remains true within our cultures as well (63). Interestingly, when I subjected normal human organoids to high concentrations of CHIR99021, I did observe an increase in the expression of both *ATP4A* and *GIF* relative to moderate Wnt (Figure 2.6). This observation aligns with the findings of Fischer et al. where parietal cell number was increased following *Rspo3* overexpression (28). However, transcript abundance was remarkably low relative to what is observed *in vivo*. In my studies of marker gene expression in patient samples, I observed an approximate 2,000- to 30,000-fold reduction in mRNA abundance of *GIF* in organoids relative to full thickness biopsies. While *ATP4A* abundance was similar to *GIF* in full thickness human biopsy tissue, it was typically not detected within \ standard organoid cultures. My observation of increased *ATP4A* and *GIF* expression in high Wnt organoids does however present a possible mechanism through which Wnt positively regulates parietal cell development.

The ability to generate *in vitro* models with parietal cells could help elucidate the mechanisms underscoring various types of disease in the corpus such as FGPs. Numerous studies have demonstrated that BMP signaling appears to be a dominant force governing parietal cell development as overexpression of BMP inhibitor noggin (NOG) or epithelial deletion of *Bmpr1a* lead to oxyntic atrophy within the mouse stomach (64-66). However, organoids require supplementation with NOG for proper maintenance and growth over time (63). Therefore, it is possible that the addition of

NOG and subsequent inhibition of the BMP signaling pathway inhibits parietal cell development within culture. Future studies could expand upon these mechanisms to develop conditions which enable enrichment of parietal cells. Combination with our Wnt studies could thus help determine *in vitro* whether Wnt regulates parietal cell function or identity.

4.5 Summary of Future Directions

Throughout this chapter, I presented potential future directions for the continued study of Wnt signaling regulation of the human gastric corpus epithelium. Below are several highlighted studies with available models that I believe would encompass the next steps for this research.

I would utilize lineage tracing techniques to observe cell fate following conditional heterozygous or homozygous deletion of *Apc* within corpus and antral progenitors, as well as within chief cells of the corpus. This could be accomplished by an *Lrig1-CreER^{T2};Apc$^{fl/fl}$;R26-LSL-tdTomato* mouse model to target antral and corpus isthmus progenitors, and a *Gif-CreER^{T2};Apc$^{fl/fl}$;R26-LSL-tdTomato* mouse model to target chief cells (33, 41). Alternatively, a *Stmn1CreER^{T2}* driver could be utilized for corpus isthmus progenitors (35). I would expect heterozygous loss of *Apc* to induce lineage tracing from progenitors to all differentiated cell types in the corpus and antrum. However, this may be more skewed towards deep glandular neck cells in the corpus in line with heightened Wnt sensitivity. Following homozygous deletion of *Apc*, I would expect cells within the corpus to either be rapidly lost (~24 hours following recombination), or to differentiate

towards a chief/neck lineage and no longer contribute to clonal expansion. I would expect chief cells with heterozygous loss of *Apc* to maintain their quiescence, but to be lost following homozygous *Apc* deletion.

Furthermore, I would combine Wnt activation models (*Apc-cKO*) with Wnt inhibition models (*Rspo3* inhibition) to determine if the high Wnt signaling environment of the corpus precludes the inability to tolerate homozygous loss of *Apc* within mouse tissue. As a dual genetic model would be technically difficult, the aforementioned *Stmn1-CreER^{T2};Apc$^{fl/fl}$* could be treated with LGR5 ECD, as described by Yan et al., to pharmacologically inhibit RSPO signaling and therefore reduce the Wnt signaling environment (48). If *Apc$^{-/-}$* cells were retained within this model and led to neoplasia, this would indicate that the signaling environment plays a major role in underscoring the regional differences between the corpus and the antrum.

To assay potential differences in Wnt sensitivity between the corpus epithelium of mice and humans, I would conduct CHIR growth experiments using corpus organoids derived from each species, as outlined in Chapter 2 (Figure 2.1). This could also be expanded to additional regions of the gastrointestinal tract, such as small intestinal organoids where there are known differences in Wnt tolerance and disease manifestation. This could also be expanded to include antral polyps from FAP patients which are more likely to carry adenomatous change, however the rarity and pathologic danger of these polyps make acquisition for research purposes difficult.

I would also focus on developing an accurate mouse model of FGPs. Thus far, only deletion of H^+/K^+-ATPase subunits have been demonstrated to lead to an FGP-like phenotype with cystically dilated glands (25, 26). Lineage tracing within these models,

such as with a *Stmn1-CreER^{T2}* driver for isthmus cells and *Gif-CreER^{T2}* driver for chief cells in a *Cre+;R26-LSL-tdTomato;Atp4b$^{-/-}$* mouse, would provide interesting perspectives on the cells-of-origin for these FGPs (25). Although this model better reflects sporadic polyposis arising from chronic use of PPIs, this model could still provide insight into Wnt-dependent FGPs. Additionally, *Stmn1/Gif-CreER^{T2};Apc$^{fl/+}$;R26-LSL-tdTomato* mice could be given a proton-pump inhibitor or DMP-777 to add additional challenge following *Apc* loss. This could potentially convert the observed hyperplasia phenotype into an FGP phenotype, although that mechanism is unproven.

To investigate how Wnt regulates isthmus progenitor cells *in vivo*, I would use an *Lrig1-CreER^{T2};R26-LSL-tdTomato* or *Stmn1CreER^{T2};R26-LSL-tdTomato* mouse model to lineage trace progenitor cell fate following Wnt activation. I would activate Wnt signaling using Adenovirus to express RSPO3, as demonstrated in the intestinal study by Yan et al. (48). I would prefer Adenovirus over a genetic overexpression model using *Myh11CreER^{T2}* driver as such lineage tracing studies would require two independent Cre drivers leading to an overly complex genetic model. I would expect this model to demonstrate enhanced lineage tracing towards neck and chief cells as our *in vitro* models suggest. These experiments could also be conducted in *Lrig1/Stmn1-CreER^{T2};R26-LSL-tdTomato;Lgr4$^{fl/fl}$* models to test the hypothesis that LGR4 might regulate Wnt sensitivity in isthmus progenitors (29). If LGR4 plays a role in regulating Wnt sensitivity in isthmus progenitors, then I would expect loss of LGR4 to either desensitize isthmus proliferation to RSPO3 overexpression or induce rapid surface cell differentiation.

To investigate Wnt regulation of chief cells, a *Mist1-CreER^{T2};R26-LSL-tdTomato* or *Gif-CreER^{T2};R26-LSL-tdTomato* mouse model could be used in combination with Adenoviral RSPO3 overexpression (67). These experiments would differ from the studies by Fischer et al. as they would investigate the origin of chief cells in the expanded base compartment induced by high Wnt signaling (28). The percentage of Tomato+ chief cells after RSPO3 induction would determine if activation of Wnt signaling induces chief cell renewal, influences isthmus progenitor cell differentiation towards a chief cell fate, or both. I would also utilize LGR5 ECD as a mechanism for lineage tracing chief cells following Wnt inhibition, as described by Yan et al. (48). Alternatively, PORCN inhibitor C59 could be utilized to reduce Wnt signaling as our lab has prior experience with this drug. These experiments would determine whether the noted reduction in chief cells by Fischer et al. is due to chief cell dedifferentiation or reduced chief cell self-renewal (28).

To investigate how Wnt regulates parietal cell differentiation, I would attempt to grow organoids without NOG or with recombinant BMP4. I would likely induce BMP signaling once organoids are matured (Day 6) to prevent premature differentiation leading to cultures crashing. The first step would be to determine whether this induced proper parietal cell differentiation through immunohistochemistry and qPCR for *GIF* and *ATP4A/B*. Following, I would repeat these experiments in low and high Wnt environments to determine how activation of Wnt signaling influenced parietal cell differentiation. For *in vivo* analysis, it is possible that the aforementioned lineage tracing studies in combination with Wnt activation and/or inhibition would provide insight into these mechanisms.

Finally, I would conduct single cell analyses on high Wnt organoids. Single cell sequencing after growth in low and high Wnt signaling conditions could provide further insight into distinct populations of cells which exist within each culture. This would also provide insight into the percentage of cells which have a differentiated phenotype versus an undifferentiated, progenitor-like phenotype at this timepoint. Serial analysis of high Wnt organoids, namely from the 5 μM CHIR99021 condition, could also be conducted to observe differentiation over time. Bioinformatics analysis would therefore allow lineage mapping to determine how neck, chief, and potentially parietal cells arise over time in the presence of high Wnt signaling.

Another important question remaining from these experiments is which cells are responsible for demonstrating progenitor potential and giving rise to new organoids following passage. I would first utilize mouse organoids derived from a *Stmn1-GFP* or a *Gif-GFP* model to explore this concept (28, 35). GFP+ and GFP- cells from either model could be sorted after 6 days growth in low or high CHIR and then replated as single cells. Organoid formation efficiency from each population would provide insight into how Wnt regulates cell-specific progenitor potential. Furthermore, mature organoids originating from each pool could be assayed for mRNA expression in order to determine how chief cells versus isthmus cells give rise to differentiated cells following Wnt reduction. It is possible that these experiments could be repeated within human organoids; however, this would require the use of CRISPR or viral transfection to induce genetic change such as GFP expression.

4.6 Moving Beyond Traditional Organoid Models

Organoids have long been considered the gold standard for studying human gastrointestinal epithelial tissue as they are easily generated and maintained over long periods of time. However, while the *in vivo* epithelium is patterned by complex basal-luminal gradients of signaling factors, current organoid techniques require suspended growth in a homogenous pro-proliferative, anti-differentiation medium. This leads to organoids lacking any definitive architecture or cellular organization that would enable studying complex features of homeostasis and disease progression. The lack of parietal cells in corpus organoids represents an additional critical flaw in their design and demonstrates a need for improved systems to study human tissue *in vitro*.

Emerging platforms are being developed to produce *in vitro* or *ex vivo* models that closely mirror the architecture and environment that is present within tissue systems *in vivo*. Work by Boccellato and Wölffling et al. have established 2D polarized mucusoids through the use of an air-liquid interface as an approach to study pathways regulating differentiation in the antrum and corpus (66, 68). Hinman et al. have created 3D structures to grow colonic epithelium which leads to compartmentalization of cell types upon exposure to various chemical gradients (69). Growing human organoids in the presence of stroma also may lead to improved models as two independent studies have demonstrated that stromal cells can increase the number of parietal cells *in vitro* (70, 71).

The creation of these platforms will enable more precise study of human epithelial physiology and eventually could lead to phasing out traditional animal models as technology continues to advance. Furthermore, they could carry significant clinical

importance as primary patient tissue could be grown and used for personalized medicine applications. The development of these platforms however requires intimate knowledge and understanding of the key mechanisms which regulate cell function and identity. My work on Wnt signaling not only provides insights that will enable us to improve upon our current organoid models but will also help develop the next generation of research tools.

4.7 Conclusion

In conclusion, the work within this thesis describes a role for Wnt signaling in regulating homeostasis and disease progression within the human gastric corpus. Wnt signaling is distinctly associated with disease throughout the gastrointestinal epithelium, so understanding the mechanisms through which Wnt regulates cellular function and identity could impact the development of new therapies for patients. Through using primary tissue biopsies derived from patients, my work directly translates to our understanding of human gastric physiology.

4.8 References

1. Busslinger GA, Weusten BLA, Bogte A, Begthel H, Brosens LAA, and Clevers H. Human gastrointestinal epithelia of the esophagus, stomach, and duodenum resolved at single-cell resolution. *Cell Rep* 34: 108819, 2021.

2. Flanagan DJ, Barker N, Costanzo NSD, Mason EA, Gurney A, Meniel VS, Koushyar S, Austin CR, Ernst M, Pearson HB, Boussioutas A, Clevers H, Phesse TJ, and Vincan E. Frizzled-7 Is Required for Wnt Signaling in Gastric Tumors with and Without Apc Mutations. *Cancer Res* 79: 970-981, 2019.

3. de Lau W, Peng WC, Gros P, and Clevers H. The R-spondin/Lgr5/Rnf43 module: regulator of Wnt signal strength. *Genes Dev* 28: 305-316, 2014.

4. Ruffner H, Sprunger J, Charlat O, Leighton-Davies J, Grosshans B, Salathe A, Zietzling S, Beck V, Therier M, Isken A, Xie Y, Zhang Y, Hao H, Shi X, Liu D, Song Q, Clay I, Hintzen G, Tchorz J, Bouchez LC, Michaud G, Finan P, Myer VE, Bouwmeester T, Porter J, Hild M, Bassilana F, Parker CN, and Cong F. R-Spondin potentiates Wnt/beta-catenin signaling through orphan receptors LGR4 and LGR5. *PLoS One* 7: e40976, 2012.

5. Sigal M, Logan CY, Kapalczynska M, Mollenkopf HJ, Berger H, Wiedenmann B, Nusse R, Amieva MR, and Meyer TF. Stromal R-spondin orchestrates gastric epithelial stem cells and gland homeostasis. *Nature* 548: 451-455, 2017.

6. Lamlum H, Ilyas M, Rowan A, Clark S, Johnson V, Bell J, Frayling I, Efstathiou J, Pack K, Payne S, Roylance R, Gorman P, Sheer D, Neale K, Phillips R, Talbot I, Bodmer W, and Tomlinson I. The type of somatic mutation at APC in familial adenomatous polyposis is determined by the site of the germline mutation: a new facet to Knudson's 'two-hit' hypothesis. *Nat Med* 5: 1071-1075, 1999.

7. Albuquerque C, Baltazar C, Filipe B, Penha F, Pereira T, Smits R, Cravo M, Lage P, Fidalgo P, Claro I, Rodrigues P, Veiga I, Ramos JS, Fonseca I, Leitao CN, and Fodde R. Colorectal cancers show distinct mutation spectra in members of the canonical WNT signaling pathway according to their anatomical location and type of genetic instability. *Genes Chromosomes Cancer* 49: 746-759, 2010.

8. Albuquerque C, Breukel C, van der Luijt R, Fidalgo P, Lage P, Slors FJ, Leitao CN, Fodde R, and Smits R. The 'just-right' signaling model: APC somatic mutations are selected based on a specific level of activation of the beta-catenin signaling cascade. *Hum Mol Genet* 11: 1549-1560, 2002.

9. Lewis A, Segditsas S, Deheragoda M, Pollard P, Jeffery R, Nye E, Lockstone H, Davis H, Clark S, Stamp G, Poulsom R, Wright N, and Tomlinson I. Severe polyposis in Apc(1322T) mice is associated with submaximal Wnt signalling and increased expression of the stem cell marker Lgr5. *Gut* 59: 1680-1686, 2010.

10. Leedham SJ, Rodenas-Cuadrado P, Howarth K, Lewis A, Mallappa S, Segditsas S, Davis H, Jeffery R, Rodriguez-Justo M, Keshav S, Travis SP, Graham TA, East J, Clark S, and Tomlinson IP. A basal gradient of Wnt and stem-cell number influences regional tumour distribution in human and mouse intestinal tracts. *Gut* 62: 83-93, 2013.

11. McCracken KW, Aihara E, Martin B, Crawford CM, Broda T, Treguier J, Zhang X, Shannon JM, Montrose MH, and Wells JM. Wnt/beta-catenin promotes gastric fundus specification in mice and humans. *Nature* 541: 182-187, 2017.

12. Broda TR, McCracken KW, and Wells JM. Generation of human antral and fundic gastric organoids from pluripotent stem cells. *Nat Protoc* 14: 28-50, 2019.

13. Hayakawa Y, Ariyama H, Stancikova J, Sakitani K, Asfaha S, Renz BW, Dubeykovskaya ZA, Shibata W, Wang H, Westphalen CB, Chen X, Takemoto Y, Kim W, Khurana SS, Tailor Y, Nagar K, Tomita H, Hara A, Sepulveda AR, Setlik W, Gershon MD, Saha S, Ding L, Shen Z, Fox JG, Friedman RA, Konieczny SF, Worthley DL, Korinek V, and Wang TC. Mist1 Expressing Gastric Stem Cells Maintain the Normal and Neoplastic Gastric Epithelium and Are Supported by a Perivascular Stem Cell Niche. *Cancer Cell* 28: 800-814, 2015.

14. Douchi D, Yamamura A, Matsuo J, Melissa Lim YH, Nuttonmanit N, Shimura M, Suda K, Chen S, Pang S, Kohu K, Abe T, Shioi G, Kim G, Shabbir A, Srivastava S, Unno M, Bok-Yan So J, Teh M, Yeoh KG, Huey Chuang LS, and Ito Y. Induction of Gastric Cancer by Successive Oncogenic Activation in the Corpus. *Gastroenterology* 161: 1907-1923 e1926, 2021.

15. Galiatsatos P, and Foulkes WD. Familial adenomatous polyposis. *Am J Gastroenterol* 101: 385-398, 2006.

16. Kinzler KW, and Vogelstein B. Lessons from hereditary colorectal cancer. *Cell* 87: 159-170, 1996.

17. Groden J, Thliveris A, Samowitz W, Carlson M, Gelbert L, Albertsen H, Joslyn G, Stevens J, Spirio L, Robertson M, and et al. Identification and characterization of the familial adenomatous polyposis coli gene. *Cell* 66: 589-600, 1991.

18. Knudson AG. Two genetic hits (more or less) to cancer. *Nat Rev Cancer* 1: 157-162, 2001.

19. Weiss JM, Gupta S, Burke CA, Axell L, Chen LM, Chung DC, Clayback KM, Dallas S, Felder S, Gbolahan O, Giardiello FM, Grady W, Hall MJ, Hampel H, Hodan R, Idos G, Kanth P, Katona B, Lamps L, Llor X, Lynch PM, Markowitz AJ, Pirzadeh-Miller S, Samadder NJ, Shibata D, Swanson BJ, Szymaniak BM, Wiesner GL, Wolf A, Yurgelun MB, Zakhour M, Darlow SD, Dwyer MA, and Campbell M. NCCN Guidelines(R) Insights: Genetic/Familial High-Risk Assessment: Colorectal, Version 1.2021. *J Natl Compr Canc Netw* 19: 1122-1132, 2021.

20. Paszkowski J, Samborski P, Kucharski M, Cwalinski J, Banasiewicz T, and Plawski A. Endoscopic Surveillance and Treatment of Upper GI Tract Lesions in Patients with Familial Adenomatous Polyposis-A New Perspective on an Old Disease. *Genes (Basel)* 13: 2022.

21. Wood LD, Salaria SN, Cruise MW, Giardiello FM, and Montgomery EA. Upper GI tract lesions in familial adenomatous polyposis (FAP): enrichment of pyloric gland adenomas and other gastric and duodenal neoplasms. *Am J Surg Pathol* 38: 389-393, 2014.

22. Fodde R, Kuipers J, Rosenberg C, Smits R, Kielman M, Gaspar C, van Es JH, Breukel C, Wiegant J, Giles RH, and Clevers H. Mutations in the APC tumour suppressor gene cause chromosomal instability. *Nat Cell Biol* 3: 433-438, 2001.

23. Ratner N, and Miller SJ. A RASopathy gene commonly mutated in cancer: the neurofibromatosis type 1 tumour suppressor. *Nat Rev Cancer* 15: 290-301, 2015.

24. Powell AE, Vlacich G, Zhao ZY, McKinley ET, Washington MK, Manning HC, and Coffey RJ. Inducible loss of one Apc allele in Lrig1-expressing progenitor cells results in multiple distal colonic tumors with features of familial adenomatous polyposis. *Am J Physiol Gastrointest Liver Physiol* 307: G16-23, 2014.

25. Franic TV, Judd LM, Robinson D, Barrett SP, Scarff KL, Gleeson PA, Samuelson LC, and Van Driel IR. Regulation of gastric epithelial cell development revealed in H(+)/K(+)-ATPase beta-subunit- and gastrin-deficient mice. *Am J Physiol Gastrointest Liver Physiol* 281: G1502-1511, 2001.

26. Spicer Z, Miller ML, Andringa A, Riddle TM, Duffy JJ, Doetschman T, and Shull GE. Stomachs of mice lacking the gastric H,K-ATPase alpha -subunit have achlorhydria, abnormal parietal cells, and ciliated metaplasia. *J Biol Chem* 275: 21555-21565, 2000.

27. Karam SM, and Leblond CP. Dynamics of epithelial cells in the corpus of the mouse stomach. I. Identification of proliferative cell types and pinpointing of the stem cell. *Anat Rec* 236: 259-279, 1993.

28. Fischer AS, Mullerke S, Arnold A, Heuberger J, Berger H, Lin M, Mollenkopf HJ, Wizenty J, Horst D, Tacke F, and Sigal M. R-spondin/YAP axis promotes gastric oxyntic gland regeneration and Helicobacter pylori-associated metaplasia in mice. *J Clin Invest* 132: 2022.

29. Wizenty J, Mullerke S, Kolesnichenko M, Heuberger J, Lin M, Fischer AS, Mollenkopf HJ, Berger H, Tacke F, and Sigal M. Gastric stem cells promote inflammation and gland remodeling in response to Helicobacter pylori via Rspo3-Lgr4 axis. *EMBO J* 41: e109996, 2022.

30. Bockerstett KA, Lewis SA, Noto CN, Ford EL, Saenz JB, Jackson NM, Ahn TH, Mills JC, and DiPaolo RJ. Single-Cell Transcriptional Analyses Identify Lineage-Specific Epithelial Responses to Inflammation and Metaplastic Development in the Gastric Corpus. *Gastroenterology* 159: 2116-2129 e2114, 2020.

31. Powell AE, Wang Y, Li Y, Poulin EJ, Means AL, Washington MK, Higginbotham JN, Juchheim A, Prasad N, Levy SE, Guo Y, Shyr Y, Aronow BJ, Haigis KM, Franklin JL, and Coffey RJ. The pan-ErbB negative regulator Lrig1 is an intestinal stem cell marker that functions as a tumor suppressor. *Cell* 149: 146-158, 2012.

32. Arnold K, Sarkar A, Yram MA, Polo JM, Bronson R, Sengupta S, Seandel M, Geijsen N, and Hochedlinger K. Sox2(+) adult stem and progenitor cells are important for tissue regeneration and survival of mice. *Cell Stem Cell* 9: 317-329, 2011.

33. Choi E, Lantz TL, Vlacich G, Keeley TM, Samuelson LC, Coffey RJ, Goldenring JR, and Powell AE. Lrig1+ gastric isthmal progenitor cells restore normal gastric lineage cells during damage recovery in adult mouse stomach. *Gut* 67: 1595-1605, 2018.

34. Yoshioka T, Fukuda A, Araki O, Ogawa S, Hanyu Y, Matsumoto Y, Yamaga Y, Nakanishi Y, Kawada K, Sakai Y, Chiba T, and Seno H. Bmi1 marks gastric stem cells located in the isthmus in mice. *J Pathol* 248: 179-190, 2019.

35. Han S, Fink J, Jorg DJ, Lee E, Yum MK, Chatzeli L, Merker SR, Josserand M, Trendafilova T, Andersson-Rolf A, Dabrowska C, Kim H, Naumann R, Lee JH, Sasaki N, Mort RL, Basak O, Clevers H, Stange DE, Philpott A, Kim JK, Simons BD, and Koo BK. Defining the Identity and Dynamics of Adult Gastric Isthmus Stem Cells. *Cell Stem Cell* 25: 342-356.e347, 2019.

36. Stange DE, Koo BK, Huch M, Sibbel G, Basak O, Lyubimova A, Kujala P, Bartfeld S, Koster J, Geahlen JH, Peters PJ, van Es JH, van de Wetering M, Mills JC, and Clevers H. Differentiated Troy+ chief cells act as reserve stem cells to generate all lineages of the stomach epithelium. *Cell* 155: 357-368, 2013.

37. Fujii M, Clevers H, and Sato T. Modeling Human Digestive Diseases With CRISPR-Cas9-Modified Organoids. *Gastroenterology* 156: 562-576, 2019.

38. Kebschull JM, and Zador AM. Cellular barcoding: lineage tracing, screening and beyond. *Nat Methods* 15: 871-879, 2018.

39. Barker N, van Es JH, Kuipers J, Kujala P, van den Born M, Cozijnsen M, Haegebarth A, Korving J, Begthel H, Peters PJ, and Clevers H. Identification of stem cells in small intestine and colon by marker gene Lgr5. *Nature* 449: 1003-1007, 2007.

40. Barker N, Huch M, Kujala P, van de Wetering M, Snippert HJ, van Es JH, Sato T, Stange DE, Begthel H, van den Born M, Danenberg E, van den Brink S, Korving J, Abo A, Peters PJ, Wright N, Poulsom R, and Clevers H. Lgr5(+ve) stem cells drive self-renewal in the stomach and build long-lived gastric units in vitro. *Cell Stem Cell* 6: 25-36, 2010.

41. Caldwell B, Meyer AR, Weis JA, Engevik AC, and Choi E. Chief cell plasticity is the origin of metaplasia following acute injury in the stomach mucosa. *Gut* 71: 1068-1077, 2022.

42. Mills JC, and Goldenring JR. Metaplasia in the Stomach Arises From Gastric Chief Cells. *Cell Mol Gastroenterol Hepatol* 4: 85-88, 2017.

43. Nam KT, Lee HJ, Sousa JF, Weis VG, O'Neal RL, Finke PE, Romero-Gallo J, Shi G, Mills JC, Peek RM, Jr., Konieczny SF, and Goldenring JR. Mature chief cells are cryptic progenitors for metaplasia in the stomach. *Gastroenterology* 139: 2028-2037.e2029, 2010.

44. Bockerstett KA, Lewis SA, Wolf KJ, Noto CN, Jackson NM, Ford EL, Ahn TH, and DiPaolo RJ. Single-cell transcriptional analyses of spasmolytic polypeptide-expressing metaplasia arising from acute drug injury and chronic inflammation in the stomach. *Gut* 69: 1027-1038, 2020.

45. Fischer AS, and Sigal M. The Role of Wnt and R-spondin in the Stomach During Health and Disease. *Biomedicines* 7: 44, 2019.

46. Burclaff J, Willet SG, Saenz JB, and Mills JC. Proliferation and Differentiation of Gastric Mucous Neck and Chief Cells During Homeostasis and Injury-induced Metaplasia. *Gastroenterology* 158: 598-609 e595, 2020.

47. Kabiri Z, Greicius G, Zaribafzadeh H, Hemmerich A, Counter CM, and Virshup DM. Wnt signaling suppresses MAPK-driven proliferation of intestinal stem cells. *J Clin Invest* 128: 3806-3812, 2018.

48. Yan KS, Janda CY, Chang J, Zheng GXY, Larkin KA, Luca VC, Chia LA, Mah AT, Han A, Terry JM, Ootani A, Roelf K, Lee M, Yuan J, Li X, Bolen CR, Wilhelmy J, Davies PS, Ueno H, von Furstenberg RJ, Belgrader P, Ziraldo SB, Ordonez H, Henning SJ, Wong MH, Snyder MP, Weissman IL, Hsueh AJ, Mikkelsen TS, Garcia KC, and Kuo CJ. Non-equivalence of Wnt and R-spondin ligands during Lgr5(+) intestinal stem-cell self-renewal. *Nature* 545: 238-242, 2017.

49. Lee JH, Kim S, Han S, Min J, Caldwell B, Bamford AD, Rocha ASB, Park J, Lee S, Wu SS, Lee H, Fink J, Pilat-Carotta S, Kim J, Josserand M, Szep-Bakonyi R, An Y, Ju YS, Philpott A, Simons BD, Stange DE, Choi E, Koo BK, and Kim JK. p57(Kip2) imposes the reserve stem cell state of gastric chief cells. *Cell Stem Cell* 29: 826-839.e829, 2022.

50. Famili F, Brugman MH, Taskesen E, Naber BEA, Fodde R, and Staal FJT. High Levels of Canonical Wnt Signaling Lead to Loss of Stemness and Increased Differentiation in Hematopoietic Stem Cells. *Stem Cell Reports* 6: 652-659, 2016.

51. Luis TC, Naber BA, Fibbe WE, van Dongen JJ, and Staal FJ. Wnt3a nonredundantly controls hematopoietic stem cell function and its deficiency results in complete absence of canonical Wnt signaling. *Blood* 116: 496-497, 2010.

52. Luis TC, Naber BA, Roozen PP, Brugman MH, de Haas EF, Ghazvini M, Fibbe WE, van Dongen JJ, Fodde R, and Staal FJ. Canonical wnt signaling regulates hematopoiesis in a dosage-dependent fashion. *Cell Stem Cell* 9: 345-356, 2011.

53. Matsumoto A, Takeishi S, Kanie T, Susaki E, Onoyama I, Tateishi Y, Nakayama K, and Nakayama KI. p57 is required for quiescence and maintenance of adult hematopoietic stem cells. *Cell Stem Cell* 9: 262-271, 2011.

54. Higa T, Okita Y, Matsumoto A, Nakayama S, Oka T, Sugahara O, Koga D, Takeishi S, Nakatsumi H, Hosen N, Robine S, Taketo MM, Sato T, and Nakayama KI. Spatiotemporal reprogramming of differentiated cells underlies regeneration and neoplasia in the intestinal epithelium. *Nat Commun* 13: 1500, 2022.

55. Arnason T, Liang WY, Alfaro E, Kelly P, Chung DC, Odze RD, and Lauwers GY. Morphology and natural history of familial adenomatous polyposis-associated dysplastic fundic gland polyps. *Histopathology* 65: 353-362, 2014.

56. Islam RS, Patel NC, Lam-Himlin D, and Nguyen CC. Gastric polyps: a review of clinical, endoscopic, and histopathologic features and management decisions. *Gastroenterol Hepatol (N Y)* 9: 640-651, 2013.

57. Odze RD, Marcial MA, and Antonioli D. Gastric fundic gland polyps: a morphological study including mucin histochemistry, stereometry, and MIB-1 immunohistochemistry. *Hum Pathol* 27: 896-903, 1996.

58. Martin FC, Chenevix-Trench G, and Yeomans ND. Systematic review with meta-analysis: fundic gland polyps and proton pump inhibitors. *Aliment Pharmacol Ther* 44: 915-925, 2016.

59. Tran-Duy A, Spaetgens B, Hoes AW, de Wit NJ, and Stehouwer CD. Use of Proton Pump Inhibitors and Risks of Fundic Gland Polyps and Gastric Cancer: Systematic Review and Meta-analysis. *Clin Gastroenterol Hepatol* 14: 1706-1719 e1705, 2016.

60. Fukuda M, Ishigaki H, Sugimoto M, Mukaisho KI, Matsubara A, Ishida H, Moritani S, Itoh Y, Sugihara H, Andoh A, Ogasawara K, Murakami K, and Kushima R. Histological analysis of fundic gland polyps secondary to PPI therapy. *Histopathology* 75: 537-545, 2019.

61. Radulescu S, Ridgway RA, Cordero J, Athineos D, Salgueiro P, Poulsom R, Neumann J, Jung A, Patel S, Woodgett J, Barker N, Pritchard DM, Oien K, and Sansom OJ. Acute WNT signalling activation perturbs differentiation within the adult stomach and rapidly leads to tumour formation. *Oncogene* 32: 2048-2057, 2013.

62. Huh WJ, Khurana SS, Geahlen JH, Kohli K, Waller RA, and Mills JC. Tamoxifen induces rapid, reversible atrophy, and metaplasia in mouse stomach. *Gastroenterology* 142: 21-24 e27, 2012.

63. Bartfeld S, Bayram T, van de Wetering M, Huch M, Begthel H, Kujala P, Vries R, Peters PJ, and Clevers H. In vitro expansion of human gastric epithelial stem cells and their responses to bacterial infection. *Gastroenterology* 148: 126-136.e126, 2015.

64. Bleuming SA, He XC, Kodach LL, Hardwick JC, Koopman FA, Ten Kate FJ, van Deventer SJ, Hommes DW, Peppelenbosch MP, Offerhaus GJ, Li L, and van den Brink GR. Bone morphogenetic protein signaling suppresses tumorigenesis at gastric epithelial transition zones in mice. *Cancer Res* 67: 8149-8155, 2007.

65. Maloum F, Allaire JM, Gagne-Sansfacon J, Roy E, Belleville K, Sarret P, Morisset J, Carrier JC, Mishina Y, Kaestner KH, and Perreault N. Epithelial BMP signaling is required for proper specification of epithelial cell lineages and gastric endocrine cells. *Am J Physiol Gastrointest Liver Physiol* 300: G1065-1079, 2011.

66. Wolffling S, Daddi AA, Imai-Matsushima A, Fritsche K, Goosmann C, Traulsen J, Lisle R, Schmid M, Reines-Benassar MDM, Pfannkuch L, Brinkmann V, Bornschein J, Malfertheiner P, Ordemann J, Link A, Meyer TF, and Boccellato F. EGF and BMPs Govern Differentiation and Patterning in Human Gastric Glands. *Gastroenterology* 161: 623-636 e616, 2021.

67. Choi E, Means AL, Coffey RJ, and Goldenring JR. Active Kras Expression in Gastric Isthmal Progenitor Cells Induces Foveolar Hyperplasia but Not Metaplasia. *Cell Mol Gastroenterol Hepatol* 7: 251-253 e251, 2019.

68. Boccellato F, Woelffling S, Imai-Matsushima A, Sanchez G, Goosmann C, Schmid M, Berger H, Morey P, Denecke C, Ordemann J, and Meyer TF. Polarised epithelial monolayers of the gastric mucosa reveal insights into mucosal homeostasis and defence against infection. *Gut* 68: 400-413, 2019.

69. Hinman SS, Wang Y, and Allbritton NL. Photopatterned Membranes and Chemical Gradients Enable Scalable Phenotypic Organization of Primary Human Colon Epithelial Models. *Anal Chem* 91: 15240-15247, 2019.

70. Noguchi TK, Ninomiya N, Sekine M, Komazaki S, Wang PC, Asashima M, and Kurisaki A. Generation of stomach tissue from mouse embryonic stem cells. *Nat Cell Biol* 17: 984-993, 2015.

71. Schumacher MA, Aihara E, Feng R, Engevik A, Shroyer NF, Ottemann KM, Worrell RT, Montrose MH, Shivdasani RA, and Zavros Y. The use of murine-derived fundic organoids in studies of gastric physiology. *J Physiol* 593: 1809-1827, 2015.

72. Valenta T, Hausmann G, Basler K. The many faces and functions of β-catenin. *EMBO J* 31: 2714-2736, 2012.

73. Mosimann C, Hausmann G, Basler K. Beta-catenin hits chromatin: regulation of Wnt target gene activation. *Nat Rev Mol Cell Biol* 10: 276-286, 2009.